SYNTHESIS AND BIOACTIVITIES OF SUBSTITUTED QUINOLINES AND NANOGELS

by

AIBIN SHI

B.Sc., University of Science and Technology of China, 2004

AN ABSTRACT OF A DISSERTATION

submitted in partial fulfillment of the requirements for the degree

DOCTOR OF PHILOSOPHY

Department Of Chemistry
College of Arts and Sciences

KANSAS STATE UNIVERSITY
Manhattan, Kansas

2009

Abstract

The first section of this thesis deals with the synthesis of substituted quinolines and its bioactivities against gap junction. Cancer cells are characterized by down regulated or altered gap junction intercellular communication (GJIC) activities; enhancement of GJIC would provide a pathway for the delivery of anticancer drugs. Our computational studies using Autodock found binding interactions between gap junction channels and substituted quionlines (code name PQs). Thus, a serial of PQ compounds were synthesized and their activities against GJIC were tested. Among these synthesized PQs, 6-Methoxy-8-[(3-aminopropyl) amino]-4- methyl-5-(3-trifluoromethyl-phenyloxy)quinoline (PQ1) can specifically enhance GJIC activity of T47D cells without affecting the normal MECs. The PQ1 induced apoptosis can spread throughout the gap juctions, consequently cause the decrease of cell viability and colony growth. PQ1 can attenuate tumor growth of xenograft tumors in Nu/Nu mice. Compound **7** (code PQ11) which has an IC_{50} of 15.6nM against T47D cancer cell, is a promising candidate for further pharmacological studies.

The second section of this thesis deals with the synthesis and anticancer bioactivities of PEG-PEI based nanogels. Nanogels were synthesized, encapsulated with anticancer drugs, and loaded to stem cells. Stem cells can target at the cancer cell and release the nanogel and anticancer drug to kill the cancer cell. The nontoxic PEG-PEI nanogel which can be loaded to stem cells was successfully synthesized by doubly treatment of PEI with activated PEG. Based on this nontoxic nanogel, two other types of nanogels were synthesized. In one type of nanogel, an anticancer drug, SN38 was modified and attached to the nontoxic nanogel via a tetra-peptide linker. This tetra peptide can be recognized and cut by legumain, a protein that highly over expressed in many tumors, to release the drug to tumors. In the other type of nanogel, straptavidin was attached to the nanogel which can bind to biotin and recognized by tumor. The result indicated this type of nanogel can be loaded to stem cells within 15 minutes.

SYNTHESIS AND BIOACTIVITIES OF SUBSTITUTED QUINOLINES AND NANOGELS

by

AIBIN SHI

B.Sc., University of Science and Technology of China, 2004

A DISSERTATION

submitted in partial fulfillment of the requirements for the degree

DOCTOR OF PHILOSOPHY

Department Of Chemistry
College of Arts and Sciences

KANSAS STATE UNIVERSITY
Manhattan, Kansas

2009

Approved by:

Major Professor
Dr. Duy H. Hua

Abstract

The first section of this thesis deals with the synthesis of substituted quinolines and its bioactivities against gap junction. Cancer cells are characterized by down regulated or altered gap junction intercellular communication (GJIC) activities; enhancement of GJIC would provide a pathway for the delivery of anticancer drugs. Our computational studies using Autodock found binding interactions between gap junction channels and substituted quionlines (code name PQs). Thus, a serial of PQ compounds were synthesized and their activities against GJIC were tested. Among these synthesized PQs, 6-Methoxy-8-[(3-aminopropyl) amino]-4-methyl-5-(3-trifluoromethyl- phenyloxy)quinoline (PQ1) can specifically enhance GJIC activity of T47D cells without affecting the normal MECs. The PQ1 induced apoptosis can spread throughout the gap juctions, consequently cause the decrease of cell viability and colony growth. PQ1 can attenuate tumor growth of xenograft tumors in Nu/Nu mice. Compound **7** (code PQ11) which has an IC_{50} of 15.6nM against T47D cancer cell, is a promising candidate for further pharmacological studies.

The second section of this thesis deals with the synthesis and anticancer bioactivities of PEG-PEI based nanogels. Nanogels were synthesized, encapsulated with anticancer drugs, and loaded to stem cells. Stem cells can target at the cancer cell and release the nanogel and anticancer drug to kill the cancer cell. The nontoxic PEG-PEI nanogel which can be loaded to stem cells was successfully synthesized by doubly treatment of PEI with activated PEG. Based on this nontoxic nanogel, two other types of nanogels were synthesized. In one type of nanogel, an anticancer drug, SN38 was modified and attached to the nontoxic nanogel via a tetra-peptide linker. This tetra peptide can be recognized and cut by legumain, a protein that highly over expressed in many tumors, to release the drug to tumors. In the other type of nanogel, straptavidin was attached to the nanogel which can bind to biotin and recognized by tumor. The result indicated this type of nanogel can be loaded to stem cells within 15 minutes.

Table of Contents

Structure Number Correlation List

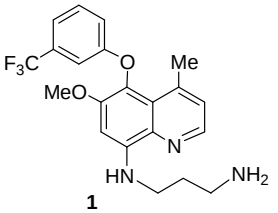

1

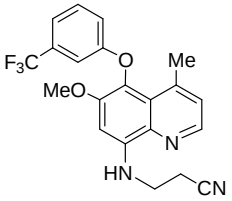

2

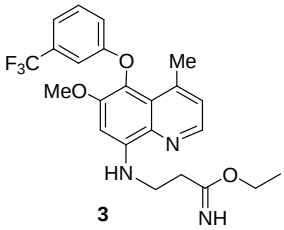

3

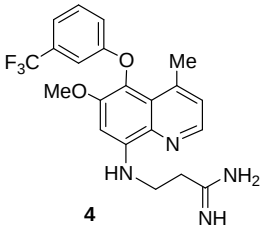

4

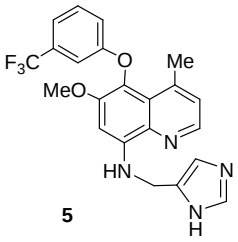

5

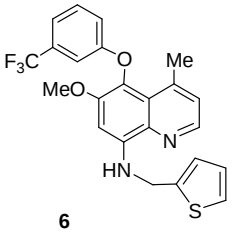

6

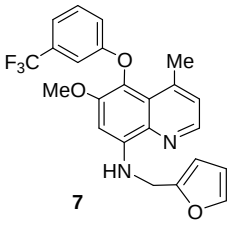

7

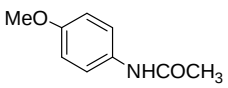

8

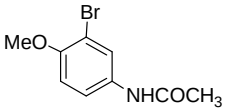

9

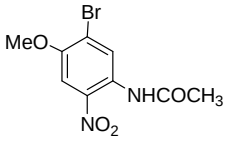

10

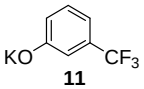

11

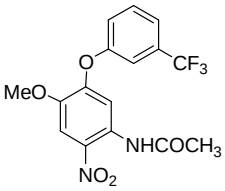

12

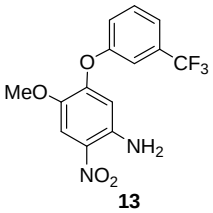

13

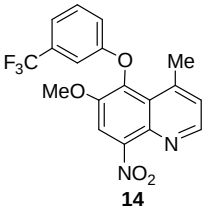

14

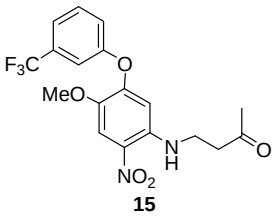

15

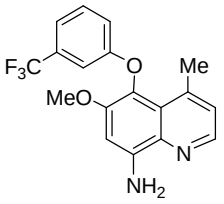

16

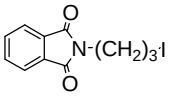

17

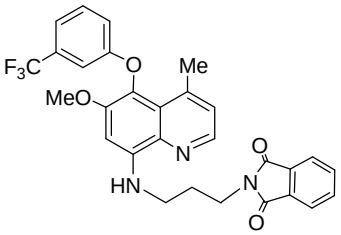

18

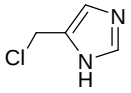

19

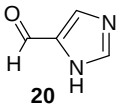

20

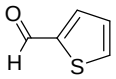

21

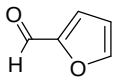

22

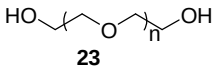

23

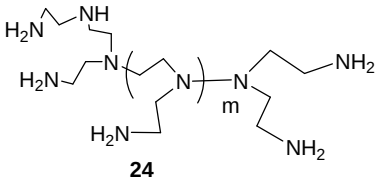

24

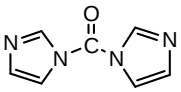

25

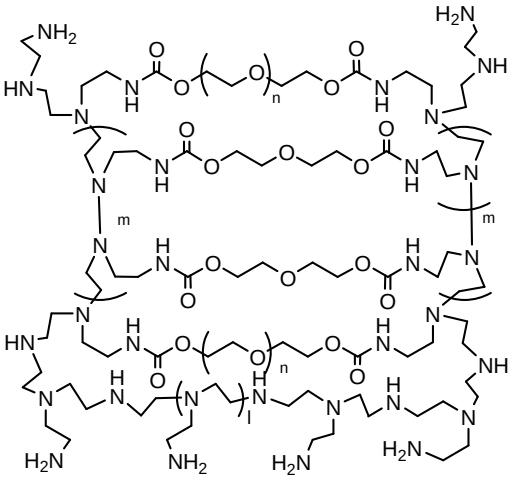

26

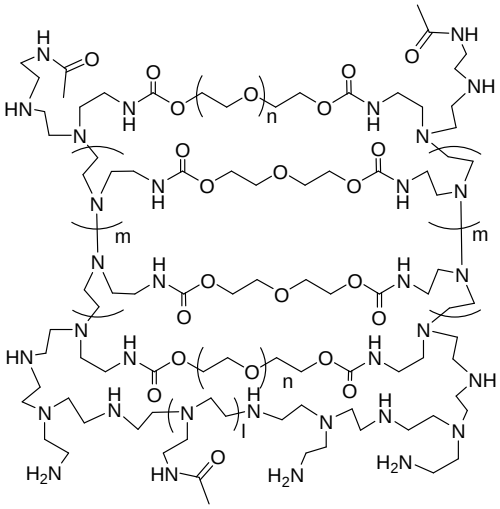

Aceterylated Nanogel
Ac-NG

27

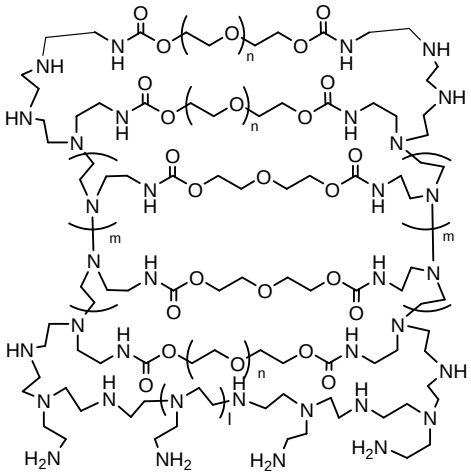

Nanogel PEI-PEG(1:6.8) NG

28

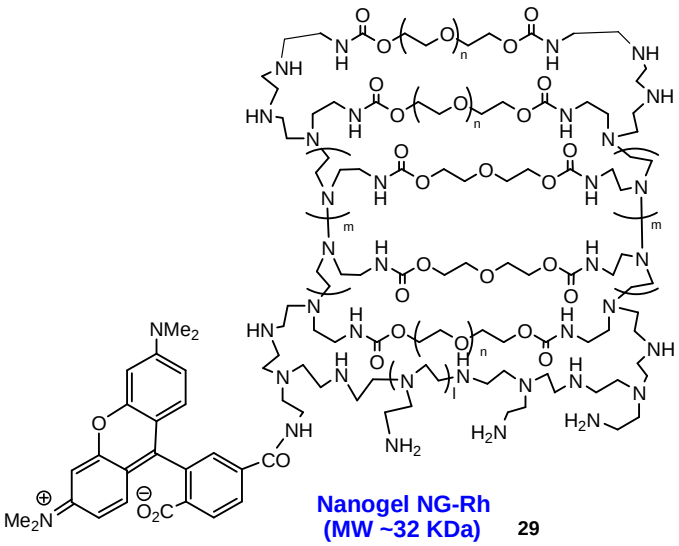

Nanogel NG-Rh
(MW ~32 KDa) **29**

AQ10

AQ10-NG

30

AQ10

AQ10-NG-Rh

31

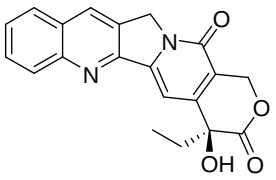

Camptothecin

32

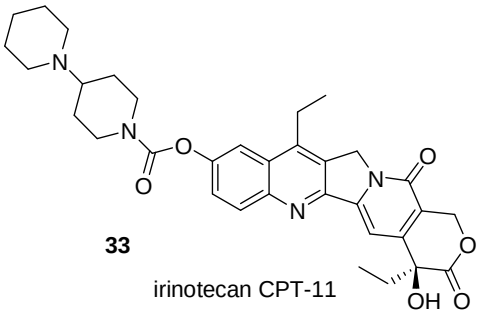

33

irinotecan CPT-11

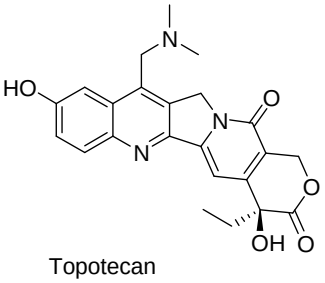

Topotecan

34

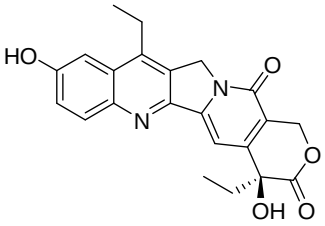

SN38

35

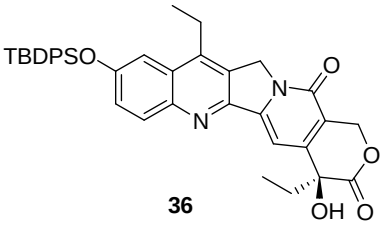

36

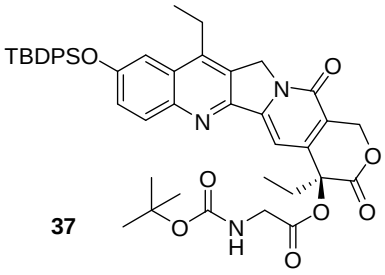

37

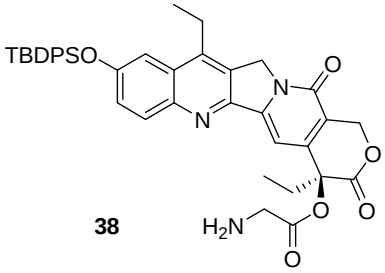

38

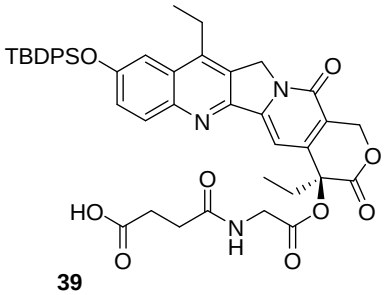

39

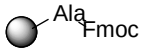

40

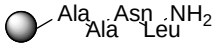

41

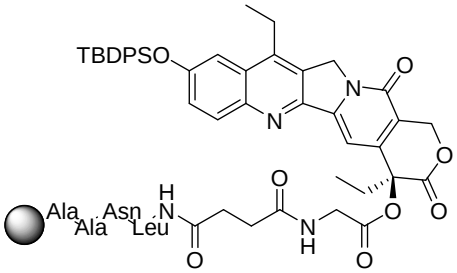

42

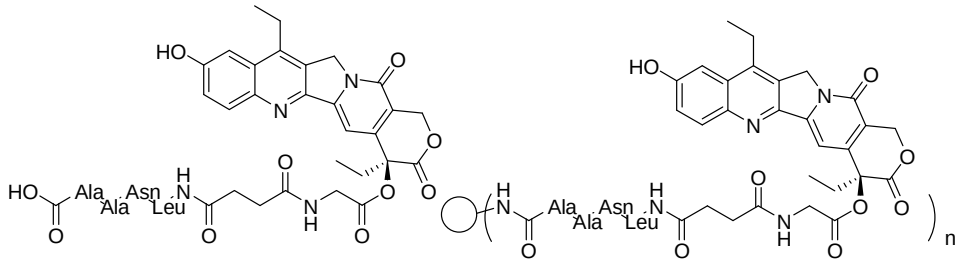

43

44

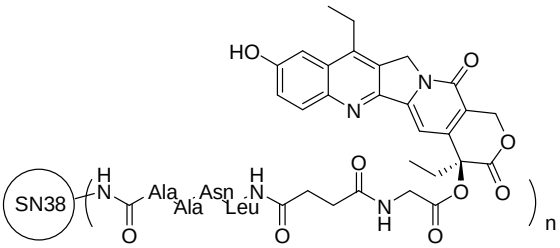

45

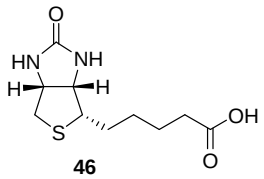

46

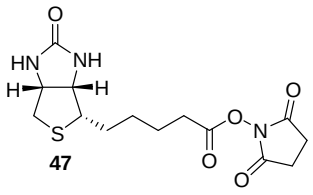

47

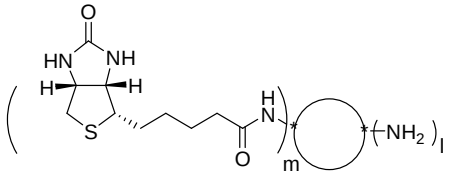

48

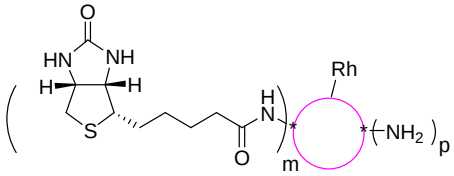

49

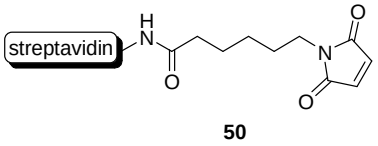

50

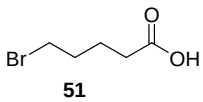

51

52

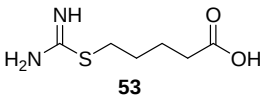

53

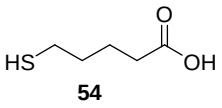

54

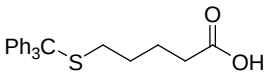

55

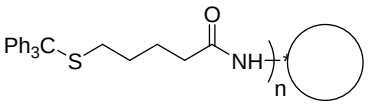

56

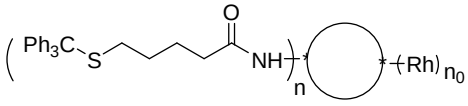

57

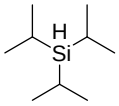

58

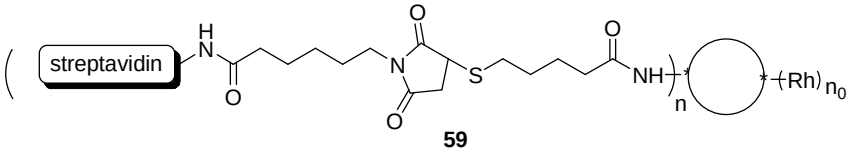

59

List of Figures

List of Schemes and Tables

List of Abbreviations

Ac2O	Acetic anhydride
Cx	Connexin
DCC	N,N’-dicyclohexylcarbodiimide
DIEA	Diisopropyl ethyl amine
DMAP	4-Dimethylaminopyridine
DMF	Dimethylformaide
EDC	N-ethyl-N’-(3-dimethylaminopropyl) carbodiimide hydrochloride
HBTU	O-Benzotriazole N,N,N',N'-tetramethyl uronium hexafluoro phosphate
MWCO	Molecular weight cut off
NHS	N-hydroxysuccinimide
NSC	Neural stem cells
PEG	Poly ethylene glycol
PEI	Poly ethylenimine
SA	Succinic Acid
Tam	Tamoxifen
TFA	Trifluoroacetic acid
TIS	Triisopropylsilane
UCMS	Umbilical cord matrix stem cells

Acknowledgements

I would like to thank my research advisor, Dr. Hua, for his guidance and instructions during my graduate study at Kansas State University. His hard working habit and positive attitude have encouraged me to work hard to achieve my goals in research and in career. He trained me to be a chemist using his vast knowledge and experience in organic chemistry and other fields. I also learned how to operate a well organized organic lab from him in this lab.

I would also like to thank Dr. Maatta, Dr. Bossmann, Dr. Aakeroy and Dr. Sorensen for their instructions and suggestions. Thanks to Dr. Blecha to be my outside chairperson of my committee. I would like to thank Ron Jackson and Tobe Eggers for the maintenance and support of instruments, Arlon Meek, Mary Dooley and Kimberly Ross for chemical orders.

Thank all my current and past labmates in Dr. Hua's lab, Kaiyan Lou, Huiping Zhao, Angelo Aguilar, Srinivas Battina, Bernard Wiredu, Sandeep Rana, Keshar Prasain, Mahendra Thapa, Weier Bao, Allan Prior, Thi Nguyen, and Laxman Pokhrel for their help in my research.

I would also like to thank all the collaborators Dr. Thu Annelise Nguyen, Dr. Gunjan Gakhar, Dr. Dolores J. Takemoto, Satyabrata Das, Dr. Chanran Ganta Dr. Rajashekar Rachakatla and Dr. Deryl Troyer for the bioactivity evaluation.

Finally I would like to thank my wife for her love and support in my life these years. Her spiritual support encouraged me to finish my graduate study during the past five years. Thank to my new boy for giving me a new life and new hope.

CHAPTER 1-Synthesis and Bioactivities of Substituted Quinolines

1.1 Introduction

Gap junctions are channels that connect two adjacent cells. Gap junctions are important channels[1] for the communication between cells as they allow a variety of compounds to pass through such as water, ions, metabolites, and secondary messengers which are smaller than 1000 Daltons.[1]

For normal cells, gap junction intercellular communication (GJIC) is highly up regulated. The apoptosis or damage signals can pass through the gap junction as well as other small molecules. Moreover, some diseases are associated with an increase in gap junction intercellular communication.[16] It is therefore necessary to find a compound that can specifically inhibit the gap junction activities.

One major difference between normal cells and cancer cells is the gap junction intercellular communication (GJIC). Cancer cells are mostly characterized by reduced or altered gap junction activities. Because of the lack of gap junction intercellular communication, the apoptosis signals can't be passed over to the cancer cells.[11] Moreover, the anti-cancer drugs can only kill cancer cells on the tumor surface which results in the demand of a large dose. In this case, it is important to find a gap junction enhancer that can increase or restore the gap junction intercellular communications between cancer cells to provide a pathway for apoptosis signals and anticancer drugs to penetrate to the inside of tumor.

Quinolines have been shown to have anticancer activities.[17-19] The effects of quinolines in modulation of multidrug resistance,[17] targeting tumor hypoxia,[18] and inhibition of tyrosine kinase[19] have been reported. Substituted quinolines were therefore examined to determine their interaction with gap junctions. Our computational docking study indicated binding between the substituted quinolines and the gap junctions.

A series of substituted quionlines (code name PQs) were synthesized in this study, and their activities on gap junctions were evaluated. The effect of PQ1 on the enhancement of gap junction on retinal and neuronal cells was studied using Lucifer yellow dye transfer assay, and the effect of PQ1 on the cell viability and colony growth of T47D breast cancer cell line was evaluated. On contrary to that of retinal and neuronal cells, the results indicated that PQ1 enhances gap junction activity and activates apoptosis leading to breast cancer cell death.

1.2 Background

1.2.1 Gap Junction Intercellular Communication

Gap Junctions function as the intercellular communication channels by allowing a passage for a variety of ions, small molecules secondary messengers and metabolites.

In vertebrates, each gap junction is composed of two connexons from two different cells. Each connexon is composed of six proteins of the connexin (Cx) family such as Cx 43 and Cx 32. For example, six Cx 43 proteins can form a connexon. To date approximately 21 of the connexins have been identified.[2]

Commonly, the connxin monomer has four helical bundles that are connected by two extracellular loops and one intracellular loop. These four transmebrane domains (TM1, TM2, TM3, and TM4) are believed to have different functions in the gap junction assembly, although their mechanisms still remain unclear. The N-terminus connected to TM1 is shorter compared to the C-terminus that binds to TM4.[5]

The phosphorylation of connexin mostly occurs on the serines[3] of the C-terminus and this phosphorylation process is shown to have important effect on the regulation of gap junction intercellular communication. The higher the expression of phosphorylated form of connexin, the lower the regulation of gap junction is observed.[4]

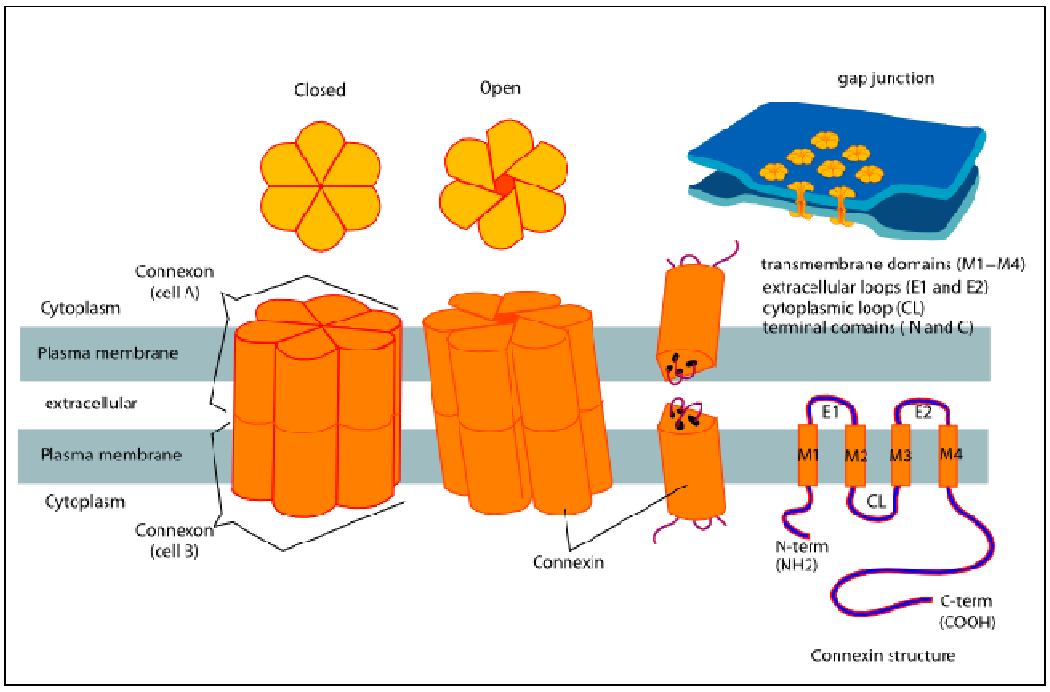

Figure 1 gap junction *http://psychology.wikia.com/wiki/Connexon*

The connexins follows the dimmer-dimmer pathway[6] to oligomerize into connexons. These connexons are then transported through the Golgi and fused to the nonjunctional plasma membrane. The connexons travel to the edge of the gap junction plaque where new gap junction channels were formed.[7, 8]

Gap junctions allow a variety of compounds to pass through including secondary messengers. Apoptosis or damage signals can also be passed from the damaged cell to its adjacent normal cells, which can spread out the damage. Researchers are thus trying to find ways to prevent this effect. One possibility is to block the gap junctions between the normal cells and the affected cells. Moreover, some of the diseases are associated with the increase of the gap junction intercellular communication (GJIC), which can be possibly treated by reducing the GJIC. Those compounds that can effectively block or inhibit the activities of gap junction channels are called gap junction inhibitors or blockers.

One significant difference between the normal cells and cancer cells is the amount of gap junctions. Unlike the normal cells that can communicate intracellularly through the gap junction channels, cancer cells are characterized by the lack of gap junctions.

As shown in figure 2, the initiated cell is suppressed by the surrounding normal cells, but the functional gap junctions are then disrupted by the cancer cell. The cancer cell that is released from the suppression grows to become a tumor without regulation.[10] Because of the lack of gap junction intercellular communication, the apoptosis signals can't be passed over to the cancer cells.[11] Moreover anti-cancer drugs could only kill the cancer cells on the tumor surface which results in the demand of a large dose.

In this case, it is necessary to open or restore the gap junction intercellular communication. The restoration of the gap junction can provide a pathway for the apoptosis signal to be delivered to the cancer cells. On the other hand, the anti-cancer drugs can also gain entrance into the internal part of the tumors, which resulted in an increase in drug sensitivity.

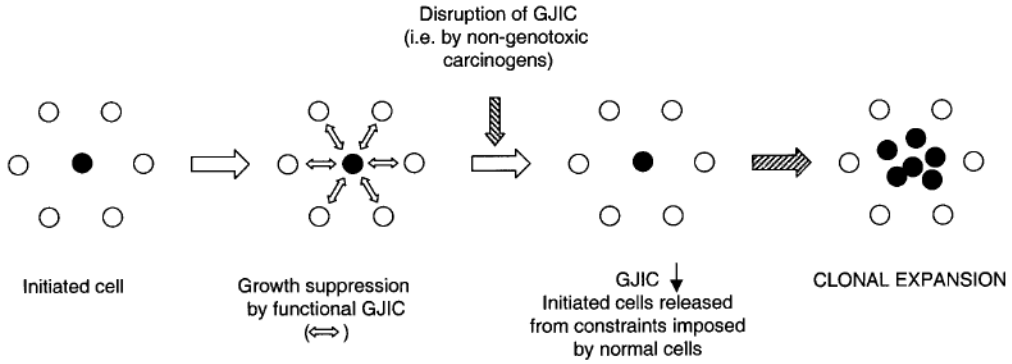

Figure 2 Disruption of GJIC in cancer cells

1.2.2 Gap Junction Inhibitors and Enhancers

Very few compounds have been reported to be gap junction inhibitors[9, 12, 16] or enhancers[13, 14, 15] despite the extensive research that has been done in this field.

Glycyrrhetinic acid, a derivative of the natural product glycyrrhizic acid isolated from the Chinese herb liquorice, is known to be an inhibitor of the gap junction. Its analog, carbenoxolone has also shown this inhibitory effect. To date no total synthesis of carbenoxolone has been reported. Resveratrol, a compound reported by Jiang[14] in 1997 that can prevent the skin cancer, has been discovered to be a gap junction enhancer.

1.2.3 Interaction of GJIC with Substituted Quinolines

Quinolines have been shown to have anticancer activities.[17-19] The effects of quinolines in modulation of multidrug resistance,[17] targeting tumor hypoxia,[18] and inhibition of tyrosine kinase have been reported.[19] Hence, substituted quinolines were examined on the interaction with gap junctions. To find new compounds that can interact with GJIC, the partial crystal structure of gap junction[20-22] was utilized as a model to develop new drugs. By using Autodock computational docking software,[23-25] the bindings of substituted quinolines (code name PQs) to the inert core of the hexameric hemichannel of gap junctions were observed. In one of the minimum energy (-0.7 kcal/mol) bound structures, interactions (close contact) between CF_3 group of PQ1 and H-N of Leu144 of connexin (2.5 Å), and OCH_3 group of PQ1 and CH_2 of Phe81 of connexin (2.0 Å) were found. Consequently, this substituted quinoline and its analogs were synthesized and their GJIC and anticancer activities were studied.

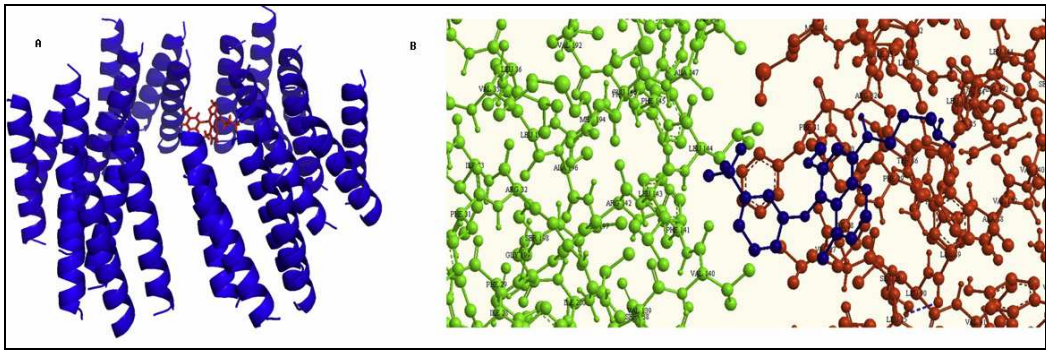

Figure 3 Interactions between PQ1 and GJIC by computational docking. In one of the minimum energy (-0.7 kcal/mol) bound structures, interactions (closed contact) between CF_3 group of PQ1 (blue) and H-N of Leu144 (green) of connexin (2.5 Å), OCH_3 group of PQ1 and CH_2 of Phe81 (orange) of connexin (2.0 Å), and NH_3^+ of PQ1 and $–O_2C$-Glu146 of connexin are found

1.3 Synthesis of Substituted Quinolines

The synthesized substituted quinolines are summarized in Figure 4.

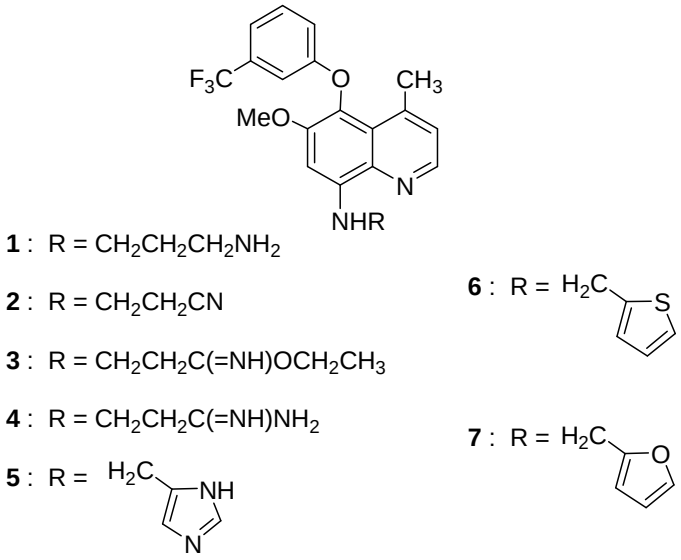

Figure 4. Structural formulas of substituted quinolines

1.3.1 Retro synthesis of compound 1

Gabriel synthesis is a synthetic method to make primary amines from alkyl halides. Compound **1** was synthesized from intermediate **16** by using a Gabriel synthesis, in which compound **16** was reacted with 3-iodopropylphthalimide followed by a treatment of hydrazine to afford a primary amine. Doebner-Miller reaction was utilized to construct the quinoline **16** from compound **13**. When treated with sodium bicarbonate in DMF, compound **13** undergo a Michael addition with methyl vinyl ketone followed by aromatization; further reduction of nitro group would give compound **16**. Compound **13** was obtained from functionalizations of N-(4-methoxyphenyl) acetamide (**8**). Bromination at C2 and nitration at C5 followed by deprotection of acetyl of starting compound **8** led to intermediate **13**.

Scheme 1 Retro-synthesis of compound **1**

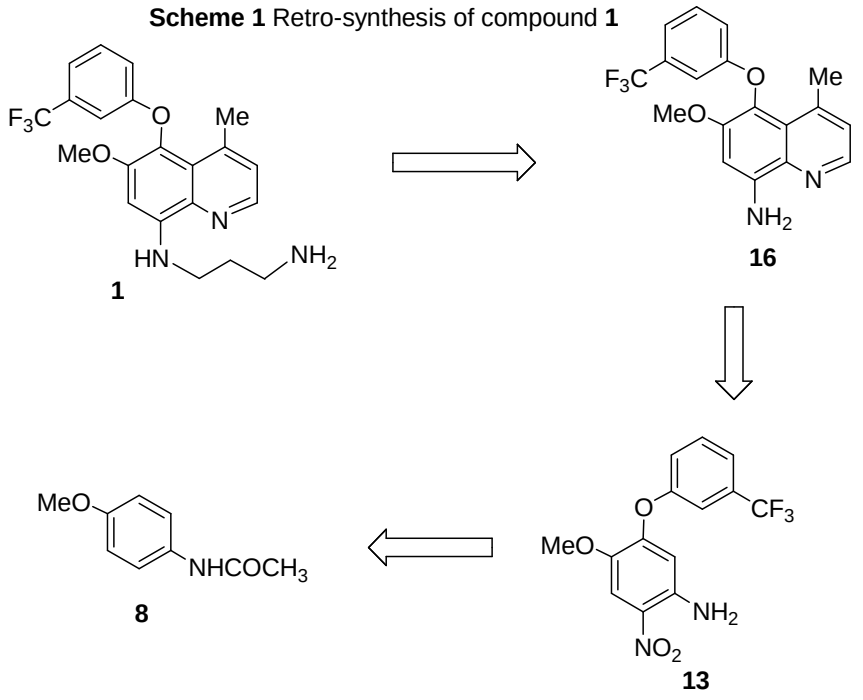

1.3.2 Synthesis of 4-amino-5-nitro-2-(3-trifluoromethylphenyloxy) anisole

A similar synthetic strategy was utilized from the literature reports[26, 27] with some modification. Starting from N-(4-methoxyphenyl) acetamide (**8**), functionalizations on C2 and C5 lead to the synthesis of 4-amino-5-nitro-2-(3-trifluoromethylphenyloxy)anisole (**13**) (scheme 1). Bromination of compound **8** at C2 in acetic acid using bromine gave N-(3-bromo-4-methoxyphenyl) acetamide (**9**) in 69% yield after recrystallized from 25% ethanol in water. Nitration of **9** at C5 by using nitric acid in acetic anhydride and acetic acid at 5°C for 3 hours gave 2-bromo-4-acetamino-5-nitroanisole[27] (**10**) in 82% yield after recrystallized from chloroform. 4-acetamino-5-nitro-2-(3-trifluoromethyl- phenyloxy) anisole (**12**) was prepared by a substitution of bromide in compound **10** with potassium 3-trifluoromethylphenoxide (**11**) in N, N-dimethylformamide (DMF) at 120 ^{o}C; the yield of this reaction was 79% after recrystallized from ethanol. The acetyl proctetction group of **12** was removed with hydrochloric acid in ethanol followed by recrystallization from ethanol to give 4-amino-5-nitro-2-(3-trifluoro- methylphenyloxy) anisole (**13**) with 95% yield.

Scheme 2. Preparation of 4-amino-5-nitro-2-(3-trifluoromethylphenyloxy)anisole (**13**)

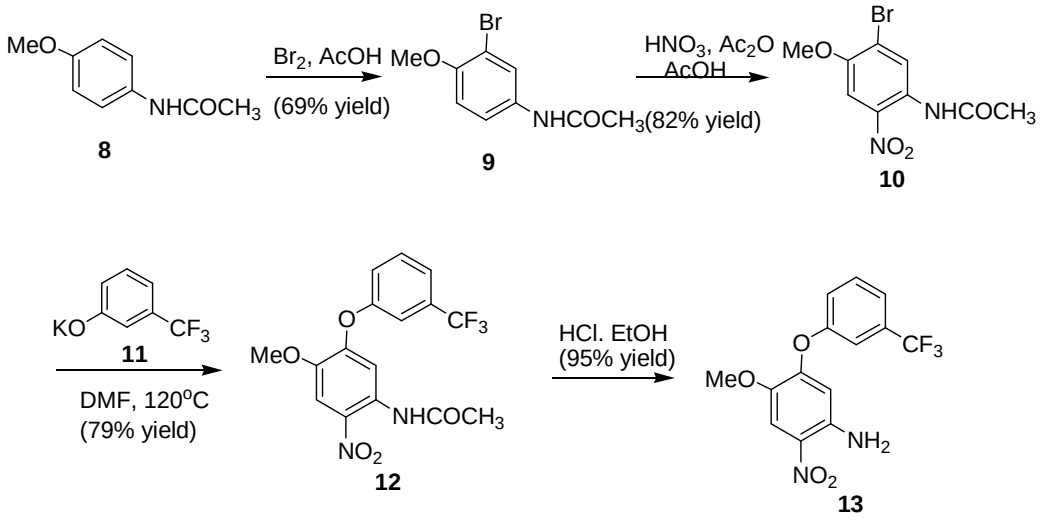

1.3.3 Synthesis of 6-Methoxy-4-methyl-8-nitro-5-(3-trifluoromethyl phenyloxy)quinoline (14)

Literature[28] has reported the construction of the quinoline via a Michael addition of vinyl methyl ketone. However, the results turned out not as simple as was reported. Vinyl methyl ketone was added to a solution of **13**, arsenic acid in 85% phosphoric acid at 100 ^{o}C (oil bath temperature); the color of the solution turned from red to dark brown immediately after the addition. After 20 minutes, the reaction[29] was worked up and a mixture of desired quinoline **14** and 1, 4-adduct **15** as well as the starting material **13** was obtained in a ratio of 1:2:1. A 24.5% yield of compound **14**, 49% yield of compound **15**, and 24% recovery of **13** were obtained after the separation by silica gel column chromatography. A higher temperature (120 ^{o}C) did not improve the yield of compound **14**, but resulted in decomposition of 1, 4- adduct **15** and starting material **13** and longer reaction time had the same effect. Excess of vinyl methyl ketone did not result in the decomposition; however the yields and ratios remained unchanged neither. Compound **15** was then treated with arsenic acid in phosphoric acid again under similar conditions as that mentioned above to give **14** and **13** along with the starting material **15** in a ratio of 1:2:1. The results indicated that the intermediate **15** can either undergo a cyclization to form the desired product **14**, or a reverse Michael addition to

provide amine **13** and vinyl methyl ketone.

Since the conjugated alkynones were also used to construct quinolines[30, 31] from aromatic amines, 3-butyn-2-one was also tested in order to simplify the synthesis. Amine **13** was treated with 3-butyn-2-one and arsenic acid in phosphoric acid at 100 ^{o}C for 20 minutes; after work up, the crude products were separated by silica gel column chromatography. The desired product **14** was obtained in a 24% yield along with 28% of recovered starting material **13** while the 1, 4-adduct was not detected. Instead, some red oligomers that can not be identified by NMR spectroscopy were obtained. This might due to polymerization of the alkynone or rapid decomposition of the 1, 4 adduct. Thus, vinyl methyl ketone was chosen to construct the quinoline ring since the 1, 4-adduct could be isolated and retreated to improve the overall yield of compound **14**.

Scheme 3. Preparation of quinoline **14** and **15**

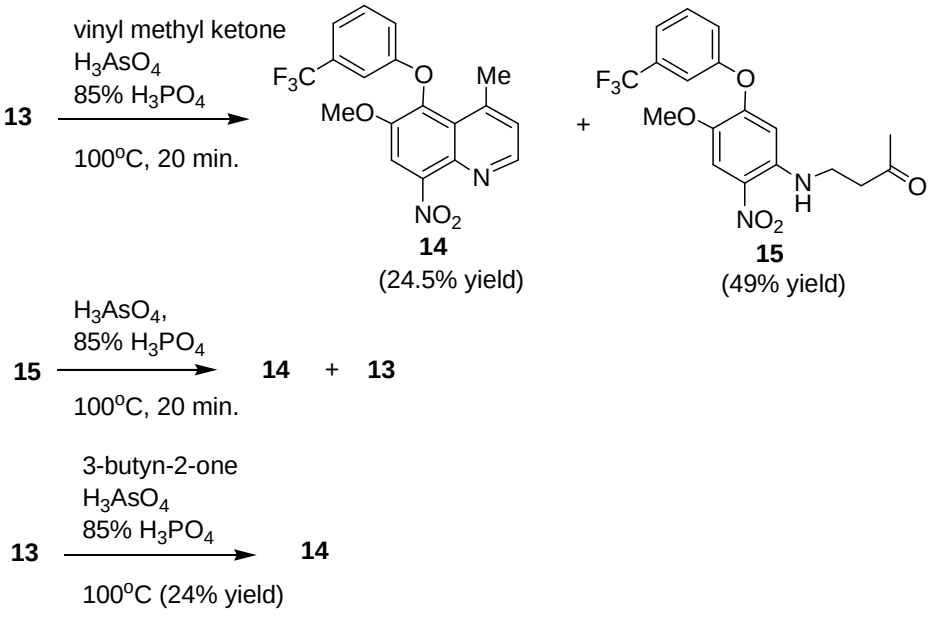

1.3.4 Synthesis of PQ1 (1)

Reduction of compound **14** with iron powder in 1% (by volume) acetic acid in water under reflux for 2 hours gave amino quinoline **16** in 96% yield as a red solid. Base on the amino function group, compound **16** was served as the precursor for a series of different substituted quinolines as shown in Figure 1. Since compound **16** was red in color and strongly UV active while all the substituted quinolines had a yellow or red color, the purification of product by silica gel column chromatography was easily achieved by tracking the color. Treatment of amino quinoline **16** with Iodide **17** and sodium bicarbonate in DMF at 80 ^{o}C for 48 hours[32] gave the alkylated compound **18** as a yellow solid in 72% yield. Removal of the amino protecting group of compound **18** with hydrazine in refluxing ethanol finished substituted quinoline **1** as a yellow solid in 80% yield. Since compound **1** had very poor solubility in aqueous media, its succinic acid salt was prepared by treatment with 1 equivalent of succinic acid in methanol, diluted with water and lyophilized to yield the succinic salt in quantitative yield. The code name for the succinic salt of compound **1** is PQ**1.**

Scheme 4. Synthesis of substituted quinoline **1**(**PQ1**)

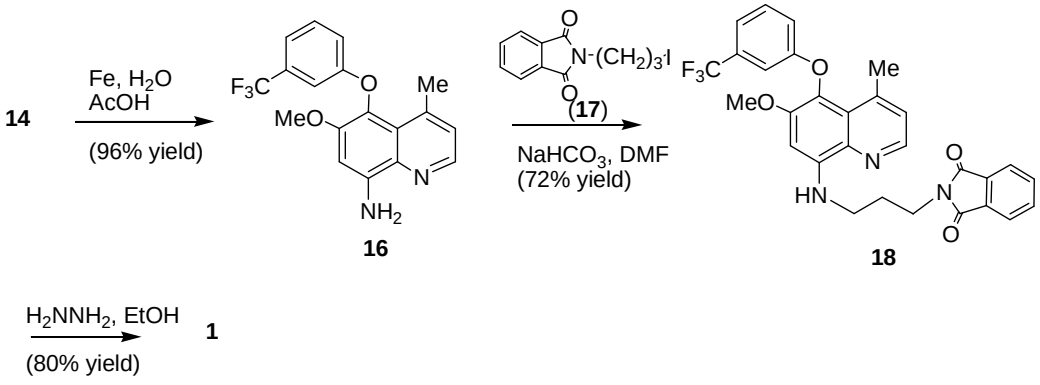

1.3.5 Synthesis of PQ6-PQ8

Compound **16** was treated with acrylonitrile in phenol at 100 °C for two days[33] in a sealed tube to give compound **2** as a Michael addition product in 50% yield along with 20% of recovered starting material **16**. No reaction was found when ethanol[34] was used as a solvent instead of phenol. Ethanolysis[35] of compound **2** by the treatment with saturated HCl (gas) in ethanol and benzene in a sealed tube at room temperature for 3 days afforded a 69% yield of ethyl imidate **3** as a yellow solid. Compound **3** was then treated with ammonia gas in ethanol[36] at 50 °C for 6 hours in a sealed tube to produce amidine **4** in 57% yield along with 13% recovery of starting material **2**. Their succinic salts were made by adding 1 equivalent of succinic acid in methanol followed by diluting with water and lyophilization. The code names of the succinic salts for compound **2**, **3**and **4** were PQ6, PQ7 and PQ8, respectively.

Scheme 5. Synthesis of compounds **2**-**4**

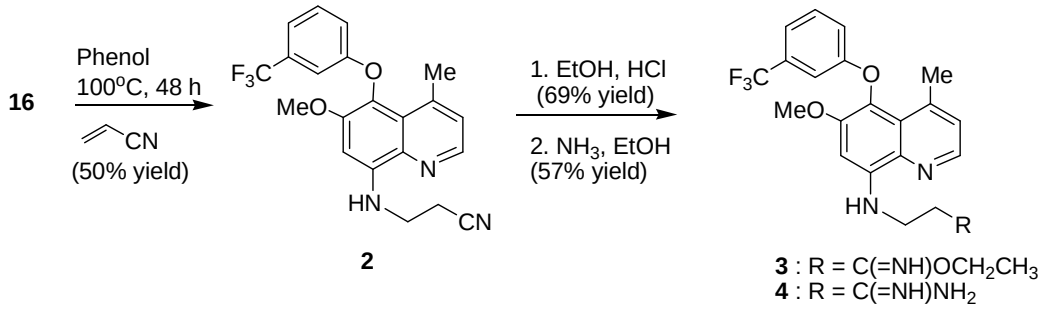

1.3.6 Synthesis of PQ9-PQ11

Initially, we were trying to synthesize quinoline **5** by using nuclearphilic substitution of the aromatic amine **16** with 5-(chloromethyl)-1H-imidazole **19**. Compound **16** was treated with **19** and sodium bicarbonate in DMF at 80 °C for two days, however, no reaction was detected. This might be due to the instability of compound **19**. Imidazole **19** can absorb moisture very rapidly and decompose at room temperature.

Synthesis of quinolines **5-7** was accomplished via a reductive amination[37] of aromatic amine **16** and with an aldehyde. Treatment of **16** with aldehyde **20** in methanol-acetic acid for 1 hour at room temperature followed by the addition of sodium cyanoborohydride afforded compound **5** as a yellow solid in 79% yield. Aldehyde **20** was obtained by the oxidation of 5-hydroxymethylimidazole with manganese dioxide in methanol[38] at room temperature (99% yield). Treatment of compound **16** with aldehyde **21** and **22** separately utilizing the same procedure as mentioned above gave quinolines **6** and **7**, respectively. Their succinic salts were made by adding 1 equivalent of succinic acid in methanol followed by diluting with water and lyophilization. The code names of the succinic salts for compound **5**, **6** and **7** were PQ9, PQ10 and PQ11 respectively.

Scheme 6. Synthesis of substituted quinolines **5** ~ **7**.

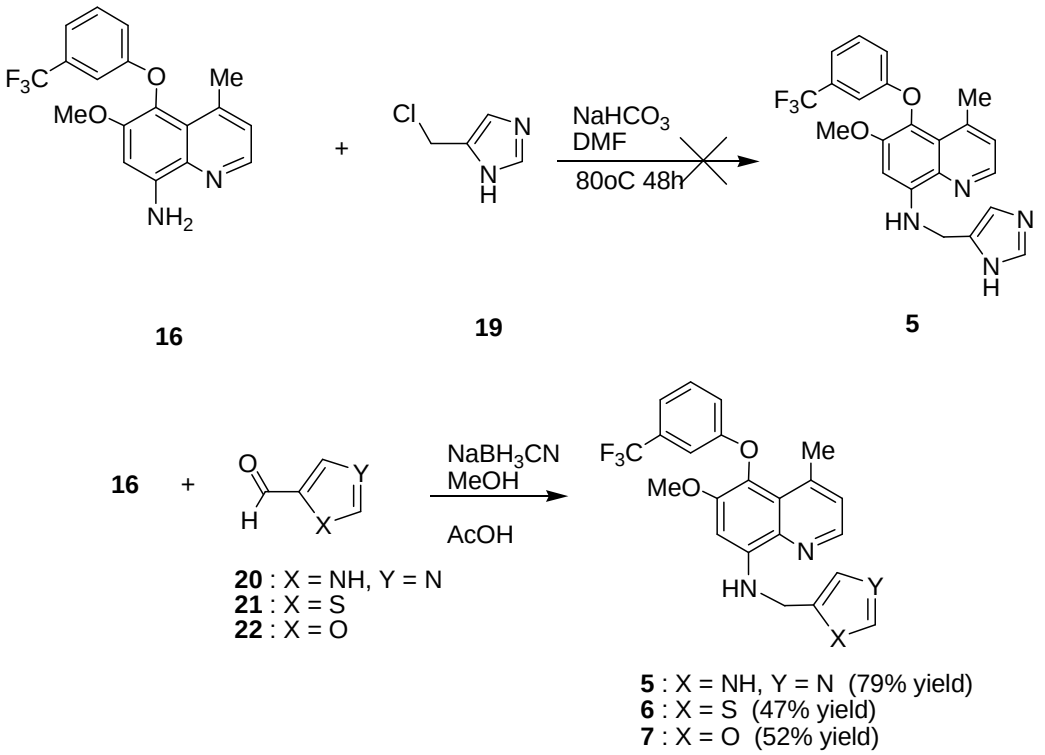

1.4 Results and Discussions

Breast cancer, the most common type of cancer in women worldwide, [39] is one of the highest death rate cancers for women in the United States. Breast cancer cells also have reduced or altered gap junction intercellular communications. The growth activity of cancer cells is negatively related to the capability of communication[40] through gap junction; thus one feasible way to reduce the growth of tumor is to restore or enhance the gap junction[41, 42] in breast cancer cells. A small molecule that can activate the GJIC would provide a possible way to load the anticancer drugs to breast cancer cells. Our autodocking computation shows the interaction of PQ1 with the connexin 43 hemichannels; thus PQ1 has been chosen and its effect on gap junctions has been evaluated. The bioactivity evaluations on T47D cells were done by our collaborator, Dr. Thu Annelise Nguyen and her student Gunjan Gakhar. The bioactivity on R28 cells regarding the inhibition of gap junction were tested by Dr. Dolores J. Takemoto and her student Satyabrata Das.

1.4.1 Effect of PQ1 in GJIC in T47D Breast Cancer Cells

The effect of PQ1 on the GJIC activity in T47D breast cancer cells was tested. Scrape load/dye transfer assay was utilized (Figure 5). In this experiment, the white dash line indicates the initial cutting site. Rhodamine-dextran, which was a relatively large molecular dye that can't pass through the gap junction channels, was used to mark the cutting site. To the right side of the cutting site, different doses of PQ1 were given to the cells compared to the control. Lucifer yellow was used as a dye that can travel through any gap junctions that are present. The top panel shows the T47D cancer cell while the bottom shows the normal cell. For the control with media alone or treated with succinic acid, the Lucifer yellow (green in color) can't travel to the right side due to the lack of gap junction. When treated with PQ1, the travel of the Lucifer yellow was obviously increased as the concentration of PQ1 increased. The results indicated that PQ1 can significantly increase the gap junction activity in T47D cells compared to the control using scrape load/dye transfer assay (Figure 5A, top panels).

While for the human primary epithelial cells (MEC, normal cells, Figure 5A, bottom panels), the Lucifer yellow dye were uniformly transferred due to the existing high level of gap junction activity[43-45] in these cells. A graphical representation demonstrated that 200 nM PQ1 causes an 8.5-fold increase in distance of dye transfer compared to control (Figure 5B).

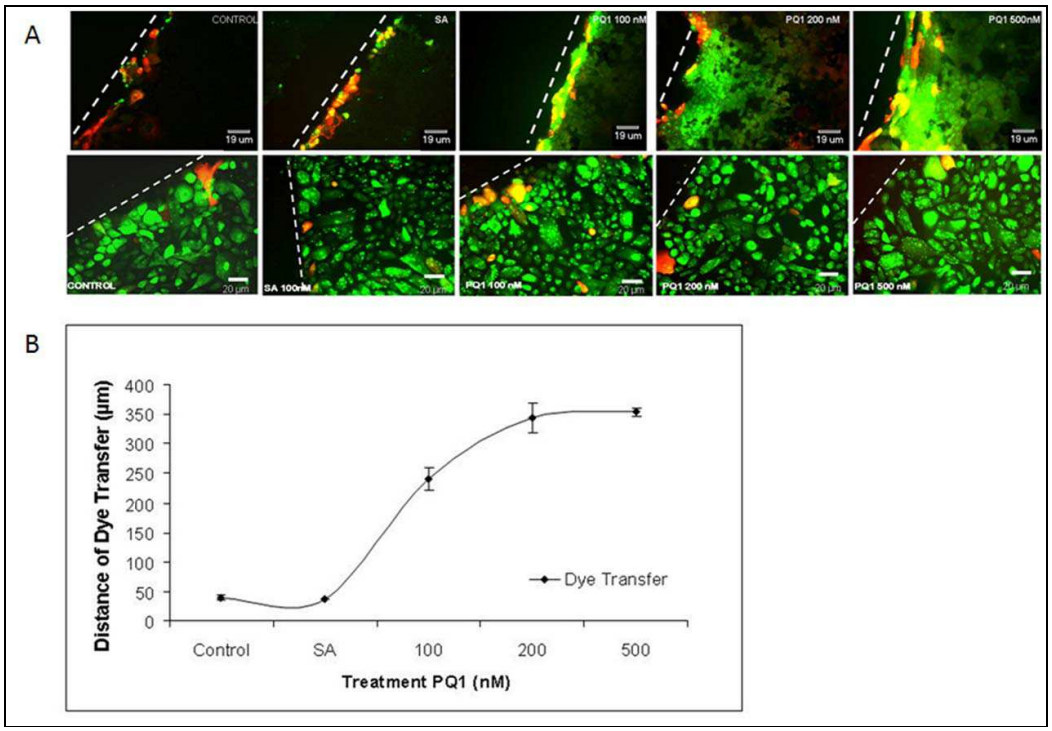

Figure 5. Effect of PQ1 in Gap Junction Activity (data collected from Dr. Thu Annelise Nguyen and Dr. Gunjan Gakhar). A top) T47D and A bottom) MEC cells were treated with 0, 100, 200, and 500 nM PQ1 for 1 hour. Controls are media alone and succinic acid. B) Graphical presentation of experiments shows the distance of dye transfer of T47D cells.

1.4.2 Effect of PQ1 in T47D Cancer Cell Colony Growth

The above result on the GJIC of T47D breast cancer cells indicated that PQ1 can cause an increase in the GJIC activities of T47D cells. For most cancer cells, the cell growth ability is related to the GJIC, the higher the GJIC in cancer cells, the lower the growth of cancer cells. Thus, we would expect that PQ1 can inhibit the growth of T47D breast cancer cells by enhancing the GJIC.

The effect of PQ1 in T47D cancer cell colony growth formation was examined. As

shown in Figure 6, T47D and MEC cells were treated with 10, 100, 1000, and 10,000 nM PQ1 for 7 days. Individual cell colonies which were larger than 50 μm were counted. A graphical presentation of three experimental results is presented below in log scale of PQ1 concentration. The treatment of 100 nM PQ1 inhibited 66% of colony growth compared to the control, while having no effect on the normal cells. This suggested that treatment of PQ1 can increase the GJIC activity and subsequently decrease colony growth of T47D cells.

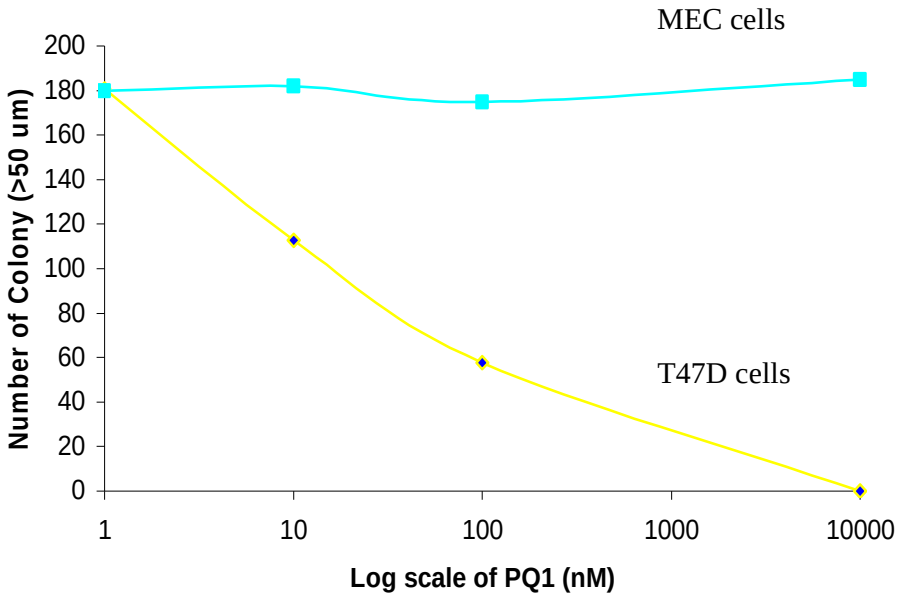

Figure 6 Effects of Substituted Quinolines on T47D and MEC Cells (data collected from Dr. Thu Annelise Nguyen and Dr. Gunjan Gakhar). Base agar plates were prepared containing 0.8% agar and 0.4% agar in Ham's F12. Cells (5×10^4 cells/33 mm2 well) were suspended in 100 μl of Ham's F12 with 0.4% agar and plated. These plates were maintained at 37°C for 7 days and examined for the presence of colonies. Individual colonies of 50 μm or greater were examined. T47D cells were treated with 1, 10 and 100 nM PQ1 and SA (succinic acid) as a solvent control. Individual colonies of 50 μm or greater were examined. Statistical significance, $*p<0.05$, of at least three experiments.

1.4.3 Effect of PQ1 on Cell Viability

PQ1 restored the GJIC on T47D cells, and caused a decrease in the colony growth of T47D breast cancer cell. This indicated an inhibition of the tumor growth. As for the treatment of cancer cells, the cell viability is another important factor. Would PQ1 kill the T47D cells to cause an inhibition of the colony growth?

Thus the cell viabilities of PQ1 in T47D and MEC cells were also determined by using MTT assay. Results demonstrated that at 200nM PQ1 has 67% cell viability compared to the controls (Figure 7). 1 μM PQ1 can further decrease cell viability to 50% in T47D cells; however, treatments of 100 and 200 nM PQ1 have 95% and 103% MEC cell viabilities respectively as compared to the control. This indcated PQ1 had no cytotoxic effect to normal MECs even at 500 nM.

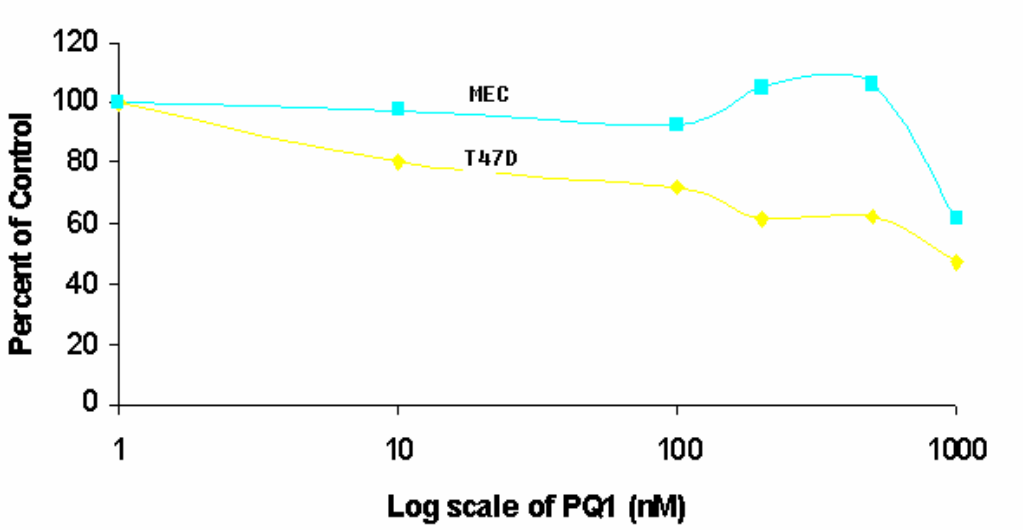

Figure 7 Effect of PQ1 on Cell Viability (data collected from Dr. Thu Annelise Nguyen and Dr. Gunjan Gakhar). T47D and MEC cells were treated with various concentrations of PQ1 for 24 hours. MTT assay was performed with adherent cell cultures using a culture medium free of phenol red and of serum. Solution containing MTT was metabolized by the cells (incubation period 3 hours). After solubilization of the MTT crystals with the solubilization solution MTT, the amount of dye was measured spectrophotometrically at 540 nm.

1.4.4 Effect of PQ1 on the Expression of Connexins

Gap junctions are composed of connexins (Cx). To date, about 20 different connexins have been identified. The nominations are based on the structure and molecular weight; for example, Cx43 is a connexin protein with a molecular weight at about 43 kDa.

Not much research has been done in the study of different functions of connexins. The most common studied connexins are Cx26, Cx32, and Cx43 which are shown to be related to the bioactivities of cancer cells. In most cancer cells, the connexins are well expressed but can not assemble together to form gap junctions. Examination of the changes of connexins on T47D breast cancer cells when treated with PQ1 may provide a pathway to understand the mechanism of the enhancement of gap junction intercellular communications.

The analysis of changes in gap junctional proteins was performed after the treatment of PQ1. Three common connexins, Cx26, Cx32, and Cx43 were checked using western blot analysis. The results indicated that PQ1 had no effect on the expression of these connexins. However, a decrease in phosphorylated Cx43 was observed when T47D cells were treated with 500 nM PQ1. This indicated that PQ1 can cause a direct decrease in phosphorylation of Cx43 without affecting the expression of connexins. The increase of GJIC (Figure 5) was consistent with the decrease of phosphorylation of Cx43 since upregulation of GJIC activity was dependent on the unphosphorylated connexins.

1.4.5 Effect of PQ1 on Active Caspase 3

When treated with PQ1, T47D cells were under apoptotic conditions sincee mitochondrial damage was observed. Thus the effect of PQ1 on apoptosis was evaluated by detecting the active form of caspase 3. A 200 nM PQ1 caused a 1.5-fold increase of active caspase 3 compared to the control. The decrease of caspase 3 at higher concentration was due to the cytotoxic response of the cells. This result indicated that PQ1 can induce apoptosis to T47D cells.

1.4.6 Effect of PQ1 on Tumor Growth in Nu/Nu Mice

The above results demonstrated that PQ1 can enhance the GJIC activities on T47D breast cancer cells and inhibit the cell and colony growth at nM scale. The anti-tumor effect of PQ1was also tested in animal model (Figure 8). Nu/Nu mice were injected with T47D breast cancer cells. After the xenograft tumor grown to a certain size, a 1 µM PQ1 or 10 µM tamoxifen (a known drug used for comparison) was injected directly into the tumor. The three control animals along with a tamoxifen-treated animal were euthanized after day 6 due to the systemic abnormality. The PQ1-treated group demonstrated a decrease in tumor size compared to control, even at day 2. A 70% decrease of tumor growth with PQ1 treatment for only one injection was observed at day 6 compared to control. This indicated that PQ1 is a promising anti-cancer drug for the T47D breast cancer.

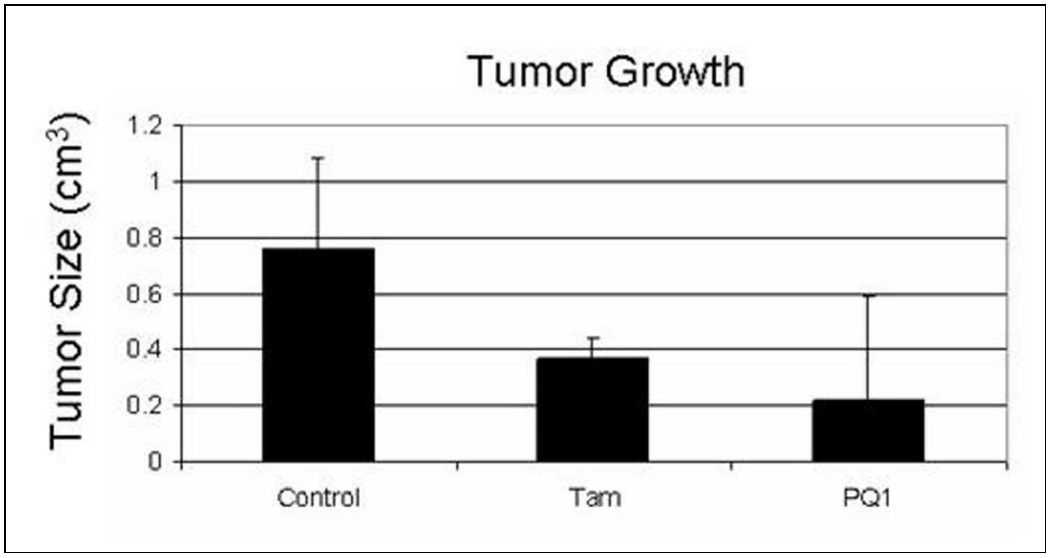

Figure 8 Xenograft Tumor Growths of T47D Cells in Nu/Nu Mice (data collected from Dr. Thu Annelise Nguyen and her student Gunjan Gakhar). Mice was inoculated with 17ßestradiol (1.7 mg/pellet) before the injection of 1 x 10^7 T47D cells subcutaneously into the inguinal region of mammary fat pad. Animals received treatment at 1 µM PQ1 or 10 µM tamoxifen. The results after 6 days of injection show a decrease in tumor growth of PQ1-treated animals compared to control or tamoxifen.

1.4.7 Anti-tumor Effects of PQ analogs

Since the PQ1 demonstrated a promising anti-tumor effect on T47D breast cancer cells, the quinolines **1-7** were tested against T47D cells using trypan blue exclusion assay. Among these compounds, The IC_{50} of quinoline **7** is 15.6 nM (Table 1), even lower than PQ1 which is 119 nM. The study of anti-cancer effects of compound 7 is now carrying on in Dr. Thu Annelise Nguyen's lab.

Compound	**1**	**2**	**3**	**4**	**5**	**6**	**7**
IC_{50} value (nM)	119 ± 21	378 ± 79	1974 ± 404	519 ± 102	1276 ± 246	3732 ± 696	15.6 ± 3.0

Table 1 Cell Viabilities using Trypan Blue Exclusion (data collected from Dr. Thu Annelise Nguyen and her student Gunjan Gakhar). T47D breast cancer cells were treated with various concentrations of **1** – **7** for 2 days. A cell suspension was mixed with trypan blue dye and then visually examined to determine whether cells take up or exclude dye. The numbers of live cells (excluded dye) were quantified and IC_{50} values for each compound were determined.

Retinal ischemia[46-48] is a major cause of vision loss. The apoptotic signals will pass from ischemic cells to adjacent normal cells via gap junction, resulting in the spread of damage.[49] A gap junction inhibitor[50-54] that can block the GJIC may provide a way to prevent further damage during ischemia. PQ1 was sent to Dr. Dolores J. Takemoto and Satyabrata Das to test the effect on gap junction activities on R28 retinal normal cells.

1.4.8 Effect of PQ1 on Retinal R28 Cells

Based on the computational docking[23-35] results, the binding between PQ1 and gap junction hemi channels indicated that the quinoline compounds could be potential gap junction inhibitors. Thus, PQ1 and its analogs were tested for the gap junction activities on normal retinal R28 cells. Lucifer yellow dye transfer experiments were carried out on R28 cells. For the control (Figure 9A top panel), no PQ1 was loaded, which allowed the dye to be transferred far from the loading site to the right suggesting a high level of gap junction intercellular communication. While for PQ1 treatment

(Figure 9A bottom), the dye transfer was much less pronounced due to the inhibition of GJIC. The results (Figure 9) demonstrated that after 10 µM for 40 minutes, PQ1 inhibited the Lucifer yellow dye transfer by 90%, while mefloquine[55, 56] (MQ), a known gap junction inhibitor, at the same dose can only inhibit 60%.

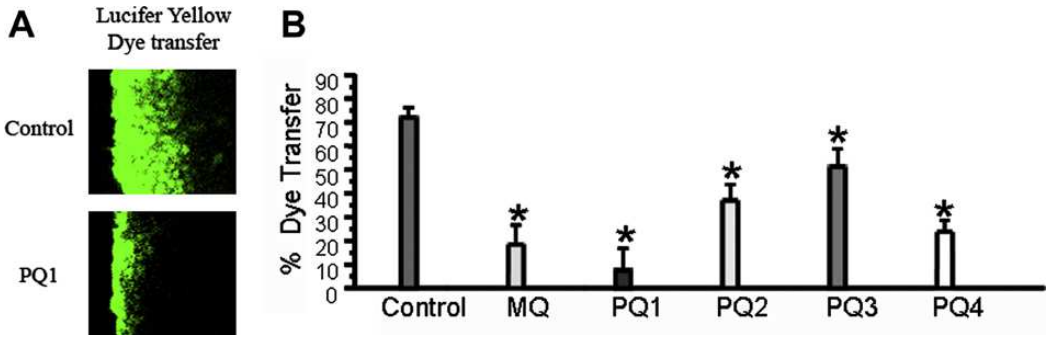

Figure 9 PQ1 inhibition of gap junction dye transfer activity in retinal neurosensory R28 cells in culture (data collected from Dr. Dolores J. Takemoto and Satyabrata Das). R28 cells were grown in 6-well plates with coverslips. When cells reached 90% confluency, gap junction dye transfer activity was performed as described in Materials and methods. (A) The transfer of Lucifer yellow dye in the control and PQ1 treated cells. (B) Bar graph of percentage dye transfer in R28 cells after treatment with the different PQs and Mefloquine (MQ). Application of PQ1 significantly (*) inhibited gap junction activity.

1.4.9 Effect of PQ1 on Protection against Apoptosis

The Lucifer yellow dye transfer experiment indicated that PQ1 can inhibit the GJIC activities on R28 cells. Would the inhibition of GJIC prevent the apoptosis passing from the damaged cells to the adjacent normal cells?

PQ1 was further tested for the protection against apoptosis induced by the treatment of cobalt dichloride. In this experiment, R28 cells were treated with differing dosages of PQ1 and $CoCl_2$. Caspase-3 was examined to indicate the level of apoptosis. Without pre-treatment of PQ1, $CoCl_2$ at 500 µM can activate caspase-3 which indicated the activation[57, 58] of apoptosis. However, pre-incubation of R28 with PQ1 at 10 µM for 40 minutes can block the activation significantly. $CoCl_2$ also caused stabilization of HIF1a that confirmed induction hypoxia. Treatment with PQ1 alone did not cause activation of caspase 3 or stabilization of HIF1a respectively. PQ1,

$CoCl_2$ or a combination of both did not cause any change in the Cx43 gap junction protein levels or phosphorylation, which indicated the PQ1 did not cause the down-regulation of gap junctions.

The result from the apoptosis assay shown in Figure 10 demonstrated that pre-treatment of R28 cells with 10 µM PQ1 for 40 minutes can protect the cells significantly form undergoing apoptosis induced by $CoCl_2$ (Figure 10A), while the treatment of PQ1 alone did not cause serious damage to the cells, even after 36 hours.

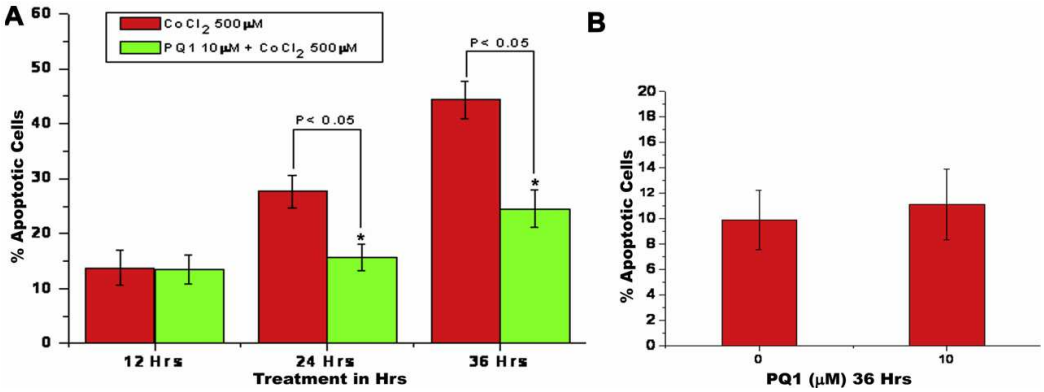

Figure 10 Apoptotis assay using the Annexin V-FITC Kit (data collected from Dr. Dolores J. Takemoto and Satyabrata Das). (A) Representative flow cytometer images of R28 cells with different treatments of PQ1 and/or CoCl2. The y-axis quantifies the number of cells stained with propidium iodine and the x-axis quantifies number of cells stained with Annexin V-FITC. (B,C) Histogram of % apoptotic cells after treatment with CoCl2 and PQ1. The percentage of apoptotic cells represents cells that are Annexin V-FITC positive and both propidium iodide and Annexin V-FITC positive after different time periods.

1.5 Conclusion

PQ1 was synthesized employing a tandem Michael addition followed by an electrophilic aromatic substitution reaction of substituted aniline with vinyl methyl ketone, reduction of the nitro function, and alkylation of the resulting amine moiety. Its analogs were synthesized through a reductive amination of intermidate **16** with a variety of aldehydes.

PQ1 can specifically enhance GJIC activity of T47D cells without affecting the normal MECs. The PQ1 induced apoptosis can spread throughout the gap juctions and consequently cause a decrease in cell viability and colony growth. As the first known compound to enhance GJIC activity in T47D cells, PQ1 can attenuate tumor growth of xenograft tumors in Nu/Nu mice.

Compound **7** (code PQ11) which has an IC_{50} of 15.6 nM against T47D cancer cells, is a promising candidate for further pharmacological studies.

Interestingly, higher concentrations of PQ1 test on normal retinal R28 cells can significantly block the gap junction and prevent the spread of damage.

1.6. References

1. Willecke, K.; Eiberger, J.; Degen, j.; Eckardt, D.; Romualdi, A.; Guldenagel, M.; Deutsch, U.; Sohl, G. Structural and functional diversity of connexin genes in the mouse and human genome. *Biol. Chem.* **2002**, *383*, 725-737.

2. Goodenough, D.A.; Paul, D.A. Beyond the gap: functions of unpaired connexon channels. *Nat. Rev., Mol. Cell Biol.* **2003**,*4*, 285- 294.

3. Lampe, P.D.; Cooper, C.D.; King, T.J.; Burt, J.M. Analysis of Connexin43 phosphorylated at S325, S328 and S330 in normoxic and ischemic heart. *Journal of Cell Science* **2006**, *119*, 3435-3442.

4. Gemel, J.; Lin, X.; Veenstra, R.D.;and Beyer, E.C. N-terminal residues in Cx43 and Cx40 determine physiological properties of gap junction channels, but do not influence heteromeric assembly with each other or with Cx26. *Journal of Cell Science* **2006**, *119*, 2258-2268.

5. Ahmad, S.; Martin, P.E.M; Evans, W.H. Assembly of gap junction channels. *Eur. J. Biochem.* **2001**, *268*, 4544-4552.

6. Falk, M. M. Biosynthesis and structural composition of gap junction intercellular membrane channels. *Eur. J. Cell Biol.* **2000**, *79*, 564-574.

7.Lauf, U.; Giepmans, B.N.G.; Lopez, P.; Braconnot, S.; Chen, S.; Falk, M.M. Dynamic trafficking and delivery of connexons to the plasma membrane and accretion to gap junctions in living cells. *PNAS*, **2002**, *99*, 10446-10451.

8. Bukauskas, F.F.; Verselis, V.K. Gap junction channel gating. *iochimica et Biophysica Acta.***2004**, *1662*, 42-60.

9. Ke, F.; Fang, S.; Lee, M.; Sheu, S.; Lai, S.; Chen, Y.; Huang, F.; Wang, P.S.; Stocco, D.M.; Hwang, J. Lindane, a gap junction blocker, suppresses FSH and transforming growth factor 1-induced connexin43 gap junction formation and steroidogenesis in rat granulosa cells. *Journal of Endocrinology*. **2005**, *184*, 555-566.

10. Chipman, J.K.; Mally, A.; Edwards, G. O. Disruption of Gap Junctions in Toxicity and Carcinogenicity. *Toxicological Sciences.* **2003**, *71*, 146-153.

11. Farahani, R.; Pina-Benabou, H.; Kyrozis, A.; Siddiq, A.; Barradas, P.C.; Chiu, F.C.; Cavalcante, A.; Lai, J.C.; Stanton, P.K.; Rozental, R. Alterations in metabolism and gap junction expression may determine the role of astrocytes as ‘‘good amaritans” or executioners, *Glia*, **2005**, *50*, 351-361.

12. Das, S.; Lin, D.; Jena, S.; Shi, A.; Battina, S.; Hua, D.H.; Allbaugh, R.; Takemoto, D.J. Protection of retinal cells from ischemia by a novel gap junction inhibitor. *Biochemical and Biophysical Research Communications.* **2008**, *373*, 504-508.

13. Leone, S.; Fiore, M.; Lauro, M.G.; Pino, S.; Cornetta, T.; Cozzi, R. Resveratrol and X Rays Affect Gap Junction Intercellular Communications in Human Glioblastoma Cells. *Molecular Carcinogenesis.* **2008**, *47*, 587-598.

14. Jang, M.; Cai, L.; Udeani, G.O.; Slowing, K.V.; Thomas, C.F.; Beecher, C.W.; Fong, H.H.; Farnsworth, N.R.; Kinghorn, A.D.; Mehta, R.G.; Moon, R.C.; Pezzuto, J.M.; Cancer chemopreventive activity of resveratrol, a natural product derived from grapes. *Science.* **1997**, *275*, 218-220.

15. Carystinos, G.D.; Alaoui-Jamali, M.A.; Phipps, J.; Yen, L.; Batist, G. Upregulation of gap junctional intercellular communication and connexin 43 expression by cyclic-AMP and all-trans-retinoic acid is associated with glutathione depletion and chemosensitivity in neuroblastoma cells. *Cancer Chemother Pharmacol*. **2001**, *47*, 126-132.

16. Miyazato, M.; Sugaya, K.; Nishijima, S.; Oda, M.; Ogawa, Y. A gap junction blocker inhibits isolated whole bladder activity in normail rats and rats with partial bladder outlet obstruction. *Biomedical Research.* **2006**, *27*, 203-209.

17. Kawase, M.; Motohashi, N. New multidrug resistance reversal agents. *Curr. Drug Targets*, **2003**, *4*, 31-43.

18. Boyle, R. G.; Travers, S. Hypoxia: targeting the tumor. *Anti-cancer Agents in Med. Chem*. **2006**, *6*, 281-286.

19. Levitt, M. L.; Koty, P. P. Tyrosine kinase inhibitors in preclinical development. *Invest. New Drugs*, **1999**, *17*, 213-226.

20. Fleishman, S. J.; Unger, V. M.; Ben-Tal, N. Transmembrane protein structures without X-rays. *Trends Biochem Sci.* **2006,** *31(2)*, 106-13.

21. Makowski, L.; Caspar, D. L.; Phillips, W. C.; Goodenough, D. A. Gap junction structures. II.Analysis of the x-ray diffraction data. *J Cell Biol*. **1977**, *74(2)*, 629-45.

22. Veenstra, R. D. Gap junction channel structure. *Recent Res. Devel. Biophys*. **2003**, *2*, 65-94.

23. Goodsell, D. S.; Olson, A. J. Automated docking of substrates to proteins by simulated annealing. *Proteins*. **1990**, *8(3)*, 195-202.

24. Morris, G. M.; Goodsell, D. S.; Huey, R. Olson A. J. Distributed automated docking of flexible ligands to proteins: parallel applications of AutoDock 2.4. *J Comput Aided Mol Des.* **1996**, *10(4)*, 293-304.

25. Morris, G. M.; Goodsell, D.S.; Halliday, R. S.; Huey, R.; Hart, W. E.; Belew, R. K.; Olson, A. J. Automated docking using Lamarckian genetic algorithm and an empirical binding free energy function. *J. Comp. Chem.* **1998**, *19*, 1639-1662.

26. LaMontagne, P. M.; Markovac, A.; Khan, S. M. Antimalarials. 13. 5-Alkoxy analogues of 4-methylprimaquine. *J. Med. Chem.* **1982**, *25*, 964-968.

27. Lauer, W. M.; Rondestvedt, C.; Arnold, R. T.; Drake, N. L.; van Hook, J.; Tinker, J. Some derivatives of 8-aminoquinoline. *J. Am. Chem. Soc.* **1946**, *68*, 1546-1548.

28. LaMontagne, P. M.; Blumbergs, P.; Strube, R. E. Antimalarials. 14. 5-(aryloxy)-4-methylprimaquine analogues. A highly effective series of blood and tissue schizonticidal agents. *J. Med. Chem.* **1982**, *25*, 1094-1097.

29. Kawase, M.; Motohashi, N. New multidrug resistance reversal agents. *Curr. Drug Targets*, **2003**, *4*, 31-43.

30. Dade, J.; Provot, O.; Moskowitz, H.; Mayrargue, J.; Prina, E. Synthesis of 2-substituted trifluoromethylquinolines for the evaluation of leishmanicidal activity. *Chem. Pharm. Bull.* 2001, *49*, 480-483.

31. von Dieter Sicker, E. S.; Wilde, H. Ein alternativer zugang zum PQQ-triester. *Helv. Chim. Acta*, **1996**, *79*, 658-662.

32. Kaji, E.; Zen, S. Synthetic reactions of aliphatic nitro compounds. VII. Synthesis of α-amino acids from the nitroacetic ester. *Bull. Chem. Soc. Japan*, **1973**, *46*, 337-338.

33. Butskus, P. F. Cyanoethylation of aromatic amines. *Zhurnal Obshchei Khimii*, **1961**, *31*, 764-767.

34. Klenke, B.; Stewart, M.; Barrett, M. P.; Brun, R.; Gilbert, I. H. Synthesis and biological evaluation of s-triazine substituted polyamines as potential new anti-trypanosomal drugs. *J. Med. Chem*. **2001**, *44*, 3440-3452.

35. McElvain, S. M.; Nelson, J. W. Preparation of orthoesters. *J. Am. Chem. Soc*. **1942**, *64*, 1825-1827.

36. Easson, A. P. T.; Pyman, F. L. Amidines of pharmacological interest. *J. Chem. Soc*. **1931**, 2991-3001.

37. Borch, R. F.; Bernstein, M. D.; Durst, H. D. Cyanohydridoborate anion as a selective reducing agent. *J. Am. Chem. Soc.* **1971**, *93*, 2897-2904.

38. McNab, H. Synthesis of pyrrolo[1,2-c]imidazol-5-one, pyrrolo [1,2-a]imidazol-5-one, and pyrrolo[1,2-b]pyrazol-6-one (three isomeric azapyrrolizinones) by pyrolysis of Meldrum's acid derivatives. *J. Chem. Soc., Perkin Trans. 1: Org. & Bio-Org. Chem*. **1987**, *3*, 653-656.

39. Jemal, A.; Siegel, R.; Ward, E.; Murray, T.; Xu, J.; Thun, M. J. 2007. *Cancer statistics, 2007. CA Cancer J Clin*. **2007**, *57(1)*, 43-66.

40. Saez, C. G.; Velasquez, L.; Montoya, M.; Eugenin, E.; Alvarez, M. G. Increased gap junctional intercellular communication is directly related to the anti-tumor effect of all-trans-retinoic acid plus tamoxifen in a human mammary cancer cell line. *J. Cell. Biochem.* **2003**, *89(3)*, 450-61.

41. Goldberg, G. S.; Martyn, K. D.; Lau, A. F. A connexin 43 antisense vector reduces the ability of normal cells to inhibit the foci formation of transformed cells. *Mol. Carcinog.* **1994**, *11(2)*, 106-14.

42. Zhu, D.; Kidder, G. M.; Caveney, S.; Naus, C. C. Growth retardation in glioma cells cocultured with cells overexpressing a gap junction protein. *Proc. Natl. Acad. Sci. U S A*, **1992**, *89(21)*, 10218-21.

43. Loewenstein, W. R. Junctional intercellular communication and the control of growth. *Biochim. Biophys. Acta.* **1979**, *560(1)*, 1-65.

44. Loewenstein, W. R. Junctional intercellular communication: the cell-to-cell membrane channel. *Physiol. Rev.* **1981**, *61(4)*, 829-913.

45. Yamasaki, H.; Naus, C. C. Role of connexin genes in growth control. *Carcinogenesis*. **1996**, *17(6)*, 1199-213.

46. Osborne, N.N.; Casson, R.J.; Wood, J.P.; Chidlow, G.; Graham, M.; Melena, J. Retinal ischemia: mechanisms of damage and potential therapeutic strategies, Prog. Retin. *Eye Res.* **2004**, *23*, 91-147.

47. Kamphuis, W.; Dijk, F.; Bergen, A.A. Ischemic preconditioning alters the pattern of gene expression changes in response to full retinal ischemia. *Mol. Vis.* **2007**, *13*, 1892-1901.

48. Leker, R. R.; Shohami, E. Cerebral ischemia and trauma-different etiologies yet similar mechanisms: neuroprotective opportunities. *Brain Res. Rev.* **2002**, *39*, 55-73.

49. Farahani, R.; Pina-Benabou, M.H.; Kyrozis, A.; Siddiq, A.; Barradas, P. C.; Chiu, F. C.; Cavalcante, L. A.; Lai, J. C.; Stanton, P. K.; Rozental, R. Alterations in metabolism and gap junction expression may determine the role of astrocytes as ‘‘good samaritans” or executioners. *Glia.* **2005**, *50*, 351-361.

50. Thompson, R. J.; Zhou, N.; MacVicar, B. A. Ischemia opens neuronal gap junction hemichannels. *Science*. **2006**, 312, 924-927.

51. Cusato, K.; Bosco, A.; Rozental, R.; Guimaraes, C. A.; Reese, B. E.; Linden, R.; Spray, D. C. Gap junctions mediate bystander cell death in developing retina. *J. Neurosci.* **2003**, *23*, 6413-6422.

52. Lin, J. H.; Weigel, H.; Cotrina, M. L.; Liu, S.; Bueno, E.; Hansen, A. J.; Hansen, T. W.; Goldman, S.; Nedergaard, M. Gap-junction mediated propagation and amplification of cell injury. *Nat. Neurosci.* **1998**, *1*, 494-500.

53. Neijssen, J.; Herberts, C.; Drijfhout, J. W.; Reits, E.; Janssen, L.; Neefjes, J. Crosspresentation by intercellular peptide transfer through gap junctions. *Nature* **2005**, *434*, 83-88.

54. Giepmans, B. N. Gap junctions and connexin-interacting proteins. *Cardiovasc. Res.* **2004**, *62(2)*, 233-245.

55. Srinivas, M.; Kronengold, J.; Bukauskas, F. F.; Bargiello, T. A.; Verselis, V. K. Correlative studies of gating in Cx46 and Cx50 hemichannels and gap junction channels. *Biophys. J.* **2005**, *88(3)*, 1725-1739.

56. Cruikshank, S.J.; Hopperstad, M.; Younger, M.; Connors, B. W.; Spray, D. C.; Srinivas, M. Potent block of Cx36 and Cx50 gap junction channels by mefloquine. *Proc. Natl. Acad. Sci. USA.* **2004**, *101(33)*, 12364-12369.

57. Guo, M.; Song, L. P.; Jiang, Y.; Liu, W.; Yu, Y.; Chen, G. Q.; Hypoxia-mimetic agents desferrioxamine and cobalt chloride induce leukemic cell apoptosis through different hypoxia-inducible factor-1 a independent mechanisms. *Apoptosis* **2006**, *11*, 67-77.

58. Haraa, A.; Niwab, M.; Aokie, H.; Kumadad, M.; Kunisadae, T.; Oyamaa, T.; Yamamotod, T.; Kozawab, O.; Moria, H. A new model of retinal photoreceptor cell degeneration induced by a chemical hypoxia-mimicking agent, cobalt chloride. *Brain Res.* **2006**, *1109*, 192-200.

1.7 Experimental Section

General procedure: Nuclear magnetic resonance spectra were obtained at 400 MHz and 200MHz for ^{1}H and 100 MHz and 50 MHz for ^{13}C in deuteriochloroform, unless otherwise indicated. Infrared spectra are reported in wavenumbers (cm^{-1}). High-resolution Mass spectra were obtained from Maldi and ESI spectrometers. Maldi spectra were taken using 2,5-dihydroxybenzoic acid as a matrix. ESI spectra were acquired on a LCT Premier (Waters Corp., Milford MA) time of flight mass spectrometer. The instrument was operated at 10,000 resolution (W mode) with dynamic range enhancement that attenuates large intensity signals. The cone voltage was 60eV. Spectra were acquired at 16666 Hz pusher frequency covering the mass range 100 to 1200 u and accumulating data for 2 seconds per cycle. Mass correction for exact mass determinations was made automatically with the lock mass feature in the MassLynx data system. A reference compound in an auxiliary sprayer is sampled every third cycle by toggling a "shutter" between the analysis and reference needles. The reference mass is used for a linear mass correction of the analytical cycles. Samples are presented in Methanol plus 0.1% formic acid as a 20ul loop injection using an auto injector (LC PAL, CTC Analytics AG, Zwingen, Switzerland). 4-Acetaminoanisole, vinyl methyl ketone, 3-(trifluoromethyl)phenol, and arsenic acid were obtained from Aldrich Chemical Co. 4-Hydroxymethylimidazole, thiophene-2-carboxaldehyde and 2-furaldehyde were purchased from Acros. Potassium *t*-butoxide was prepared by treating *t*-butanol with potassium metal at 85^{o}C followed by evaporating excess of *t*-butanol under vacuum. 2-Bromo-4-acetamino anisole (**9**) and 2-bromo-4-acetamino-5-nitroanisole (**10**) were prepared by following the reported procedures.[19]

N-(4-methoxyphenyl)acetamide(8)

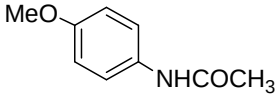

8

To a solution of 5 g (40.6mmol) of p-anisidine in 50 ml of water, 5.2 g (50.75 mmol) of acetic anhydride was added at 80 ^{o}C. The mixture was stirred at 80 ^{o}C for 20 min, then cooled down to room temperature and stirred for additional 1 hour. Crude product precipitated out as a white solid. The solid was filtered and washed with water, dried under vacuum to give 5.4 g (80.5%) of compound **8**: ^{1}H NMR ($CDCl_3$, 200MHz) δ 2.15 (s, 3H, CH_3), 3.79 (s, 3H, OCH_3), 6.84 (d, J=8.8Hz, 2H), 7.37 (d, J=9.1Hz, 2H); ^{13}C NMR δ 24.17, 55.52, 114.10 (2C), 122.25 (2C), 131.34, 156.43, 169.06.

2-Bromo-4-acetaminoanisole (9)

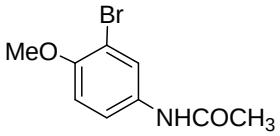

9

To a solution of 10 g (60.5 mmol) of N-(4-methoxyphenyl)acetamide (**8**) in 50 ml of glacial acetic acid, 11.6 g (72.7 mmol) of bromine was added slowly. Temperature was maintained below 50 ^{o}C while adding. The mixture was stirred at room temperature for 1 hour, poured into 400 ml of ice water with 1.2 g of sodium bisulfite, stirred until color discharged. The precipitated solid was filtered out and recrystallized from 25% ethanol in water to give 10.19 g (69%) of compound **9**: ^{1}H NMR ($CDCl_3$, 200MHz) δ 2.16 (s, 3H, CH_3), 3.87 (s, 3H, OMe), 6.83 (d, J=8.8Hz, 1H), 7.41 (d-d, J=2.5Hz, 1H), 7.67 (d, J=2.6Hz, 1H); ^{13}C NMR δ 24.11, 56.48, 111.25, 111.94, 121.05, 125.95, 132.02, 152.72, 169.47.

2-bromo-4-acetamino-5-nitroanisole (10)

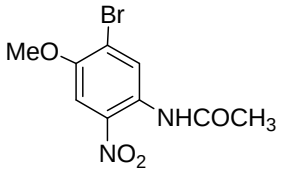

10

To a solution of 12.3 g (50.4 mmol) of 2-Bromo-4-acetaminoanisole (**9**) in 20 ml of acetic anhydride and 40 ml of acetic acid at 5 °C, 3.51 ml (54 mmol) of concentrated nitric acid was added dropwise while maintaining the temperature below 5 °C. The mixture was stirred at 5 °C for 3 hours, poured into 200 ml of ice water. The yellow precipitate was filtered out and washed with cold water, dried under vacuum to give 12 g (82.3%) of compound **10**: ^{1}H NMR($CDCl_3$, 200MHz) δ 2.28 (s, 3H, CH_3), 3.95 (s, 3H, OCH_3), 7.67 (s, 1H), 9.09 (s, 1H).

Potassium 3-(trifluoromethyl)phenoxide(11)

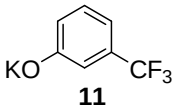

11

A mixture of 1.94 g (12 mmol) of 3-(trifluoromethyl) phenol and 1.344 g (12 mmol) of potassium *t*-butoxide was stirred at room temperature under argon for 30 min. A solution was resulted, and the by-product, *t*-butanol, was removed under vacuum and heat to give 2.40 g (100% yield) of **11** as a brown oil.

4-Acetamino-5-nitro-2-(3-trifluoromethylphenyloxy) anisole (12).

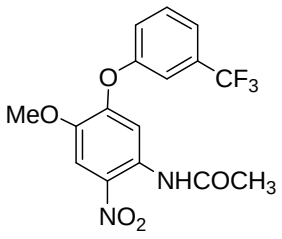

12

To 2.4 g (12 mmol) of compound **11** under argon, was added a solution of 3.0 g (10.4 mmol) of bromide **10** in 20 mL of DMF via cannula. The resulting solution was

stirred at 120 ^{o}C for 1 day. Thin layer chromatography indicated the reaction was not completed. The reaction solution was cooled to 25 ^{o}C and an additional of 2 mmol of **11** was added. The solution was stirred at 120 ^{o}C for additional 12 hours, then poured into 200 mL of ice water, and the solid was collected by filtration, washed with water, dried under vacuum, and crystallized from ethanol twice to give 3.04 g (79% yield) of compound **12** as a yellow solid.[20] ^{1}H NMR($CDCl_3$, 200MHz) δ 10.4 (s, 1 H, NH), 8.39 (s, 1 H), 7.83 (s, 1 H), 7.5 (m, 2 H), 7.3 (m, 2 H), 3.93 (s, 3 H, OMe), 2.23 (s, 3 H, CH_3); ^{13}C NMR δ 186.2, 155.7, 153.9, 142.4, 141.5, 133.0 (q, J = 30 Hz, C-CF_3), 130.9, 125.1 (q, J = 260 Hz, CF_3), 123.0, 121.7, 116.8, 116.7, 108.7, 106.6, 56.7, 21.8.

4-Amino-5-nitro-2-(3-trifluoromethylphenyloxy) anisole (13).

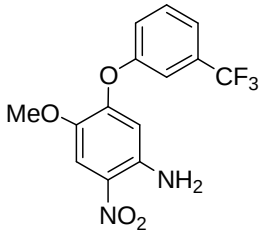

13

To a solution of 2.0 g (5.3 mmol) of compound **12** in 30 mL of ethanol under argon was added 4 mL of concentrate HCl. The reaction was heated up to reflux for 2 hours. The color turned from yellow to red. The solution was cooled to room temperature, poured into 200 mL of ice and water. The precipitate was collected by filtration, then washed with water twice and crystallized from ethanol to give 1.69 g (95% yield) of **13** as an orange solid.[20] ^{1}H NMR($CDCl_3$, 200MHz) δ 7.70 (s, 1 H), 7.5 (m, 2 H), 7.32 (m, 1 H), 7.20 (m, 2 H), 6.15 (s, 1 H), 3.87 (s, 3 H, OMe); ^{13}C NMR δ 155.6, 153.9, 142.3, 141.6, 132.8 (q, J = 33 Hz, C-CF_3), 130.9, 127.1, 123.7 (q, J = 272 Hz, CF_3), 123.1, 121.8, 116.8, 108.5, 106.5, 56.6.

6-Methoxy-4-methyl-8-nitro-5-(3-trifluoromethylphenyloxy)quinoline (14) and 4-{N-[4-methoxy-2-nitro-5-(trifluoromethylphenyloxy)] phenylamino}2-butanone (15).

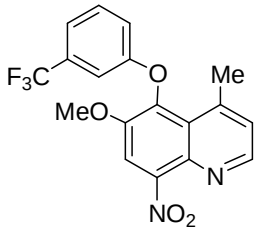

14

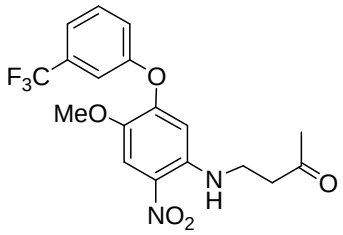

15

To a mixture of 2.0 g (6.0 mmol) of compound **13** and 1.7 g (12 mmol) of H_3AsO_4, was added 15 mL of 85% H_3PO_4. The mixture was stirred and heated to 100 ^oC, and 0.7 mL (9.0 mmol) of vinyl methyl ketone was added dropwise via a syringe. The solid compound **13** dissolved and a dark red solution was resulted. After stirring at 100 ^oC for 20 min, the reaction solution was cooled to room temperature, poured into 200 ml ice and water. The pH was adjusted to 10 by 6 M NaOH solution, and the solid precipitate was extracted by dichloromethane three times. The combined extract was washed with brine, dried ($MgSO_4$), and concentrated to give a red crude product. The combined material was column chromatographed on silica gel using a gradient mixture of hexane, diethyl ether, and dichloromethane as eluants to give 0.58 g (25% yield) of quinoline **14**, 1.21 g (50% yield) of compound **15**, and 0.50 g (25% recovery) of **13**.

Compound **14**: ^1H NMR ($CDCl_3$, 400MHz) δ 8.78 (d, *J* = 4 Hz, 1 H), 7.88 (s, 1 H), 7.40 (m, 2 H), 7.27 (m, 1 H), 7.11 (s, 1 H), 6.93 (d, *J* = 7 Hz, 1 H), 3.87 (s, 3 H, OMe), 2.74 (s, 3 H, Me); ^{13}C NMR ($CDCl_3$, 400MHz) δ 158.0, 151.0, 148.3, 146.9, 143.8, 139.9, 136.3, 132.6 (q, *J* = 30 Hz, C-CF_3), 130.6, 126.5, 126.0, 123.2 (q, *J* = 270 Hz, CF_3), 119.5, 118.3, 112.5, 111.8, 57.3, 23.4.

Compound **15**: ^1H NMR ($CDCl_3$, 400MHz) δ 8.18 (s, 1 H), 7.78 (s, 1 H), 7.50 (m, 2 H), 7.30 (m, 2 H), 6.32 (s, 1 H), 3.87 (s, 3 H, OMe), 3.40 (t, *J* = 7 Hz, 2 H), 2.75 (t, *J* = 7 Hz, 2 H), 2.17 (s, 3 H, Me). ^{13}C NMR ($CDCl_3$, 400MHz) δ 206.1, 156.2, 153.8, 142.5, 141.6, 132.5 (q, *J* = 30 Hz, C-CF_3), 130.8, 127.2, 123.7 (q, *J* = 280 Hz, CF_3), 122.2, 121.2, 115.9, 109.8, 103.0, 56.6, 42.5, 37.7, 30.4. Anal. Calcd for

$C_{18}H_{17}F_3N_2O_5$: C, 54.27; H, 4.30. Found: C, 54.02; H, 4.53.

Cyclization of compound 15 to quinoline 14.

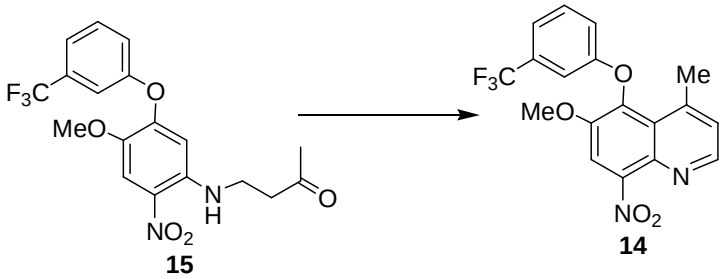

To a hot (100 ^oC) solution of 0.11 g (0.75 mmol) of H_3AsO_4 in 1 mL of 85% H_3PO_4, was added 0.15 g (0.38 mmol) of ketone **15**. The mixture was stirred at 100 ^oC for 20 min., cooled to room temperature, diluted with aqueous NH_4OH and NaOH to pH ~12, and extracted with ethyl acetate three times. The organic layer was washed with water and brine, dried ($MgSO_4$), concentrated, and column chromatographed on silica gel using a gradient mixture of hexane, dichloromethane, and diethyl ether as eluants to give 33 mg (23% yield) of **14**, 57 mg (46% yield) of **13**, and 35 mg (23% recovery) of **15**.

8-Amino-6-methoxy-4-methyl-5-(3-trifluoromethylphenyloxy) quinoline (16).

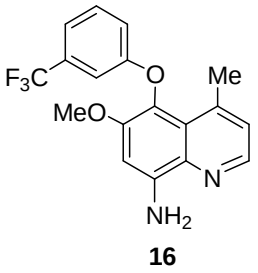

To a solution of 1 g (2.65 mmol) of **14** in 0.5 mL of acetic acid and 10 mL of water, 0.95 g (17.0 mmol) of iron was added at room temperature. The mixture was stirred at 100^oC for 2 h, cooled to room temperature, and extracted with dichoromethane three times. The combined extract was washed with aqueous $NaHCO_3$, and brine, dried ($MgSO_4$), concentrated, and column chromatographed on silica gel using a gradient mixture of hexane, dichloromethane, and diethyl ether as eluents to give 0.78 g (85%

yield) of **16**.[22] ^{1}H NMR ($CDCl_3$, 400MHz)δ 8.46 (d, *J* = 4 Hz, 1 H), 7.34 (t, *J* = 8 Hz, 1 H), 7.22 (d, *J* = 8 Hz, 1 H), 7.15 (m, 2 H), 6.93 (d, *J* = 8 Hz, 1 H), 6.79 (s, 1 H), 5.15 (bs, 2 H, NH_2), 3.80 (s, 3 H, OMe), 2.63 (s, 3 H, Me); ^{13}C NMR ($CDCl_3$, 400MHz) δ 159.7, 150.5, 145.6, 143.7, 142.8, 141.5, 137.7, 134.0, 132.0 (q, *J* = 30 Hz, C-CF_3), 130.2, 125.1, 124.6, 123.1 (q, *J* = 270 Hz, CF_3), 118.3, 112.1, 97.9, 56.6, 23.3.

6-Methoxy-8-(3-phthalimidopropylamino)-4-methyl-5-(3-trifluoromethylphenyloxy)-quinoline (18).

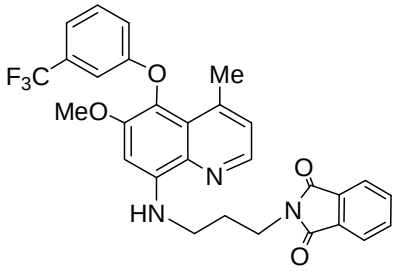

18

A solution of 1.0 g (2.86 mmol) of **16**, 0.9 g (2.9 mmol) of 3-iodopropylphthalimide (**17**) and 0.22 g (2.6 mmol) of $NaHCO_3$ in 10 mL of DMF was stirred under argon at 80°C for 48 h. The reaction mixture was cooled to 25°C, diluted with 100 mL of water, and extracted four times with ethyl acetate. The combined extract was washed with brine, dried ($MgSO_4$), concentrated, and column chromatographed on silica gel using a gradient mixture of ethyl acetate and methanol as eluants to give 0.37 g (72% yield based on reacted **16**) of compound **18** and 0.69 g (77% recovery) of **16**. Compound **18**: ^{1}H NMR ($CDCl_3$, 400MHz) δ 8.37 (d, *J* = 4 Hz, 1 H), 7.85 (m, 2 H), 7.73 (m, 2 H), 7.34 (t, *J* = 7 Hz, 1 H), 7.23 (d, *J* = 7 Hz, 1 H), 7.05 (m, 2 H), 6.92 (d, *J* = 7 Hz, 1 H), 6.54 (bs, 1 H, NH), 6.45 (s, 1 H), 3.92 (t, *J* = 7 Hz, 2 H), 3.82 (s, 3 H, OMe), 3.44 (q, *J* = 7 Hz, 2 H), 2.60 (s, 3 H, Me), 2.20 (pent, *J* = 7 Hz, 2 H); ^{13}C NMR ($CDCl_3$, 400MHz) δ 168.7, 159.9, 151.0, 145.0, 144.4, 142.6, 134.4, 134.2, 133.9, 132.3, 130.2 (q, *J* = 30 Hz, C-CF_3), 125.8, 125.2, 124.1 (q, *J* = 260 Hz, CF_3), 123.5, 123.3, 118.3, 118.1, 112.3, 92.9, 56.8, 41.2, 36.2, 28.2, 23.3. Anal. Calcd for $C_{29}H_{24}F_3N_3O_4$: C, 65.04; H, 4.52. Found: C, 64.95; H, 4.71.

6-Methoxy-8-[(3-aminopropyl)amino]-4-methyl-5-(3-trifluoromethylphenyloxy)quinoline (1).

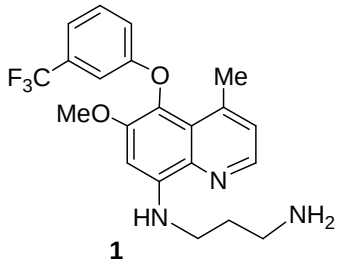

1

A solution of 0.35 g (0.65 mmol) of phthalimide **18** in 10 mL of 65% hydrazine and 10 mL of ethanol was refluxed under argon for 3 hours. After cooling the solution to 25^{o}C, it was diluted with 10% aqueous KOH solution and extracted with dichloromethane three times. The combined extract was washed with brine, dried (K_2CO_3), concentrated, and column chromatographed on silica gel using a gradient mixture of dichloromethane and methanol as eluants to give 0.21 g (80% yield) of **1** ^{1}H NMR ($CDCl_3$, 400MHz) δ 8.40 (d, *J* = 4 Hz, 1 H), 7.34 (t, *J* = 8 Hz, 1 H), 7.21 (d, *J* = 8 Hz, 1 H), 7.06 (m, 2 H), 6.93 (d, *J* = 8 Hz, 1 H), 6.48 (s, 1 H), 6.4 (bs, 1 H, NH), 3.83 (s, 3 H, OMe), 3.42 (t, *J* = 8 Hz, 2 H), 2.99 (t, *J* = 8 Hz, 2 H), 2.62 (s, 3 H, Me), 1.98 (pent, *J* = 8 Hz, 2 H), 1.80 (bs, 2 H, NH_2); ^{13}C NMR ($CDCl_3$, 400MHz) δ 160.0, 151.1, 145.0, 143.5, 142.7, 132.2 (q, *J* = 30 Hz, C-CF_3), 130.2, 125.2, 123.1 (q, *J* = 270 Hz, CF_3), 118.4, 118.2, 112.2, 107.5, 92.9, 56.8, 41.6, 40.4, 33.1, 23.4. Anal. Calcd for $C_{21}H_{22}F_3N_3O_2$: C, 62.21; H, 5.47. Found: C, 62.07; H, 5.62. The succinic acid salt was prepared by treating 0.457 g (1.12 mmol) of the quinoline with 0.134 g (1.13 mmol) of succinic acid in 5 ml of methanol. The resulting solution was diluted with 50 ml of water and lyophilized to give a quantitative yield of the succinic acid salt of **1**.

6-Methoxy-8-[(2-cyanoethyl)amino]-4-methyl-5-(3-trifluoromethylphenyloxy)quinoline (2).

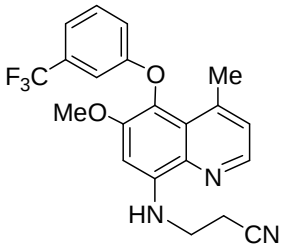

2

A solution of 0.57 g (1.6 mmol) of amine **16** and 86 mg (1.6 mmol) of acrylonitrile in 2 mL of phenol was heated in a sealed tube at 100°C for 2 days. The mixture was cooled to 25°C, diluted with dichloromethane, washed with 1 N NaOH, water, and brine, dried ($MgSO_4$), concentrated and column chromatographed on silica gel using a mixture of hexane:CH_2Cl_2:diethyl ether (4:4:1) to give 0.20 g (50% yield) of compound **2** and 0.11 g (20% recovery) of **16**. Compound **2**: ^{1}H NMR ($CDCl_3$, 400MHz) δ 8.43 (d, *J* = 4 Hz, 1 H), 7.36 (t, *J* = 8 Hz, 1 H), 7.23 (d, *J* = 8 Hz, 1 H), 7.08 (m, 2 H), 6.94 (d, *J* = 8 Hz, 1 H), 6.71 (t, *J* = 7 Hz, 1 H), 6.52 (s, 1 H, NH), 3.85 (s, 3 H, OMe), 3.78 (q, *J* = 7 Hz, 2 H), 2.82 (t, *J* = 7 Hz, 2 H), 2.63 (s, 3 H, Me); ^{13}C NMR ($CDCl_3$, 400MHz) δ 159.7, 150.8, 145.5, 143.1, 143.0, 134.0 132.3 (q, *J* = 30 Hz, C-CF_3), 132.0, 131.7, 130.3, 127.0, 125.5, 124.7, 122.9 (q, *J* = 270 Hz, CF_3), 118.3, 112.2, 93.6, 57.1, 39.8, 23.3, 18.4; HRMS calcd for $C_{21}H_{19}F_3N_3O_2$ ($M+H^+$) 402.1429, found 402.1422.

Ethyl 3-{8-[6-Methoxy-4-methyl-5-(3-trifluoromethylphenyloxy) quinolinyl]amino}-propanoimidate (3).

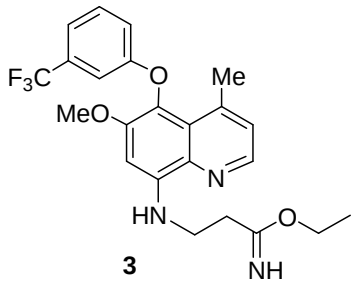

3

To a cold (0°C) solution of 0.16 g (0.41 mmol) of cyanide **2** in 3 mL of ethanol and 3 mL of benzene, hydrogen chloride gas was introduced for 5 min. The gas inlet was removed and the reaction vessel was sealed and stirred at 25°C for 3 days. The solvent was removed under vacuum and the crude product was column chromatographed using a mixture of hexane:CH_2Cl_2:diethyl ether (4:4:1) as an eluant to give 0.12 g (69% yield) of compound **3**: ^{1}H NMR ($CDCl_3$, 400MHz) δ 8.41 (d, *J* = 4 Hz, 1 H), 7.34 (t, *J* = 8 Hz, 1 H), 7.22 (d, *J* = 8 Hz, 1 H), 7.08 (m, 2 H), 6.93 (d, *J* = 8 Hz, 1 H), 6.59 (bs, 1 H, NH), 6.54 (s, 1 H), 4.20 (q, *J* = 7 Hz, 2 H), 3.84 (s, 3 H, OMe), 3.69 (t, *J* = 7 Hz, 2 H), 2.80 (t, *J* = 7 Hz, 2 H), 2.62 (s, 3 H, Me), 1.29 (t, *J* = 7 Hz, 3 H); ^{13}C NMR ($CDCl_3$, 400MHz) δ 172.3, 159.9, 151.0, 145.5, 145.1, 144.2, 142.8, 134.0, 132.0 (q, *J* = 30 Hz, C-CF_3), 130.2, 126.1, 125.3, 124.6, 124.0 (q, *J* = 270 Hz, CF_3), 118.4, 112.3, 93.3, 61.0, 56.9, 39.4, 34.4, 23.3, 14.4; HRMS calcd for $C_{23}H_{26}F_3N_3O_3$ ($M+2^+$) 449.1926, found 449.1687. Anal. Calcd for $C_{23}H_{24}F_3N_3O_3$: C, 61.74; H, 5.41. Found: C, 61.65; H, 5.49.

Ethyl 3-{8-[6-Methoxy-4-methyl-5-(3-trifluoromethylphenyloxy) quinolinyl]amino}-propionamidine (4).

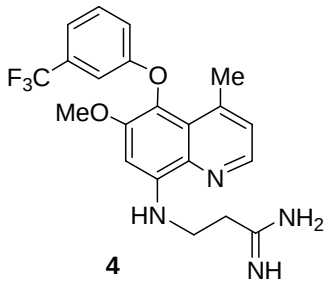

4

To a solution of 40 mg (0.09 mmol) of imidate **3** in 2 mL of ethanol, ammonia gas was introduced for 5 min. The reaction vessel was sealed and stirred at 50°C for 6 h. After removal of ethanol, the crude product was column chromatographed on silica gel using a gradient mixture of hexane, dichloromethane, diethyl ether and methanol as eluants to give 21 mg (57% yield) of amidine **4** and 5 mg (13% recovery) of imidate **3**. Compound **4**: ^{1}H NMR ($CDCl_3$, 400MHz) δ 8.41 (d, *J* = 4 Hz, 1 H), 7.35 (t, *J* = 8 Hz, 1 H), 7.23 (d, *J* = 8 Hz, 1 H), 7.08 (m, 2 H), 6.94 (d, *J* = 8 Hz, 1 H), 6.60 (s, 1 H), 6.55 (bs, 1 H), 5.69 (bs, 1 H, NH), 5.40 (bs, 1 H, NH), 3.84 (s, 3 H, OMe), 3.73 (q, *J* = 7 Hz, 2 H), 2.72 (t, *J* = 7 Hz, 2 H), 2.62 (s, 3 H, Me); ^{13}C NMR ($CDCl_3$, 400MHz) δ 173.6, 159.8, 151.0, 145.2, 144.2, 142.9, 134.0, 131.8 (q, *J* = 30 Hz, C-CF_3), 130.2, 126.3, 125.7, 125.3, 124.6, 124.5 (q, *J* = 270 Hz, CF_3), 118.4, 112.2, 93.7, 56.9, 39.8, 30.5, 23.4; Anal. Calcd for $C_{21}H_{21}F_3N_4O_2$: C, 60.28; H, 5.06. Found: C, 61.01; H, 5.27.

6-Methoxy-8-[(4-imidazolylmethyl)amino]-4-methyl-5-(3-trifluoromethylphenyloxy)-quinoline (5).

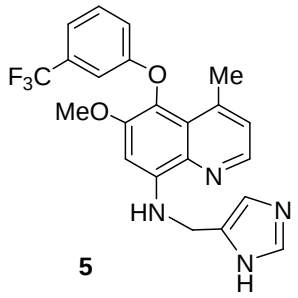

5

The following procedure serves as a general procedure for the reductive amination reaction.

A solution of 0.18 g (0.51 mmol) of quinoline **16** and 55 mg (0.57 mmol) of aldehyde **9**[28] in 5 mL of methanol was stirred at 25°C under argon for 1 h. To it, 10 mg of acetic acid was added, and the solution was stirred for 1 h, and 96 mg (1.5 mmol) of sodium cyanoborohydride was added. After stirring for 3 h, the solution was diluted with aqueous NH_4Cl and extracted with dichloromethane twice. The combined extract was washed with brine, dried ($MgSO_4$), concentrated, and column chromatographed using a gradient mixture of hexane, ethyl acetate, and methanol as eluants to give 0.18 g (79% yield) of compound **1.5** and 14 mg (8% recovery) of compound **16**. Compound **5**: ^{1}H NMR ($CDCl_3$, 400MHz) δ 8.41 (d, *J* = 4 Hz, 1 H), 7.66 (s, 1 H), 7.33 (t, *J* = 8 Hz, 1 H), 7.22 (d, *J* = 8 Hz, 1 H), 7.08 (m, 3 H), 6.92 (d, *J* = 8 Hz, 1 H), 6.78 (bs, 1 H, NH), 6.60 (s, 1 H), 4.60 (s, 2 H), 3.78 (s, 3 H, OMe), 2.62 (s, 3 H, Me); ^{13}C NMR ($CDCl_3$, 400MHz) δ 159.9, 151.0, 145.1, 144.4, 142.8, 135.2, 134.0, 132.3 (q, *J* = 30 Hz, C-CF_3), 130.2, 126.2, 125.2, 124.5, 124.2 (q, *J* = 270 Hz, CF_3), 118.2, 116.3, 112.3, 95.3, 93.9, 56.8, 41.5, 23.3; HRMS calcd for $C_{22}H_{20}F_3N_4O_2$ ($M+H^+$) 429.1538, found 429.1521.

6-Methoxy-8-[(2-thiophenylmethyl)amino]-4-methyl-5-(3-trifluoromethylphenyloxy)-quinoline (6).

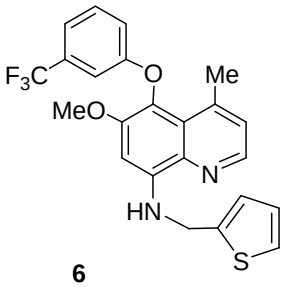

6

A similar procedure as that described above was carried out using 0.12 g (0.34 mmol) of quinoline **16** and 42 mg (0.38 mmol) of 2-thiophenecarboxaldehyde to give 72 mg (47% yield) of quinoline **6** and 43 mg (36% recovery) of starting material **16** after column chromatographic purification. Compound **6**: ^{1}H NMR ($CDCl_3$, 400MHz) δ 8.41 (d, *J* = 4 Hz, 1 H), 7.33 (t, *J* = 8 Hz, 1 H), 7.21 (m, 2 H), 7.09 (m, 3 H), 6.99 (d, *J* = 8 Hz, 1 H), 6.92 (d, *J* = 8 Hz, 1 H), 6.85 (bs, 1 H, NH), 6.58 (s, 1 H), 4.75 (s, 2 H), 3.77 (s, 3 H, OMe), 2.62 (s, 3 H, Me); ^{13}C NMR ($CDCl_3$, 400MHz) δ 159.8, 150.9, 145.2, 144.0, 142.9, 142.6, 134.0, 132.3 (q, *J* = 30 Hz, C-CF_3), 130.2, 127.1, 126.4, 125.5, 125.2, 124.9, 124.5, 124.2 (q, *J* = 280 Hz, CF_3), 118.3, 118.2, 112.3, 94.0, 56.7, 43.3, 23.3; HRMS calcd for $C_{23}H_{20}F_3N_2O_2S$ ($M+H^+$) 445.1197, found 445.1183.

6-Methoxy-8-[(2-furanylmethyl)amino]-4-methyl-5-(3-trifluoromethylphenyloxy)-quinoline (7).

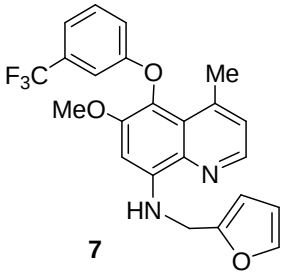

7

A similar procedure as that described above was carried out using 0.17 g (0.47 mmol)

of quinoline **16** and 50 mg (0.52 mmol) of 2-furancarboxaldehyde to give 0.11 g (52% yield) of quinoline **7** and 20 mg (12% recovery) of starting material **16** after column chromatographic purification. Compound **7**: ^{1}H NMR ($CDCl_3$, 400MHz) δ 8.41 (d, *J* = 4 Hz, 1 H), 7.41 (s, 1 H), 7.33 (t, *J* = 8 Hz, 1 H), 7.21 (d, *J* = 8 Hz, 1 H), 7.09 (m, 2 H), 6.92 (d, *J* = 8 Hz, 1 H), 6.76 (bt, *J* = 5 Hz, 1 H, NH), 6.60 (s, 1 H), 6.35 (m, 2 H), 4.56 (d, *J* = 5 Hz, 2 H), 3.80 (s, 3 H, OMe), 2.62 (s, 3 H, Me); ^{13}C NMR ($CDCl_3$, 400MHz) δ 159.9, 152.5, 150.9, 145.2, 144.1, 142.8, 142.3, 134.1, 132.2 (q, *J* = 30 Hz, C-CF_3), 130.2, 126.4, 125.2, 124.5, 124.1 (q, *J* = 280 Hz, CF_3), 118.4, 118.2, 112.3, 110.6, 107.5, 93.8, 56.8, 41.3, 23.3; HRMS calcd for $C_{23}H_{20}F_3N_2O_3$ ($M+H^+$) 429.1426, found 429.1532.

CHAPTER 2-Synthesis and Bioactivities of Nanogels

2.1 Introduction

In the current field of medical research, one problem that need to be addressed is the discovery of a proper drug carrier.[1-2] Most of the drugs are small organic compounds that are not soluble in aqueous media. Since the development of nanotechnology, nanopaticles have been widely studied as one of the possible systems that can control the release of many small molecules.[3-6] Micelles,[7] immunoliposomes,[8] liposomes,[9,10] lipoplexes,[11] and cell-pentrating peptiedes[12] have been reported for the intra-cytoplasmic drug delivery. Polymeric nanogels based on Poly Ethylene Glycol (PEG) has more recently emerged as a promising system for the drug delivery[5, 13-15] due to the biocompatibility and high solubility in aqueous media. Poly Ethylene imine (PEI) combined with PEG has been reported to be utilized as a nonviral gene delivery material. The PEI can be crosslinked with PEG to form a more stable nanogel which is water soluble and less toxic[6, 16-18] compared to PEI alone.[13, 17-20]

Specification is currently another problem in the realms of drug delivery. The delivery of the drug directly into the tumor to reduce the dosage and minimize the side effects of the drugs is currently a challenging endeavor. Recently, research on stem cells demonstrated that umbilical cord matrix stem cells (UCMS) can engraft near or even within the tumors when administered to tumor-bearing mice.[21] This indicated that UCMS may severe as a potential delivery vehicles to carry and release the nanogels into tumors

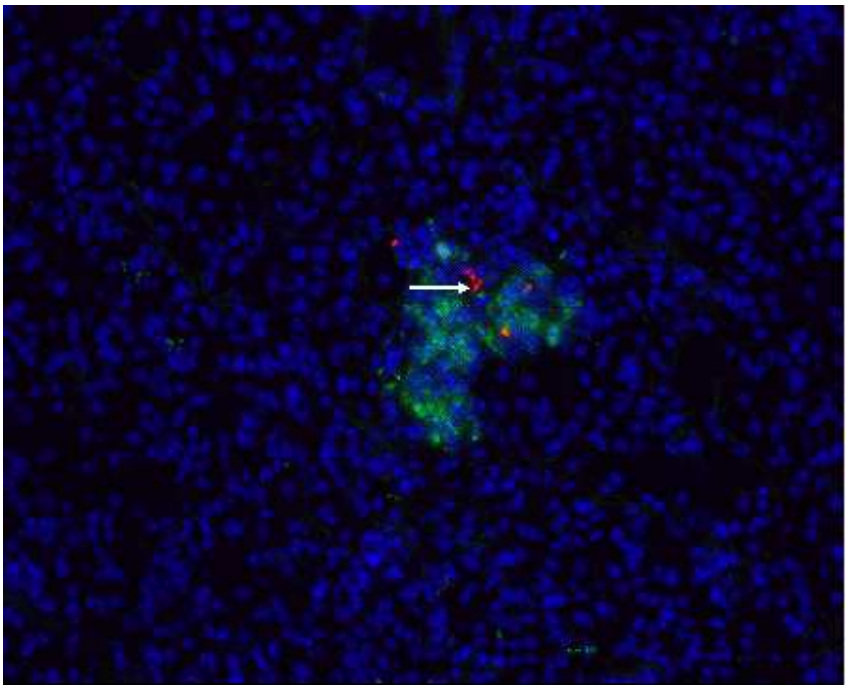

Figure 11 Dye-loaded UCMS cells (red cells) were detected in small breast tumor (green) but not in the surrounding normal lung tissue (blue).

In this study, we synthesized three types of nanogels and encapsulated them with different anticancer drugs. These nanogels were internalized into the stem cells and subsequently evaluated to determing their abilities in releasing drugs to the cancer cells. All the bioactivities were evaluated by Dr. Chanran Ganta and Dr. Rajashekar Rachakatla in Dr. Deryl Troyer's lab.

2.2 Tpye I Nanogel

The PEI bought from Aldrich was purified by a Sephacryl S200 chromatograph column to obtain PEI with a much more uniformed molecular weight.[6] The medium fractions were collected and used for the synthesis of nanogel.

2.2.1 Synthesis of Toxic PEG-PEI Nanogel

Initially, the nanogel was prepared by following the reported procedure[6] with a few modifications. Poly ethylene glycol (PEG) has been widely utilized in recent cancer research due to its water solubility and bio-compatibility. PEG can also be functionalized on the hydroxyl groups. The activation of PEG was achieved by treatment with 1, 1'-carbonyldiimidazole in distilled dry acetonitrile at 40^{o}C for 2 hours. The resulting light yellow solution was dialyzed twice with 800 ml of 10% ethanol in deionized water at 4 ^{o}C for 4 hours using a membrane with a molecular weight cut off (MWCO) of 3500 Dalton. It is very crucial to keep the temperature low at 4 ^{o}C since higher temperature would result in the hydrolysis of the activated PEG. The desired product was lyophilized immediately to give a white solid.

To make the nanogel, 1 g of purified PEI (MW around 25 KDa) was dissolved in 300 ml deionized water, and a solution of 1 g of activated PEG in 5 ml dichloromethane was then added drop wise to the PEI solution at room temperature. A white suspension was resulted due to the heterogeneous solvent system which was sonicated for 15 minutes. The organic solvent dichloromethane was removed on a rotary evaporator to afford a transparent solution which was subsequently dialyzed with 1000 ml 10% ethanol in deionized water at room temperature using a membrane with molecular weight cut off (MWCO) of 12 KDa-14 KDa. Since the activated PEG was around 8 KDa, the activated PEG was successfully separated from the nanogel. Lyophlization of the resulting solution afforded the desired nanogel as a white light powder.

Based on the method we used for the synthesis, the structure of the nanogel was tenatively proposed and is shown in Scheme 7. This proposed structure has not yet been confirmed.

Scheme 7 Synthesis of PEG-PEI Nanogel (**26**)

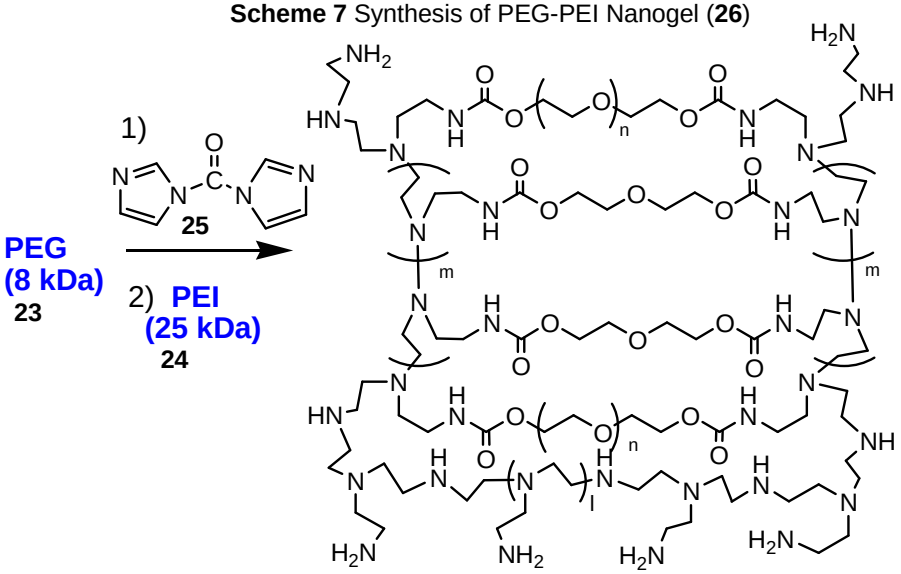

Nanogel NG-PEG-PEI
26

As a drug carrier, the nanogel should be nontoxic to stem cells. However, after being evaluated on the cell line, the naogel prepared above was toxic to the cells. The proton NMR spectrum of nanogel revealed a ratio of 1:4 for the CH_2N:CH_2O (methylene protons) respectively. We anticipated that the ratio of the PEG to PEI was what played an important role in the toxicity of the nanogel. The higher ratio of PEI in the nanogel would indeed result in a higher toxicity[16, 18] of the nanogel since PEG is highly biocompatible.

Two strategies were investigated. One possibility is to block some of the free amino groups of the PEI that might have played a role to cause the toxicity of the nanogel and another possibility is to increase the ratio of PEG by optimizing the synthetic procedure.

2.2.2 Synthesis of Acetylated Nanogel (Ac-NG)

Acetic anhydride was utilized to block part of the free amino groups of nanogel **26**. Acetylation on the amino groups of 1:4 ratio nanogel **26** was achieved by treatment of the nanogel with acetic anhydride in acetonitrile at 50 ^{o}C for 12 hours followed by dialysis and lyophilization. The acetylated nanogel was evaluated against the cancer cells and the results indicated that this nanogel was nontoxic to the cells.

Scheme 8. Synthesis of acetylated PEG-PEI Nanogel (**Ac-NG**)

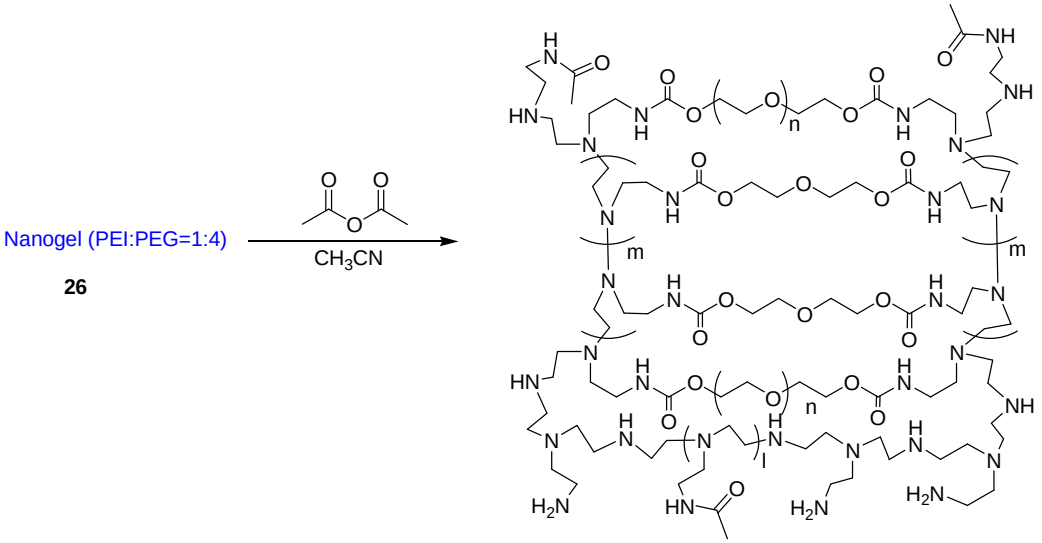

2.2.3 Synthesis of Nontoxic PEG-PEI Nanogel (NG)

To increase the ratio of PEG, the sonication (after the adding of activated PEG into PEI solution) time was optimized. Instead of 15 minutes, the nanogel was sonicated for 30 minutes or 60 minutes, and the results showed that the ratio of CH_2N:CH_2O (methylene protons) remained unchanged 1:4 in the proton NMR spectrum. The same result was obtained when the volume of deionized water was reduced from 300 ml to 200 ml. This indicated that an increase of sonication time or an increase in concentration does not affect the PEI: PEG ratio. When double the amount of activated PEG was used, the composition of the resulting nanogel still remained unchanged, as a

1:4 ratio of the CH_2N :CH_2O (methylene protons) was again observed.

The toxic nanogel (1.16 g) was further treated again with 1g of activated PEG following the same procedure to afford 1.32 g of a new nanogel. The results indicated that the CH_2N:CH_2O (methylene protons) ratio of the new nanogel had changed from 1:4 to 1:6.8. When tested on the stem cells, this nanogel was nontoxic to the cells. As shown in Figure 12, nanogel PEI: PEG (1:4) resulted in 80% inhibition of Pan 02 cell growth at 0.04 mg/ml while nanogel PEI: PEG (1:6.8) still had 90% cell viability at even 0.1 mg/ml. Based on the optimization, one single treatment of PEI with activated PEG resulted in a partially cross-linked nanogel; the ratio of CH_2N:CH_2O was about 1:4 which was toxic to stem cells; double treatment with activated PEG would increase the CH_2N:CH_2O ratio to 1:6.8 which was nontoxic to stem cells.

Scheme 9 Synthesis of nontoxic nanogel (PEI:PEG=1:6.8) **NG**

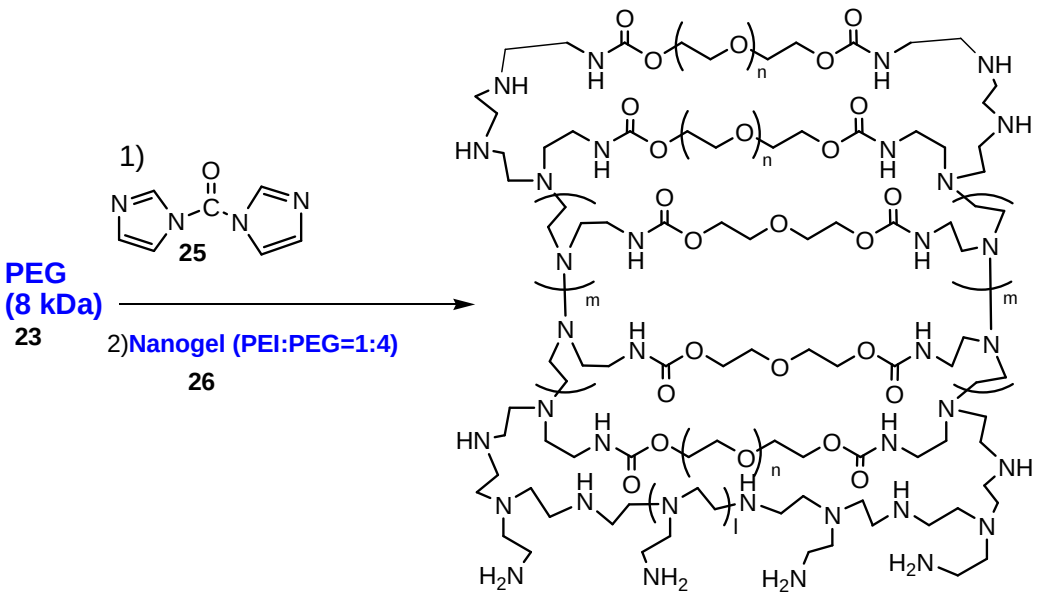

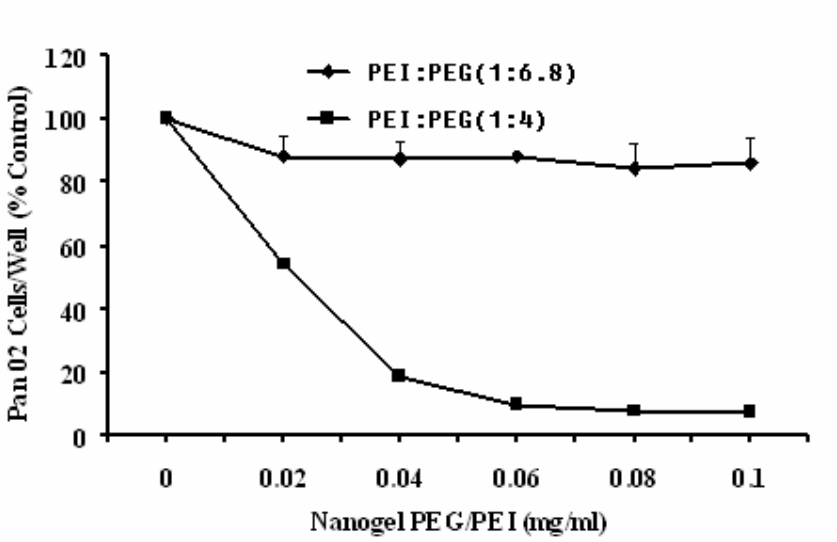

Figure 12 Cell viability of PAN 02 cell treated with PEI: PEG (1:4) and PEI: PEG (1:6.8) nanogels. Pan 02 cells were seeded in a 96 well plate and after reaching 70% confluency, the media was replaced with fresh medium containing nanogel PEI: PEG (1:4 or 1:6.8) at different concentrations and incubated for 48 hours. MTT assays were performed.

2.2.4 Synthesis of Rhodamine Attached Nanogel (NG-Rh)

Since the nanogel was not florescent, it was difficult to detect whether it was up-taken by the stem cells or not. Rhodamine B dye was subsequently attached to the nanogel as an indicator. Rhodamine B was covalently linked to the nanogel. The activation of the carboxylic acid group of rhodamine B was accomplished by reaction with Hydroxybenzotriazole (HOBt), Dicyclohexylcarbodiimide (DCC) and *N*-Hydroxysuccinimide (NHS) in DMF at 55 ^{o}C for 2.5 hours. The activated rhodamine dye was then treated with nanogel **28** in acetonitrile at 40 ^{o}C for 12 hours. The resulting pink solution was dialyzed with a 12KDa-14KDa MWCO membrane in a solution of 10% ethanol in deionized water at 25 ^{o}C for 24 hours to remove the excess rhodamine. The rhodamine attached nanogel **29** was obtained as a pink powder after lyophilization.

Scheme 10 Synthesis of Rhodamine attached Nanogel (**NG-Rh**)

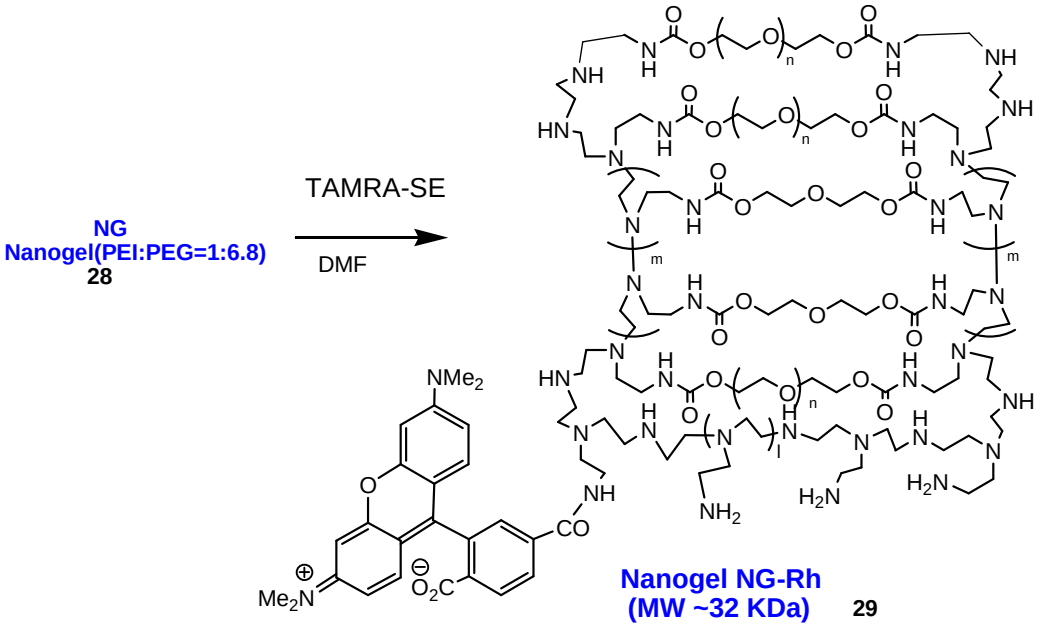

2.2.5 Encapsulation of AQ10 into Nanogel

An anthraquinone derivative, AQ10, has been reported[22-24] to have toxicities against some cancer cell lines by triggering apoptosis and causing inter-nucleosomal DNA fragmentation. AQ10 was utilized as an anticancer drug to target at Pan 02 cancer cell lines. The dosage effect of AQ10 alone against Pan02 was evaluated. The results indicated that 2 ug/ml (9.2 μM) would reduce the cell viability to around 70% while 4 ug/ml (18.4 μM) can further decrease it to 25%.

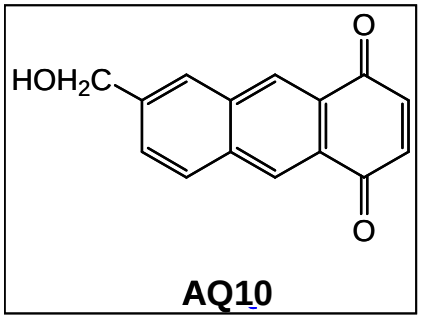

Figure 13 Structure of AQ10

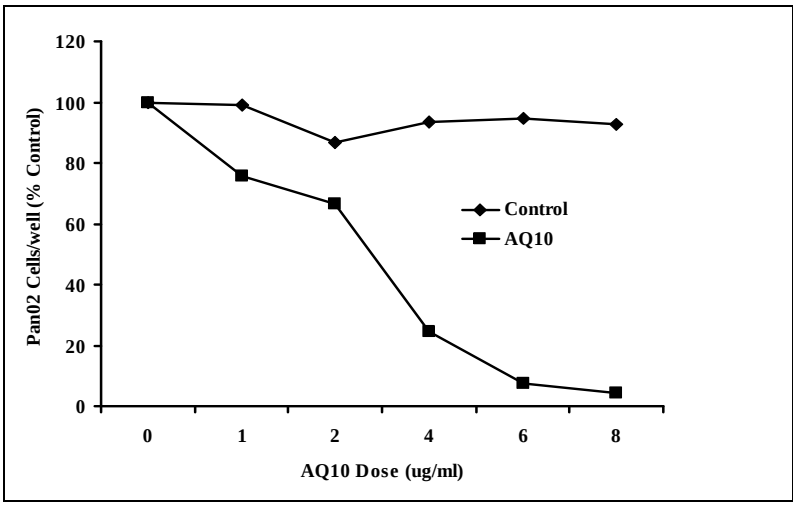

Figure 14 Cell viability of Pan 02 cells when treated with different dosages of AQ10. Pan 02 cells were seeded in a 96 well plate and after reaching 70% confluency, the media was replaced with fresh medium containing AQ10 or control (DMSO) at different concentrations and incubated for 48 hours. MTT assays were performed.

AQ10 was then encapsulated into the NG synthesized as shown below in Scheme 11. 50 mg of NG was dissolved in 5 ml of deionized water and mixed well with a solution of 0.5 mg AQ10 in 1 ml of acetonitrile. The resulting solution was lyophilized immediately to give a quantitative yield of 1% AQ10 with NG (by weight ratio) as a brown powder. Other drugs gave different weight ratios of encapsulation, and were accomplished by a similar procedure.

Scheme 11. Encapsulation of AQ10 into nanogels

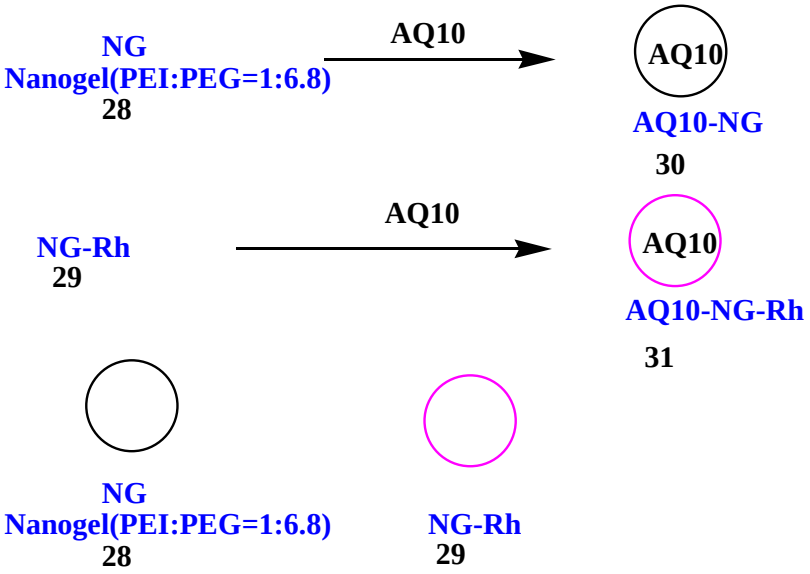

2.2.6 Loading of Nanogel (NG-Rh) to Stem Cells (UCMS)

Umbilical Cord Matrix Stem (UCMS) cells were used as a carrier for the nanogel and anticancer drugs. The incorporation of the nanogels into the stem cells was studied. As shown in Figure 15 and 16, UCMS cells were loaded with rhodamine attached nanogel **29** (NG-Rh) at different time points. The internalized NG-Rh was observed by a fluorescent microscope followed by imaging. As cells gained more NG-Rhs, the nanoparticles were distributed throughout the cytoplasm. The loading kinetics over a period ranging from 30 minutes to 36 hours was determined. The maximum loading of nanogel **29** was achieved at 24 hours, which was 5% of the total loaded nanogel.

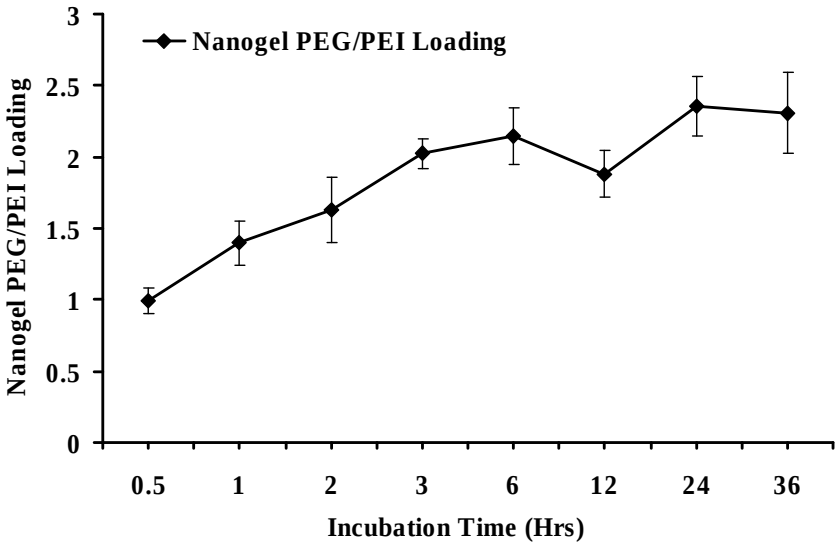

Figure 15 Loading kinetics of nanogel (NG-Rh) into stem cell. Nanogel **29** loading into stem cells increased with time following incubation of nanogel PEG/PEI with UCMS cells. Nanoparticles loaded was normalized to total cellularprotein

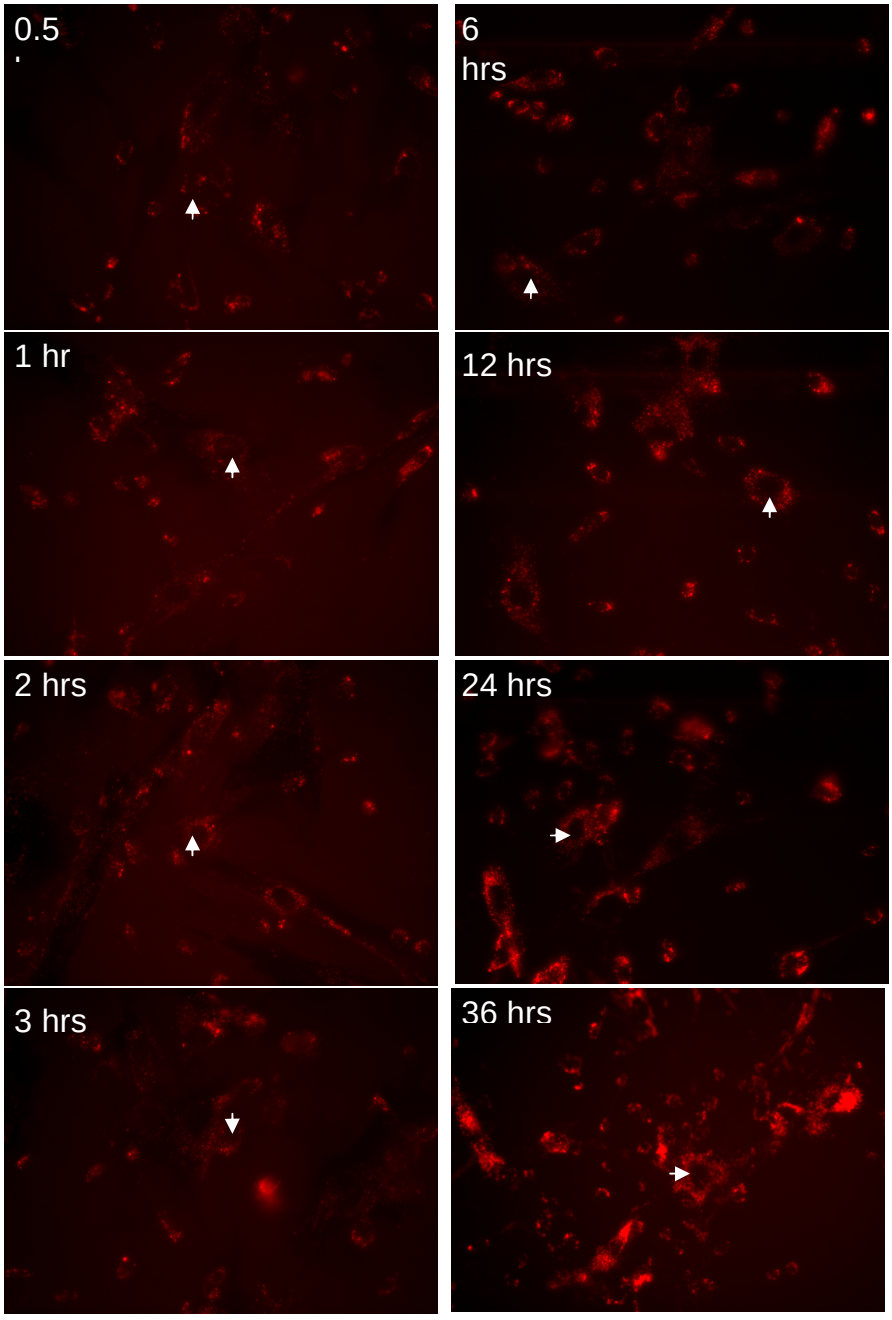

Figure 16 Nanogel (NG-Rh) up taken by stem cells at different time points. The punctuate red fluorescence indicates rhodamine labeled nanoparticle internalized by the stem cells (Arrow indicates cell nucleus)

2.2.7 Viability of Stem Cells Loaded with AQ10-NG-Rh

The results shown above indicated that nanogels actually internalized into the stem cells. Then the next question is whether the stem cells can survive during the transportation of nanogel to the tumor since AQ10 loaded nanogel **31** (AQ10-NG-Rh) is toxic to Pan 02 cancer cells. The cell viability evaluation of stem cells upon the treatment of AQ10-NG-Rh was subsequently performed. The results demonstrated that when treated with 0.1 mg/ml of nanogel **31** (AQ10-NG-Rh) for 48 hours, the stem cell still had a 100% viability.

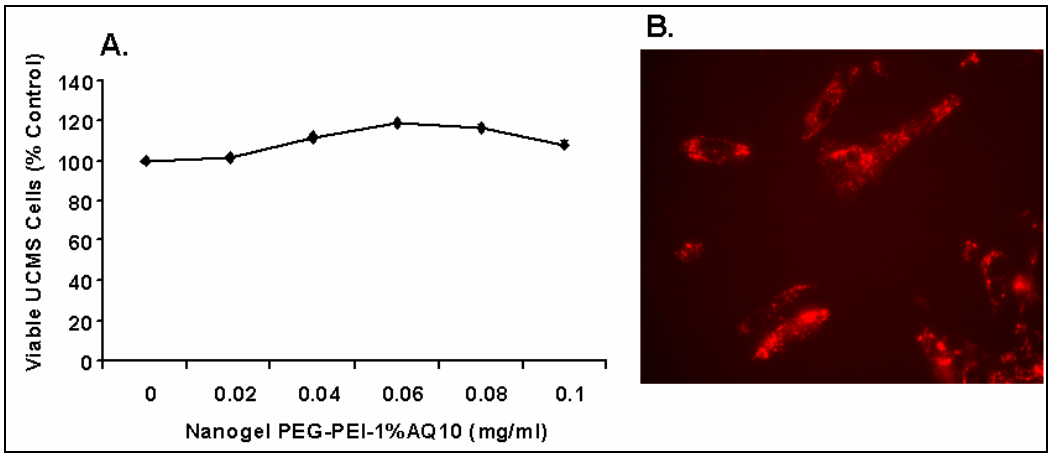

Figure 17 Cell viabilities of stem cells upon treatment of nanogel (AQ10-NG-Rh). Stem cells were treated with different concentration of nanogel (AQ10-NG-Rh) and incubated for 48 hours. MTT assay results are shown in panel A. The fluorescence images after 48 hours are shown in panel B.

2.2.8 AFM Image of Nanogel (AQ10-NG)

The size of 1% AQ10-NG was studied by Atomic Force Microscopy (AFM) using a tapping mode with a high aspect ration tip. Several samples were examined. The images were similar, and two of them are shown in the top panel of Figure 18. The zoom-in images in the middle panel show the round particles with diameter of approximately 23 nm and height of approximately 1 nm. Some aggregations of small nanogels to short fibril-like materials were also observed as can be seen in the bottom panel.

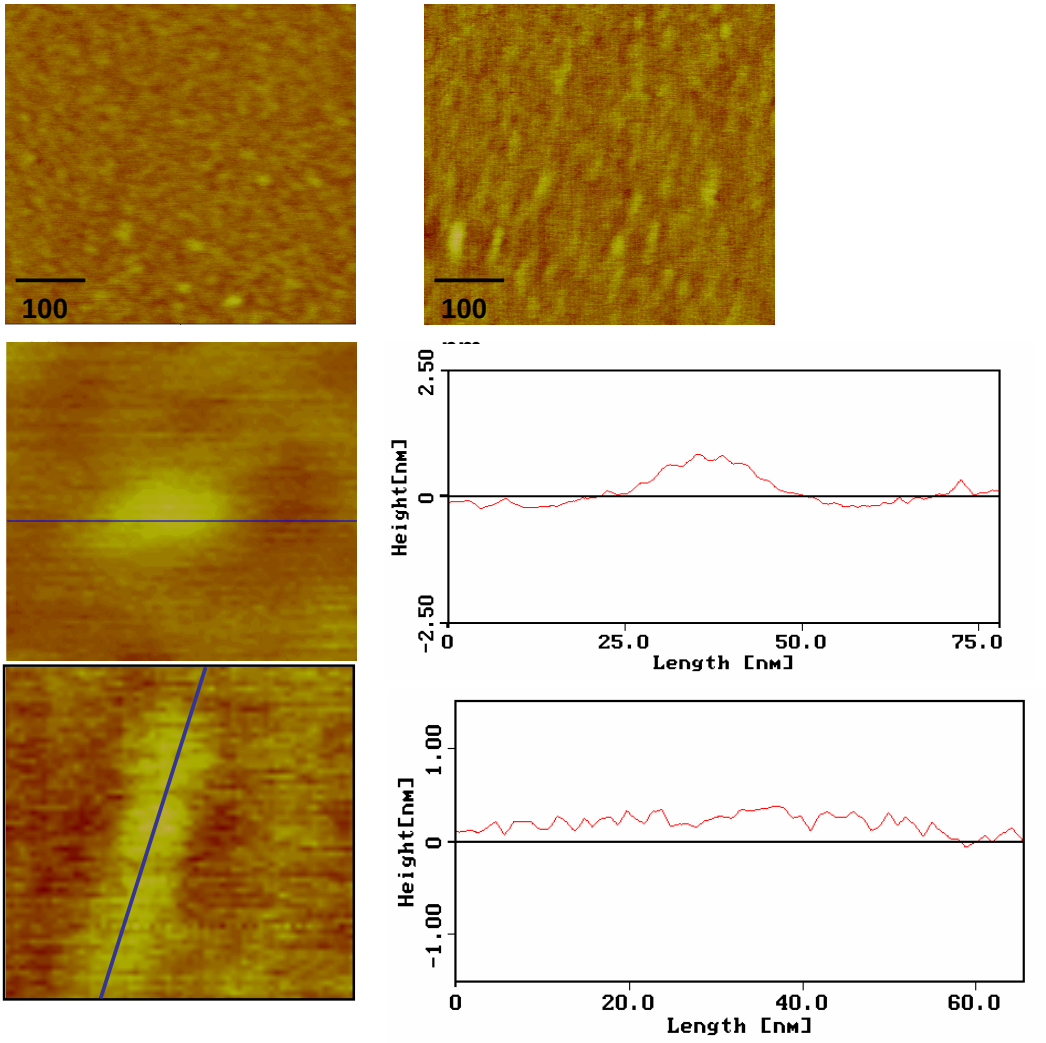

Figure 18 AFM image of nanogel (AQ10-NG). Top panels: AFM images of AQ10-NG-Rh sample at two different locations on mica. Middle left panel: a zoom-in AFM image of a nanogel (AQ10-NG) particle and its width and height are shown in middle right panel. Bottom left panel: a zoom-in AFM image of an aggregated nanogel (AQ10-NG) particle and its height and width are shown in bottom right panel.

2.2.9 Results of AQ10-NG on Pan 02 Cells

The AQ10 loaded nanogel **30** (AQ10-NG) was tested on the inhibition of Pan 02 cell proliferation in a dose-dependent manner. The results showed that nanogel **28** (NG) had no significant inhibition effects on the Pan 02 cell proliferation as compared to the control. When treated with AQ10 encapsulated nanogel **30**, the Pan 02 cell viability decreased significantly to around 60% at 0.06 mg/ml dosage and with a further rduction to 30% at 0.08 mg/ml dosage. Since there was only 1% of AQ10 by total weight of the nanogel, 0.06mg/ml of nanogel only contained 0.6 μg/ml (2.8 μM) of AQ10. As a comparison, when treated with AQ10 alone, 2 μg/ml (9.2 μM) AQ10 can only reduce the cell viability to about 70%. The results indicated that the AQ10 was about four times more effective when encapsulated with nanogel than alone. Due to the low solubility of AQ10 in water, it can not be loaded into the cells effectively; however, when incorporated into the nanogel which is highly soluble in water, a more efficient loading of AQ10 into the cells resulted, which allowed for a decrease in dosage.

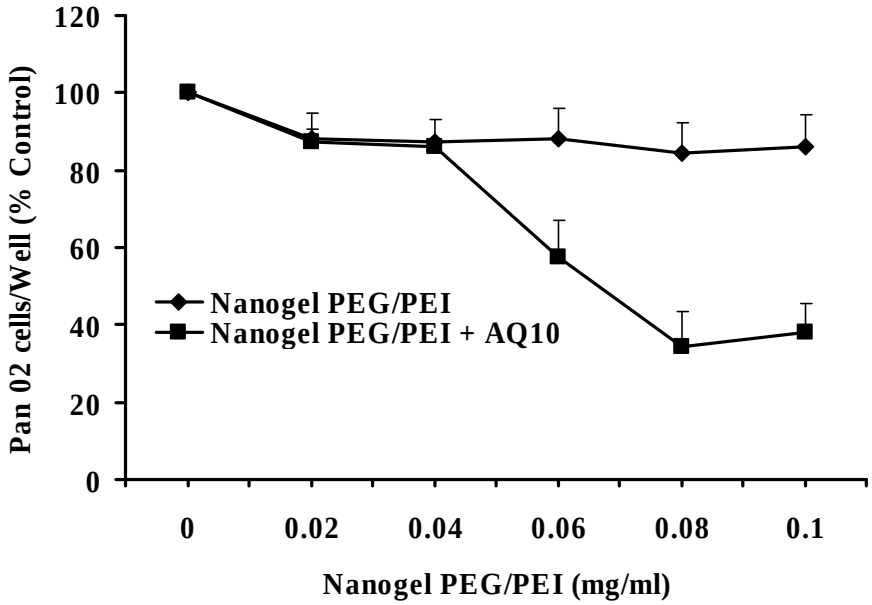

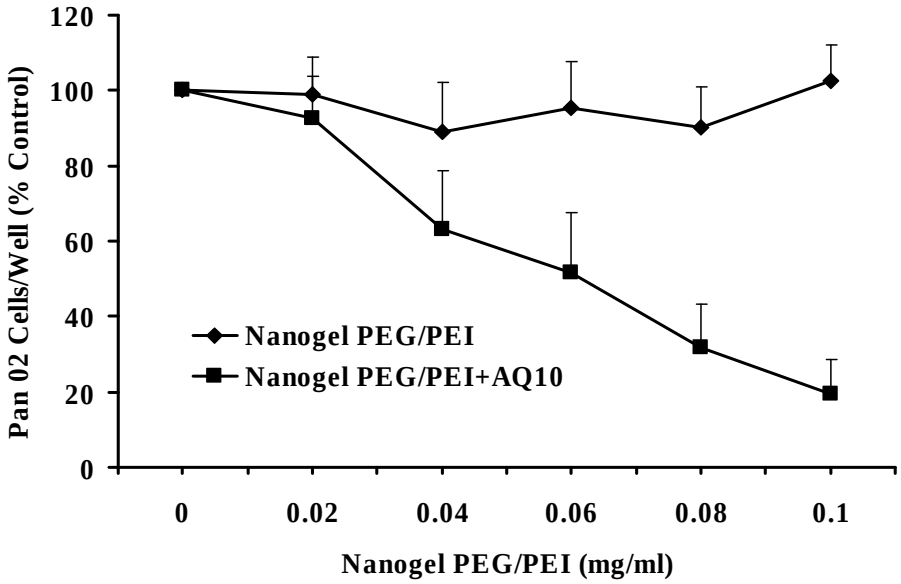

Figure 19 Dose effects of nanogel (NG) and 1% AQ10-nanogel (AQ10-NG) on Pan 02 cell viability. Pan 02 cells were seeded in a 96 well plate and after reaching 70% confluency, the media was replaced with fresh medium containing nanogel (NG or AQ10-NG) at different concentrations. Following incubation for 48 hours cell proliferation assays were performed. MTT assay results were shown in top panel and hemocytometer-trypan blue exclusion results were shown in the bottom panel.

In summary, the synthesis of nontoxic PEG-PEI nanogel (NG) was achieved by double treatments of PEI with activated PEG. PEG-PEI nanogels can be loaded with anticancer drug (AQ10) and release the drug to kill the cancer cell Pan 02 and the drug dosage was significantly lower when combined with nanogel than the drug alone. Attached rhodamine on the nanogels can indicate the location of nanogels in the cell system and the rhodamine attached nanogel was internalized into the UCMS cells. These results suggested that the nanogel is a novel anticancer drug carrier which could be incorporated into stem cells. The stem cell can be used as a delivery vehicle to specifically release the nanogel with anticancer drugs to cancer cells.

2.3 Type II Nanogels

When we carefully examine this delivery system above, there are two major concerns: 1. the capability of the nanogel to load with anticancer drugs; and 2) the internalization capability of nanogel into UCMS cells. If only a limited amount of anticancer drugs can be encapsulated to the nanogel, it may not be efficient enough to attenuate or inhibit the cancer growth. The nanogel with AQ10 above contained only 1% (by weight) of anticancer drug. We had successfully encapsulated up to 5% (by weight) while higher percentages failed. This problem may not be crucial if the anticancer drug is sensitive. However, for some less powerful drugs, even 5% encapsulation would result in a higher dosage of nanogels. Nevertheless, the lower the capability of incorporation of nanogel into the stem cells, the larger the quantity of nanogels and anticancer drugs would be required. The results showed above that only about 5% of the total nanogels can be internalized into the stem cells. Hence, increasing the amount of anticancer drug in the nanogels and the incorporation capability of the nanogel into the stem cells would significantly improve the efficiency of nanogel drug delivery system.

2.3.1 Background of SN38 and Legumain

Camptothecin (CPT) is a natural product isolated[25] from the bark and stem of a plant native to China. It has remarkable anticancer activities[26] in tumor cells. CPT selectively binds to DNA enzyme topoisomerase I (TOP1) during the cleavage of DNA which then causes DNA damage and apoptosis.[27] The oxygen atoms on the lactone E ring of CPT bind to the enzyme, and the hydroxyl group binds to aspartic acid 533 on the side chain of the enzyme.[28] Only the S configuration of the chiral carbon is active, and the opening of lactone E ring would result in a loss of activity.[29, 30]

However, the low solubility and substantial toxicity of camptothecin prevents its development and use in clinical trials.[31] Several analogs have been synthesized. In 1997, two analogs with much a higher water solubility, topotecan and irinotecan (CPT-11) were approved by the U.S. Food and Drug Administration as anticancer

agents. The most active analog so far is SN38 (7-ethyl-10-hydroxy-camptothecin) which is also the active metabolite of CPT-11 produced by esterase-mediated hydrolysis. Unfortunately, like camptothecin, SN38 has even lower water-solubility. Moreover, less than 10% of CPT-11 would be converted to its active ingredient SN38 in human body system.[32-34] Another limitation is that the lactone E ring of SN38 can be easily opened[34-36] and therefore loss in the activity before reaching the tumor site. Hence, increasing the solubility of SN38 and preventing the ring opening reaction may have therapeutic benefits. Hong Zhao and his coworkers linked SN38 with poly ethylene glycol to stabilize the compound and increase the solubility.[37] The results demonstrated much higher anticancer activity compared to CPT11.

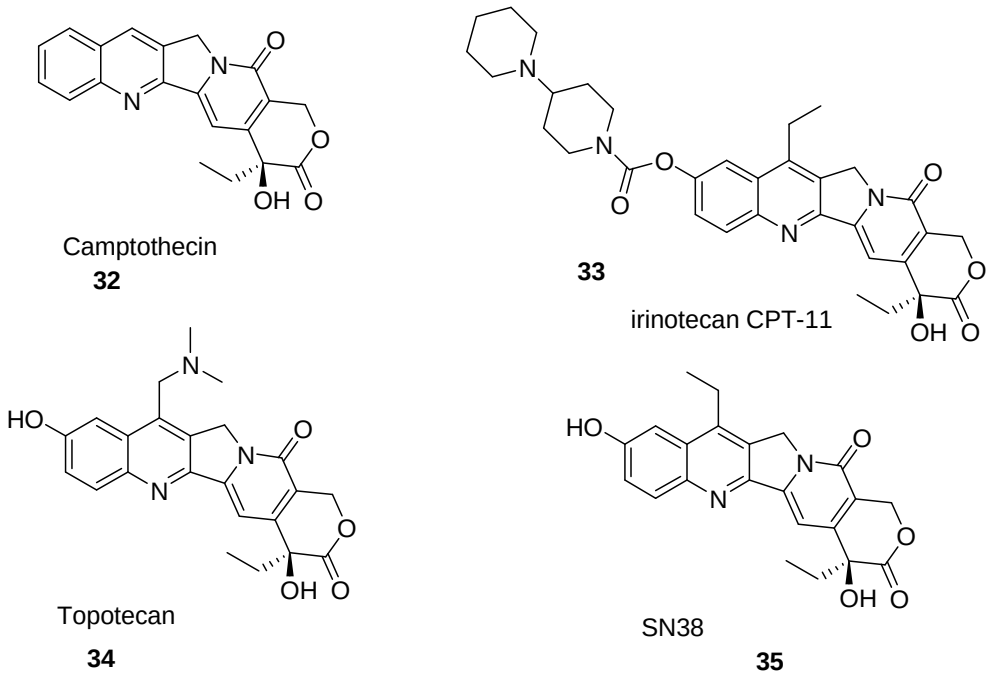

Figure 20 Camptothecin and some of its analogs.

Legumain, [38-41] a gene that encodes a cysteine protease that can specifically hydrolyze an asparaginyl bond, [42] is highly expressed in many tumors[43] due to the down-regulation of its inhibitors such as cystatin C.[44] However, the activity of legumain could be inhibited by such cystheine protease inhibitors in normal tissues. Hence, legumain could be a potential targeting candidate[45] for drug delivery. A short, specifically designed peptide sequence that contains one asparagine and links with an anticancer drug would be recognized and hydrolyzed by legumain; thus, the anticancer drug could be released to the tumor. In a report by Wenyuan Wu and her coworkers, [38] a prodrug using a short peptide with 4 amino acids (Ala-Ala-Asn-Leu) that is linked with doxorubincin was synthesized and tested. The results indicated that legumain can actually recognized the sequence and cut right in between asparagine and leucine to release doxorubincin linked with leucine, which was further converted to the end product doxorubincin.

As to our nanogel system, we firstly tested the simple encapsulation with 1% and 5% of SN38 into the nanogel; however, even at 5% the SN38 system did not show much enhanced efficiency than the SN38 alone. It also turned out that higher percentage of SN38 can not be successfully encapsulated into nanogels. Thus, another method was developed by attaching the SN38 prodrug to the outside of the nanogel with a short peptide linker. SN38 was modified at the hydroxyl group of the lactone E ring to have a carboxylic acid functional group at the end that can be linked to the amino end of the peptide. The same sequence of peptide (Ala-Ala-Asn-Leu) was synthesized by solid phase peptide synthesis and then coupled with modified SN38. This prodrug was covalently attached to the outside of nanogel that still had free amino groups. To enhance the activity and increase the loading efficiency, 5% of SN38 was encapsulated into the prodrug nanogel.

2.3.2 Synthesis of SN38 linkers

Synthesis of SN38 derivatives with a side chain linker was accomplished by following the literature reported method[37] with some modifications. 10-OH on A ring was selectively protected with t-butyl-diphenylsilyl chloride and triethylamine in dichloromethane under reflux for overnight. Initially, the SN38 was not soluble in dichloromethane; the suspension was yellow after the adding of triethylamine. A greenish solution was formed when the reaction finished. However, the reported recrystallization[37] using dichloromethane and petroleum ether was not efficient to obtain the pure product. The compound was purified by a silica gel column chromatography using 80:2 dichloromethane and methanol as the eluant. The yield was 100% as compared to 65% from the literature report.

Scheme 12

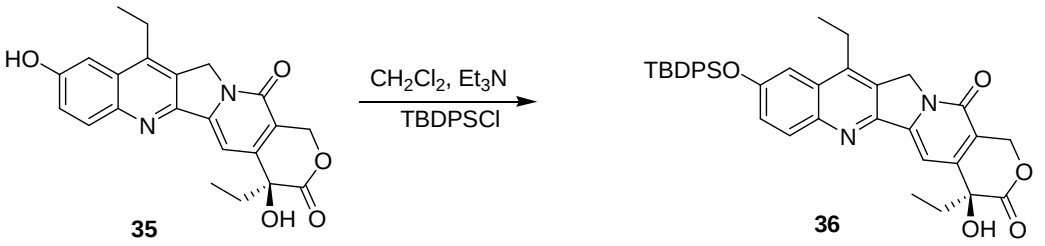

35 **36**

Boc-Glycine was coupled with the hydroxyl group on the lactone E ring of compound **36** in dichloromethane using N-ethyl-N'- (3-dimethylaminopropyl) carbodiimide hydrochloride (EDC) and 4-Dimethylaminopyridine (DMAP) as coupling reagents at 0 ^{0}C for overnight. Pure product **37** was obtained as a green solid after work up in a yield of 96%. The Boc-protecting group was removed in a solution of 2 M HCl in dioxane at room temperature for 1 hour. Compound **38** was obtained as a brown solid in 99% yield.

Scheme 13

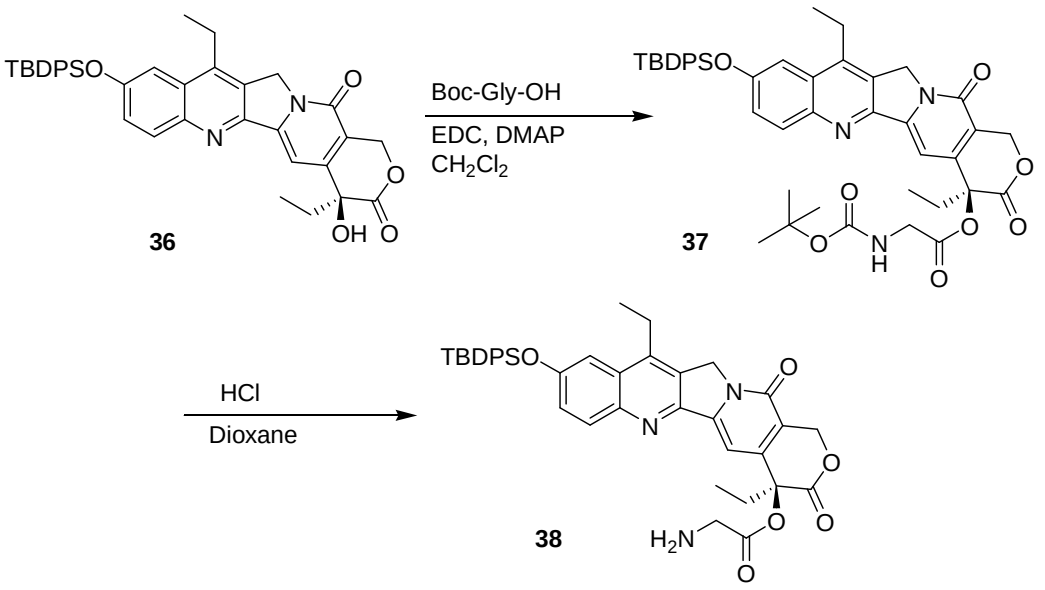

36 **37** **38**

In order to couple SN38 derivatives to the peptide on the amino end, the amine end of compound **38** was converted into a carboxylic acid by reacting compound **38** with succinic anhydride in dioxane at 90 ^{0}C for 1 hour. Silica gel column chromatography using 15:1 dichloromethane and methanol gave compound **39** as a brown solid in 96% yield.

Scheme 14

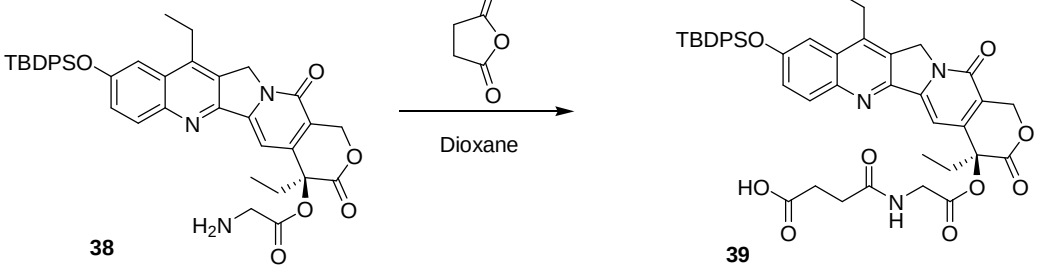

38 **39**

2.3.3 Synthesis of Peptides

The 4 amino acids peptide (Ala-Ala-Asn-Leu) was synthesized using microwave Fmoc solid-phase peptide synthesis. All the Fmoc protected amino acids and resins (Fmoc-Ala-NovaSyn TGA) were purchased from CEM. The resin was firstly deprotected using a solution of 20% of piperidine in DMF followed by washing with 100 ml DMF, and coupling with Fmoc-Ala-OH using O-Benzotriazole N,N,N',N'-tetramethyl uronium hexafluoro phosphate (HBTU) and Diisopropyl ethyl amine (DIEA) in DMF. The other two amino acids were attached respectively by repeating the deprotection, wash, coupling and wash cycle. After the final deprotection and wash, the Resin-Ala-Ala-Asn-Leu-NH_2 (Resin-Peptide **41**) was obtained as a solid.

Scheme 15 Synthesis of Resin-Peptide

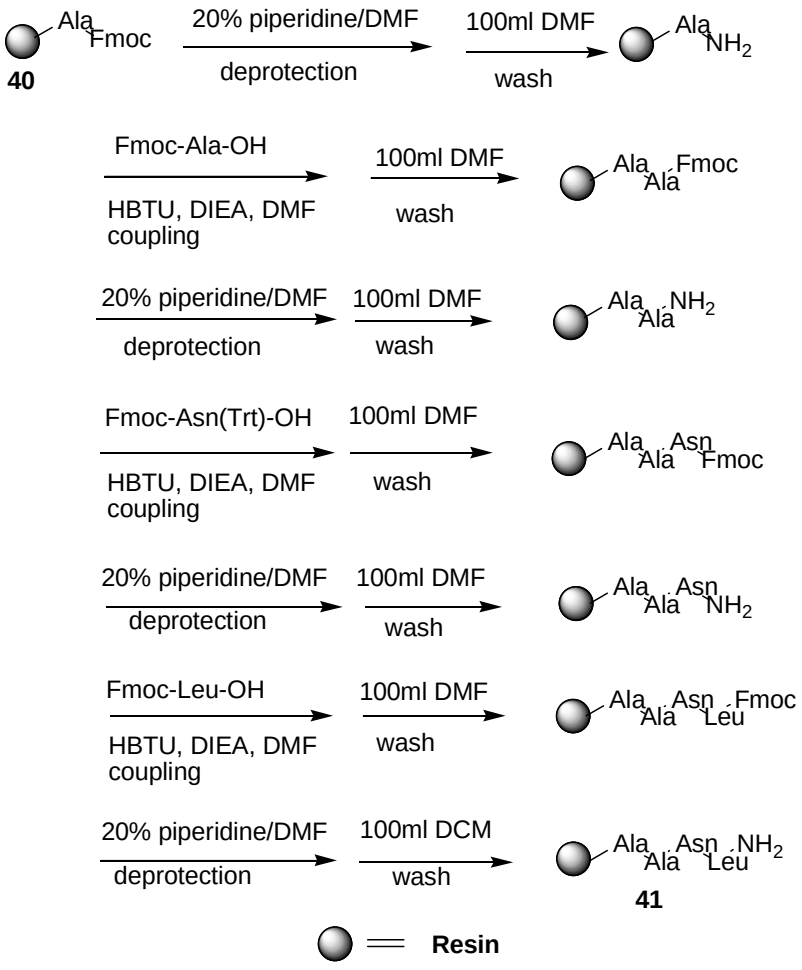

2.3.4 Synthesis of Peptide-SN38 (43)

Compound **39** was activated by HBTU and DIEA in DMF, and this mixture was then added to the reaction vessel that contained the resin-peptide. After coupling, the reaction vessel was washed with 100 ml of dichloromethane to remove any by-product and starting reagents while the product was attached to the solid resin. To cleave the Peptide-SN38 off the resin, a cleavage solution of 95% trifloroacetic acid (TFA), 2.5% water and 2.5% triisopropylsilane (TIS) was prepared and added to the reaction vessel immediately. This cleavage program was repeated twice to enhance the cleavage of the peptide. The Peptide-SN38 was collected by filtration; and the resin was washed with 4 ml dichloromethane twice. After removal of the solvent, the crude Peptide-SN38 was further purified by HPLC equipped with a UV detector. There was only about a 20% yield for the final coupling and cleavage reactions as most of the materials were lost during the work up and HPLC purification.

Scheme 16 Synthesis of Peptide-SN38 (**43**)

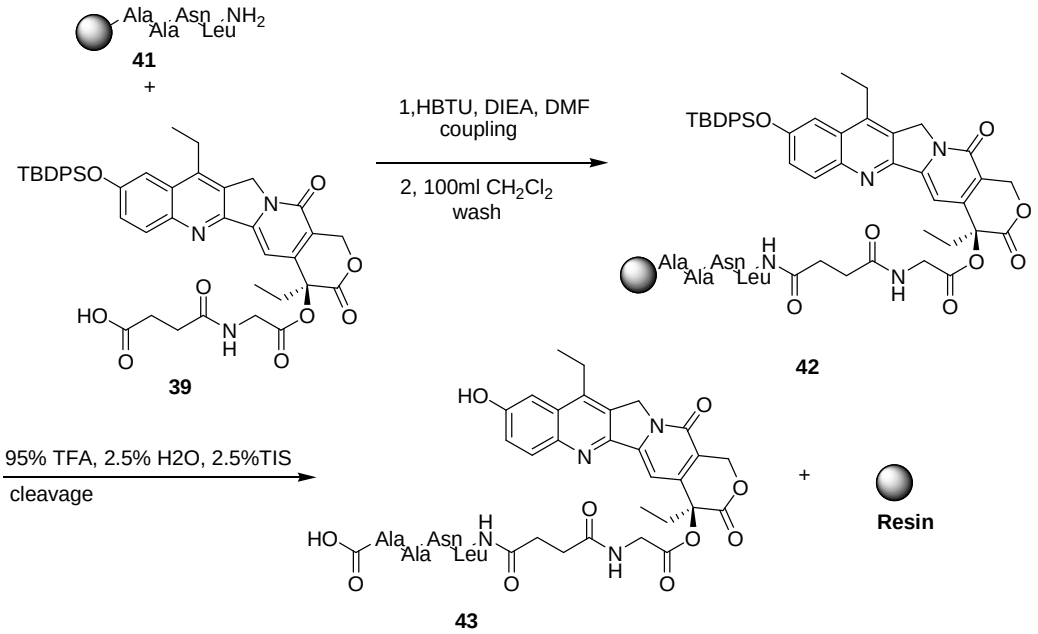

2.3.5 Synthesis of SN38-NG-Peptide-SN38 (45)

The coupling of nanogel with peptide-SN38 was accomplished by using N-ethyl-N'-(3-dimethylaminopropyl)carbodiimide hydrochloride (EDC) and 4-dimethylaminopyridine (DMAP) in dichloromethane. After the outside peptide-SN38 chain was attached to the nanogel, 5% (by weight) of SN38 was encapsulated into the nanogel system. Since the SN38 was UV active it could be tracked by confcal microscope; no rhodamine dye was attached.

Scheme 17 Synthesis of SN38-NG-Peptide-SN38 (**45**)

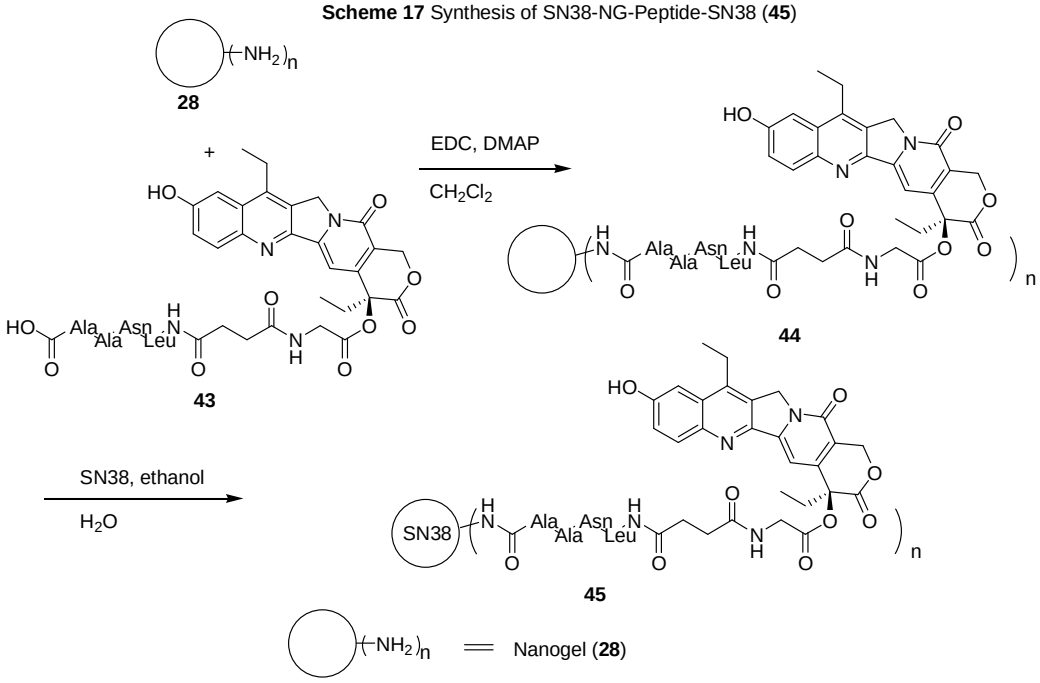

2.3.6 Results and Discussions

Nanogels NG-Peptide-SN38 (**44**) and SN38-NG-Peptide-SN38 (**45**) were tested on B-16 melanoma cancer cells. B-16 cells were chosen due to their rapid proliferation. As shown in Figure 21, when loaded with NG-Peptide-SN38 (**44**) at 0.1 mg/ml which contained no SN38 inside, the viabilities of B16 went down dramatically. 25% viability was observed on the first day and around 20% on the second day, however, it raised up to 60% on the third day and 100% on the forth day due to its proliferation ability and over expression of legumain. The results demonstrated that nanogel **44** was indeed toxic to cancer cells due to the outside attachment of SN38 which was probably cut off and released causing the toxicity. However, a higher dosage or more toxic nanogel that can further lower the cell viability to less than 25% on the first day was required.

SN38-NG-Peptide-SN38 (**45**) was expected to be more powerful than NG-Peptide-SN38 (**44**) since **45** is encapsulated with 5% of SN38 inside the nanogel. The results shown that when treated with the same concentration of **45** (0.1mg/ml), the viabilities of B16 decreased to 18% on the first day as compared to 25% for **44**; even on the forth day, the cell viabilities still remained around 10% for nanogel **45**. SN38-NG-Peptide-SN38 (**45**) can inhibit the growth of B16 at a much lower dosage. As shown in figure 21 (bottom panel), when B16 was loaded with **45** at 0.025 mg/ml, the cell viability remained less than 20% even on the forth day; while for **44**, cell viabilities all increased to around 100% again on the forth day.

These results suggested that, without the encapsulation of SN38 inside, the SN38 outside chain attached nanogel **44** was toxic to cancer cells, which might have been cleaved by legumain. The encapsulation of SN38 significantly increased the toxicity of nanogel which showed inhibition of B16 growth at concentrations lower than 0.025mg/ml.

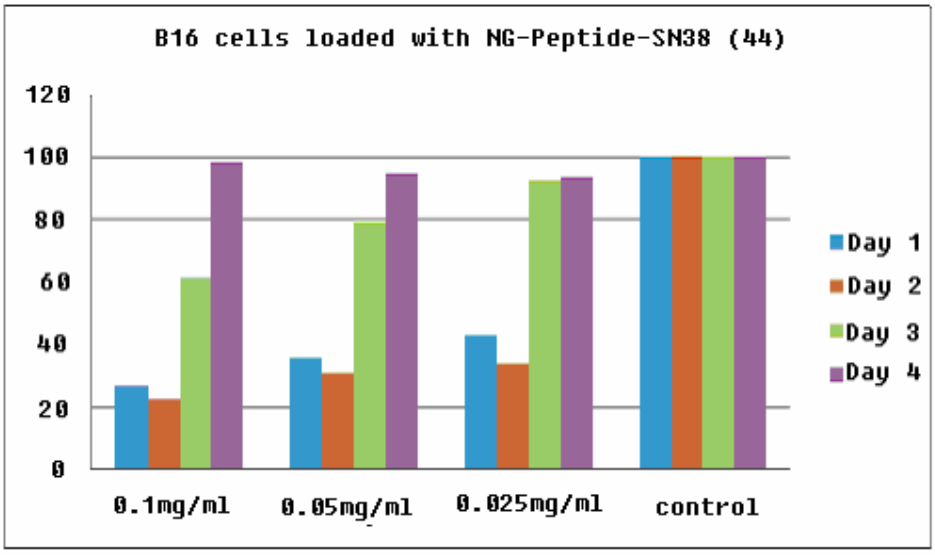

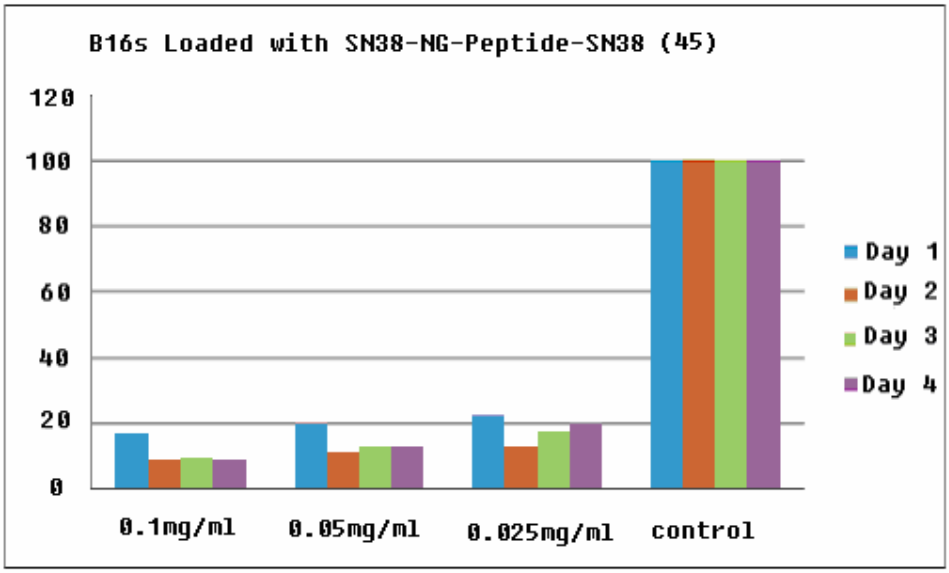

Figure 21 Dose effects of type II nanogels on B16 cell viability. B16 cells were seeded in a 96 well plate and after reaching 70% confluency, the media was replaced with fresh medium containing nanogel (**44** or **45**) at different concentrations. Following incubation for 96 hours cell proliferation assays were performed every 24 hours. Result of nanogel **44** was shown on top panel and that of nanogel **45** was shown on bottom panel

B16 cells were treated with nanogels and legumain together. As shown in Figure 22 (top panel), legumain itself caused no toxicity to cancer cells. When B16 cells were treated with nanogel **44** (no encapsulation of SN38) at 0.05mg/ml, without legumain, the cell viability was about 44% on the first day. When 0.1mg/ml of legumain was added, the cell viability decreased to about 38% on the first day. Similar effects were observed when nanogel **45** was tested.

Without the addition of extra legumain, the B16 cells could still express legumain, which can therefore cleave the peptide and release the drug SN38, and subsequently cause the inhibition. However, since the media was replaced on the first day, the initial concentration of legumain was low. When added with extra legumain, a further down regulation was observed due to the higher concentration of legumain.

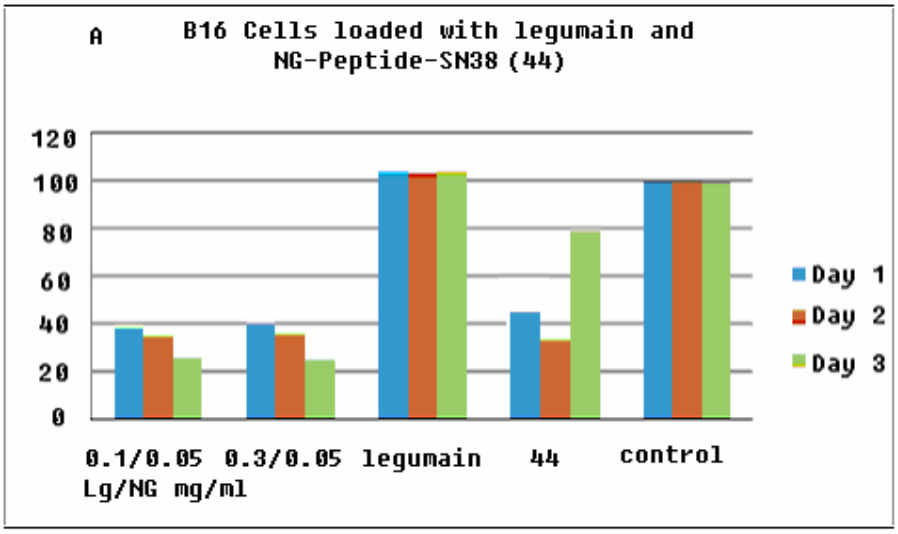

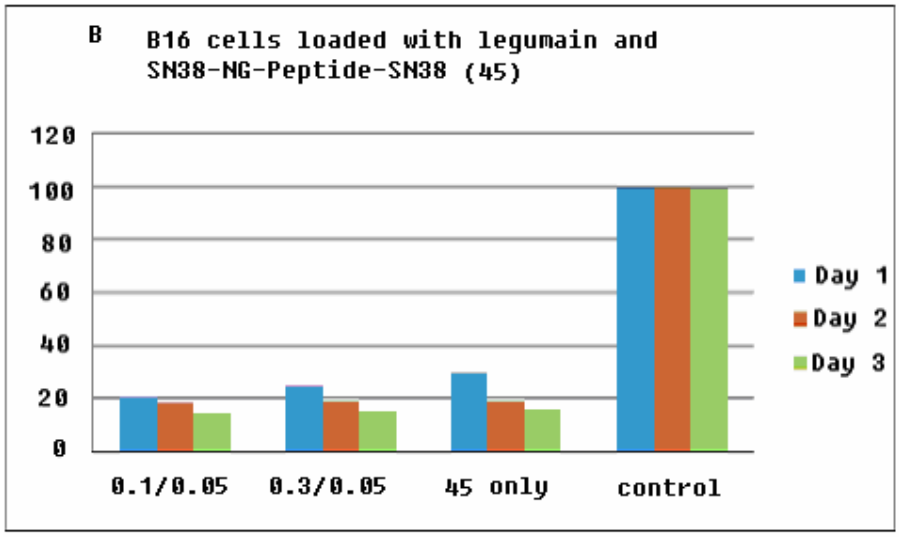

Figure 22 Dose effects of type II nanogels with legumain on B16 cell viability. B16 cells were seeded in a 96 well plate and after reaching 70% confluency, the media was replaced with fresh medium containing nanogel (**44** or **45**) and legumain at different concentrations. Following incubation for 72 hours cell proliferation assays were performed every 24 hours. Result of nanogel **44** was shown on panel A and that of nanogel **45** was shown on panel B.

Nanogel **45** was tested on the cell viability of neural stem cells (NSC). Since stem cells would serve as a carrier for the nanogels, it is required that stem cells can resist the toxicity of the nanogels. The results indicated that, at a concentration of 0.01mg/ml, the stem cells had about 50% viability on day 1 and 60% on day three (Figure 23), which was acceptable for the delivery of nanogels.

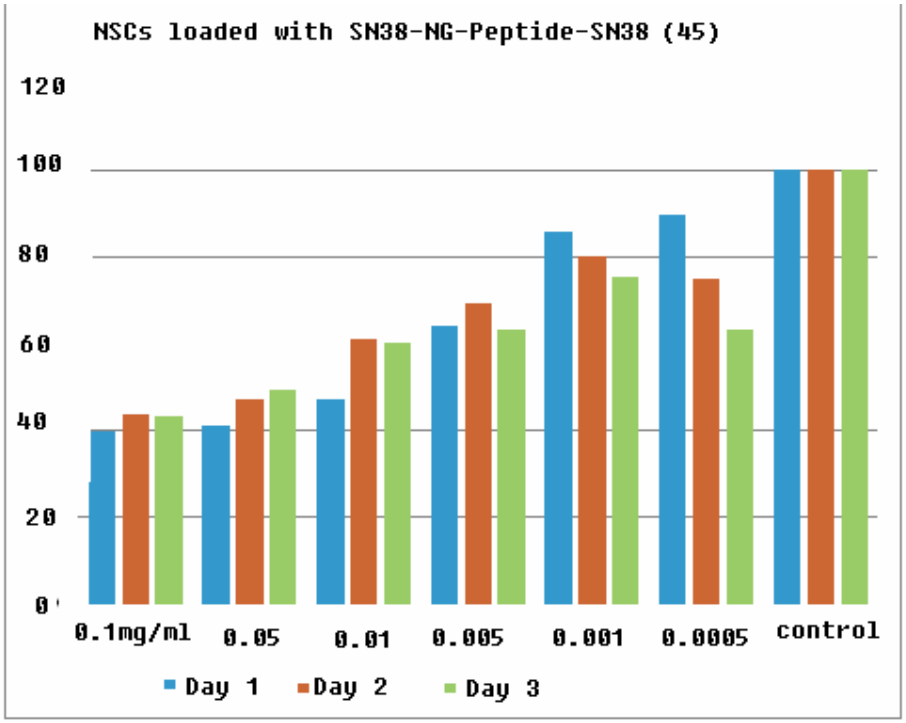

Figure 23 Dose effects of nanogel **45** on neural stem cell (NSC) viability. NSCs were seeded in a 96 well plate and after reaching 70% confluency, the media was replaced with fresh medium containing nanogel **45** at different concentrations. Following incubation for 72 hours cell proliferation assays were performed every 24 hours.

2.4 Type III Nanogels

2.4.1 Background

Biotin, also called vitamin H, is essential for the production of fatty acids needed for the cell growth. The concentration of biotin around the tumors is significantly higher than that around normal cells due to the large demand of biotin for the proliferation of the cancer cells. The biotin receptors on the cancer cell surface are usually over expressed, [47] and have been explored as candidates[48] for the targeting of cancer cells. Several approaches have been reported to enhance the drug delivery efficiency such as dendrimers,[47] pyrenes,[49] polymers,[50] and nanoparticles.[51]

Streptavidin, a protein with a molecular weight of about 52800 Daltons, is known for its high affinity for biotin. The dissociation constant (K_d) is on the order of 10^{-14} mol/L, which makes the streptavidin-biotin bond among the strongest protein-ligand

interactions.[52]

To target at the cancer cell, two approaches have been investigated. The first method involves directly attaching the biotin onto the nanogel, which is called biotinylation. This biotinylated nanogel can be recognized and picked up by cancer cells. The second approach involves attaching streptavidin onto the nanogel, which can bind to biotins around the tumor and then be caught by the cancer cells. Hence, biotinylated nanogel and streptavidin-nanogel were synthesized.

2.4.2 Synthesis of Biotinylated Nanogel

Biotin was activated by treatment with N,N'-dicyclohexylcarbodiimide (DCC) and N-hydroxysuccinimide (NHS) in DMF for 3 hours at room temperature. After filtration, the remaining solution (12 ml) was poured into diethyl ether (100 ml) to precipitate out the activated biotin. Coupling of the activated biotin with nontoxic nanogel **28** was accomplished by adding a solution of 100 mg nanogel in 1 ml acetonitrile into 3 mg of activated biotin in 1 ml of DMF followed by stirring at 50 ºC for 24 hours. Dialysis with 1000 ml of 10% ethanol in diionized water at room temperature for 24 hours using a 12kDa-14kDa molecular weight cut off membrane gave the biotinylated nanogel as a single product. Rhodamine dye was attached to the biotinylated nanogel by following a previously described procedure.

Scheme 18. Synthesis of biotinylated Nanogel (**49**)

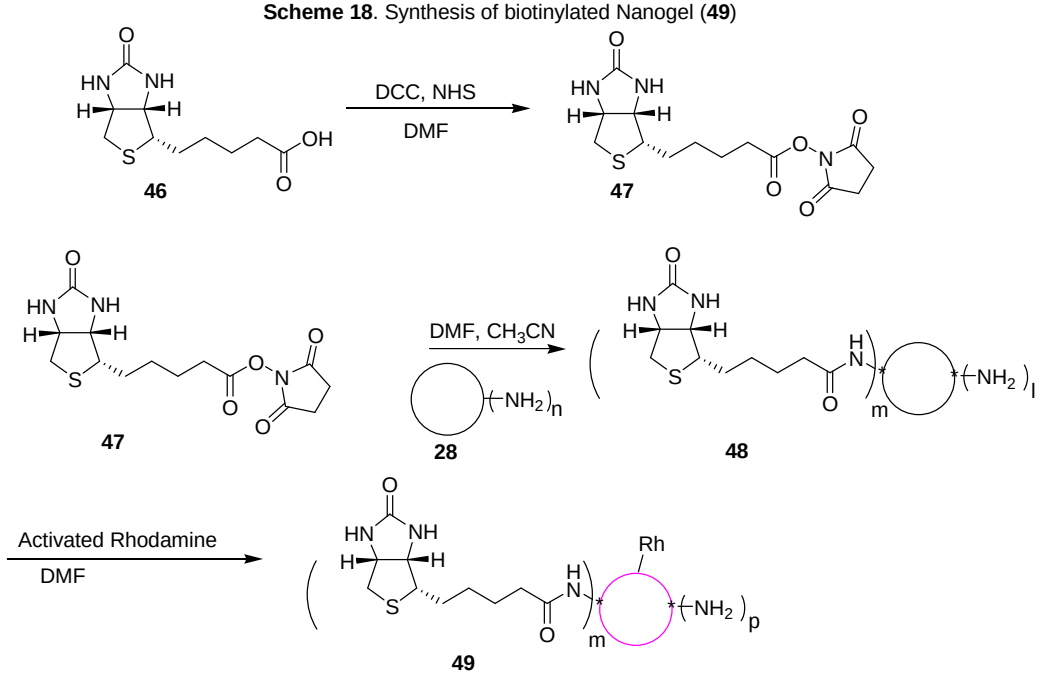

2.4.3 Synthesis of Nanogel-Streptavidin

Streptavidin maleimide was purchased from Acros, and its structure is shown below in Figure 24. The maleimide end can be attached to a thiol group that linkes to the nanogel. The amine end of the nanogel was firstly attached with a ligand that had carboxyl function group at one end and a protected thiol group at the other end.

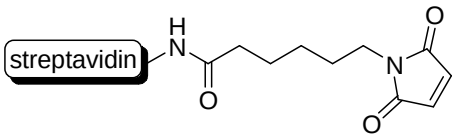

Streptavidin Maleimide (50)

Figure 24 Structure of streptavidin Maleimide

The conversion of 5-bromopentanoic acid to 5-(carbamimidoylthio) pentanoic acid was achieved by reacting 5-bromopentanoic acid with thiourea in refluxing acetone overnight.[53] The white solid product precipitated out of solution after the reaction was cooled down to room temperature. Washing with cold acetone gave desired compound as a pure product. 5-(carbamimidoylthio) pentanoic acid (**53**) reacted with sodium hydroxide at 90 ºC followed by acidic aqueous work up using sulfuric acid to

produce thiol compound **54** as the product. Since the thiol was not stable, it was protected with trityl (Trt) group using potassium hydroxide and triphenylmethyl chloride in ethanol to yield **55**.

Scheme 19 Synthesis of **55**

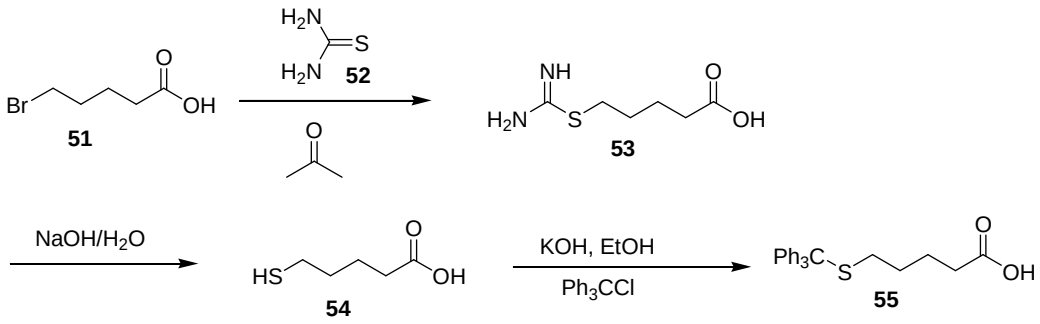

The carboxyl end of the thiol compound was directly attached to the nanogel using N, N'-dicyclohexylcarbodiimide (DCC) as a coupling reagent in dichloromethane. Thin layer chromatography (TLC) using 4:4:1 hexane: dichloromethane: diethyl ether as the elution solvent indicated the disappearance of UV active thiol compound **55** (R_f =0.4). A new UV active spot was formed which had a R_f=0.8. The dialysis in 10% of ethanol in water afforded the desired compound **56** as a white powder after lyophilization. Rhodamine dye was attached to the nanogel using freshly prepared activated rhodamine in DMF. Dialysis and lyophilizaion using an analogous procedure as described earlier gave compound **57** as a red powder.

Scheme 20. Synthesis of **57**

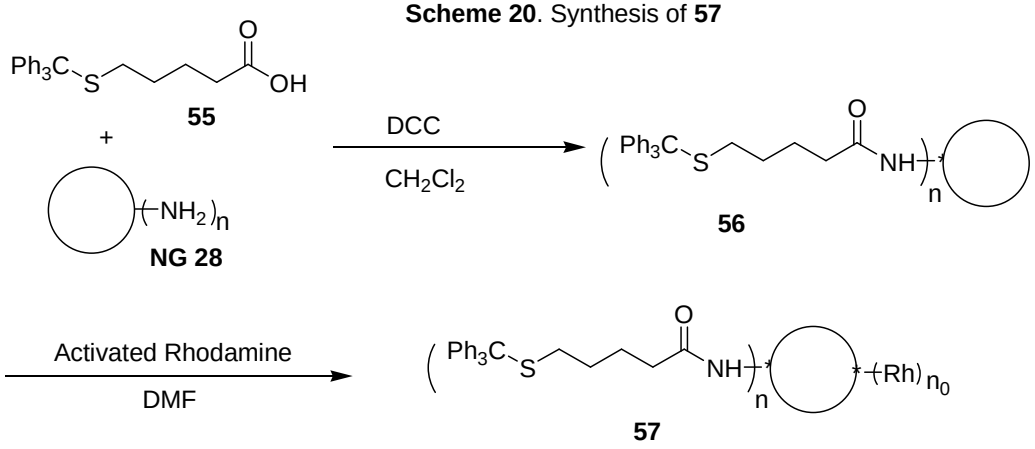

After the rhodamine was attached to the thio-nanogel, the next step involved deprotection of the thiol group and attachment of streptavidin. Compound **57** was treated with triisopropylsilane and trifluoroacetic acid in dichloromethane to remove the trityl group. The thiol intermediate was not isolated and was treated immediately with streptavidin maleimide. This was done due to the instability of thiol side chain. After the removal of solvent, the residue was dialyzed in a 10% of ethanol in water solution followed by lyophilization to give compound **59** as a pink powder.

Scheme 21. Synthesis of **59**

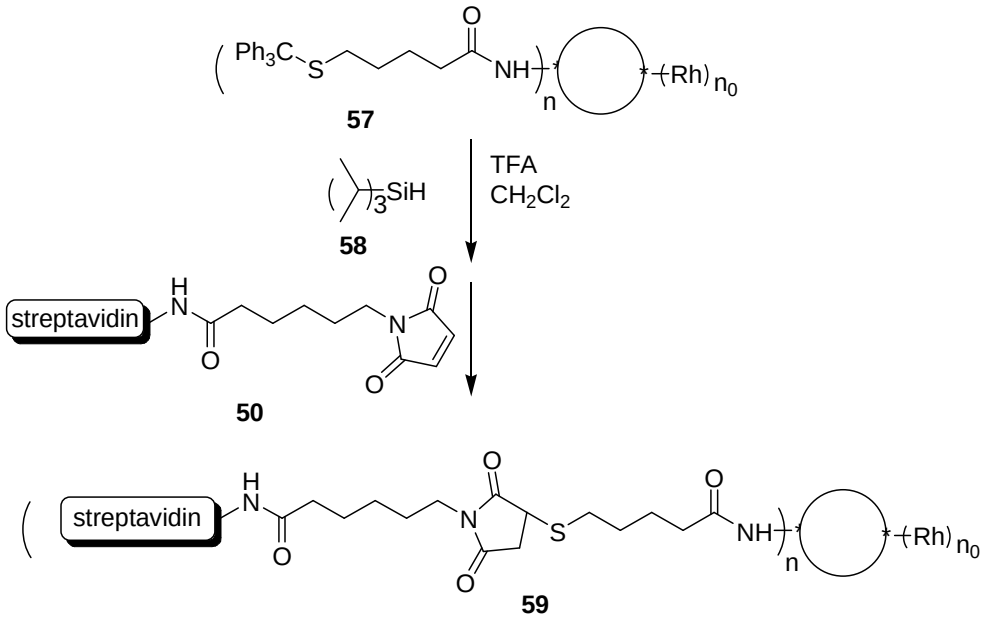

2.4.4 Results and Discussion

Stem cells were loaded with biotinylated nanogels. The results indicated that biotinylated nanogel (**49**) was not toxic against the stem cells. It could be served as a carrier for the anti-cancer drugs that target at the biotin receptor site of the cancer cells. However, biotinylated nangoel **49** can not internalize into the stem cells. Therefore, Nanogel-Streptavidin (**59**) was investigated.

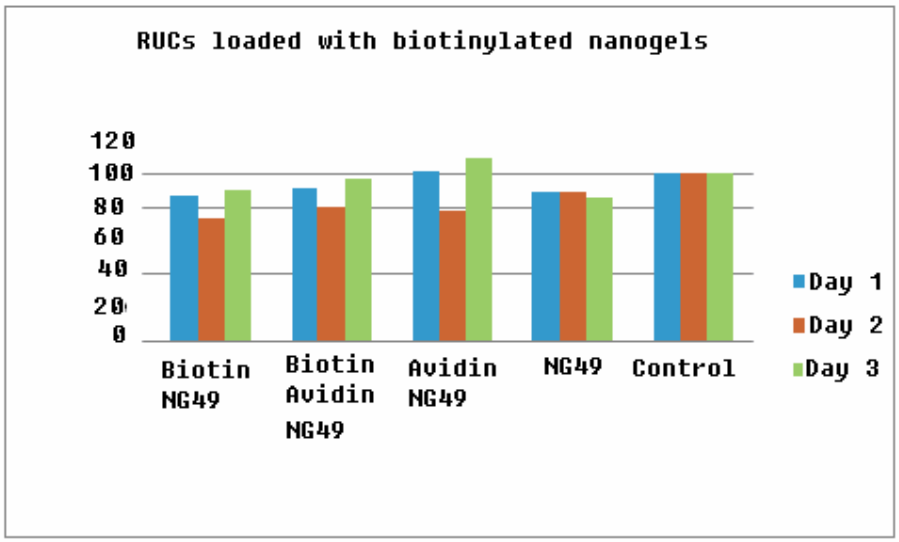

Figure 25 cell viabilities of RUCs loaded with biotinylated nanogels (**49**) RUCswere seeded in a 96 well plate and after reaching 70% confluency, the media was replaced with fresh medium containing nanogel **49** and/or biotin. Following incubation for 72 hours cell proliferation assays were performed every 24 hours.

Neural stem cells (NSC) were treated with Nanogel-Streptavidin (**59**). After 15 minutes, the confocal image was taken and the results indicated that the nanogels were loaded into the neural stem cells with a high loading efficiency. Figure 26 clearly shows the red nanogels internalized into the blue neural stem cells. When compared to all the type I and type II nanogels which took at least 12 hours to internalized into stem cells with a low loading efficiency, this type III nanogel had many benefits. Firstly, the much shorter loading time reduced the cytotoxicity of nanogels to the stem cells. Secondly, the shorter loading time also reduced the possibility of the release of anticancer drugs before reaching the tumor target. Since most of our nanogels would

release the drugs in about 2 days; a higher loading efficiency increased the loading ability of the stem cells and therefore decreases the drug dosage and minimizing the cytotoxicity of our nanogels.

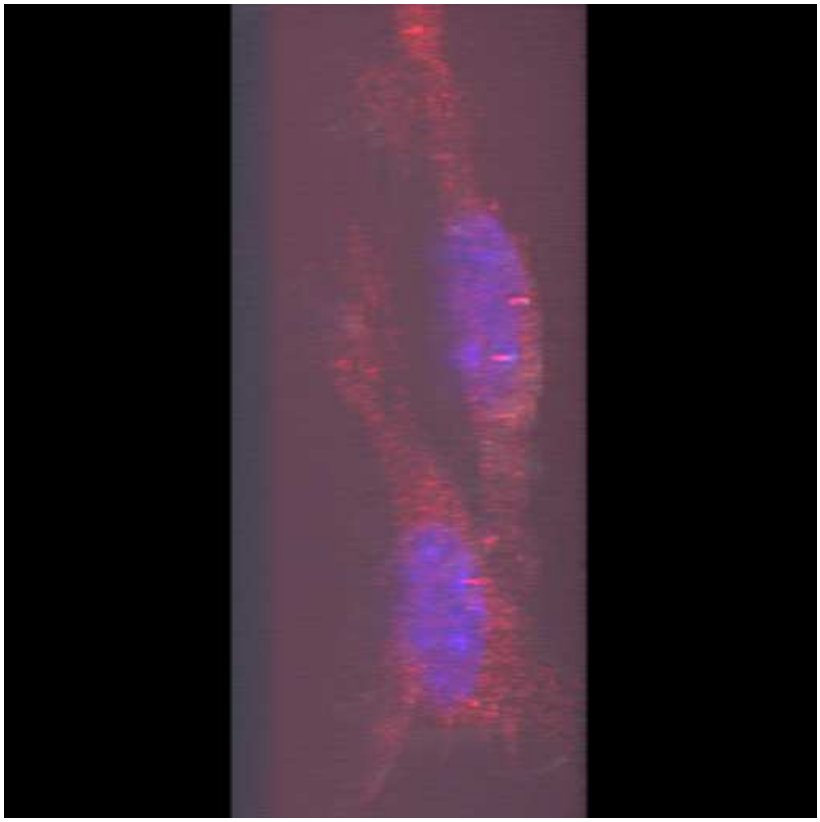

Figure 26 Stem cells (blue) loaded with nanogel-streptavidin (red) in 15mins

2.5 Conclusion

To deliver the anticancer drug to the cancer cells, a system that makes use of nontoxic nanogels and stem cells was developed. The nanogel served as a drug encapsulation material, and stem cells served as a targeting vehicle that could specifically target at the tumor site.

Type I nontoxic PEG-PEI nanogel was successful synthesized via a double treatment of PEI with activated PEG. The encapsulation of type I nanogel with anticancer drug (AQ10) enhanced the solubility of anticancer drug and consequently decreased the dosage. The sizes of the nanogel was characterized by AFM and found to be approximately 20 nm. This nanogel can be loaded into stem cells with low cytotoxicity and delivered to the tumor target.

To further enhance the toxicity, anticancer drug (SN38) was attached to the outside of Type II nanogel along with a tetrapeptide that cleavable by legumain as well as the encapsulation into inside of the nanogel. A tetra-peptide linker that can be recognized and cleaved by legumain to release the anticancer drug was attached. The results demonstrated a enhanced bioactivity against the cancer cells.

Streptavidin was attached to type III nanogels. Nanogel-Streptaividin can be loaded into neural stem cells within 15 minutes which significantly reduced the loading time compared to other nanogels.

The future work would be focused on the streptavidin nanogels (type III), new anticancer reagent will be encapsulated into type III nanogel and the bioactivities will be investigated.

2.6 References

1. Uversky, V. N.; Kabanov, A. V.; Lyubchenko, Y. L. Nanotools for Megaproblems: Probing Protein Misfolding Diseases Using Nanomedicine Modus Operandi. *J Proteome Res.* **2006**, *5*, 2505-2522.
2. Torchilin, V. Targeted pharmaceutical nanocarriers for cancer therapy and imaging. *AAPS J.* **2007**, *9*, E128-E147.
3. Cegnar, M.; Kristl, J.; Kos, J. Nanoscale polymer carriers to deliver chemotherapeutic agents to tumours. *Expert Opinion on Biological Therapy*. **2005**, *5*, 1557-1569.
4. Vinogradov, S. Colloidal microgels in drug delivery applications. *Curr Pharm Des.* **2006**, *12*, 4703-4712.
5. Vinogradov, S. V.; Batrakova, E. V.; Kabanov, A. V. Nanogels for oligo- nucleotide delivery to the brain. *Bioconjug. Chem.* **2004**, *15*, 50-60.
6. Vinogradov, S.V.; Bronich, T. K.; Kabanov, A. V. Nanosized cationic hydrogels for drug delivery: preparation, properties and interactions with cells. *Adv. Drug Deliv. Rev.* **2002**, *54*, 135-147.
7. Wang, J.; Mongayt, D.; Torchilin, V. P. Polymeric micelles for delivery of poorly soluble drugs: Preparation and anticancer activity in vitro of paclitaxel incorporated into mixed micelles based on poly (ethylene glycol)-lipid conjugate and positively charged lipids. *J. Drug Target* **2005**, *13*, 73-80.
8. Torchilin, V. Immunoliposomes and PEGylated immunoliposomes: possible use for targeted delivery of imaging agents. *Immunomethods.* **1994**, *4*, 244-258.
9. Winterhalter, M.; Lasic, D. D. Liposome stability and formation: Experimental parameters and theories on the size distribution. *Chem. Phys. Lipids.* **1993**, *64*, 35-43.
10. Torchilin, V. Recent advances with liposomes as pharmaceutical carriers. *Nat. Rev. Drug Discov.* **2005**, *4*, 145-160.
11. Elouahabi, A.; Ruysschaert, J. M. Formation and intracellular trafficking of lipoplexes and polyplexes. *Mol. Ther.* **2005**, *11*, 336-347.

12. Kerkis, A.; Hayashi, M.; Yamane, T.; Kerkis, I. Properties of cell penetrating peptides (CPPs). *IUBMB. Life.* **2006**, *58*, 7-13.

13. Sung, S.; Min, S.; Cho, K.; Lee, S.; Min, Y.; Yeom, Y.; Park, J. Effect of polyethylene glycol on gene delivery of polyethylenimine. *Biol. Pharm. Bull.* **2003**, *26*, 492-500.

14. Boussif, O.; Lezoualc'h, F.; Zanta, M. A.; Mergny, M. D.; Scherman, D.; Demeneix, B.; Behr, J. P. Lab. C. A versatile vector for gene and oligonucleotide transfer into cells in culture and in vivo: polyethylenimine. *PNAS.* **1995**, *92*, 7297-7301.

15. Goula, D.; Benoist, C.; Mantero, S.; Merlo, G.; Levi, G.; Demeneix, B. A. Polyethylenimine-based intravenous delivery of transgenes to mouse lung. *Gene Ther.* **1998**, *5*, 1291-1295.

16. Vinogradov, S. V.; Zeman, A. D.; Batrakova, E. V.; Kabanov, A. V. Polyplex Nanogel formulations for drug delivery of cytotoxic nucleoside analogs. *J. Control Release.* **2005**, *107*, 143-157.

17. Vinogradov, S. V.; Batrakova, E. V.; Li, S.; Kabanov, A. V. Mixed Polymer Micelles of Amphiphilic and Cationic Copolymers for Delivery of Antisense Oligonucleotides. *J. Drug Target.* **2004**, *12*, 517-526.

18. Dong, W.; Jin, G.; Li, S.; Sun, Q.; Ma, D.; Hua, Z. Cross-linked polyethylenimine as potential DNA vector for gene delivery with high efficiency and low cytotoxicity. *Acta. Biochim. Biophys. Sin. (Shanghai).* **2006**, *38*, 780-787.

19. Vinogradov, S. V.; Bronich, T. K.; Kabanov, A. V. Self-assembly of polyamine-poly (ethylene glycol) copolymers with phosphorothioate oligonucleotides. *Bioconjug. Chem.* **1998**, 9, 805-812.

20. Erbacher, P.; Bettinger, T.; Belguise-Valladier, P.; Zou, S; Coll, J. L.; Behr, J. P.; Remy, J. S. Transfection and physical properties of various saccharide, poly(ethylene glycol), and antibody-derivatized polyethylenimines (PEI). *Gene Med*. **1999**, *1*, 210-222.

21. Rachakatla, R. S.; Marini, F.; Weiss, M. L.; Tamura, M.; Troyer, D. Development of human umbilical cord matrix stem cell-based gene therapy for experimental lung tumors. *Cancer Gene Therapy.* 2007, *14(10)*, 828-835.

22. Perchellet, E. M.; Wang, Y.; Weber, R. L.; Sperfslage, B. J.; Lou, K.; Crossland, J.; Hua, D. H.; Perchellet, J. P. Synthetic 1,4-anth- racenedione analogs induce cytochrome c release, caspase-9, -3, and -8 activities, poly(ADP-ribose) polymerase-1 cleavage and inter- nucleosomal DNA fragmentation in HL-60 cells by a mechanism which involves caspase-2 activation but not Fas signaling. *Biochem. Pharmacol.* **2004**, *67*, 523-537.

23. Hua, D. H.; Lou, K.; Battina, S. K.; Zhao, H.; Perchellet, E. M.; Wang, Y.; Perchellet, J. P. Syntheses, molecular targets and antitumor activities of novel triptycene bisquinones and 1,4-anthracenedione analogs. *Anticancer Agents Med. Chem.* **2006**, *6*, 303-318.

24. Vinogradov, S. V.; Kohli, E.; Zeman, A. D. comparison of Nanogel Drug Carriers and their Formulations with Nucleoside 5'-Triphosphates. *Pharm. Res.* **2006**, *23*, 920-930.

25. Wall, M. E.; Wani, M. C.; Cook, C. E.; Palmer, K. H.; McPhail, A. I.; Sim, G.A. Plant antitumor agents. I. The isolation and structure of camptothecin, a novel alkaloidal leukemia and tumor inhibitor from camptotheca acuminate. *J. Am. Chem. Soc.* **1966**, *88*, 3888-3890.

26. Gottlieb, J. A.; Guarino, A. M.; Call, J. B.; Oliverio, V. T.; Block, J. B. Preliminary pharmacologic and clinical evaluation of camptothecin sodium. *Cancer Chemother. Rep.* **1970**, *54*, 461-470.

27. Pommier, Y. Topoisomerase I inhibitors: camptothecins and beyond. *Nat. ReV. Cancer.* **2006**, *6*, 789-802.

28. Pommier, Y.; Redon, C.; Rao, V. A.; Seiler, J. A.; Sordet, O.; Takemura, H.; Antony, S.; Meng, L.; Liao, Z.; Kohlhagen, G. Repair of and checkpoint response to topoisomerase I-mediated DNA damage. *Mutat. Res.* **2003**, *532*, 173-203.

29. Ulukan, H.; Swaan, P. W. Camptothecins, a review of their chemotherapeutical potential. *Drugs.* **2002**, *62(2)*, 2039-2057.

30. Lu, A. J.; Zheng, Z. S.; Zou, H. J.; Luo, X. M.; Jiang, H. L. 3D-QSAR study of 20 (S)-camptothecin analogs. *European Journal of Medicinal Chemistry.* **2007**, *42(4)*,

307-314.

31. Zhang, J. A.; Xuan, T.; Parmar, M.; Ma, L.; Ugwu, S.; Ali, S.; Ahmad, I. Development and characterization of a novel liposome-based formulation of SN-38. *Int. J. Pharm.* **2004**, *270*, 93-107.

32. Chabot, G. G. Clinical pharmacokinetics of irinotecan. *Clin. Pharmacokinet.* **1997**, *33*, 245-259.

33. Senter, P. D.; Beam, K. S.; Mixan, B.; Wahl, A. F. Identification and activities of human carboxylesterases for the activation of CPT-11, a clinically approved anticancer drug. *Bioconjugate Chem.* **2001**, *12*, 1074-1080.

34. Slatter, J. G.; Schaaf, L. J.; Sams, J. P.; Feenstra, K. L.; Johnson, M. G.; Bombardt, P. A.; Cathcart, K. S.; Verburg, M. T.; Pearson, L. K.; Compton, L. D. Miller, L. L.; Baker, D. S.; Pesheck, C. V.; Lord, R. S. Pharmacokinetics, metabolism, and excretion of irinotecan (CPT-11) following i.v. infusion of [14C]CPT-11 in cancer patients. *Drug Metab. Dispos.* **2000**, *28*, 423-433.

35. Mathijssen, R. H. J.; Van Alphen, R. J.; Verweij, J.; Loos, W. J.; Nooter, K.; Stoter, G.; Sparreboom, A. Clinical pharmacokinetics and metabolism of irinotecan (CPT-11). *Clin. Cancer Res.* **2001**, *7*, 2182-2194.

36. Smith, N. F.; Figg, W. D.; Sparreboom, A. Pharmacogenetics of irinotecan metabolism and transport: an update. *Toxicol. In Vitro.* **2006**, *20*, 163-175.

37. Zhao, H.; Rubio, B.; Sapra, P.; Wu, D.; Reddy, P.; Sai, P.; Martinez, A.; Gao, Y.; Lozanguiez, Y.; Longley, C.; Greenberger, L. M.; Horak, I. D. Novel Prodrugs of SN38 Using Multiarm Poly(ethylene glycol) Linkers. *Bioconjugate Chem.* **2008**, 19 (4), 849-859.

38. Wu, W.; Luo, Y.; Sun, C.; Liu, Y.; Kuo, P.; Varga, J.; Xiang, R.; Reisfeld, R.; Janda, K. D.; Edgington, T. S.; Liu, C. Targeting Cell-Impermeable Prodrug Activation to Tumor Microenvironment Eradicates Multiple Drug-Resistant Neoplasms. *Cancer Res.* **2006**, *66(2)*, 970-980.

39. Ishii S. Legumain: asparaginyl endopeptidase. *Methods Enzymol.* **1994**, *244*, 604-615.

40. Kembhavi, A. A.; Buttle, D. J.; Knight, C. G.; Barrett, A. J. The two cysteine

endopeptidases of legume seeds: purification and characterization by use of specific fluorometric assays. *Arch Biochem Biophys.* **1993**, *303*, 208-213.

41. Schlereth, A.; Becker, C.; Horstmann, C.; Tiedemann, J.; Muntz, K. Comparison of globulin mobilization and cysteine proteinases in embryonic axes and cotyledons during germination and seedling growth of vetch (Vicia sativa L.). *J. Exp. Bot.* **2000**, *51*, 1423-1433.
42. Chen, J. M.; Dando, P. M.; Rawlings, N. D. Cloning, isolation, and characterization of mammalian legumain, an asparaginyl endopeptidase. *J. Biol. Chem.* **1997**, *272*, 8090-8098.
43. Liu, C.; Sun, C.; Huang, H.; Janda, K.; Edgington, T. Overexpression of legumain in tumors is significant for invasion/metastasis and a candidate enzymatic target for prodrug therapy. *Cancer Res.* **2003**, *63*, 2957-2964.
44. Alvarez-Fernandez, M.; Barrett, A. J.; Gerhartz, B.; Dando, P. M.; Ni, J.; Abrahamson, M. Inhibition of mammalian legumain by some cystatins is due to a novel second reactive site. *J. Biol. Chem.* **1999**, *274*, 19195-19203.
45. Folkman, J. Angiogenesis in cancer, vascular, rheumatoid and other disease. *Nat. Med.* **1995**, *1*, 27-31.
46. Mochizuki, H.; Oikawa, Y.; Yamada, H.; Kusakabe, S.; Shiihara, T.; Murakami, K.; Kato, K.; Ishiguro, J.; Kosuzume, H. Antibacterial and pharmacokinetic properties of M14659, a new injectable semisynthetic cephalosporin. *J. Antibiotics.* **1987**, *3*, 377-391.
47. Yang, W.; Cheng, Y.; Xu, T.; Wang, X.; Wen, L. Targeting cancer cells with biotin-dendrimer conjugates. *European J. Medicinal Chem.* **2009**, *44*, 862-868.
48. Russell-Jones, G.; McTavish, K.; McEwan, J.; Vitamin-mediated targeting as a potential mechanism to increase drug uptake by tumors. *J. Inorg. Biochem.* **2004**, *98*, 1625-1633.
49. Marek, M.; Kaiser, K.; Gruber, H.J. Biotin-pyrene conjugates with poly (ethylene glycol) spacers are convenient fluorescent probes for avidin and streptavidin. *Bioconjugate. Chem.* **1997**, *8*, 560-566.
50. Cannizzaro, S. M. A novel biotinylated degradable polymer for cellinteractive

applications. *Biotechnol. Bioeng*. **1998**, *58*, 529-535.

51. Na, K. Self-assembled nanoparticles of hydrophobically-modified polysaccharide bearing vitamin H as a targeted anti-cancer drug delivery system. *Eur. J. Pharm. Sci.* **2003**, *18*, 165-173.
52. Laitinen, O. H.; Hytonen, V. P.; Nordlund, H. R.; Kulomaa, M. S. Genetically engineered avidins and streptavidins. *Cell Mol Life Sci.* **2006**, *63(24)*, 2992-3017.
53. Han, S.; Moore, R. A.; Viola, R. E. Synthesis and evaluation of alternative substrates of arginase. *Bioorganic Chemistry*. **2002**, *30*, 81-94.

2.7 Experimental Section

Separation of PEI

A chromatographic column was packed using Sephacryl S200, flashed with deionized water. 7.0 g (0.28 mmol) of PEI (MW ~25 kDa) was dissolved in 20 ml of deionized water and loaded to the column. Deionized water was used as eluant by gravity, no additional pressure was applied. After 6 hours, the middle fractions were collected to give 3.64 g (0.146 mmol) of PEI (MW ~25 kDa). ^{1}H NMR (D_2O) δ 2.72 (bs, CH_2N), 2.68 (bs, CH_2N); the number of hydrogens cannot be determined from integration due to the overlap of two signals above.

Activation of PEG

To a solution of 2.0 g (0.25 mmol) of PEG (MW 8 kDa) in 7 mL of dry acetonitrile under argon was added 0.41 g (2.5 mmol) of 1,1'-carbonyldiimidazole, and the solution was stirred at 40^{o}C for 2 hours. The crude product was purified by dialysis using a MWCO 3500 Dalton membrane twice with 1000 mL of 10% ethanol in deionized water at 4^{o}C for 4 hours. The solution was lyophilized to give 1.84 g of activated PEG. ^{1}H NMR ($CDCl_3$) δ 7.69 (s, 1 H, ArH), 7.11 (s, 2 H, ArH), 3.62 (s, 190 H, CH_2O).

Preparation of nanogel PEG-PEI (28)

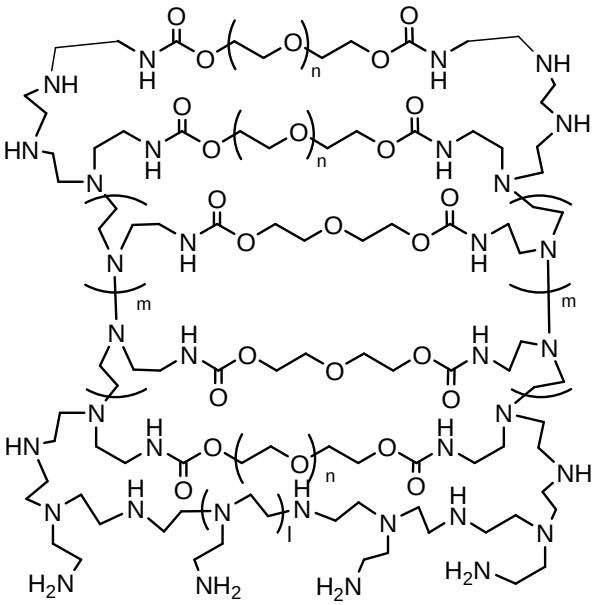

Nanogel PEI-PEG(1:6.8) NG

28

Nanogel (polyethyleneglycol)-(polyethylenimine) [NG(PEG)(PEI)] (the molecular weight of PEG is ~8 kDa and that of PEI is ~25 kDa) was prepared by following a similar micellar method (Vinogradov et al., 2006) starting from activated polyethylene glycol (activation with 1,1'-carbonyldiimidazole; ~125 μmol were used) and polyethylenimine (PEI; ~40 μmol were used) (Scheme 1). To a solution of 1.0 g (40 μmol) of PEI (MW ~25 kDa) in 300 mL of deionized water was added dropwise a solution of 1.0 g (125 μmol) of activated PEG (MW ~8 kDa) in 2 mL of dichloromethane. The solution turned to a white suspension due to the heterogeneous solvent system. The white suspension was sonicated in a water bath for 15 minutes; longer sonication did not improve the quality of nanogel. The organic solvent dicholoromethane was removed on a rotary evaporator resulting in a transparent solution. The solution was dialyzed with a 12K – 14K MWCO membrane in 1000 mL of 10% ethanol in deionized water for 1 day at 25^{o}C and lyophilized to give nanogel PEG-PEI. This nanogel was again treated with 1.0g (125 μmol) of activated PEG in 2 mL of dichloromethane and worked up as that mentioned above to give 1.32 g of nanogel PEG-PEI as a white powder. ^{1}H NMR (D_2O) δ 3.70 (s, area 44, CH_2O),

3.40 – 2.60 (m, area 6.5, CH_2N). Based on the weight of the product, we estimate that the molecular weight of the nanogel is ~33 KDa (for each mole of PEI, one mole of PEG is added). The initial treatment of PEI with activated PEG provided a partial cross-linkage of PEG, in which for each mole of PEI, there is ~ 0.5 mole of PEG attached. This partial linking PEG-PEI is toxic to stem cells.

Synthesis of aceterylated nanogel PEG-PEI (27)

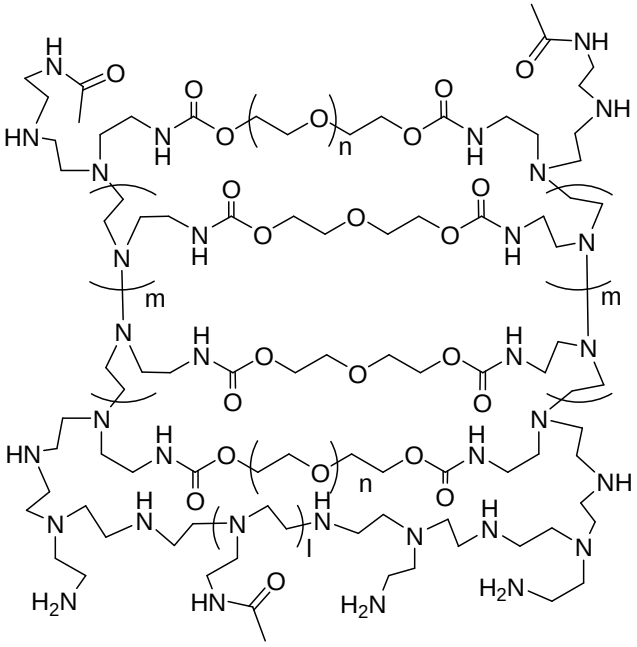

27 Aceterylated Nanogel Ac-NG

To a solution of 100 mg 1:4 ratio of CH2N:CH2O nanogel in 1 ml acetonitrile under argon, was added 200 µL of acetic anhydride at room temperature. The resulting was stirred at 50°C for 12 hours, cooled to 25°C, dialyzed with a 12k – 14 kDa MWCO membrane in 100 ml of 10% ethanol in deionized water at room temperature for 1 day, and lyophilized to give 103 mg of aceterylated nanogel as a white powder.

Synthesis of nanogel PEG-PEI-rhodamine(29)

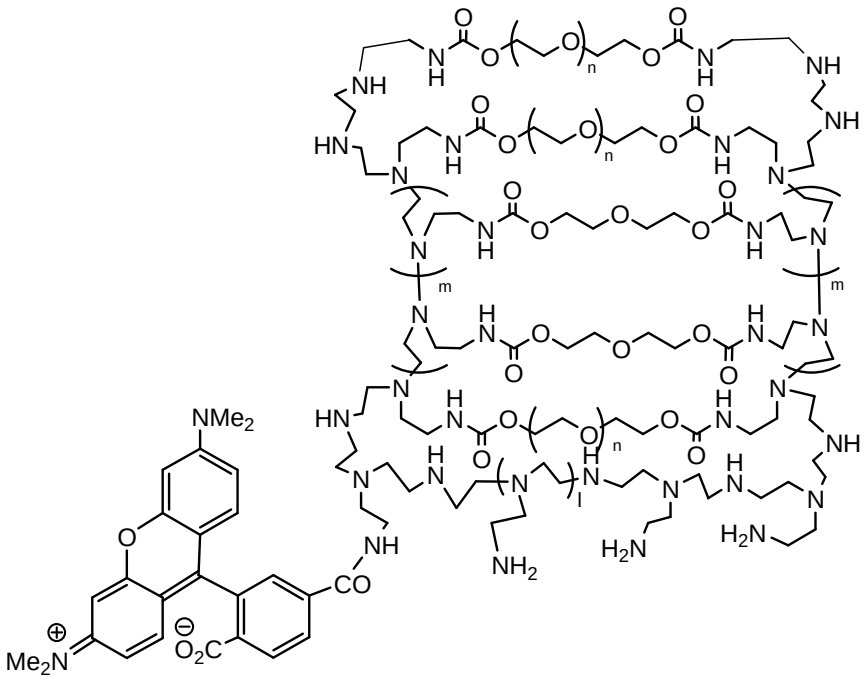

To A mixture of 15 mg (32 μmol) of 6-Carboxytetramethylrhodamine (TAMRA), 6.52 mg (48 μmol) of HOBT, 9.9 mg (48 μmol) of DCC and 4.44 mg (39 μmol) of *N*-hydroxysuccinimide under argon, 1 mL of dry DMF was added via syringe at 25°C. The resulting solution was stirred at 50-55°C for 2.5 hours, cooled to room temperature, and added a solution of 400 mg of nanogel PEG-PEI in 1mL of dry acetonitrile. The solution was stirred at 40°C for 12 hours, cooled to 25°C, dialyzed with a 12k - 14kDa MWCO membrane in 1000 ml of 10% ethanol in deionized water at room temperature for 1 day, and lyophilized to give 186 mg of PEG-PEI-rhodamine as a pink powder. ^{1}H NMR (D_2O) δ 8.50 (s, area 0.03), 8.10 (m, area 0.015), 7.90 (m, area 0.015), 7.73 (m, area 0.015), 7.37 (m, area 0.06), 3.70 (s, area 100, CH_2O), 3.20 – 2.60 (m, area 14.7, CH_2N). UV-vis (H_2O), λ_{max} = 557 nm and ε_{max} = 1.57 x 10^4 M^{-1}•cm^{-1} (assuming the MW ~33 KDa).

Inclusion of AQ10 (1%) in Nanogel PEG-PEI-rhodamine

AQ10

AQ10-NG-Rh

31

To a solution of 50 mg of PEG-PEI-rhodamine in 5 mL of deionized water, was added 0.5 mg (2.1 μmol) of AQ10 in 1 mL of acetonitrile. The resulting solution was lyophilized to give 50.5 mg of PEG-PEI-rhodamine-AQ10 as a pink powder. Inclusion of 5% AQ10 was done by the similar method describe above.

TBDPS-SN38 (36)

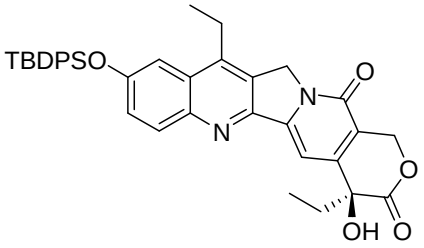

To a suspension of 60 mg (0.15 mmol) SN38 in 10 ml distilled dichloromethane under argon, were added 300 μL t-butyl-diphenylsilyl chloride and 300 μL triethylamine at room temperature. The reaction was heated up to reflux for 12 hours. A greenish solution was resulted. After cooled down to room temperature, the solution was diluted with 20 ml dichloromethane and washed with 20 ml 0.1N HCl, 20 ml 1% sodium bicarbonate, 20 ml water and 20 ml brine respectively. The organic layer was dried over $MgSO_4$ and concentrated. Crude product was purified by a silica gel column chromatography using 80:2 dichloromethane and methanol as eluants to give 96 mg (100%) of compound 2.2 : ^{1}H NMR(400 MHz, $CDCl_3$): δ (t, J=7.6Hz, 3H), 1.02 (t, J=7.4Hz, 3H), 1.18(s, 9H), 1.83-1.93(m, 2H), 2.64(q, J=7.6Hz, 2H), 3.68(s, 1H), 5.12(s, 2H), 5.26(d, J=15.6Hz, 1H), 5.71(d, J=16.4Hz, 1H), 7.08(d, J=2.5Hz, 2H), 7.35-7.49(m, 7H), 7.57(s, 1H), 7.76-7.78(m, 4H), 8.05(d, J=9.2Hz, 1H).

TBDPS-SN38-Gly-Boc (37)

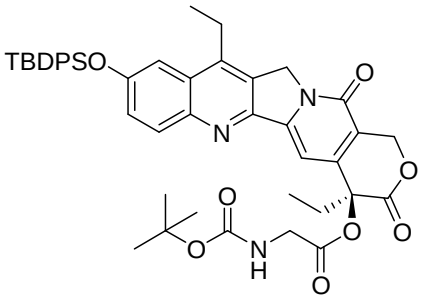

To a solution of 75 mg (0.12 mmol) of compound 2.2 and 42 mg (0.24 mmol) of Boc-Gly-OH in 5 ml distilled dichloromethane under argon at 0□, were added 46 mg (0.24 mmol) of N-ethyl-N'- (3-dimethylaminopropyl)carbodiimide hydrochloride (EDC) and 8 mg (0.06 mmol) of 4-Dimethylaminopyridine (DMAP). The solution was stirred at 0□ for 12 hours. After warm up to room temperature, the solution was diluted with 20 ml of dichloromethane, and then washed with 1% sodium bicarbonate, water, 0.1N HCl and water respectively. The organic layer was washed with brine and dried over $MgSO_4$, concentrated and vacuum dried to give 90 mg (96%) of compound **37**: ^{1}H NMR(400 MHz, $CDCl_3$): δ 0.88 (t, J=7.8Hz, 3H), 0.96 (t, J=7.6Hz, 3H), 1.18(s, 9H), 1.40(s, 9H), 2.10-2.31(m, 2H), 2.65 (q, J=7.6Hz, 2H), 3.64 (s, 2H), 5.10 (d, J=1.9Hz, 2H), 5.37 (d, J=17.0Hz, 1H), 5.66(d, J=17.0Hz, 1H), 7.08 (s, 1H), 7.12 (d, J=2.4Hz, 1H), 7.37-7.50 (m, 7H), 7.75(d, J=6.6Hz, 4H), 8.02 (d, J=9.2Hz, 1H).

TBDPS-SN38-Gly (38)

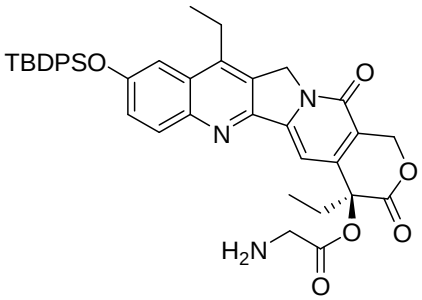

A solution of 75 mg (0.1 mmol) compound **37** in 2M HCl in dioxane under argon was stirred at room temperature for 1 hour. Saturated aqueous sodium bicarbonate solution was added until basic after the reaction was done. The aqueous solution was extracted with dichloromethane 3 times. The organic extract was washed with brine, dried ($MgSO_4$), and concentrated to give 65 mg (99%) of compound **38**: ^{1}H NMR(400 MHz,

$CDCl_3$): δ 0.89 (t, J=7.8Hz, 3H), 0.96 (t, J=7.6Hz, 3H), 1.17(s, 9H), 2.15-2.31(m, 2H), 2.65 (q, J=7.6Hz, 2H), 3.64 (s, 2H), 5.10 (d, J=1.9Hz, 2H), 5.37 (d, J=17.0Hz, 1H), 5.66(d, J=17.0Hz, 1H), 7.08 (s, 1H), 7.12 (d, J=2.4Hz, 1H), 7.36-7.50 (m, 7H), 7.75(d, J=6.6Hz, 4H), 8.02 (d, J=9.2Hz, 1H).

TBDPS-SN38-Gly-Succinyl (39)

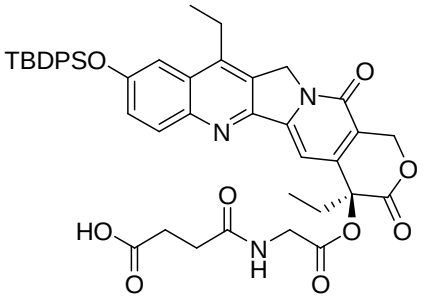

A solution of 50 mg (0.07 mmol) of compound **38** and 11 mg (0.1 mmol) of succinic anhydride in 3 ml distilled dioxane under argon was heated up to 90□ for 1 hour. After cooled down to room temperature, the solution was diluted with 20 ml of 0.1N HCl, and then extracted with ethyl acetate 4 times. The organic extract was washed with brine, dried ($MgSO_4$), concentrated and column chromatographed on silica gel using 15:1 dichloromethane and methanol to give 55 mg (96% yield) of compound **39** : ^{1}H NMR(400 MHz, $CDCl_3$): δ 0.89 (t, J=7.6Hz, 6H), 1.17(s, 9H), 2.19-2.38 (m, 2H), 2.60-2.70 (m, 6H), 4.07-4.20 (m, 2H), 5.11 (s, 2H), 5.39 (d, J=17.1Hz, 1H), 5.60 (d, J=17.2Hz, 1H), 7.12 (d, J=2.4Hz, 1H), 7.36-7.50 (m, 7H), 7.75(d, J=6.8Hz, 4H), 8.12 (d, J=9.4Hz, 1H); ^{13}C NMR(200MHz, $CDCl_3$) δ 7.58, 13.38, 19.64, 23.14, 26.60, 30.10, 31.07, 32.12, 41.75, 49.37, 67.43, 97.11, 110.53, 120.51, 126.70, 127.14, 128.21, 130.46, 132.07, 135.59, 144.18, 144.77, 145.46, 146.36, 149.23, 155.41, 157.36, 167.58, 168.63, 171.08, 172.33, 175.68; HRMS calcd for $C_{44}H_{45}N_3O_9SiNa$ ($M+Na^+$) 810.2822, found 810.2829.

Resin-Tetrapeptide(Ala-Ala-Asn-Leu) (41)

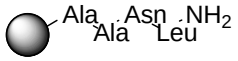

To a reaction vessel with 2.4 g (0.2mmol) of Fmoc-Ala-NovaSyn TGA (resin) was added 14 ml 20% of piperidine in DMF at room temperature. The reaction vessel was set down to the Discover Microwave Peptide Synthesizer. Select and run the deprotection program (Temp=75°C, Power=50 W, Time=3 min) twice. After cooled down to 50°C, solvent was filtrated and the residue in reaction vessel was washed with 80 ml of DMF. A freshly prepared solution of 312 mg (1.0 mmol) of Fmoc-Ala-OH, 380 mg (1.0 mmol) of HBTU (O-Benzotriazole N,N,N',N'-tetramethyl uronium hexafluoro phosphate) and 0.33 ml diisopropylethyl amine in 8 ml of DMF was added to the reaction vessel with deprotected resin alanine inside. Select and run the coupling program (Temp=75°C, Power=25W, Time=5min) twice. After cooled down to 50°C, filter off the solvent and wash the solid with 80 ml DMF. Fmoc-Asn(Trt)-OH and Fmoc-Leu-OH were attached to the resin similarly by following the same deprotection and coupling procedure. After the final deprotection of Fmoc at the leucine end, the solvent was removed and resin-peptide was washed with 80 ml of dichloromethane instead of DMF.

Tetrapeptide-SN38 (**43**)

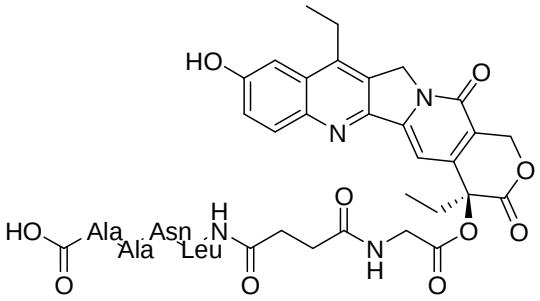

To a reaction vessel with 0.05 mmol resin-peptide, were added a freshly prepared solution of 45 mg (0.06 mmol) compound **39** and 190 mg (0.5 mmol) of HBTU in 10 ml DMF and 500 μL diisopropylethyl amine. The reaction vessel was put in the microwave peptide synthesizer. Run the SN38 program (Temp=80°C, Power=60 W, Time=60 min). The yellow solution turned to brown after cooled down to 50°C. The organic solution was filtered off; and the resin solid was washed with 100 ml of

dichloromethane. A freshly prepared cleavage solution with 250 µL of triisopropylsilane and 250 µL of water in 9.5 ml trifloroacetic acid was added to the reaction vessel. Run the cleavage program (Temp=38°C, Power=20W, Time=18 min). After cooled down to room temperature, the cleavage solution was collected by filtration; and the resin solid was washed with 4 ml of dichloromethane twice which was combined to the cleavage solution. The solvent was removed on the rota-vapor. A silica gel column chromatography using hexane, ethyl acetate and methanol as solvents gave 30 mg of compound **43** as a yellow solid. ^{1}H NMR (400 MHz, $CDCl_3$) δ 0.90 (t, J=7.6Hz, 3H), 0.98 (t, J=7.4Hz, 3H), 1.11-1.33 (m, 6H), 1.18 (s, 9H), 1.50-1.73 (m, 6H), 1.87 (m, 2H), 2.04-2.23 (m, 2H), 2.63 (m, 8H), 3.59 (m, 2H), 4.07 (m, 2H), 4.14-4.37 (m, 2H), 5.13 (s, 2H), 5.33 (d, J=17.1Hz, 1H), 5.63 (d, J=17.2Hz, 1H), 7.12 (d, J=2.4Hz, 1H), 7.36-7.50 (m, 7H), 7.75(d, J=6.8Hz, 4H), 8.18 (s, 1H).

Nanogel-Tetrapeptide-SN38 (44)

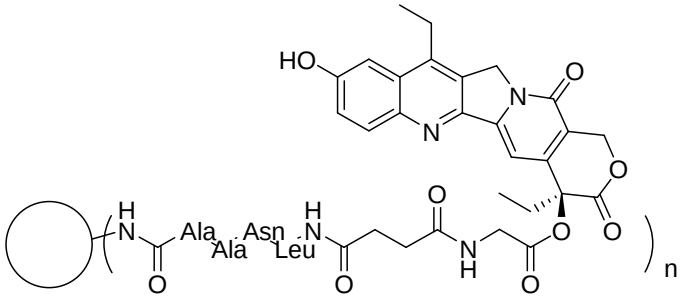

To a solution of 20 mg (0.017 mmol) of peptide-SN38, 16 mg (0.083 mmol) of N-ethyl-N'-(3-dimethylamino- propyl) carbodiimide hydrochloride (EDC) and 16 mg (0.131 mmol) of 4-Dimethylaminopyridine (DMAP) in 10 ml of dichloromethane at 0°C under argon, was added 60 mg of nanogel **28** (PEG:PEI=6.8:1, nontoxic). The solution was stirred at 0°C for 4 hours and then heated up to 40°C for 12 hours. After cooled down to room temperature, the solvent was removed on a rota-vapor. The residue was dissolved again in 5 ml of ethanol and dialyzed in 1000 ml of 10% ethanol in water at room temperature for 24 hours using a 3500 Dalton molecular weight cut off membrane. Lyophilization gave 70 mg of compound **44**. ^{1}H NMR (400 mHz, D_2O) δ 0.9–1.4 (m, CH_3 of amino acids and SN38, t-butyl of SN38), 1.9-2.1 (m, CH-C=O of

amino acids and SN38), 2.4-3.2 (m, CH_2 of PEI and SN38), 3.6-3.9 (m, CH_2 of PEG), 6.8-6.9 (Ar-H), 7.2 (Ar-H).

Nanogel-SN38-Tetrapeptide-SN38 (45)

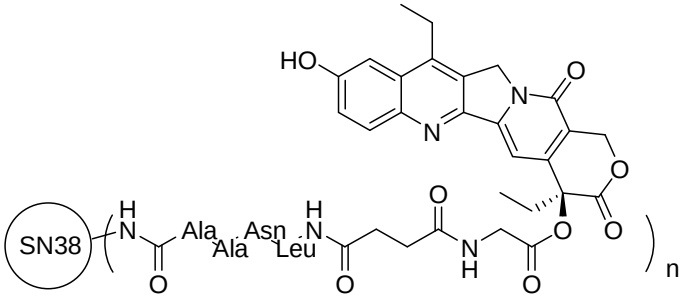

To a solution of 60 mg compound in 15 ml of diionized water, was added a suspension of 3 mg (5% by weight to nanogel) of SN38 in 2 ml of ethanol. The combined solution was stirred for 1 minute and lyophilized immediately to give 63 mg of product. ^{1}H NMR (400 MHz, D_2O) δ 0.9−1.4 (m, CH_3 of amino acids and SN38, t-butyl of SN38), 1.9-2.1 (m, CH-C=O of amino acids and SN38), 2.4-3.2 (m, CH_2 of PEI and SN38), 3.6-3.9 (m, CH_2 of PEG), 6.8-6.9 (Ar-H), 7.2 (Ar-H).

Activation of Biotin (47)

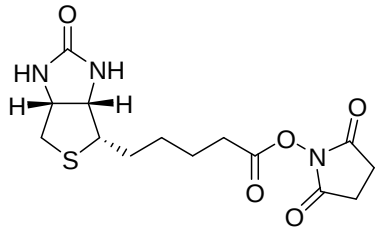

To a solution of 400 mg (1.64 mmol) biotin in 12 ml of DMF, 200 mg (1.74 mmol) of DCC and 340 mg (1.65 mmol) of NHS were added at room temperature under argon. The mixture was stirred at room temperature for 3 hours. White precipitates came out and was filtered off to obtain a transparent solution. 100 ml of diethyl ether was added to the crude solution to precipitate out the activated biotin. After dried under vacuum for 24 hours, 390 mg (70%) of activated biotin was obtained. ^{1}H NMR (200 MHz, DMSO-D_6) δ 1.43-1.64 (m, 6H, CH_2-C), 2.67 (t, J=7.3Hz, 2H), 2.81 (s, 4H), 3.11 (d, J=11.7Hz, 2H), 3.35 (s, 1H), 4.15 (d, J=4Hz, 1H), 4.27 (t, J=4.8Hz, 1H), 6.39 (s, 1H,

N-H), 6.45 (s, 1H, N-H).

Biotinylated Nanogel (48)

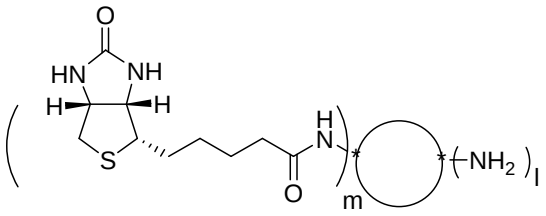

To a solution of 100 mg nontoxic nanogel **28,** a solution of 3 mg (8.8 µmol) of activated biotin in 1 ml of DMF was added at room temperature under argon. The mixture was stirred at 50°C for 24 hours, dialyzed with 1000 ml of 10% ethanol in diionized water at room temperature using a 12kDa-14kDa molecular weight cut off membrane, and lyophilized to give 98 mg of biotinylated nanogel as a light green powder. ^{1}H NMR (400 MHz, D_2O) δ 0.88 (CH_2), 1.09 (CH_2), 2.60-2.95 (CH_2-N), 3.70-3.98 (CH_2-O), 7.12 (s, N-H), 7.48 (s, N-H).

Rhodamine attached Biotinylated Nanogel (49)

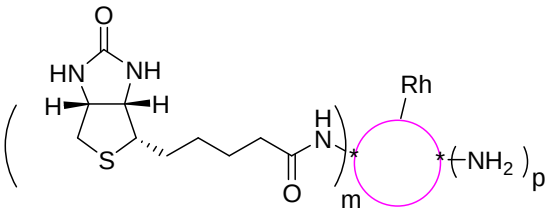

52

Activated rhodamine dye was attached to the biotinylated nanogel by following a similar procedure described above.

To A mixture of 15 mg (32 µmol) of 6-Carboxytetramethylrhodamine (TAMRA), 6.52 mg (48 µmol) of HOBT, 9.9 mg (48 µmol) of DCC and 4.44 mg (39 µmol) of *N*-hydroxysuccinimide under argon, 1 mL of dry DMF was added via syringe at 25^{o}C. The resulting solution was stirred at 50-55^{o}C for 2.5 hours, cooled to room temperature, and added a solution of 100 mg of biotinylated nanogel (**48**) in 1mL of dry acetonitrile. The solution was stirred at 40^{o}C for 12 hours, cooled to 25^{o}C, dialyzed with a 12k - 14kDa MWCO membrane in 1000 ml of 10% ethanol in deionized water at room

temperature for 1 day, and lyophilized to give 100 mg of PEG-PEI-rhodamine as a pink powder.

5-(carbamimidoylthio) pentanoic acid[53] (53)

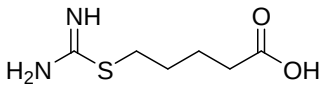

To a solution of 3.0 g (16.6 mmol) of 5-bromopentanoic acid in 150 ml of distilled acetone, was added 0.6 g (7.9 mmol) of thiourea at room temperature. The solution was heated up to reflux for 12 hours. White precipitates came out when cooled down to room temperature. The solvent solution was filtered off; and the remaining white solid was washed with cold acetone. 1.3 g (93.5%) of 5-(carbamimidoylthio) pentanoic acid was obtained. ^{1}H NMR (200MHz, DMSO-D_6) δ 1.55 (t, J=3.3Hz, 4H), 2.23 (t, J=6.6Hz, 2H), 3.17 (t, J=6.6Hz, 2H), 8.99 (d, J=22.3H, 3H); ^{13}C NMR δ 174.34, 170.00, 33.03, 29.97, 28.00, 23.34.

5-mercaptopentanoic acid (54)

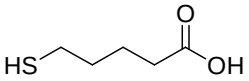

To a solution of 1.2 g (6.8 mmol) of 5-(carbamimidoylthio) pentanoic acid in 13 ml of water, was added 4.08 g (102 mmol) of sodium hydroxide at room temperature. The solution was heated up to reflux for 24 hours. After the solution cooled down to room temperature, 2M sulfuric acid was added until acidic (pH=2). The solution was extracted with dichloromethane 4 times; the combined organic extract was washed with sodium thiosulfate and brine, and then dried over magnesium sulfate. The solvent was removed on rota-vapor to give 720 mg (79%) of 5-mercaptopentanoic acid. ^{1}H NMR (200MHz, $CDCl_3$) δ 1.32 (t, J=6.9Hz, 1H, SH), 1.60-1.80 (m, 4H, 2CH_2), 2.37 (t, J=6.9Hz, 2H, CH_2-C=O), 2.50 (q, J=6.6Hz, 2H, CH_2-S); ^{13}C NMR δ 180.19, 33.64, 33.33, 24.31, 23.43.

5-(tritylthio)pentanoic acid (55)

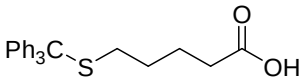

To a solution of 80 mg (0.6 mmol) of 5-mercaptopentanoic acid **54** in 10 ml distilled ethanol at room temperature under argon, was added 100 mg (1.8 mmol) of potassium hydroxide. The solution was stirred at room temperature for 20 min. 335 mg (1.2 mmol) of chlorotriphenyl- methane was added. The solution was stirred at room temperature for 12 hours and then diluted with 20 ml of water, acidified with 2M sulfuric acid, extracted with ethyl acetate. The organic extract was washed with brine and dried over magnesium sulfate. Solvent was removed on a rota-vapor. The crude product was applied to a silica gel column chromatography using hexane, ethyl acetate and methanol as eluants. 100 mg (44%) of compound **55** was obtained as oil. ^{1}H NMR (400 MHz, $CDCl_3$) δ 1.40 (p, J=7.2Hz, 2H), 1.58 (p, J=7.2Hz, 2H), 2.14-2.22 (m, 4H), 7.20-7.42(m, 15H, Ar-H).

Nanogel-Thiolinker (56)

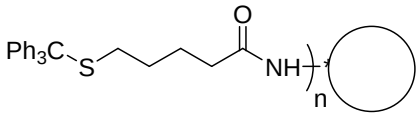

To a solution of 20 mg (0.05 mmol) of 5-(tritylthio)pentanoic acid in 3 ml of distilled dichloromethane under argon, was added 20 mg (0.1 mmol) of N,N'-dicyclohexylcarbodiimide (DCC). The solution was stirred at room temperature for 12 hours and turned to a white suspension. 50mg of nanogel **28** (PEG: PEI=6.8:1, nontoxic) was added to the suspension and stirred for 12 hours at room temperature. Thin layer chromatography indicated the disappearance of 5-(tritylthio)pentanoic acid; and the reaction was stopped. The solvent was removed on rota-vapor. The residue was dissolved in 10ml of water and dialyzed in 1000 ml of 10% ethanol in water at room temperature for 24 hours using a 3500 Dalton molecular weight cut off membrane. Lyophilization gave 35 mg of product. ^{1}H NMR (200 MHz, $CDCl_3$) δ 1.32 (CH_2), 1.75 (CH_2), 2.10-2.80 (CH_2-N), 23.65-3.72 (CH_2-O), 7.25-7.40 (Ar-H).

Nanogel-Thiolinker-Rhodamine (57)

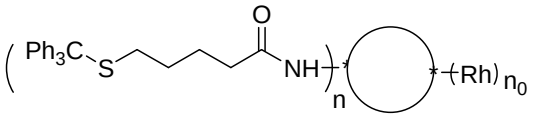

To A mixture of 3 mg (6 μmol) of 6-Carboxytetramethylrhodamine (TAMRA), 1.3 mg (9 μmol) of HOBT, 2 mg (9 μmol) of DCC and 0.9 mg (8 μmol) of *N*-hydroxysuccinimide under argon, 0.2 mL of dry DMF was added via syringe at 25°C. The resulting solution was stirred at 50-55°C for 2.5 hours, cooled to room temperature, and added to a solution of 35mg of compound in 2ml of DMF. The mixture was stirred for 12 hours at 40 °C, cooled to 25°C, dialyzed with a 3500 Dalton molecular weight cut off membrane in 1000ml of 10% ethanol in deionized water at room temperature for 1 day, and lyophilized to give 35 mg of PEG-PEI-rhodamine as a pink powder.

Nanogel-Rhodamine-Thiolinker-Streptavidin (59)

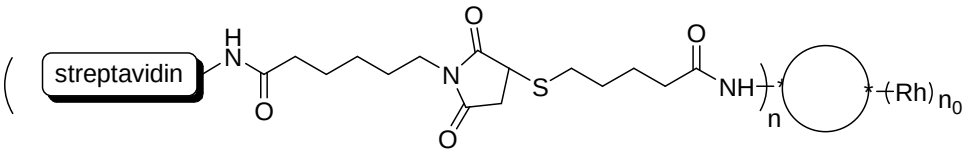

To a solution of 35 mg of compound in 8 ml of dichloromethane at room temperature under argon, 300 μL of trifloroacetic acid and 300 μL of triisopropylsilane were added. The color of the solution turned from pink to red upon the adding. The mixture was stirred at 25°C for 2 hours, and added to a solution of 2 mg streptavidin maleimide in 2 ml of dichloromethane, stirred at room temperature for 12 hours. The mixture was then dialyzed in 1000 ml of 10% ethanol in water using a 12-14kDa molecular weight cut off membrane at 25°C for 24 hours, and lyophilized to give 30 mg of pink powder.

Appendices: 1H and 13C NMR spectra

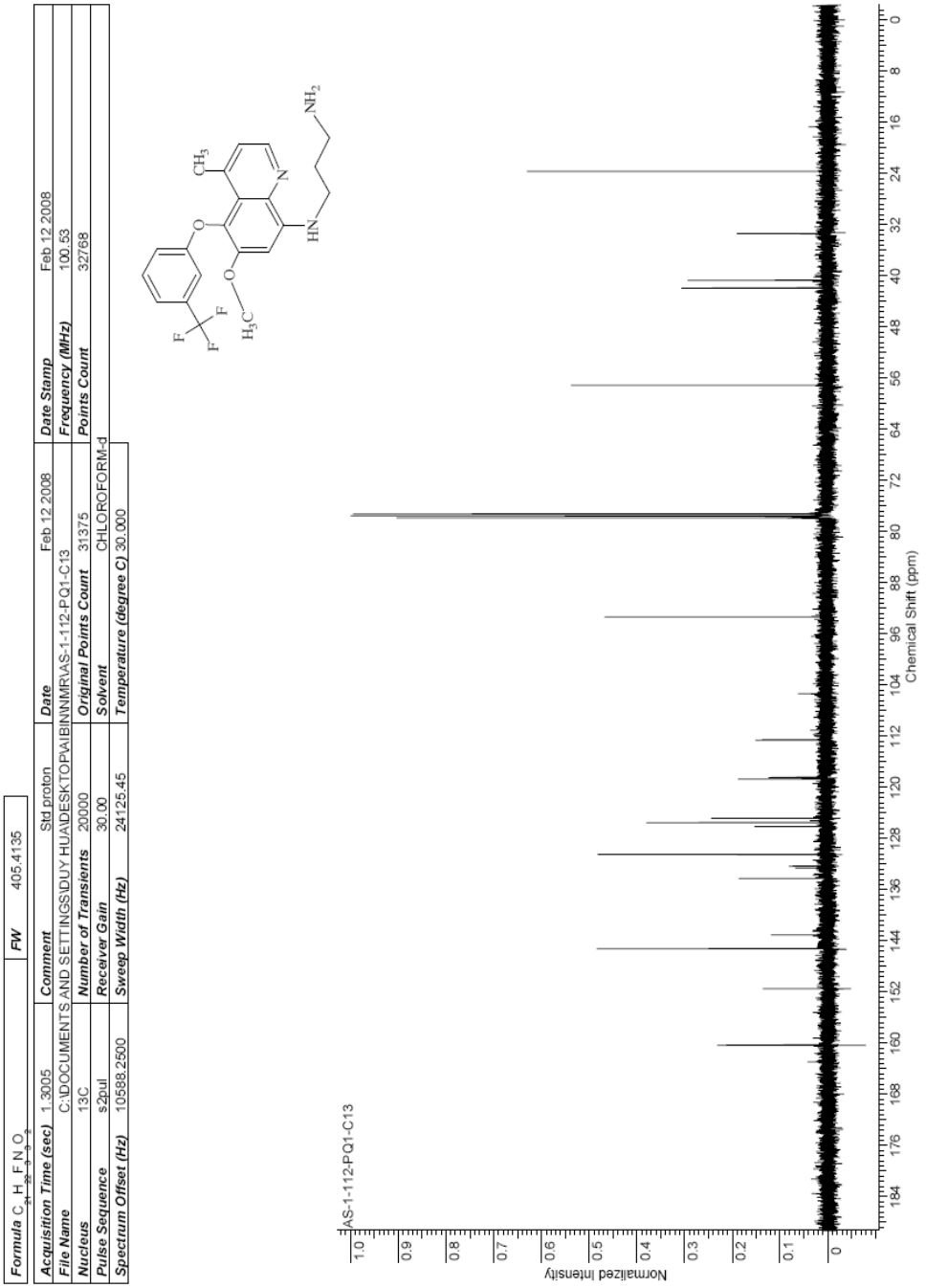

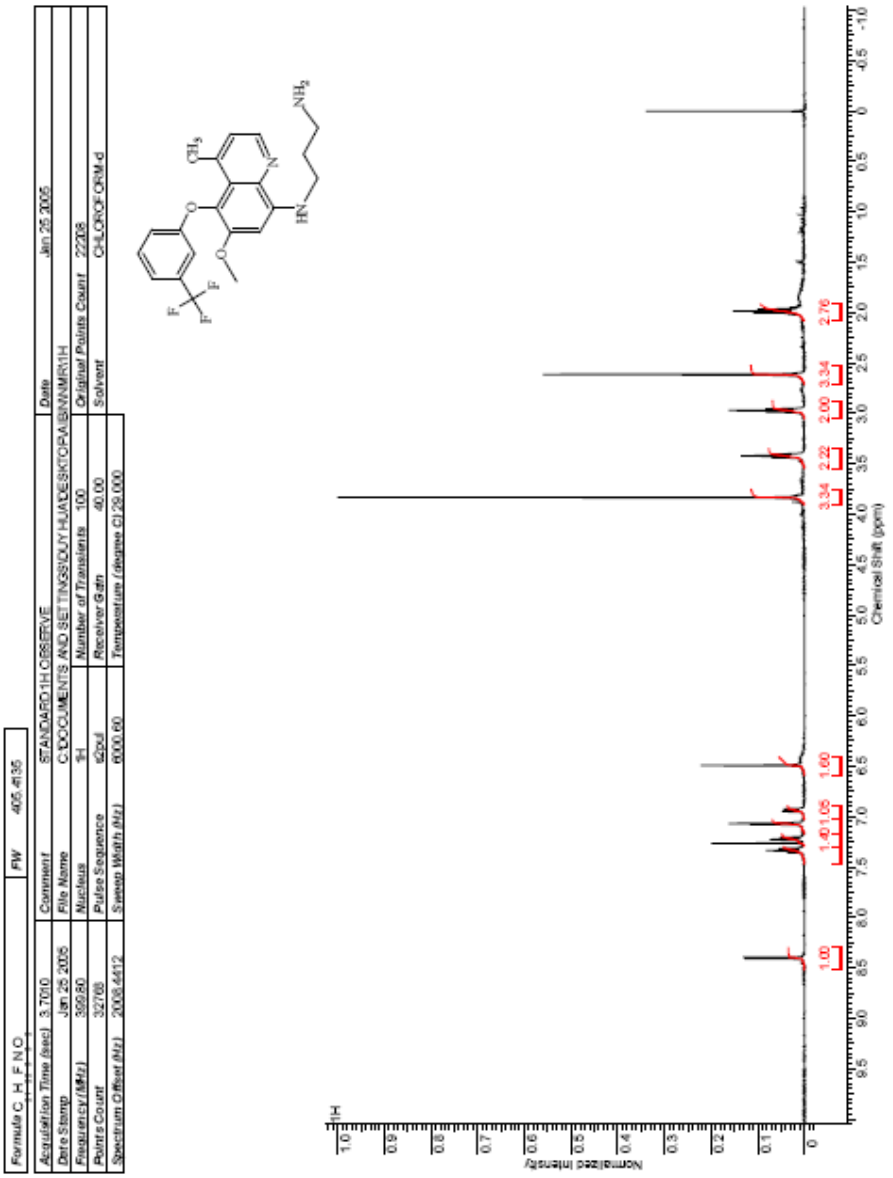
Formula C H F N O FW 405.435
Acquisition Time (sec) 3.7010 Comment STANDARD 1H OBSERVE Date Jan 25 2005
Date Stamp Jan 25 2005 File Name C:\DOCUMENTS AND SETTINGS\DUY HUA\DESKTOP\A\BNNMR1H
Frequency (MHz) 399.80 Nucleus 1H Number of Transients 100 Original Points Count 22208
Points Count 32768 Pulse Sequence s2pul Receiver Gain 40.00 Solvent CHLOROFORM-d
Spectrum Offset (Hz) 2008.4412 Sweep Width (Hz) 6000.60 Temperature (degree C) 29.000
1H
Normalized Intensity
Chemical Shift (ppm)
1.00
1.40
1.05
1.00
3.34
2.22
2.00
3.34
2.76

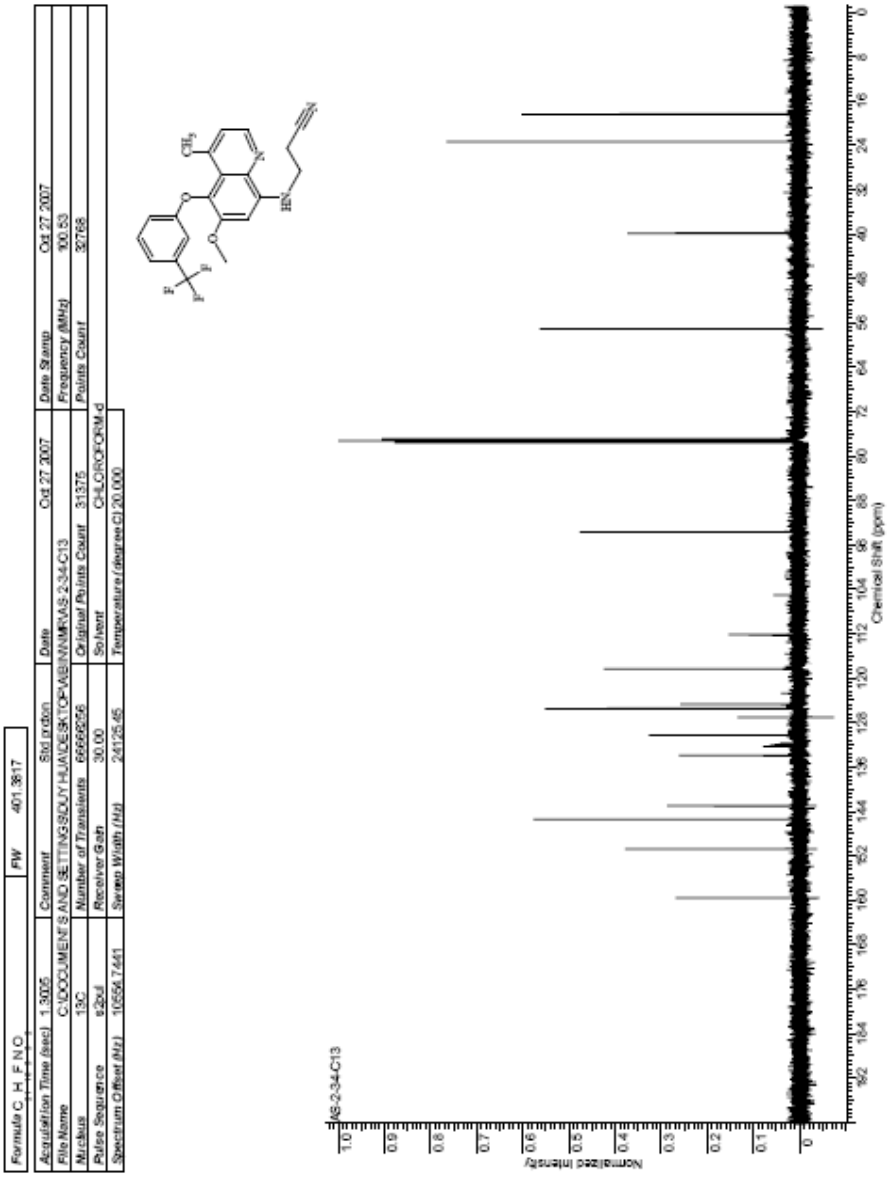
Formula C H F N O FW 401.3817
Acquisition Time (sec) 1.3005 Comment Std proton Date Oct 27 2007 Date Stamp Oct 27 2007
File Name C:\DOCUMENTS AND SETTINGS\DUY HUA\DESKTOP\ABI\NMR\AS-2-34-C13 Frequency (MHz) 100.53
Nucleus 13C Number of Transients 6666656 Original Points Count 31375 Points Count 32768
Pulse Sequence s2pul Receiver Gain 30.00 Solvent CHLOROFORM-d
Spectrum Offset (Hz) 10556.7441 Sweep Width (Hz) 24125.45 Temperature (degree C) 20.000
AS-2-34-C13
Normalized Intensity
Chemical Shift (ppm)

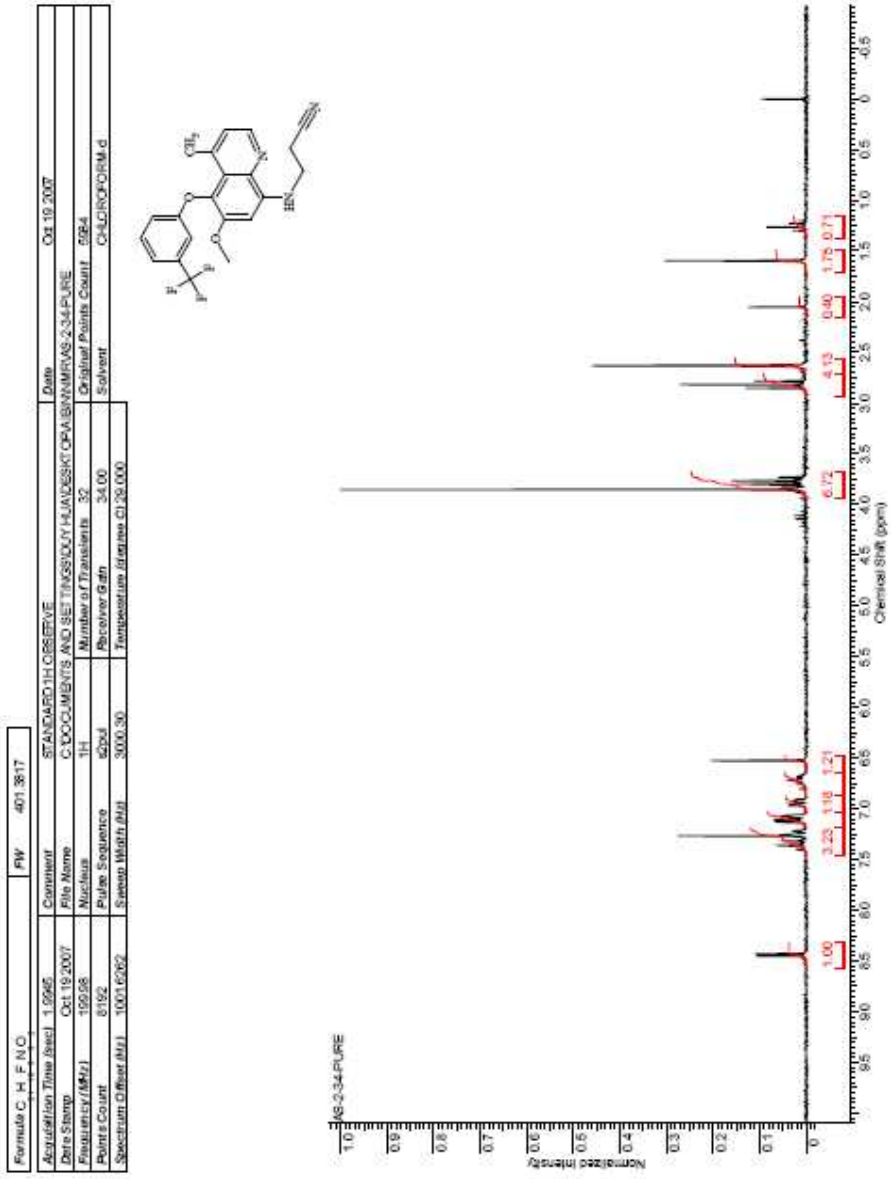
Formula C H F N O FW 401.3817
Acquisition Time (sec) 1.9945 Comment STANDARD 1H OBSERVE Date Oct 19 2007
Date Stamp Oct 19 2007 File Name C:\DOCUMENTS AND SETTINGS\DOUYHUA\DESKTOP\A\BIYAMIRIVA\6-234-PURE
Frequency (MHz) 199.98 Nucleus 1H Number of Transients 32 Original Points Count 5984
Points Count 8192 Pulse Sequence s2pul Receiver Gain 34.00 Solvent CHLOROFORM-d
Spectrum Offset (Hz) 1001.6062 Sweep Width (Hz) 3000.30 Temperature (degree C) 28.000
6-234-PURE
Normalized Intensity
Chemical Shift (ppm)
1.00
3.23
1.18
1.21
6.72
4.13
0.90
1.75
0.71

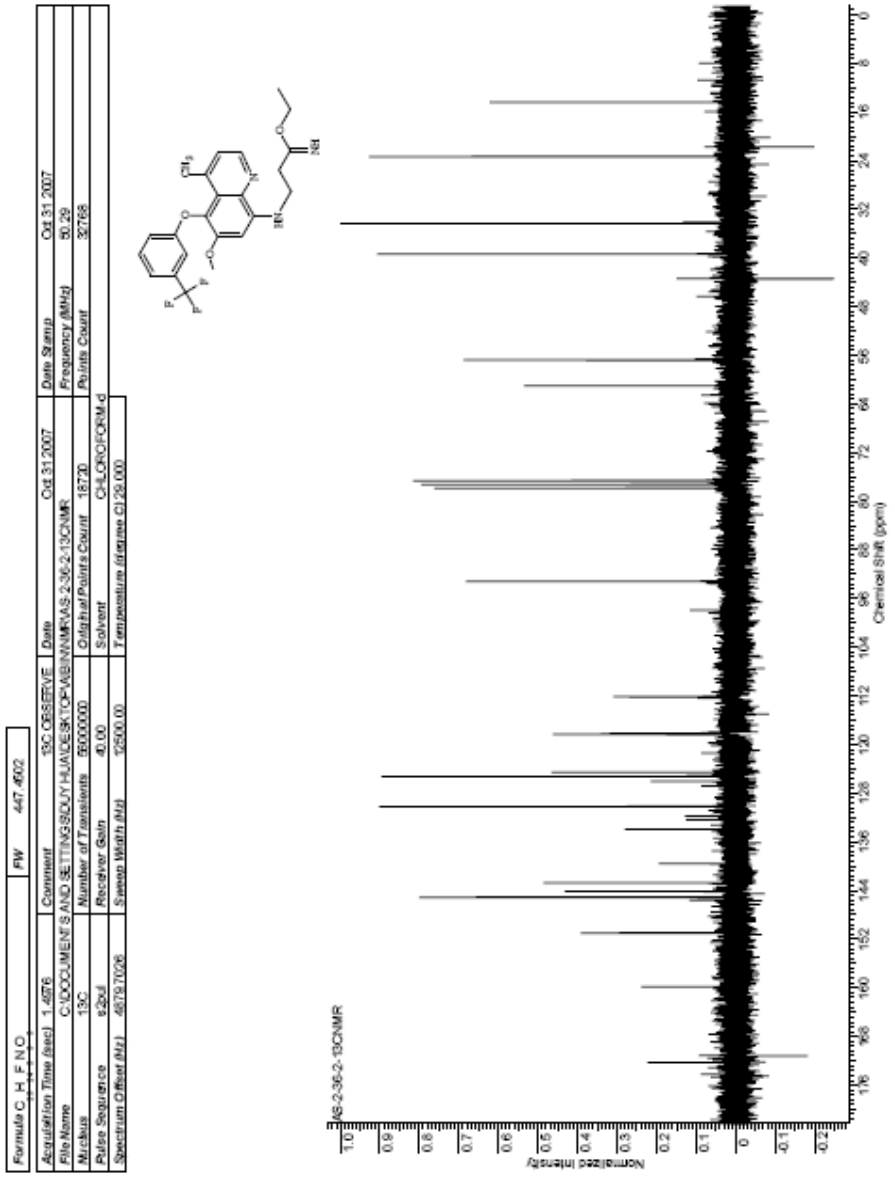
Formula C H F N O
FW 447.4002
Acquisition Time (sec) 1.4976
Comment 13C OBSERVE
Date Oct 31 2007
Date Stamp Oct 31 2007
File Name C:\DOCUMENTS AND SETTINGS\DUY HUA\DESKTOP\ABBVNMR\AS-2-36-2-13CNMR
Frequency (MHz) 50.29
Nucleus 13C
Number of Transients 8000000
Original Points Count 16720
Points Count 32768
Pulse Sequence s2pul
Receiver Gain 40.00
Solvent CHLOROFORM-d
Spectrum Offset (Hz) 4679.7006
Sweep Width (Hz) 9250.00
Temperature (degree C) 29.000
AS-2-36-2-13CNMR
Normalized Intensity
Chemical Shift (ppm)

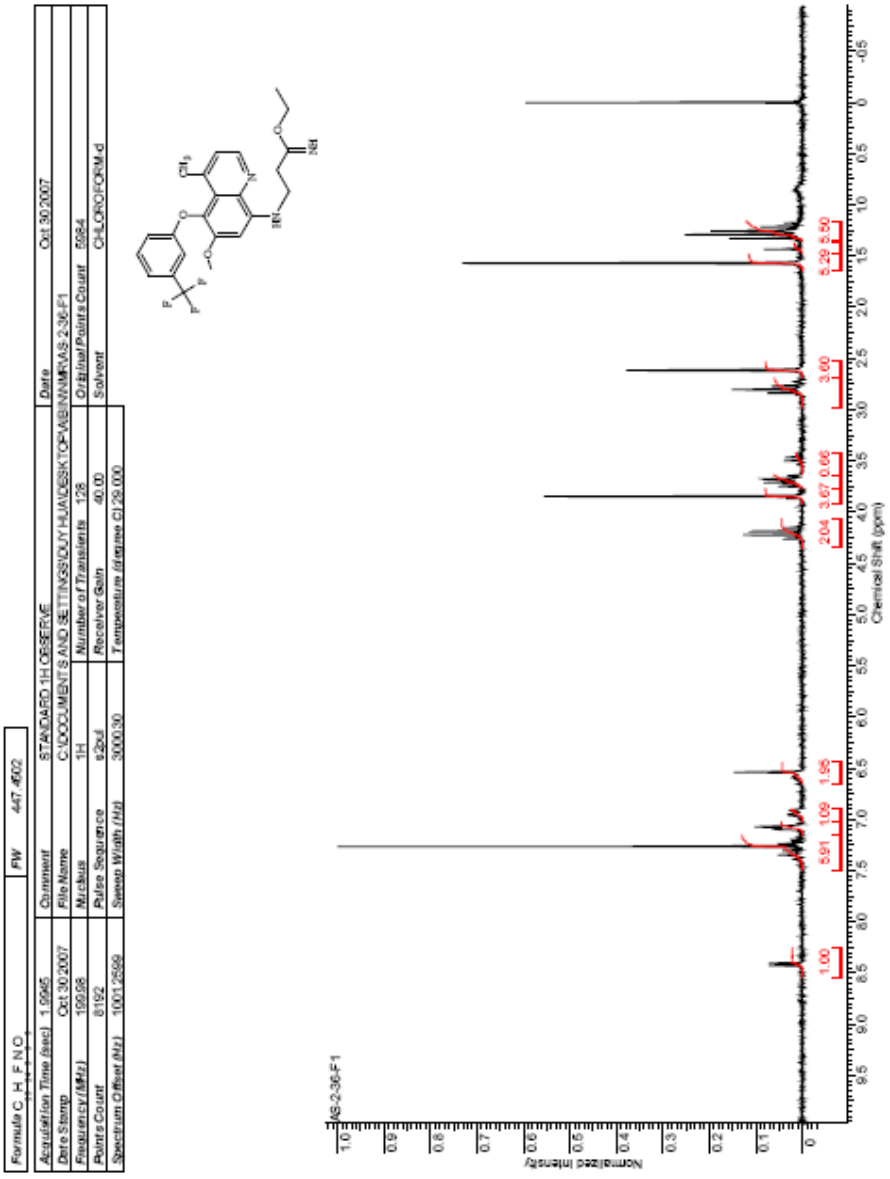
Formula C H F N O FW 447.402
Acquisition Time (sec) 1.9945 Comment STANDARD 1H OBSERVE Date Oct 30 2007
Date Stamp Oct 30 2007 File Name C:\DOCUMENTS AND SETTINGS\DOYHUA\DESKTOP\AB\NMR\AS-2-36-F1
Frequency (MHz) 199.98 Nucleus 1H Number of Transients 128 Original Points Count 5984
Points Count 8192 Pulse Sequence s2pul Receiver Gain 40.00 Solvent CHLOROFORM-d
Spectrum Offset (Hz) 1001.2568 Sweep Width (Hz) 3000.00 Temperature (degree C) 29.000
AS-2-36-F1
Normalized Intensity
Chemical Shift (ppm)
1.00
8.91
1.09
1.95
2.04
3.67
0.66
3.60
8.29
8.50

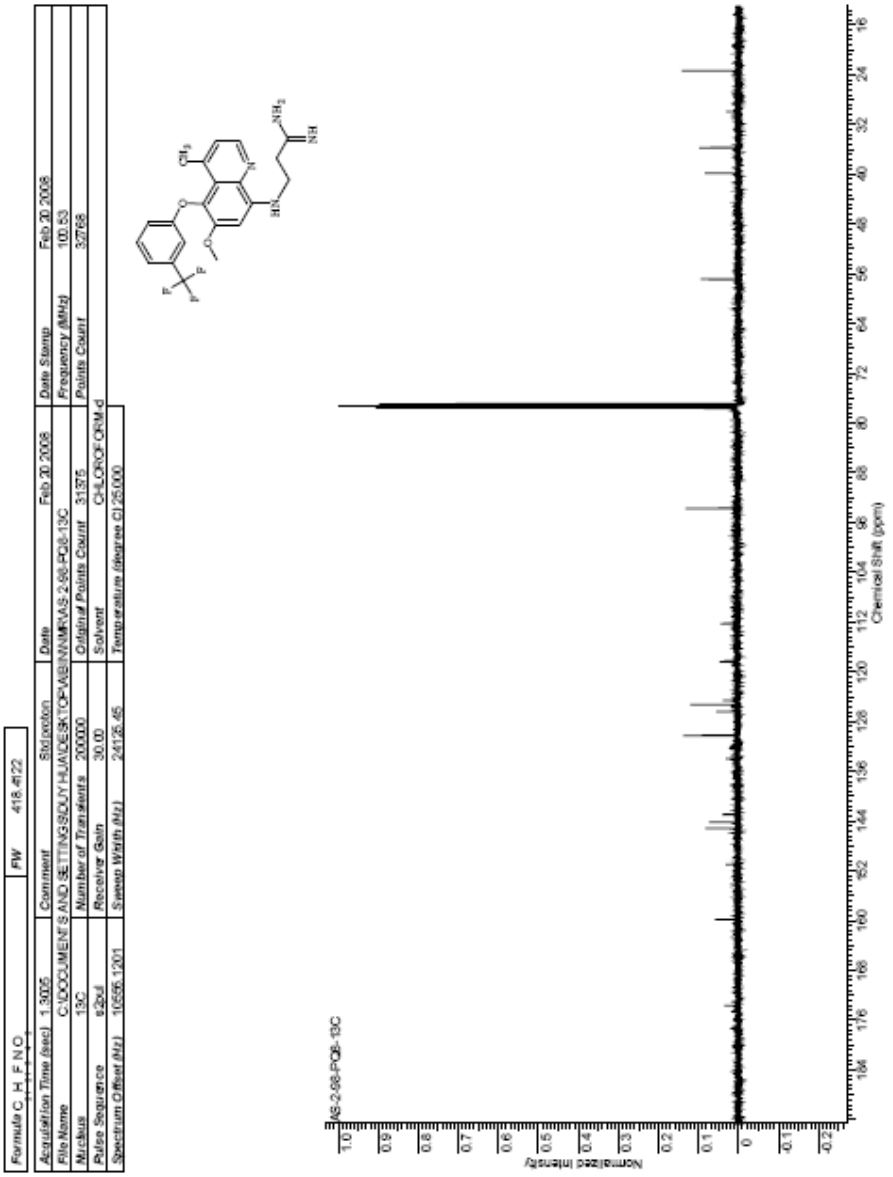
Formula C H F N O FW 418.472
Acquisition Time (sec) 1.3005 Comment Skipodon Date Feb 20 2008 Date Stamp Feb 20 2008
File Name C:\DOCUMENTS AND SETTINGS\DUY HUA\DESKTOP\ABI\NMR\AS-2-66-FQ8-13C Frequency (MHz) 100.53
Nucleus 13C Number of Transients 200000 Original Points Count 31375 Points Count 32768
Pulse Sequence s2pul Receiver Gain 30.00 Solvent CHLOROFORM-d
Spectrum Offset (Hz) 10556.1201 Sweep Width (Hz) 24126.45 Temperature (degree C) 25.000
AS-2-66-FQ8-13C
Normalized Intensity
Chemical Shift (ppm)

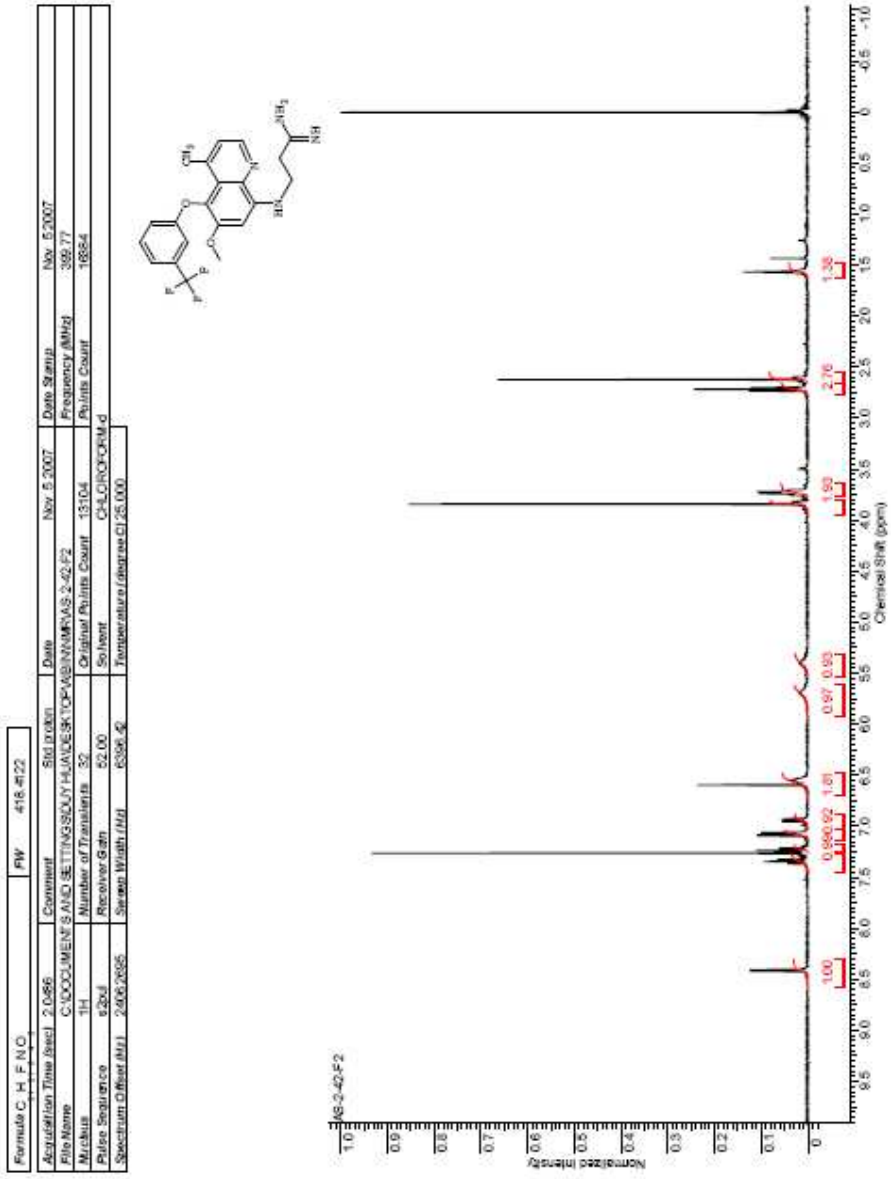
Formula C H F N O
FW 418.462
Acquisition Time (sec) 2.0486
Comment Std proton
Date Nov 5 2007
Date Stamp Nov 5 2007
File Name C:\DOCUMENTS AND SETTINGS\DUY HUA\DESKTOP\ABINNIMRAS 2-42-F2
Frequency (MHz) 399.77
Nucleus 1H
Number of Transients 32
Original Points Count 13104
Points Count 16864
Pulse Sequence s2pul
Receiver Gain 52.00
Solvent CHLOROFORM-d
Spectrum Offset (Hz) 2006.2695
Sweep Width (Hz) 6594.46
Temperature (degree C) 25.000
NS-2-42-F2
Normalized Intensity
Chemical Shift (ppm)
1.00
0.99
0.92
1.01
0.97
0.93
1.93
2.76
1.38

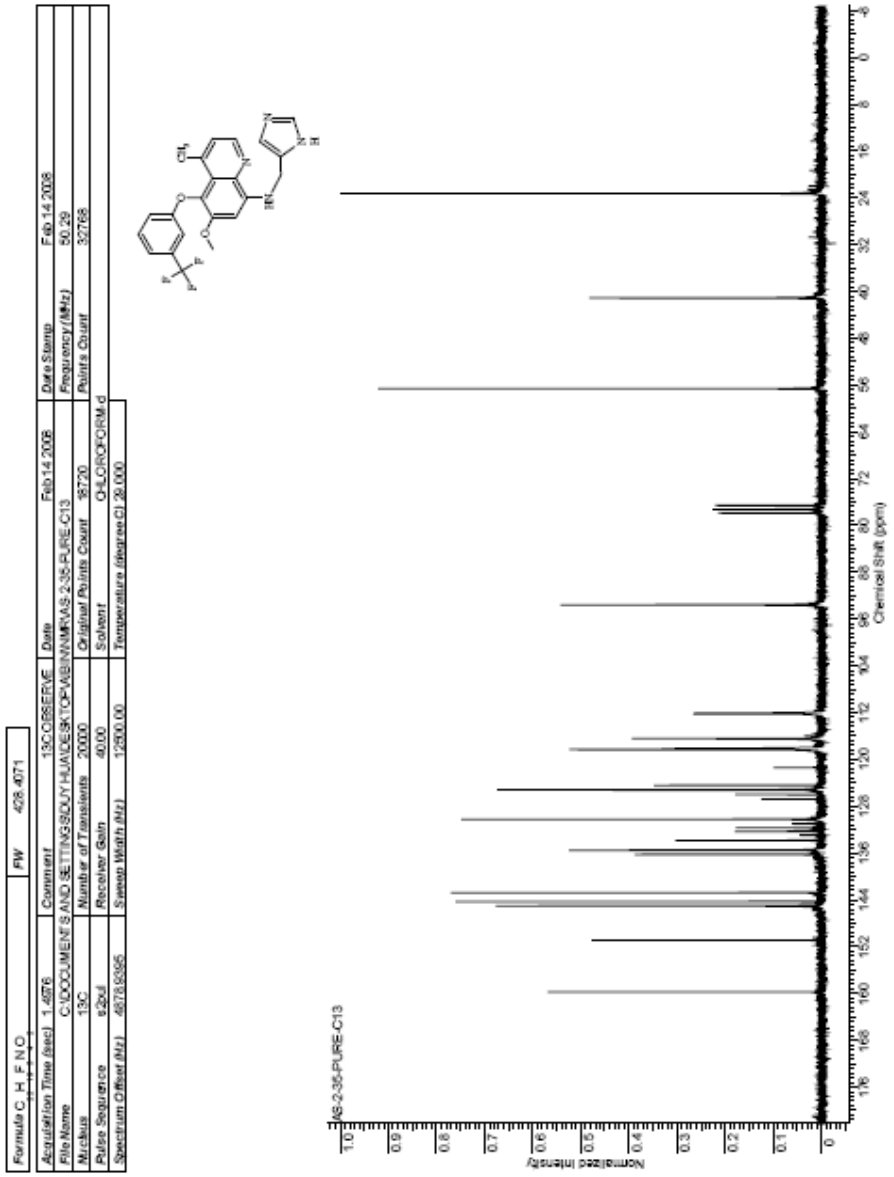
Formula C H F N O FW 428.4071
Acquisition Time (sec) 1.4976 Comment 13COBSERVE Date Feb 14 2008
File Name C:\DOCUMENTS AND SETTINGS\DUY HUA\DESKTOP\ABINNMR\AS-2-35-PURE-C13 Frequency (MHz) 50.29
Nucleus 13C Number of Transients 20000 Original Points Count 16720 Points Count 32768
Pulse Sequence s2pul Receiver Gain 4000 Solvent CHLOROFORM-d
Spectrum Offset (Hz) 4678.9395 Sweep Width (Hz) 12500.00 Temperature (degree C) 28.000
AS-2-35-PURE-C13
Normalized Intensity
Chemical Shift (ppm)

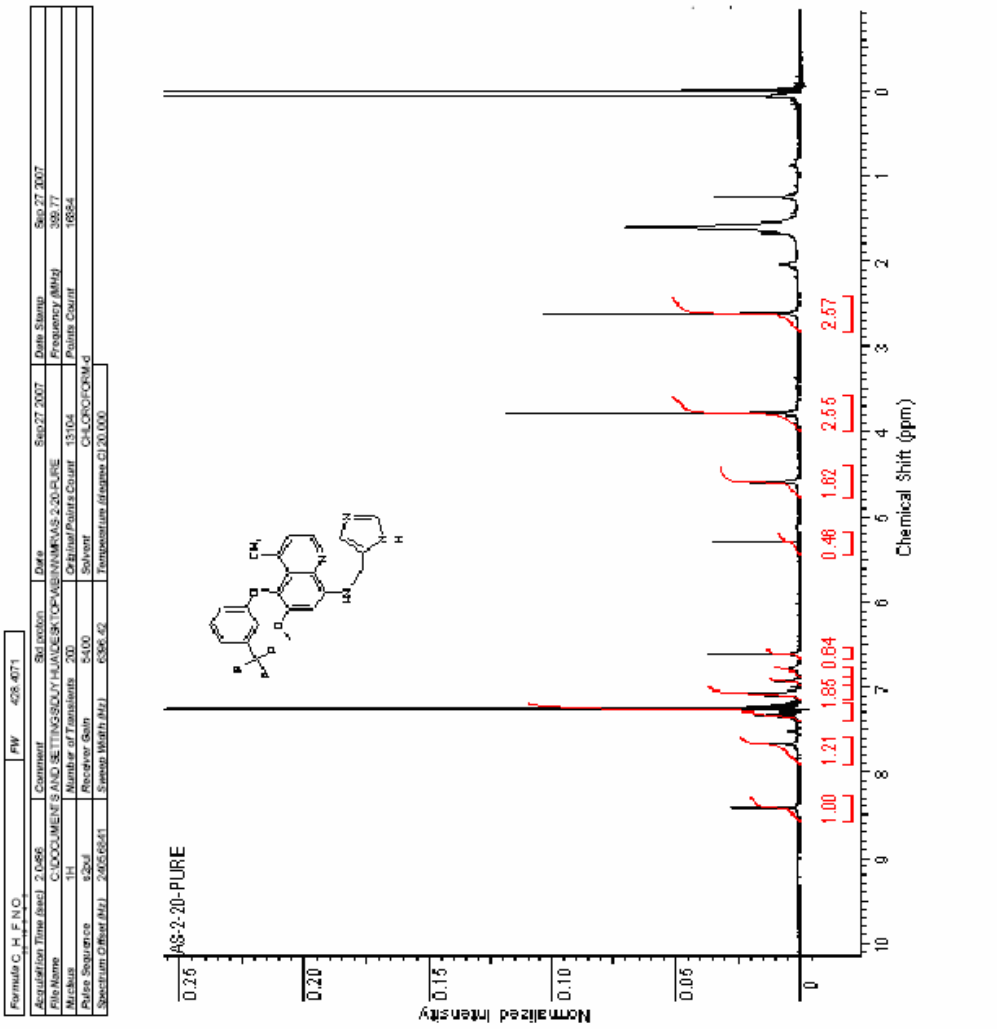
Formula C_H_F_N_O_
FW 408.4071
Acquisition Time (sec) 2.0486
Comment
Solvent
Date
Sep27 2007
Date Stamp
Sep 27 2007
File Name C:\DOCUMENTS AND SETTINGS\DUY HUA\DESKTOP\AES\NMR\AS-2-20-PURE
Frequency (MHz) 399.77
Nucleus 1H
Number of Transients 200
Original Points Count 13104
Points Count 16854
Pulse Sequence s2pul
Receiver Gain 5400
Solvent CHLOROFORM-d
Spectrum Offset (Hz) 2405.6641
Sweep Width (Hz) 6396.42
Temperature (degree C) 20.000
AS-2-20-PURE
1.00
1.21
1.85
0.64
0.46
1.82
2.56
2.57
Normalized Intensity
Chemical Shift (ppm)

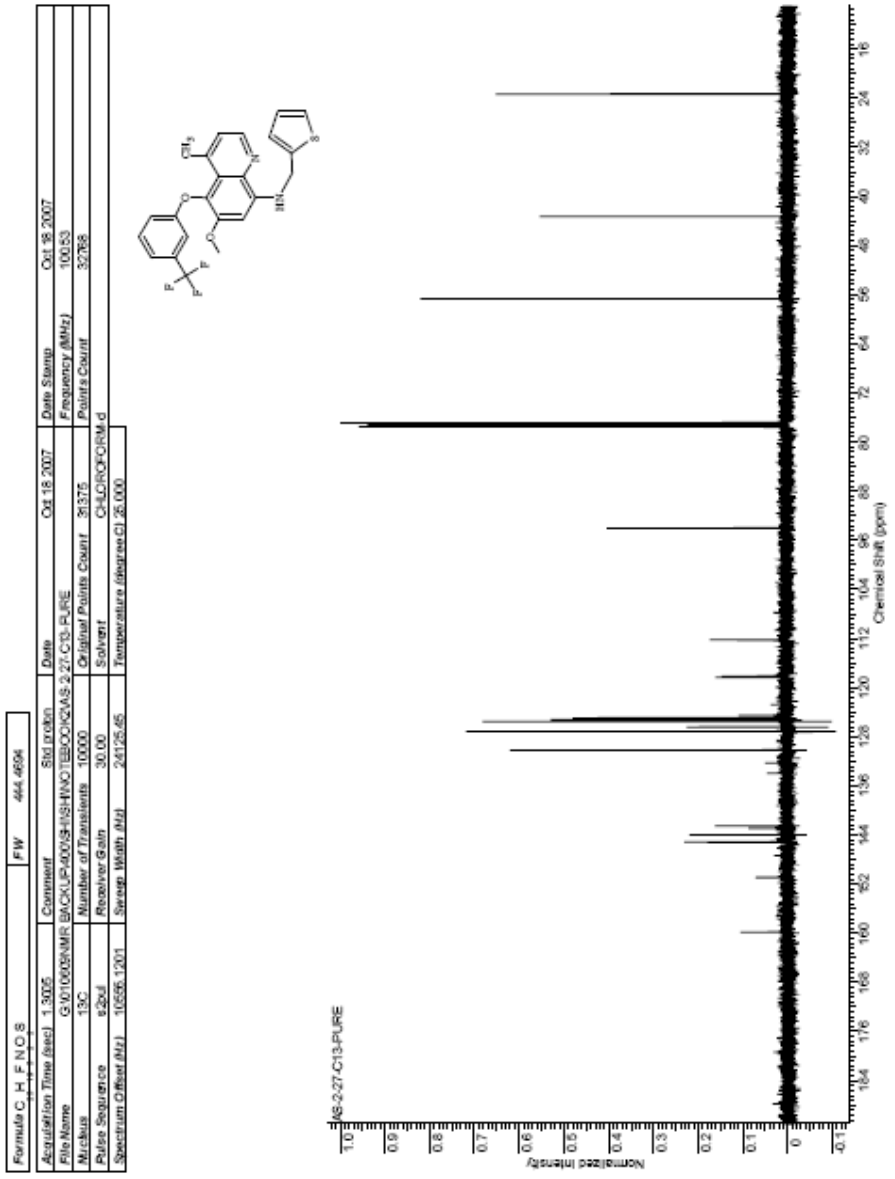
Formula C H F N O S
FW 444.4694
Acquisition Time (sec) 1.3005
Comment Std proton
Date Oct 18 2007
Date Stamp Oct 18 2007
File Name G:\01\0005\MR BACKUP\400\SH\NOTEBOOK\AS-2-27-C13-PURE
Frequency (MHz) 100.53
Nucleus 13C
Number of Transients 10000
Original Points Count 31375
Points Count 32768
Pulse Sequence s2pul
Receiver Gain 30.00
Solvent CHLOROFORM-d
Spectrum Offset (Hz) 10556.1201
Sweep Width (Hz) 24125.45
Temperature (degree C) 26.000
AS-2-27-C13-PURE
Normalized Intensity
Chemical Shift (ppm)

Formula C H F N O S		FW 444.4694					
Acquisition Time (sec)	2.0466	Comment	Std proton	Date	Oct 18 2007	Date Stamp	Oct 18 2007
File Name	C:\DOCUMENTS AND SETTINGS\DUY HUA\DESKTOP\AB\NNMR\AS 2-27-PURE					Frequency (MHz)	399.77
Nucleus	1H	Number of Transients	64	Original Points Count	13104	Points Count	16384
Pulse Sequence	s2pul	Receiver Gain	42.00	Solvent	CHLOROFORM-d		
Spectrum Offset (Hz)	2403.5369	Sweep Width (Hz)	6596.42	Temperature (degree C)	25.000		

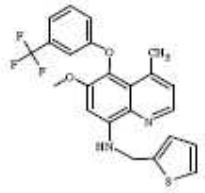

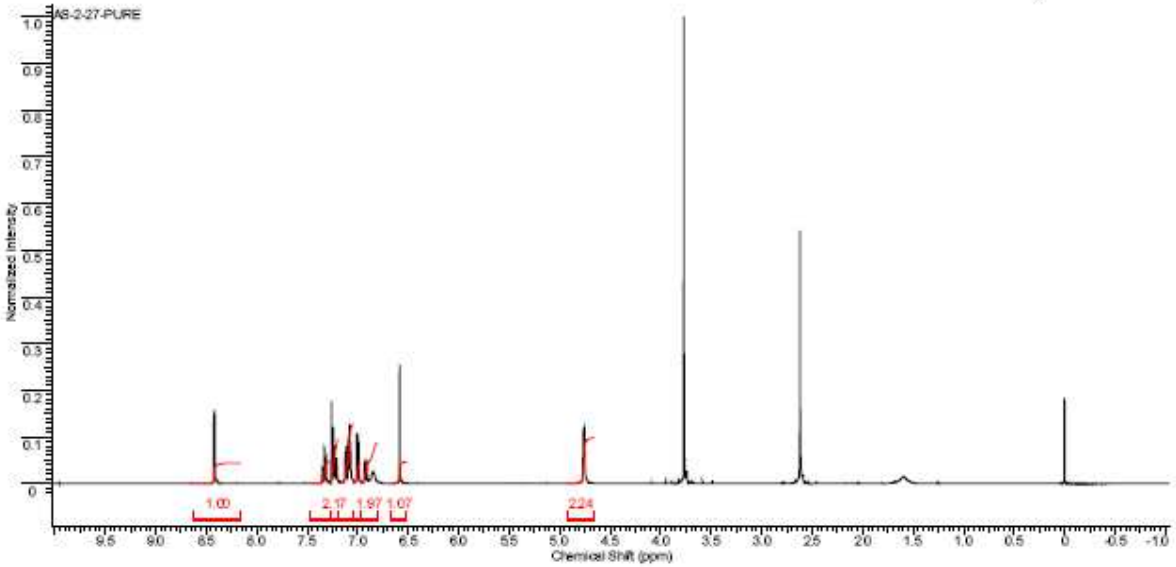

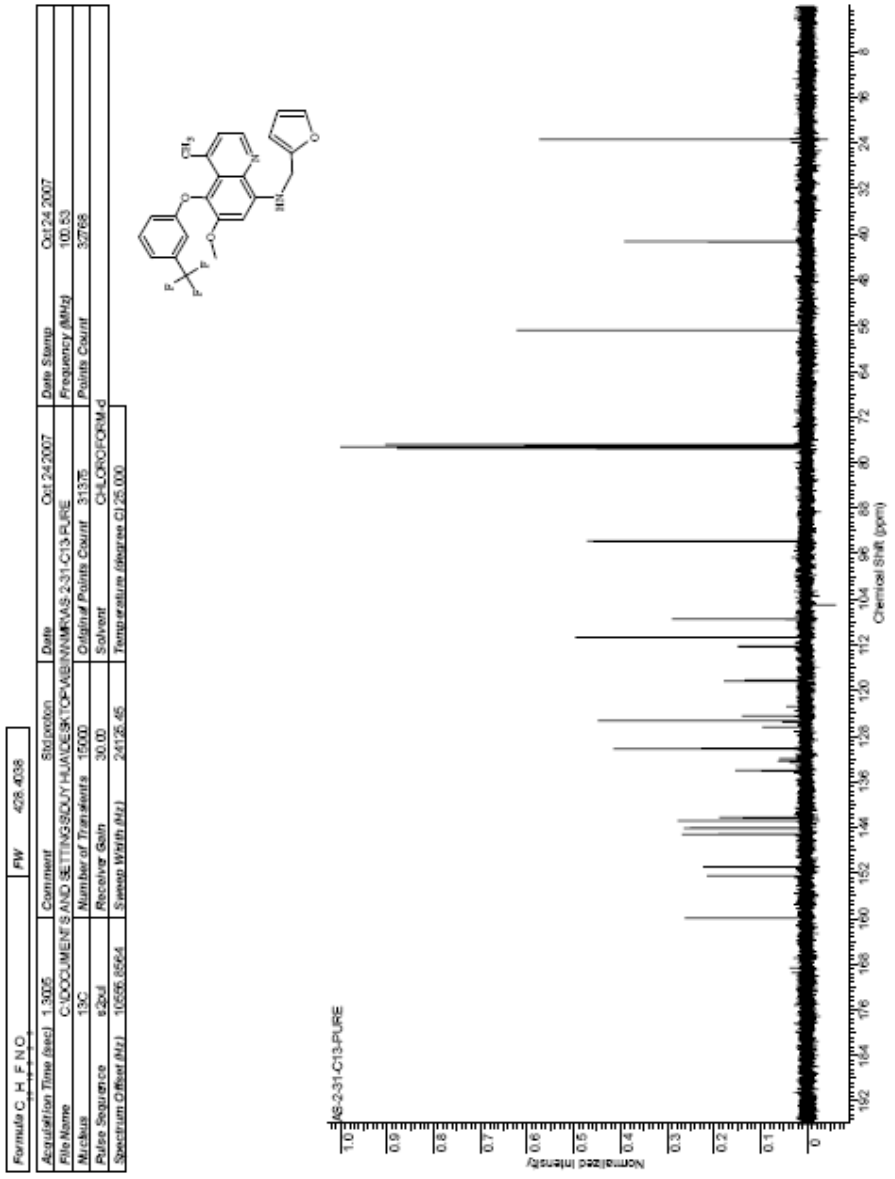
Formula C H F N O
FW 428.4038
Acquisition Time (sec) 1.3005
Comment Skipcotton
Date Oct 24 2007
Date Stamp Oct 24 2007
File Name C:\DOCUMENTS AND SETTINGS\DUY HUA\DESKTOP\ABI\NMR\AS-2-31-C13-PURE
Frequency (MHz) 100.53
Nucleus 13C
Number of Transients 15000
Original Points Count 31375
Points Count 32768
Pulse Sequence s2pul
Receiver Gain 30.00
Solvent CHLOROFORM-d
Spectrum Offset (Hz) 10556.8564
Sweep Width (Hz) 24126.45
Temperature (degree C) 25.000
AS-2-31-C13-PURE
Normalized Intensity
Chemical Shift (ppm)

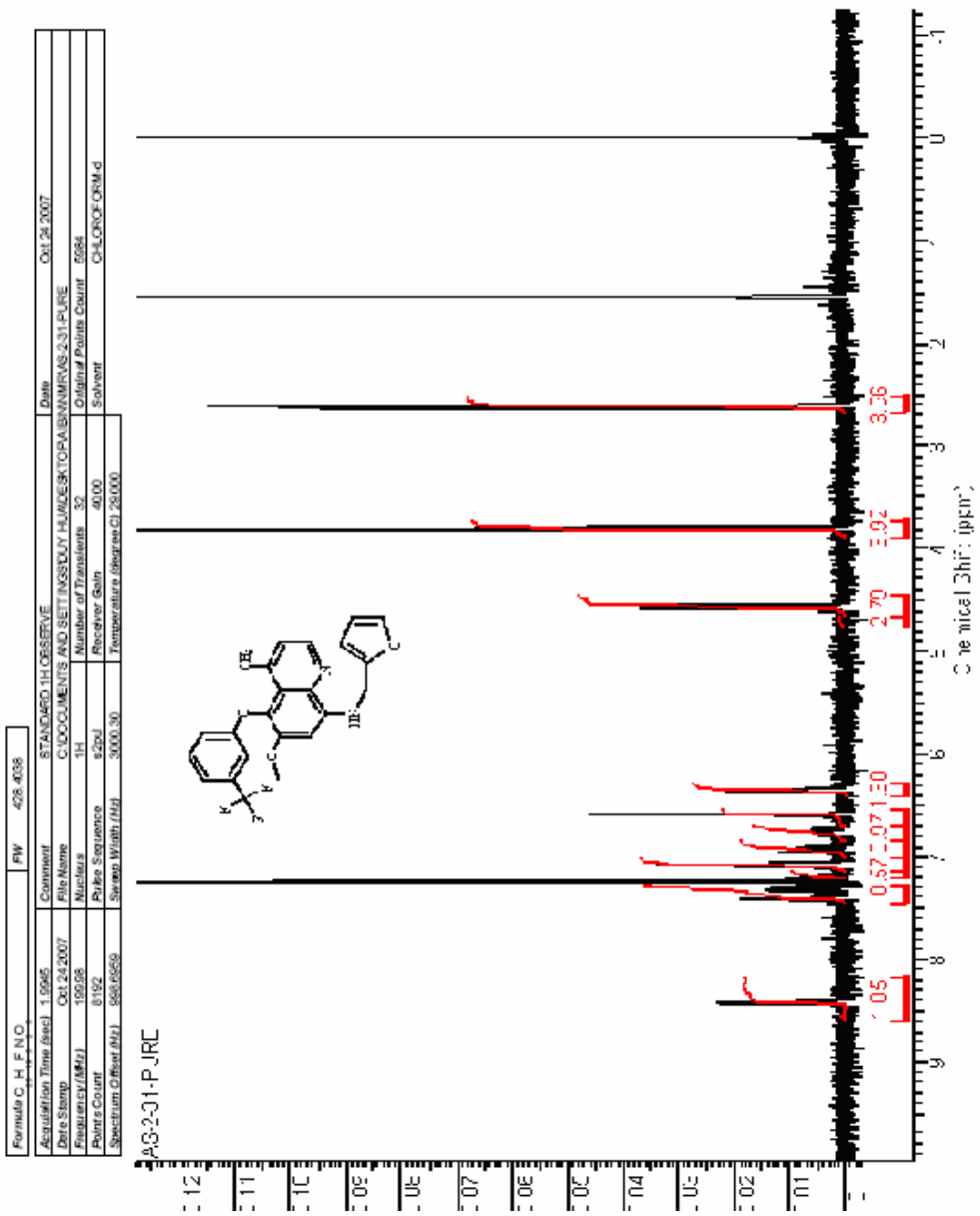
Formula C H F N O
FW 426.436
Acquisition Time (sec) 1.9945
Comment STANDARD 1H OBSERVE
Date Oct 24 2007
Data Stamp Oct 24 2007
File Name C:\DOCUMENTS AND SETTINGS\DUY HUME\SKITOPA\SKNMR\AS-2-31-PURE
Frequency (MHz) 199.98
Nucleus 1H
Number of Transients 32
Obtained Points Count 5984
Points Count 8192
Pulse Sequence s2pul
Receiver Gain 4000
Solvent CHLOROFORM-d
Spectrum Offset (Hz) 950.6858
Sweep Width (Hz) 3000.30
Temperature (degree C) 28.000
AS-2-31-PURE
2.70
3.92
3.36
Chemical Shift (ppm)

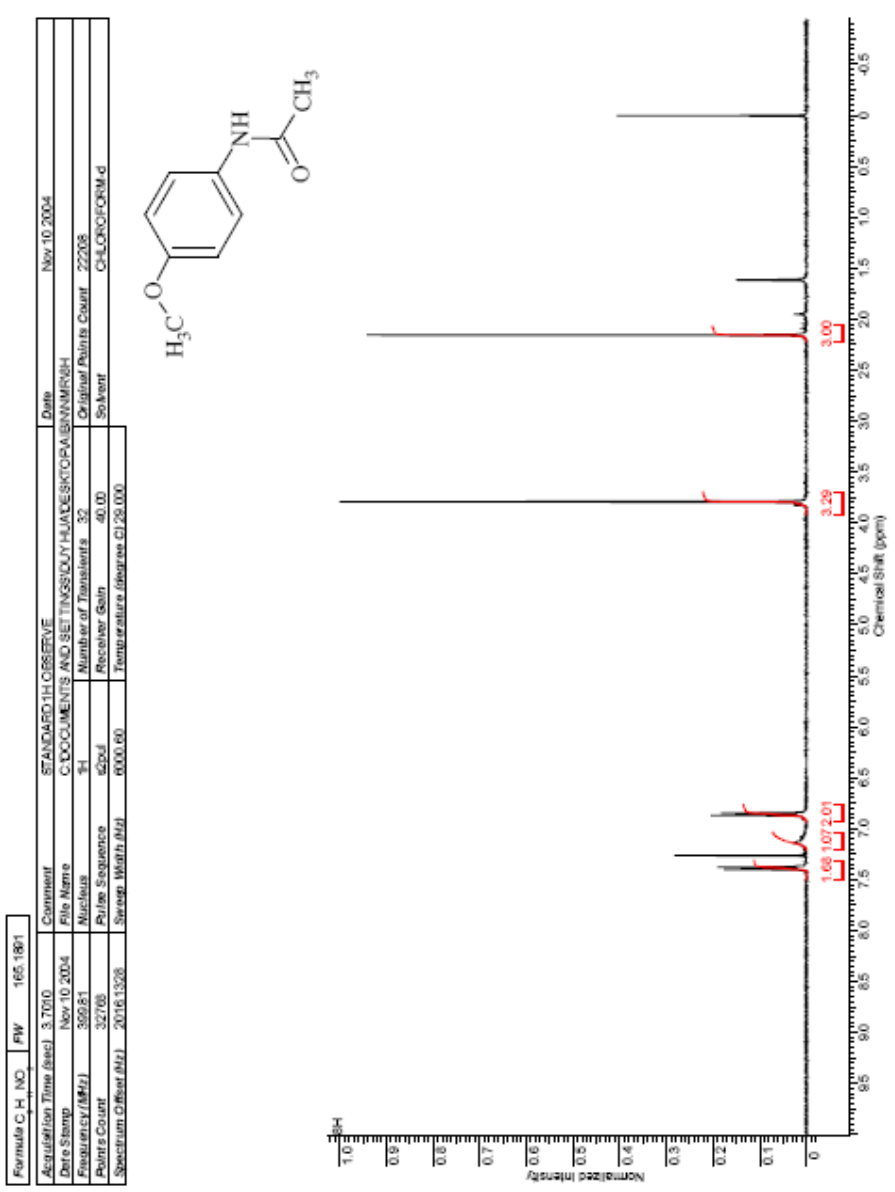
Formula C H NO FW 165.1891
Acquisition Time (sec) 3.7010 Comment STANDARD 1H OBSERVE Date Nov 10 2004
Date Stamp Nov 10 2004 File Name C:\DOCUMENTS AND SETTINGS\DOUY HUADE\SKTOP\ASBNMR\NH
Frequency (MHz) 399.81 Nucleus 1H Number of Transients 32 Original Points Count 22208
Points Count 32768 Pulse Sequence s2pul Receiver Gain 40.00 Solvent CHLOROFORM-d
Spectrum Offset (Hz) 2016.1328 Sweep Width (Hz) 6000.60 Temperature (degree C) 29.000
NH
O
CH3
H3C
O
1.68
1.07
2.01
3.29
3.00
Normalized Intensity
Chemical Shift (ppm)

Formula $C_9H_8BrNO_2$	FW	244.0662					
Acquisition Time (sec)	1.4576	Comment	13C OBSERVE			Date	Apr 30 2007
Date Stamp	Apr 30 2007	File Name	C:\DOCUMENTS AND SETTINGS\DUY HUA\DESKTOP\A\BINNMR\9C				
Frequency (MHz)	50.29	Nucleus	13C	Number of Transients	10000	Original Points Count	18720
Points Count	32768	Pulse Sequence	s2pul	Receiver Gain	40.00	Solvent	CHLOROFORM-d
Spectrum Offset (Hz)	4873.5991	Sweep Width (Hz)	12500.00	Temperature (degree C)	29.000		

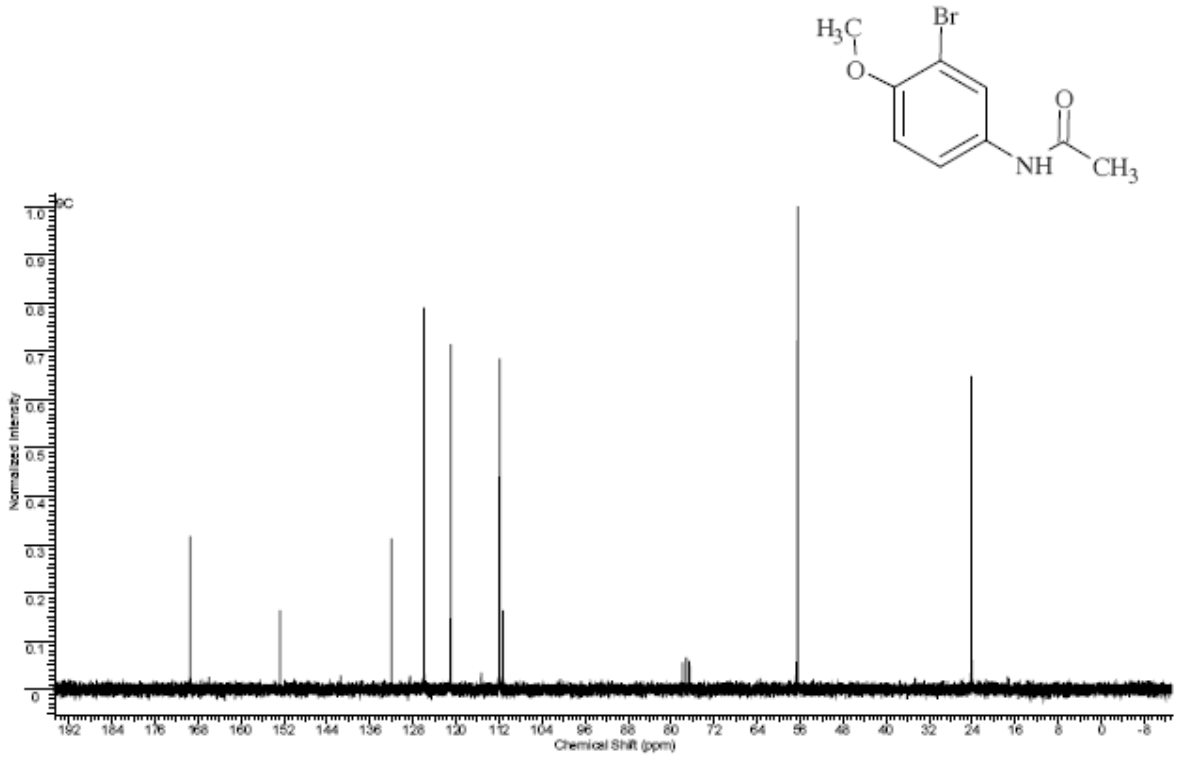

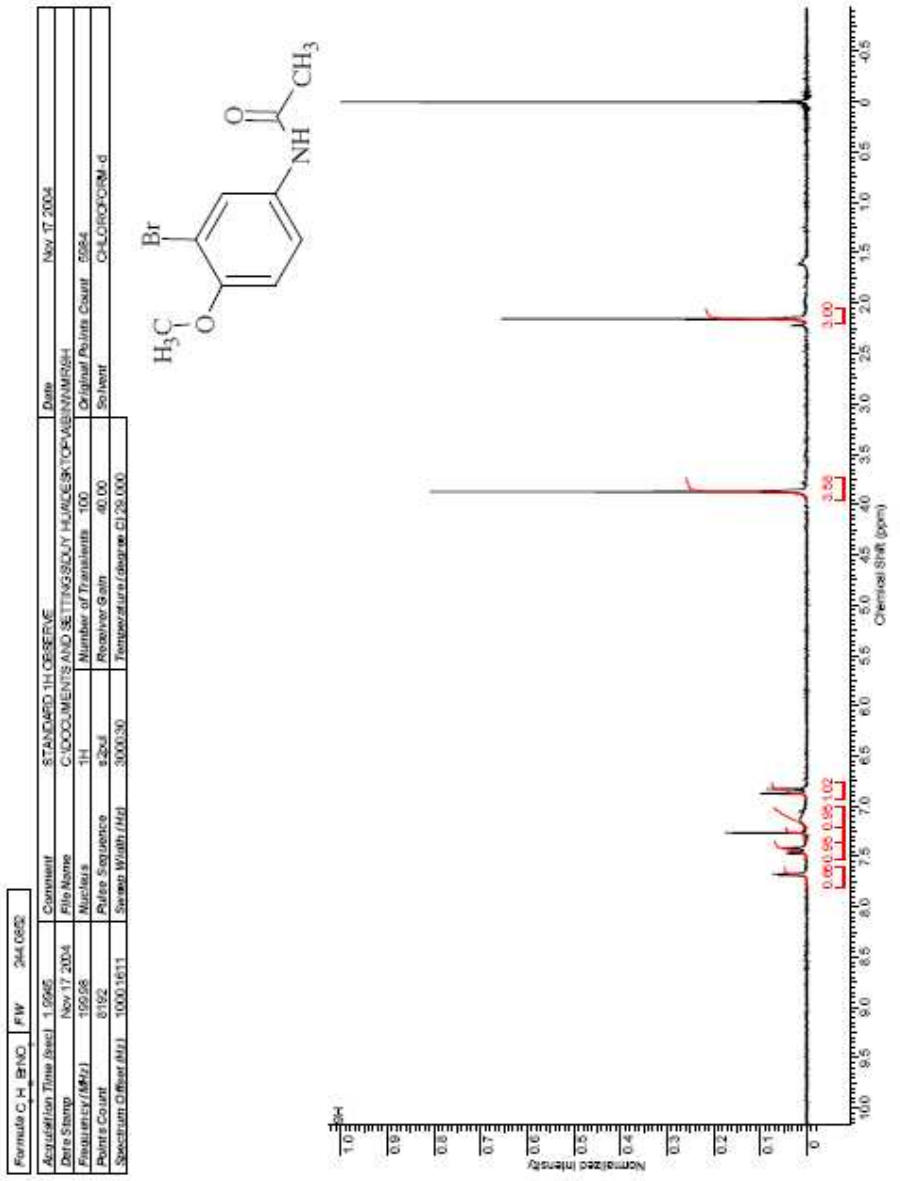
Formula C9 H9 Br NO2 FW 244.0682
Acquisition Time (sec) 1.9945
Comment STANDARD 1H OBSERVE
Date Nov 17 2004
Date Stamp Nov 17 2004
File Name C:\DOCUMENTS AND SETTINGS\DUY HUA\ESKTOP\ABENNMR\H
Frequency (MHz) 199.98
Nucleus 1H
Number of Transients 100
Original Points Count 5984
Points Count 8192
Pulse Sequence s2pul
Receiver Gain 40.00
Solvent CHLOROFORM-d
Spectrum Offset (Hz) 1000.1611
Sweep Width (Hz) 3000.30
Temperature (degree C) 29.000
Br
O
NH
CH3
H3C
O
3.00
3.89
0.95
0.98
1.02
Normalized Intensity
Chemical Shift (ppm)

Formula C9 H8 Br1 N2 O4 FW 288.0628
Acquisition Time (sec) 1.3005 Comment 8d proton Date Jun 17 2009 Date Stamp Jun 17 2009
File Name F:\AS-COMPOUND10-C13 Frequency (MHz) 100.53 Nucleus 13C Number of Transients 10000
Original Points Count 31375 Points Count 32768 Pulse Sequence s2pul Receiver Gain 30.00
Solvent CHLOROFORM-d Spectrum Offset (Hz) 10548.8616 Sweep Width (Hz) 24125.45
Temperature (degree C) 25.000
Br
O
NH
O
N+
O-
O
H3C
AS-COMPOUND10-C13
Normalized Intensity
Chemical Shift (ppm)

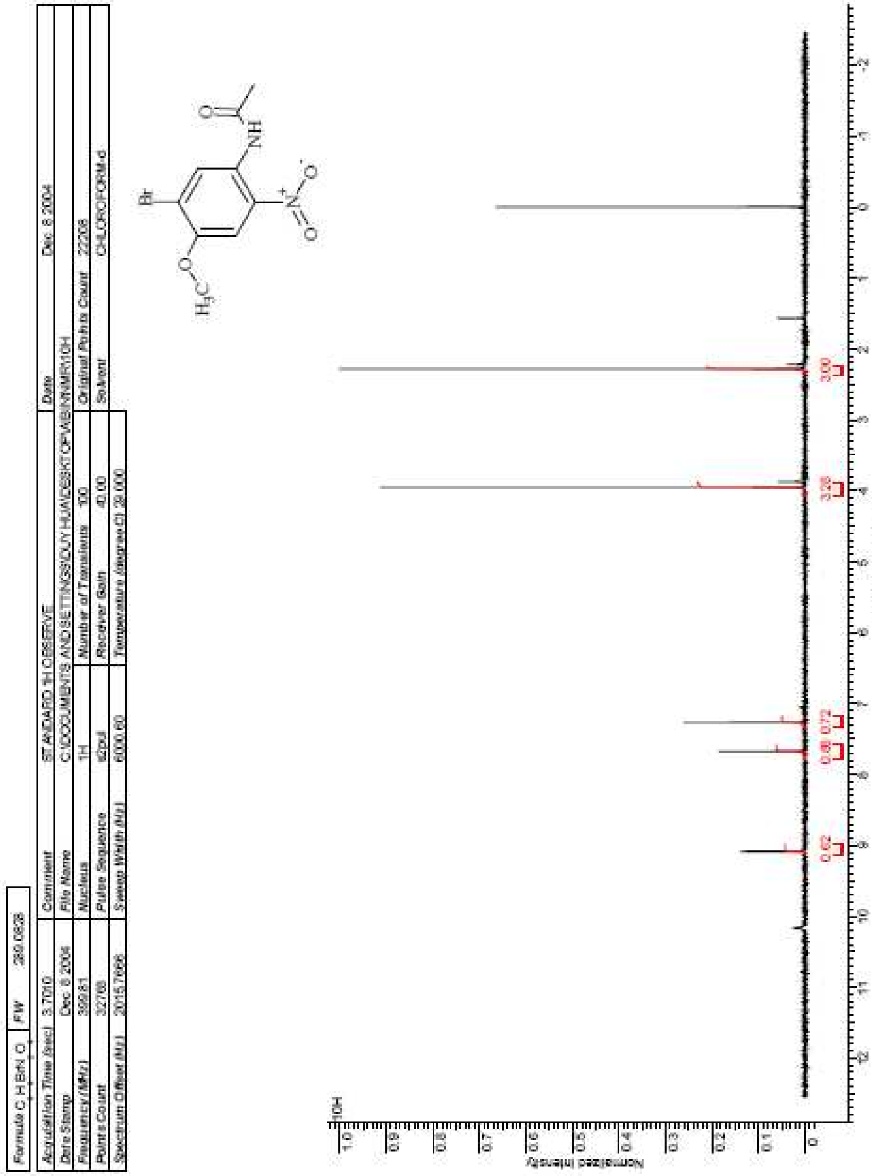

FW 289.0828
Acquisition Time (sec) 3.7010
Comment STANDARD 1H OBSERVE
Date Dec 8 2004
Date Stamp Dec 8 2004
File Name C:\DOCUMENTS AND SETTINGS\DUY HUA\DESKTOP\WBINNMR\10H
Frequency (MHz) 399.81
Nucleus 1H
Number of Transients 100
Original Points Count 22208
Points Count 32768
Pulse Sequence s2pul
Receiver Gain 40.00
Solvent CHLOROFORM-d
Spectrum Offset (Hz) 2015.7666
Sweep Width (Hz) 6000.60
Temperature (degree C) 29.000
Br
H_3C
O
NH
N^+
O^-
10H
Normalized Intensity
0.62
0.86
0.72
3.28
3.00
Chemical Shift (ppm)

Formula $C_{16}H_{11}F_6NO_4$		FW 370.2600			
Acquisition Time (sec)	1.4576	Comment	13C OBSERVE	Date	Apr 30 2006
Date Stamp	Apr 30 2006	File Name	C:\DOCUMENTS AND SETTINGS\DUY HUA\DESKTOP\WBINNMR\12C		
Frequency (MHz)	50.29	Nucleus	13C	Number of Transients 20000	Original Points Count 16720
Points Count	32768	Pulse Sequence	s2pul	Receiver Gain 40.00	Solvent CHLOROFORM-d
Spectrum Offset (Hz)	4881.6094	Sweep Width (Hz)	12500.00	Temperature (degree C) 29.000	

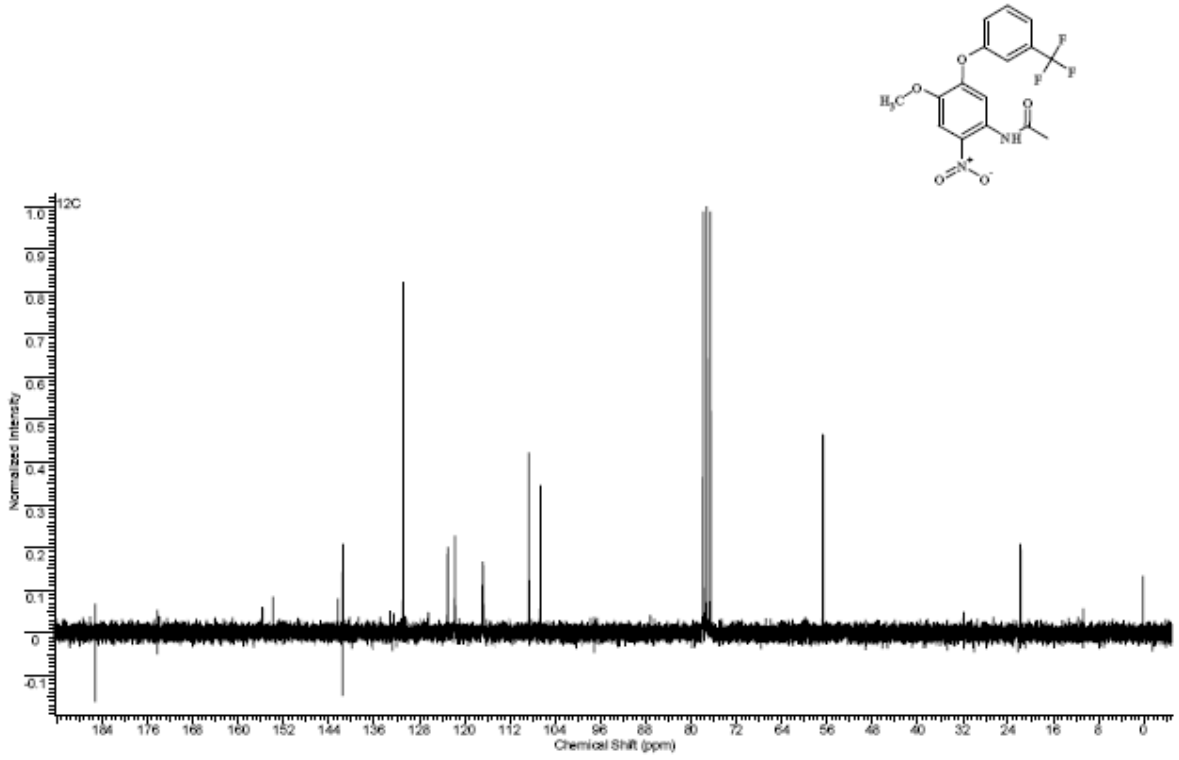

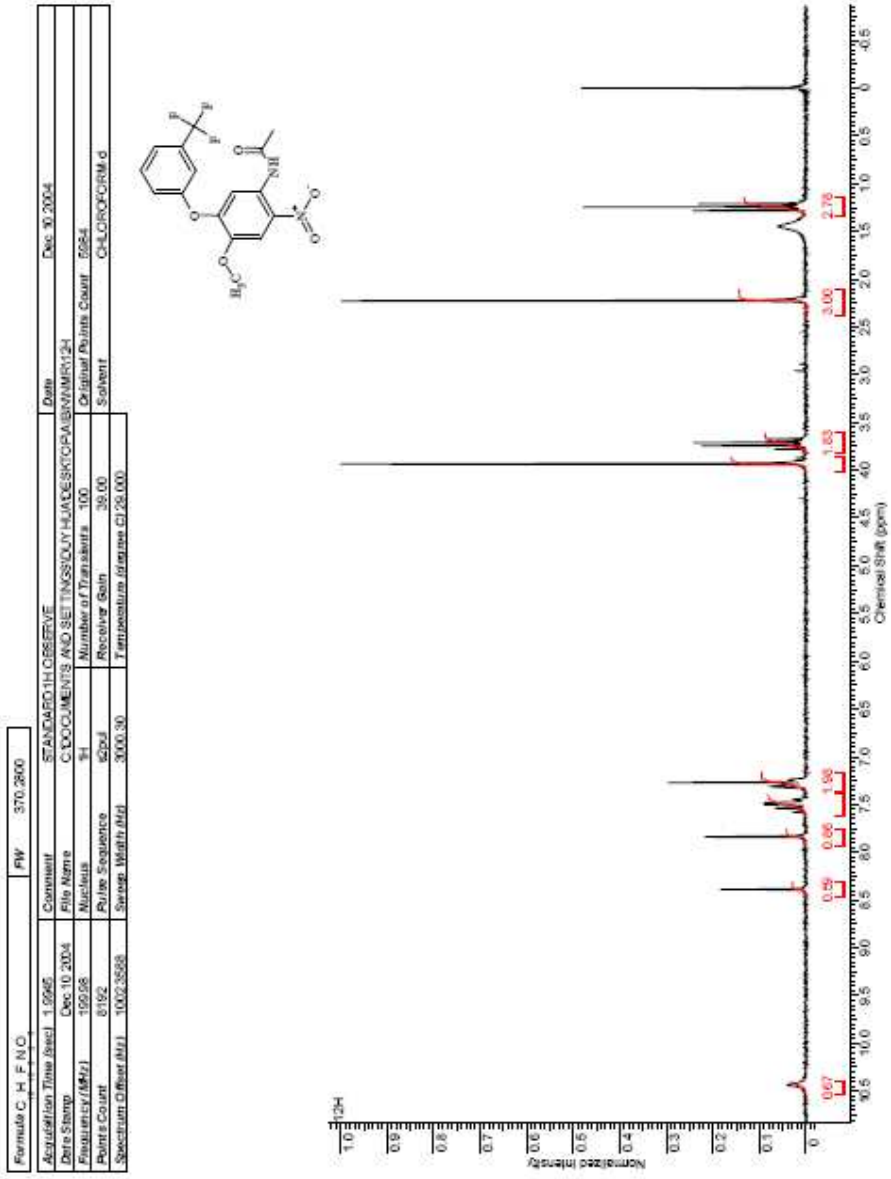
Formula C H F N O FW 370.2800
Acquisition Time (sec) 1.9945 Comment STANDARD 1H OBSERVE Date Dec 10 2004
Date Stamp Dec 10 2004 File Name C:\DOCUMENTS AND SETTINGS\DUY HUA\DESKTOP\A\BMMR\124
Frequency (MHz) 199.98 Nucleus 1H Number of Transients 100 Original Points Count 5984
Points Count 8192 Pulse Sequence s2pul Receiver Gain 39.00 Solvent CHLOROFORM-d
Spectrum Offset (Hz) 1002.3568 Sweep Width (Hz) 3000.30 Temperature (degree C) 29.000
12H
0.97
0.59
0.66
1.98
1.83
3.00
2.76
Normalized Intensity
Chemical Shift (ppm)

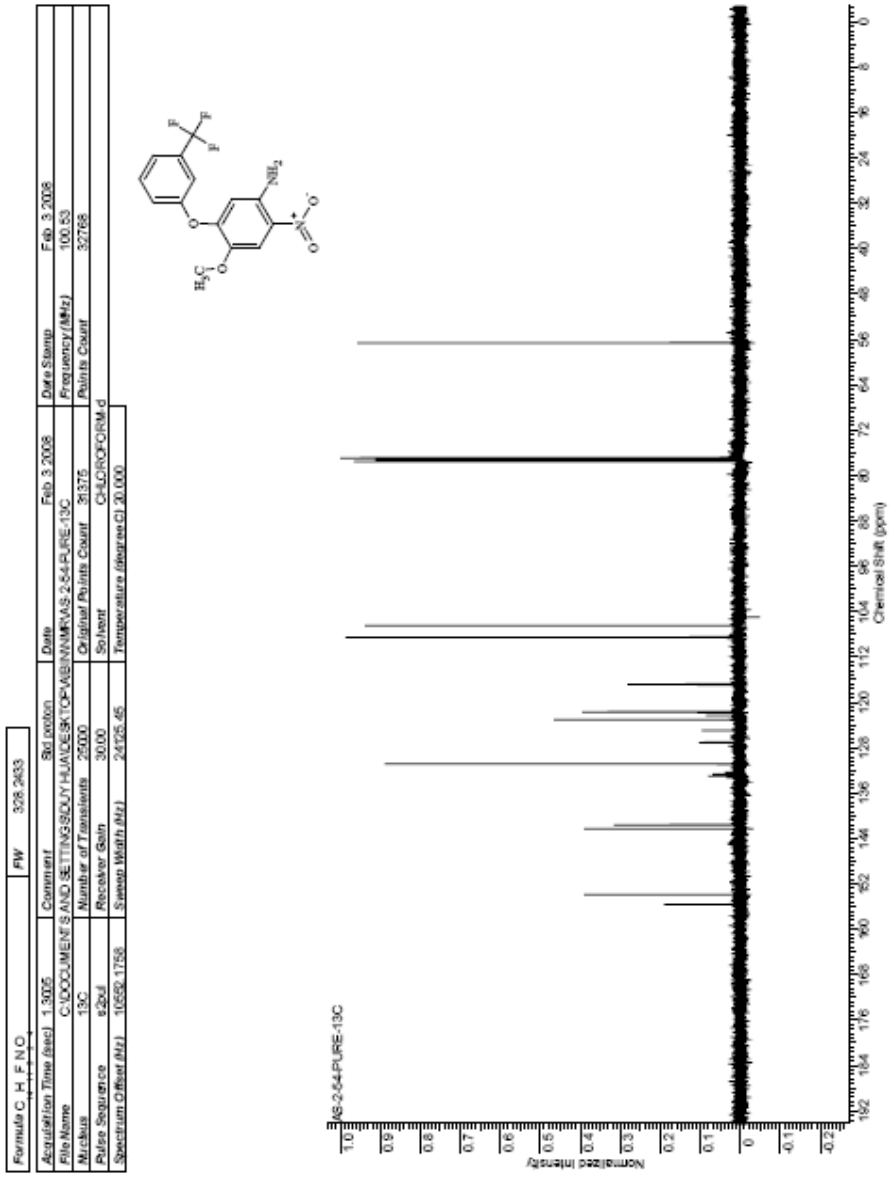
Formula C H F N O FW 328.2433
Acquisition Time (sec) 1.3005 Comment 8x1 proton Date Feb 3 2006 Data Stamp Feb 3 2006
File Name C:\DOCUMENTS AND SETTINGS\DUY HUA\DESKTOP\ABB\NMR\AS-2-54-PURE-13C Frequency (MHz) 100.53
Nucleus 13C Number of Transients 25000 Original Points Count 31375 Points Count 32768
Pulse Sequence s2pul Receiver Gain 3000 Solvent CHLOROFORM-d
Spectrum Offset (Hz) 10552.1758 Sweep Width (Hz) 24705.45 Temperature (degree C) 20.000
AS-2-54-PURE-13C
Normalized Intensity
Chemical Shift (ppm)

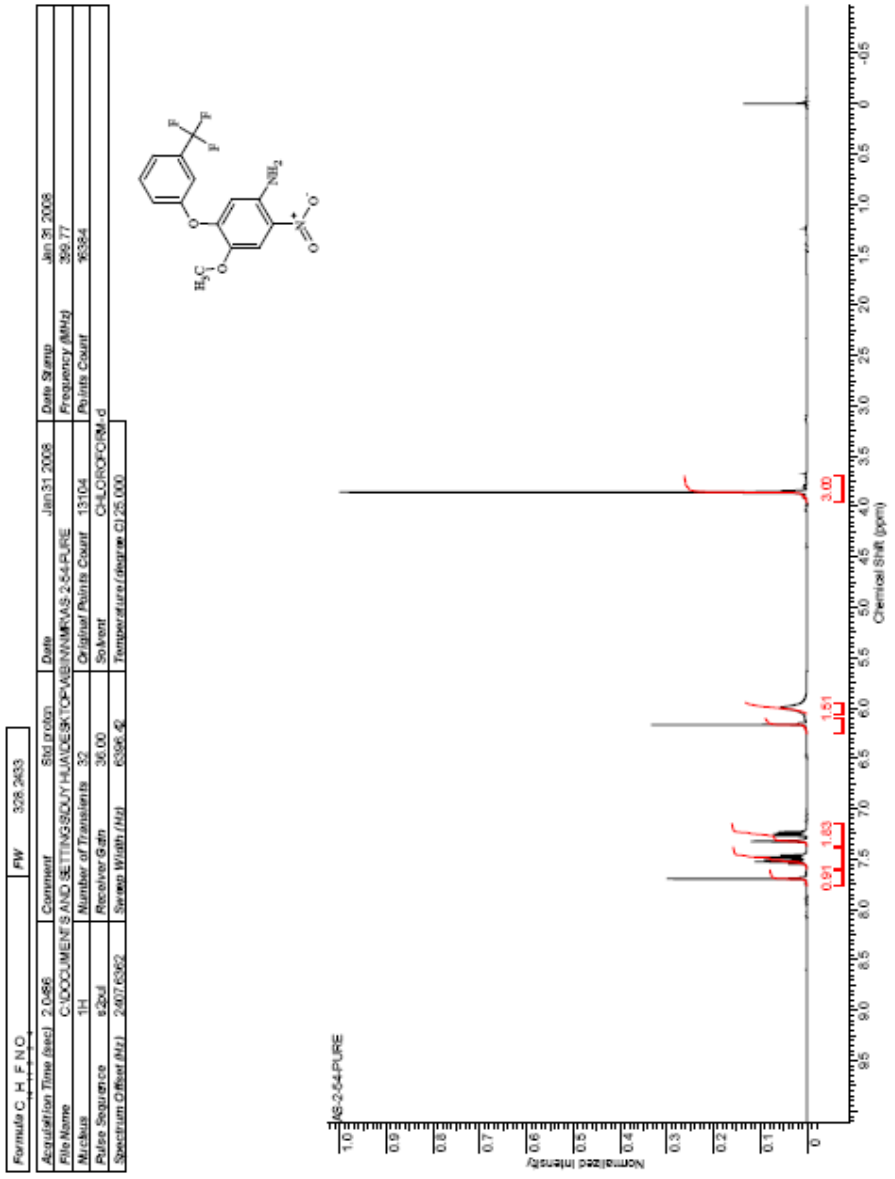
Formula C7H5F3N2O3
FW 326.2433
Acquisition Time (sec) 2.0486
Comment Std proton
Date Jan 31 2006
Date Stamp Jan 31 2006
File Name C:\DOCUMENTS AND SETTINGS\DUY HUA\DESKTOP\ABB\NMR\AS-2-54-PURE
Frequency (MHz) 399.77
Nucleus 1H
Number of Transients 32
Original Points Count 13104
Points Count 16384
Pulse Sequence s2pul
Receiver Gain 36.00
Solvent CHLOROFORM-d
Sweep Width (Hz) 6596.4
Temperature (degree C) 25.000
AS-2-54-PURE
Normalized Intensity
Chemical Shift (ppm)
0.91
1.83
1.81
3.00

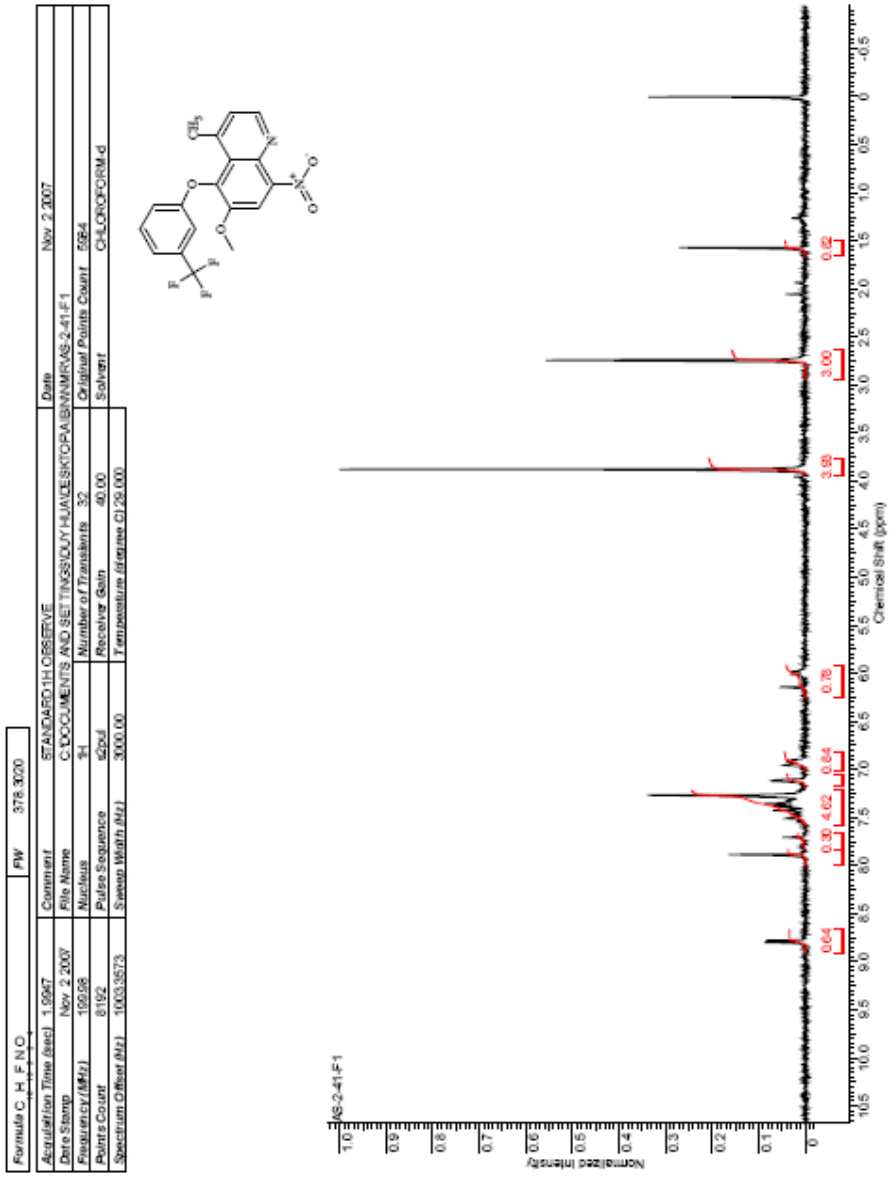
Formula C H F N O FW 378.3020
Acquisition Time (sec) 1.9947 Comment STANDARD 1H OBSERVE Date Nov 2 2007
Date Stamp Nov 2 2007 File Name C:\DOCUMENTS AND SETTINGS\DUYHUA\DESKTOP\ASBNMR\AS-2-41-F1
Frequency (MHz) 199.98 Nucleus 1H Number of Transients 32 Original Points Count 5984
Points Count 8192 Pulse Sequence s2pul Receiver Gain 40.00 Solvent CHLOROFORM-d
Spectrum Offset (Hz) 1003.3573 Sweep Width (Hz) 3000.00 Temperature (degrees C) 29.000
AS-2-41-F1
Normalized Intensity
Chemical Shift (ppm)
0.64
0.30
4.62
0.84
0.78
3.98
3.00
0.82

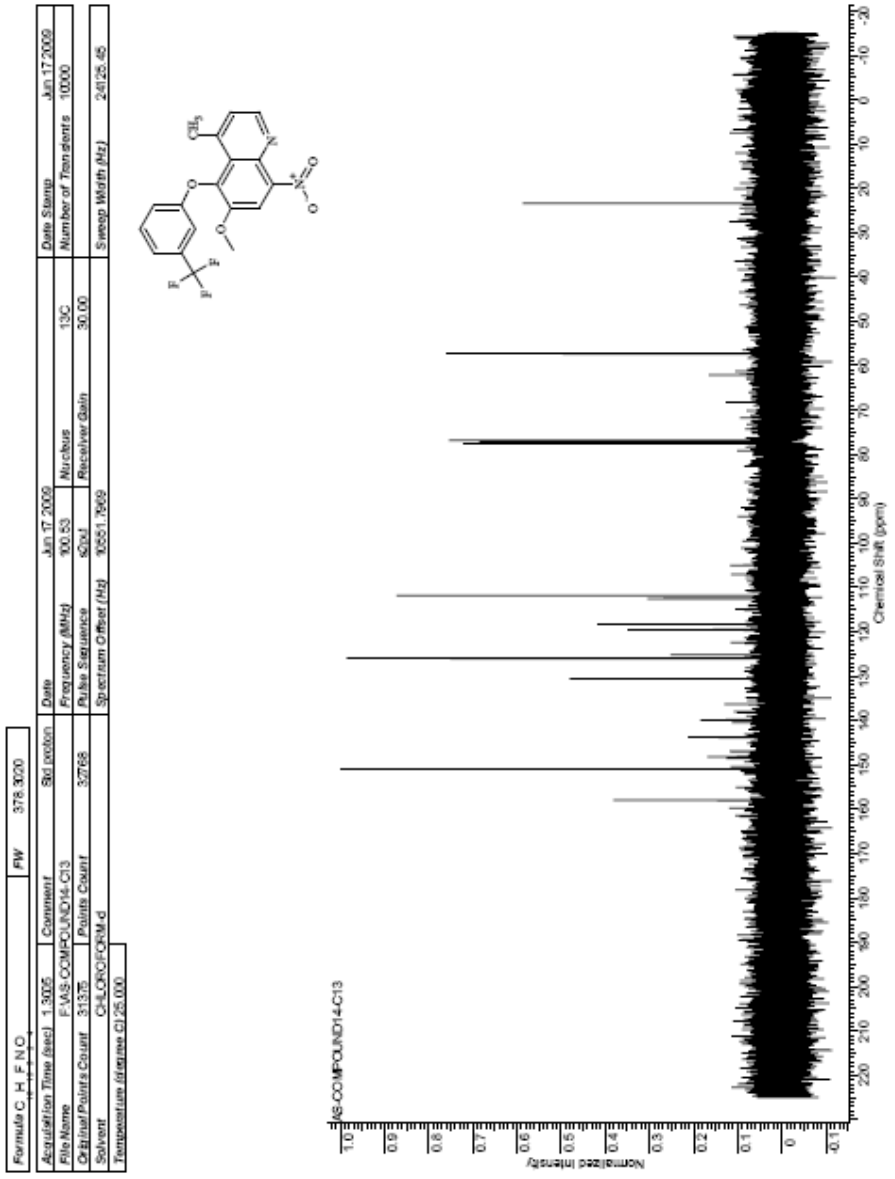
Formula C H F N O FW 378.3020
Acquisition Time (sec) 1.3005 Comment Std proton
File Name FJAS-COMPOUND14-C13
Original Points Count 31376 Points Count 32768
Solvent CHLOROFORM-d
Temperature (degree C) 25.000
Date Jun 17 2009
Frequency (MHz) 100.53
Pulse Sequence s2pul
Spectrum Offset (Hz) 10551.7969
Nucleus 13C
Receiver Gain 30.00
Date Stamp Jun 17 2009
Number of Transients 10000
Sweep Width (Hz) 24125.45
JAS-COMPOUND14-C13
Normalized Intensity
Chemical Shift (ppm)

Formula C H F N O FW 368.3832
Acquisition Time (sec) 1.3005 Comment Std proton Date Jan 30 2008 Date Stamp Jan 30 2008
File Name C:\DOCUMENTS AND SETTINGS\DUY HUA\DESKTOP\ABENNMR\15C Frequency (MHz) 100.63
Nucleus 13C Number of Transients 40000 Original Points Count 31375 Points Count 32768
Pulse Sequence s2pul Receiver Gain 30.00 Solvent CHLOROFORM-d
Spectrum Offset (Hz) 10064.3646 Sweep Width (Hz) 24175.45 Temperature (degree C) 25.000
15C
Normalized Intensity
Chemical Shift (ppm)

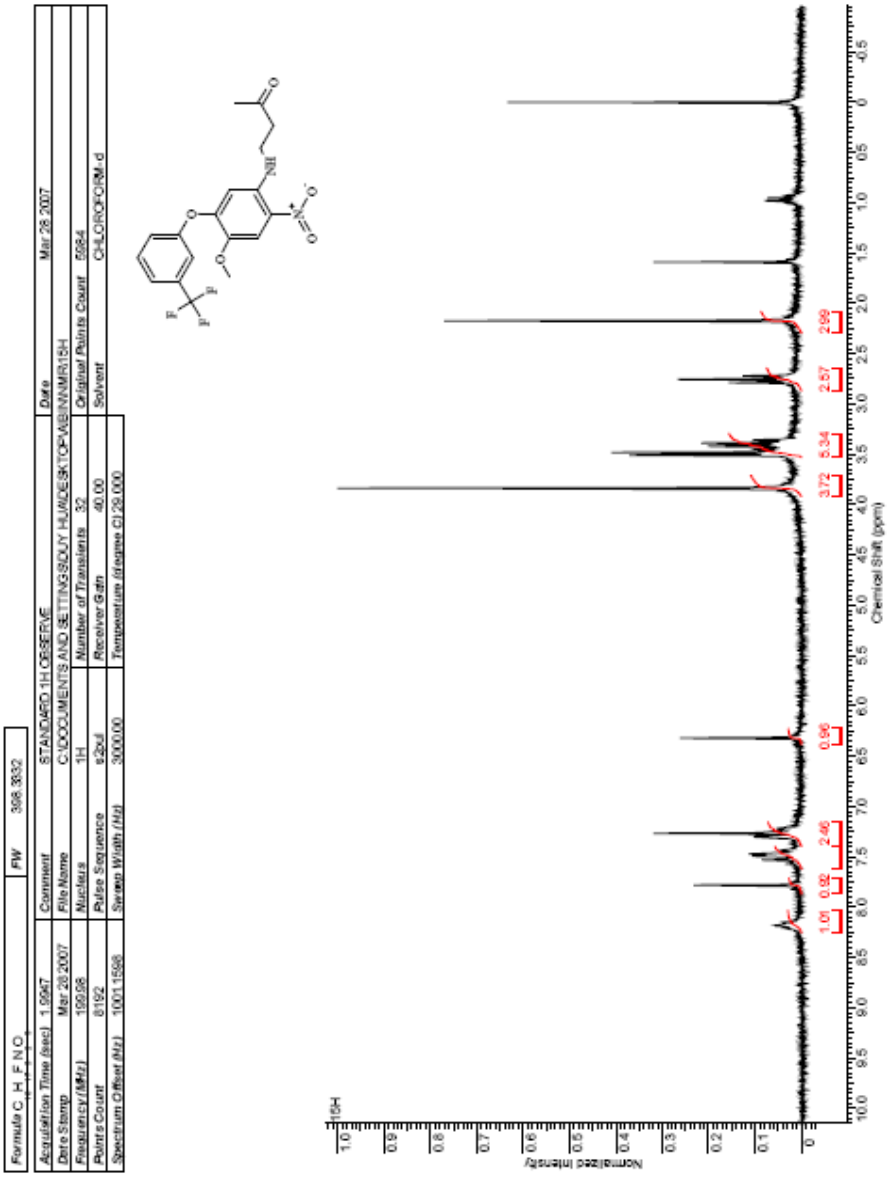
Formula C H F N O FW 368.3832
Acquisition Time (sec) 1.9947 Comment STANDARD 1H OBSERVE Date Mar 26 2007
Date Stamp Mar 26 2007 File Name C:\DOCUMENTS AND SETTINGS\DOY HURLE\DESKTOP\ABI\NMR\15H
Frequency (MHz) 199.98 Nucleus 1H Number of Transients 32 Original Points Count 5984
Points Count 8192 Pulse Sequence s2pul Receiver Gain 40.00 Solvent CHLOROFORM-d
Spectrum Offset (Hz) 1001.1586 Sweep Width (Hz) 3000.00 Temperature (degree C) 29.000
15H
1.00 0.92 2.46 0.96 3.72 5.34 2.57 2.99
Normalized Intensity
Chemical Shift (ppm)

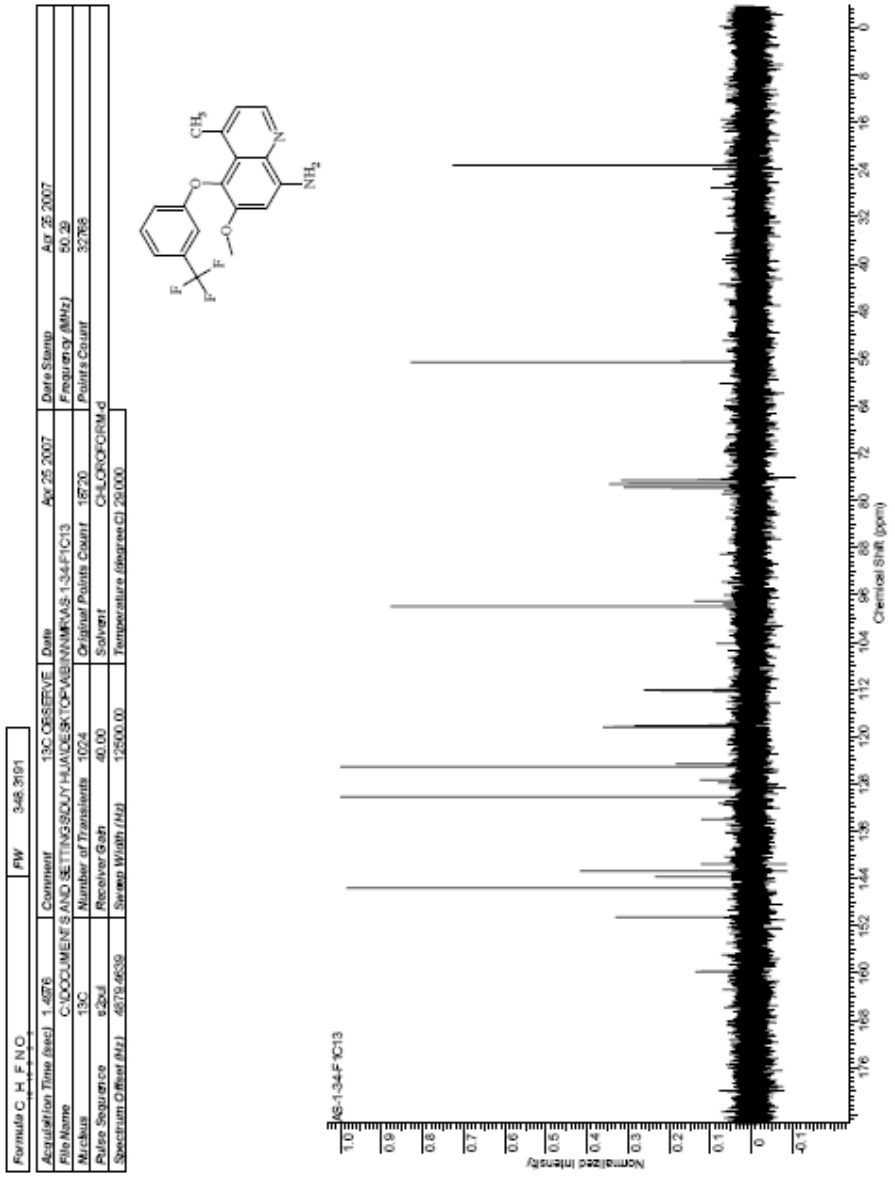
Formula C H F N O FW 348.3181
Acquisition Time (sec) 1.4976 Comment 13C OBSERVE Date Apr 25 2007 Data Stamp Apr 25 2007
File Name C:\DOCUMENTS AND SETTINGS\DUY HUA\DESKTOP\ABI\NMR\AS-1-34-F1C13 Frequency (MHz) 50.29
Nucleus 13C Number of Transients 1024 Original Points Count 16720 Points Count 32768
Pulse Sequence s2pul Receiver Gain 40.00 Solvent CHLOROFORM-d
Spectrum Offset (Hz) 4679.4658 Sweep Width (Hz) 12500.00 Temperature (degree C) 28.000
AS-1-34-F1C13
Normalized Intensity
Chemical Shift (ppm)

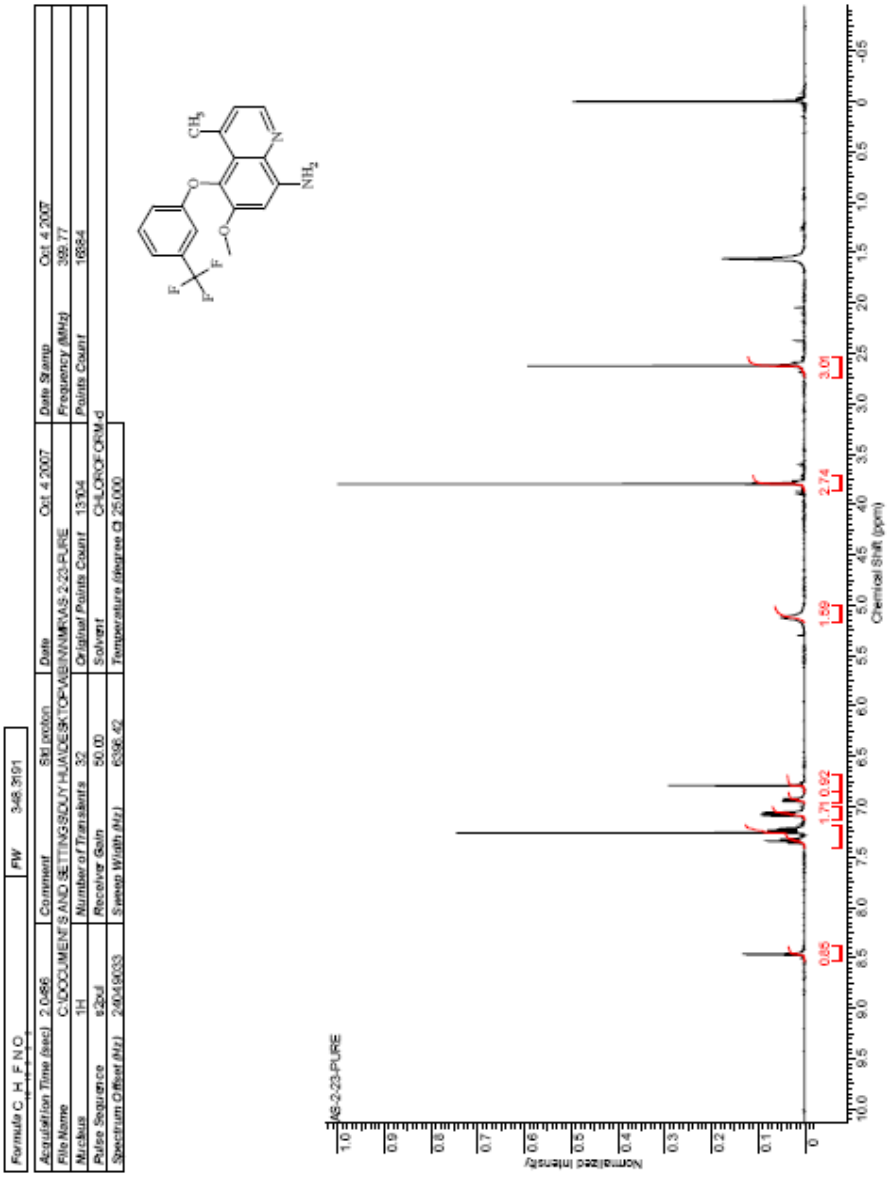
Formula C H F N O FW 348.3181
Acquisition Time (sec) 2.0486 Comment Std proton Date Oct 4 2007 Date Stamp Oct 4 2007
File Name C:\DOCUMENTS AND SETTINGS\DUY HUA\DESKTOP\ABI\NMR\AS-2-23-PURE Frequency (MHz) 399.77
Nucleus 1H Number of Transients 32 Original Points Count 13104 Points Count 16884
Pulse Sequence s2pul Receiver Gain 50.00 Solvent CHLOROFORM-d
Spectrum Offset (Hz) 2004.9003 Sweep Width (Hz) 6596.49 Temperature (degree C) 25.000
AS-2-23-PURE
Normalized Intensity
Chemical Shift (ppm)
0.85
1.71
0.92
1.59
2.74
3.01

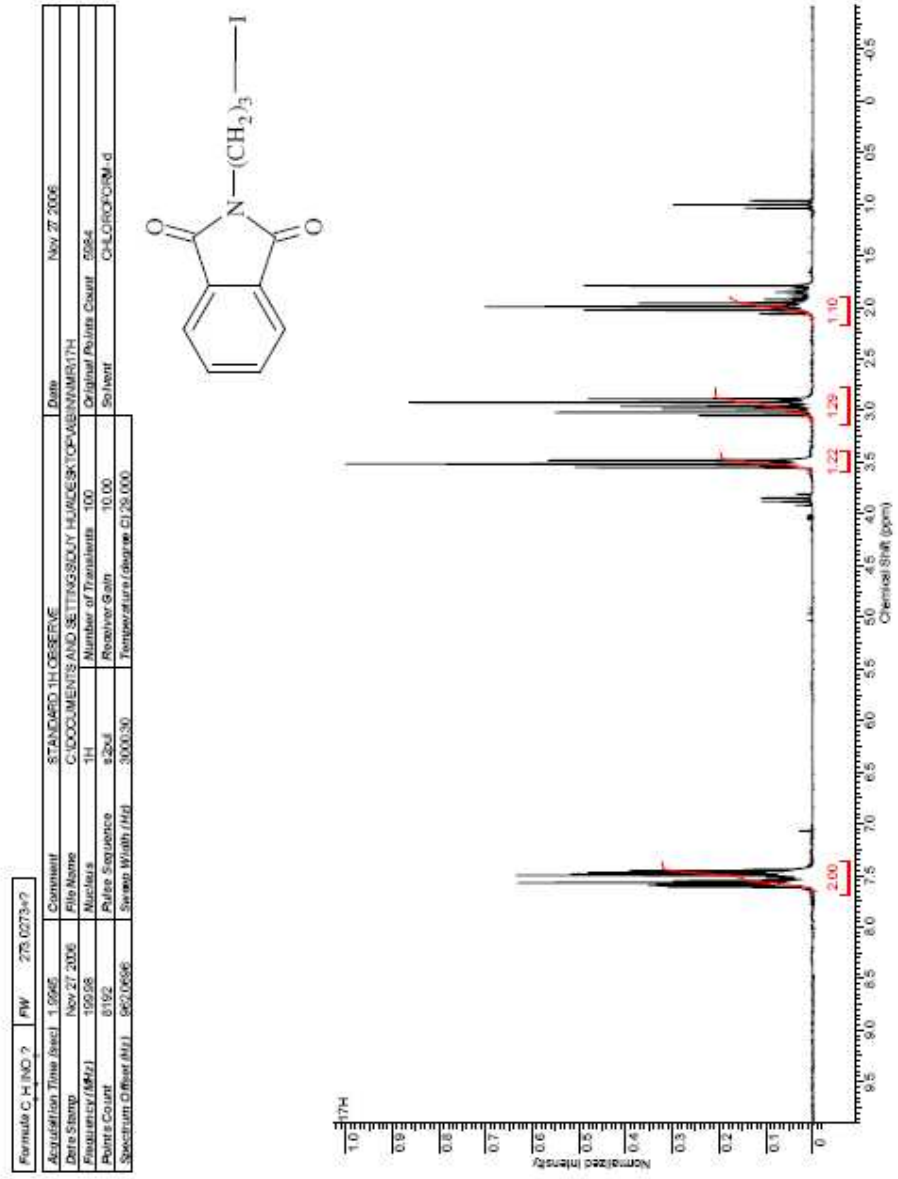
Formula C H INO 2
FW 273.0273+2
Acquisition Time (sec) 1.9945
Comment STANDARD 1H OBSERVE
Date Nov 27 2006
Date Stamp Nov 27 2006
File Name C:\DOCUMENTS AND SETTINGS\DUY HUA\ESKTOP\ABENNMR\17H
Frequency (MHz) 199.98
Nucleus 1H
Number of Transients 100
Original Points Count 5984
Points Count 8192
Pulse Sequence s2pul
Receiver Gain 10.00
Solvent CHLOROFORM-d
Spectrum Offset (Hz) 6612.0996
Sweep Width (Hz) 3000.30
Temperature (degree C) 29.000
17H
Normalized Intensity
Chemical Shift (ppm)
2.00
1.22
1.29
1.10

Formula $C_{29}H_{24}F_3N_3O_4$	FW	535.5138

Acquisition Time (sec)	1.3005	Comment	Std proton	Date	Sep 26 2007	Date Stamp	Sep 26 2007
File Name	C:\DOCUMENTS AND SETTINGS\DUY HUA\DESKTOP\WBIN\NMR\AS-2-19-C13					Frequency (MHz)	100.53
Nucleus	13C	Number of Transients	15000	Original Points Count	31375	Points Count	32768
Pulse Sequence	s2pul	Receiver Gain	30.00	Solvent	CHLOROFORM-d		
Spectrum Offset (Hz)	10553.6484	Sweep Width (Hz)	24125.45	Temperature (degree C)	20.000		

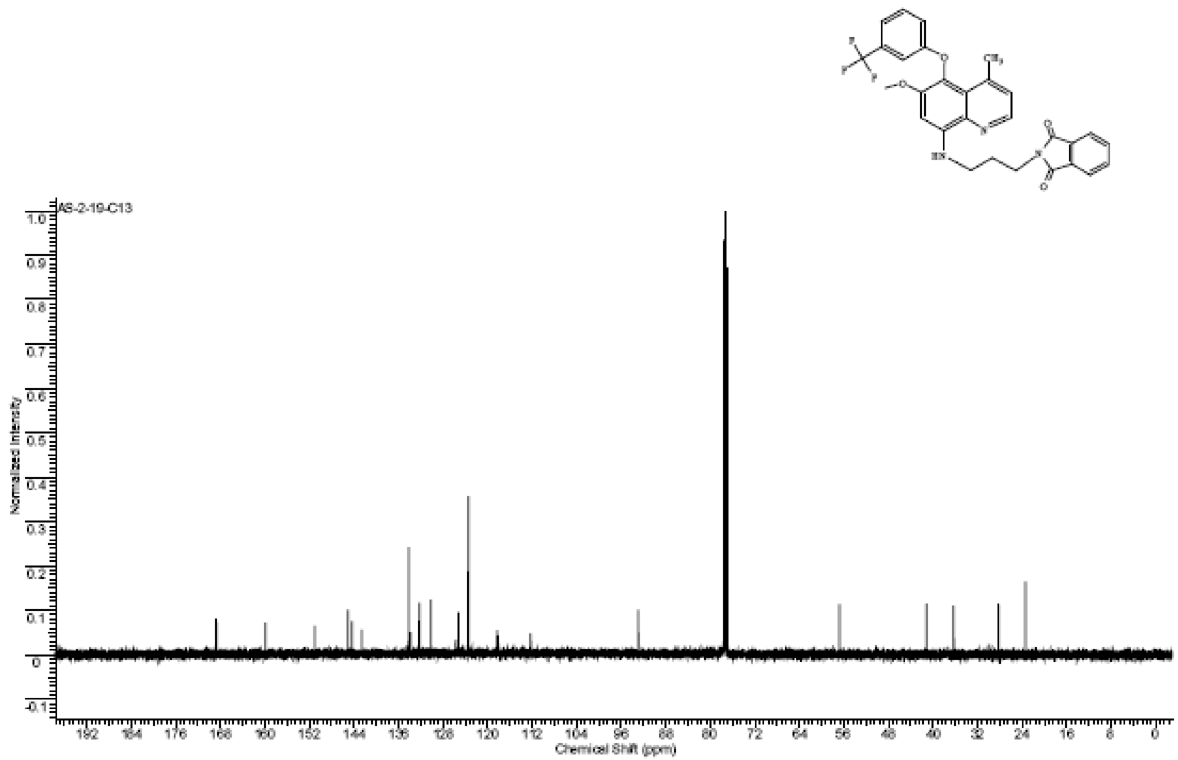

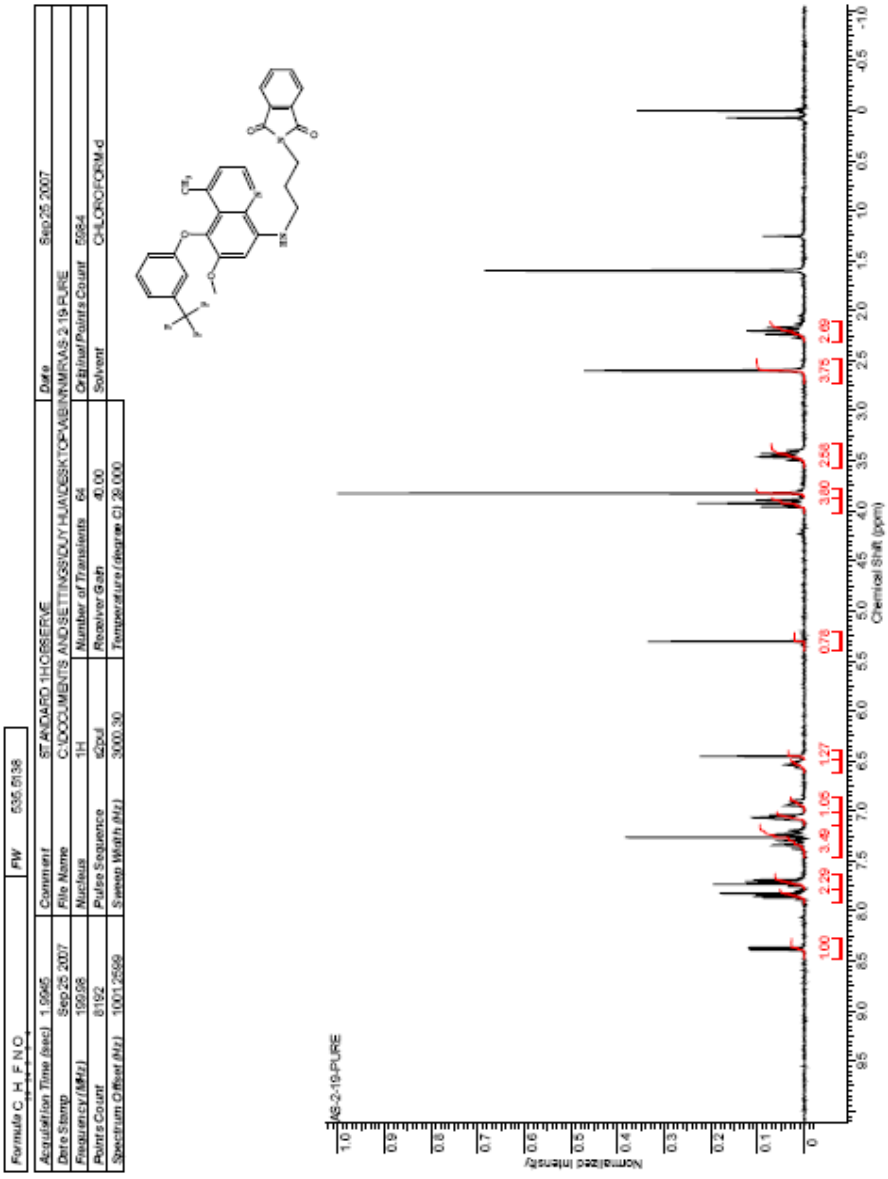
Formula C H F N O FW 535.5138
Acquisition Time (sec) 1.9945
Date Stamp Sep 25 2007
Frequency (MHz) 199.98
Points Count 8192
Spectrum Offset (Hz) 1001.4568
Comment STANDARD 1H OBSERVE
File Name C:\DOCUMENTS AND SETTINGS\DUY HUA\DESKTOP\ABI\MMRNAS-2-19-PURE
Nucleus 1H
Pulse Sequence s2pul
Sweep Width (Hz) 3003.30
Date Sep 25 2007
Number of Transients 64
Receiver Gain 40.00
Temperature (degree C) 28.000
Original Points Count 5984
Solvent CHLOROFORM-d
MS-2-19-PURE
Normalized Intensity
Chemical Shift (ppm)
1.00
2.29
3.49
1.05
1.27
0.78
3.80
2.58
3.75
2.69

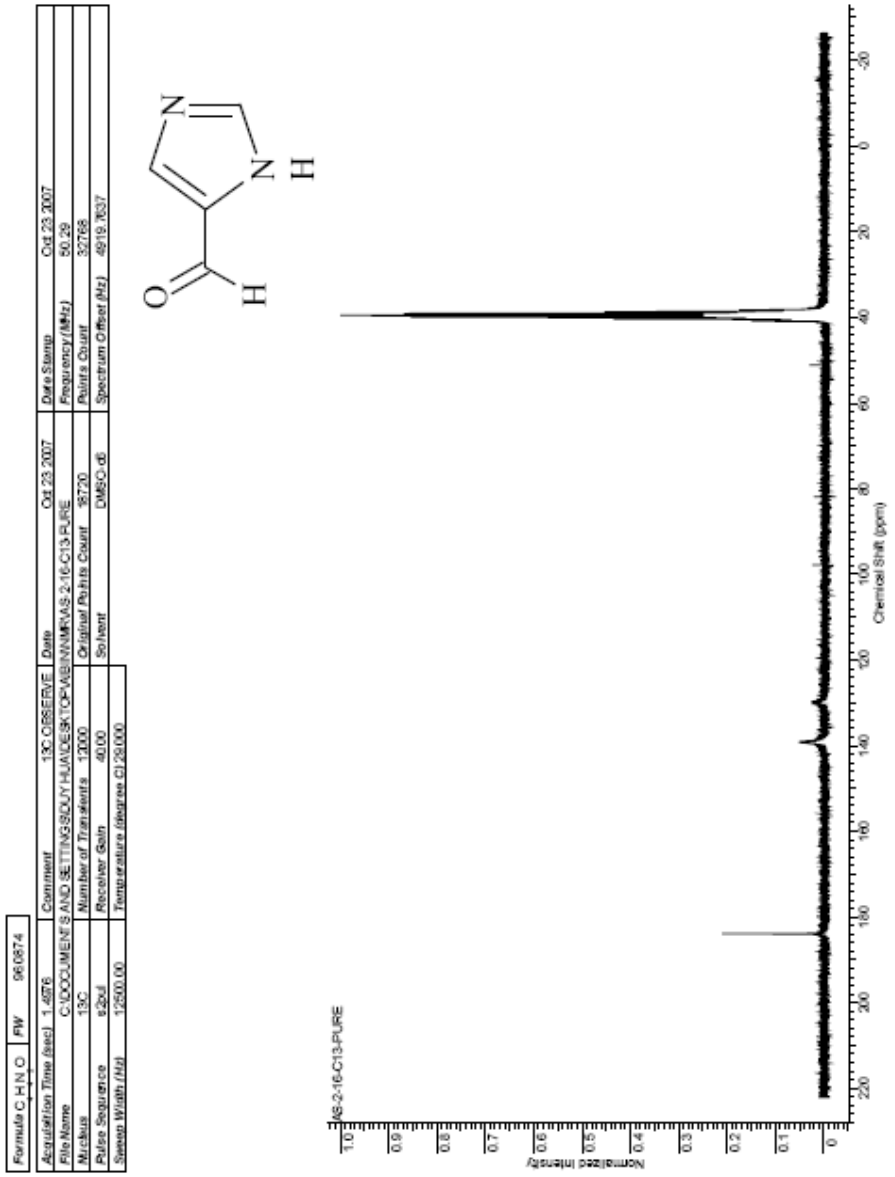
Formula C H N O FW 96.0874
Acquisition Time (sec) 1.4976
Comment 13C OBSERVE
Date Oct 23 2007
Date Stamp Oct 23 2007
File Name C:\DOCUMENTS AND SETTINGS\DUY HUA\DESKTOP\ABI\NMR\AS-2-16-C13-PURE
Frequency (MHz) 50.29
Nucleus 13C
Number of Transients 12000
Original Points Count 16720
Points Count 32768
Pulse Sequence s2pul
Receiver Gain 40.00
Solvent DMSO-d6
Spectrum Offset (Hz) 4919.7637
Sweep Width (Hz) 12500.00
Temperature (degree C) 29.000
AS-2-16-C13-PURE
Normalized Intensity
Chemical Shift (ppm)

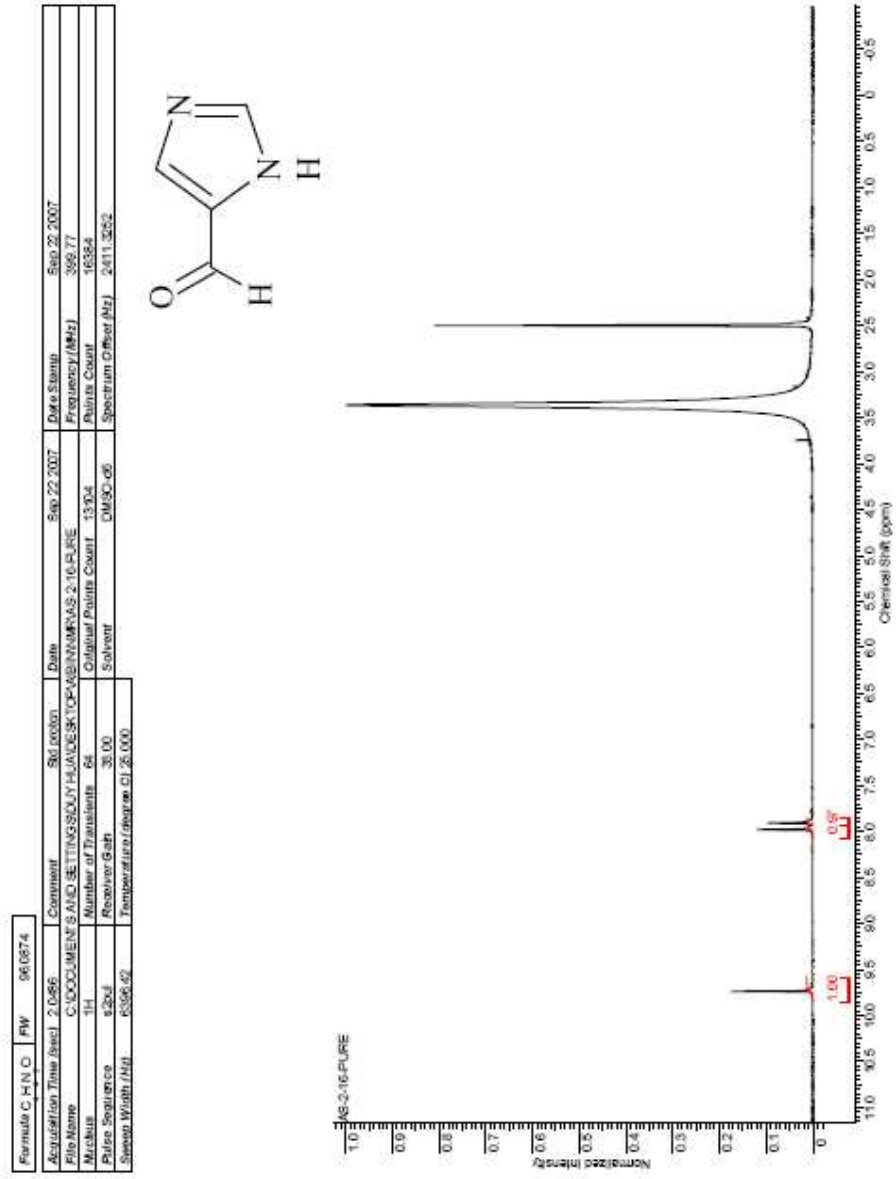
Formula C H N O FW 96.0874
Acquisition Time (sec) 2.0486 Comment Std proton Date Sep 22 2007
File Name C:\DOCUMENTS AND SETTINGS\JOY HJAVE\DESKTOP\MS\MAS-2-16-PURE
Nucleus 1H Number of Transients 64 Original Points Count 13104
Pulse Sequence s2pul Receiver Gain 35.00 Solvent DMSO-d6
Sweep Width (Hz) 6536.60 Temperature (degree C) 26.000
Date Stamp Sep 22 2007
Frequency (MHz) 399.77
Points Count 16384
Spectrum Offset (Hz) 2411.3252
O
H
N
N
H
MS-2-16-PURE
Normalized Intensity
Chemical Shift (ppm)
1.00
0.97

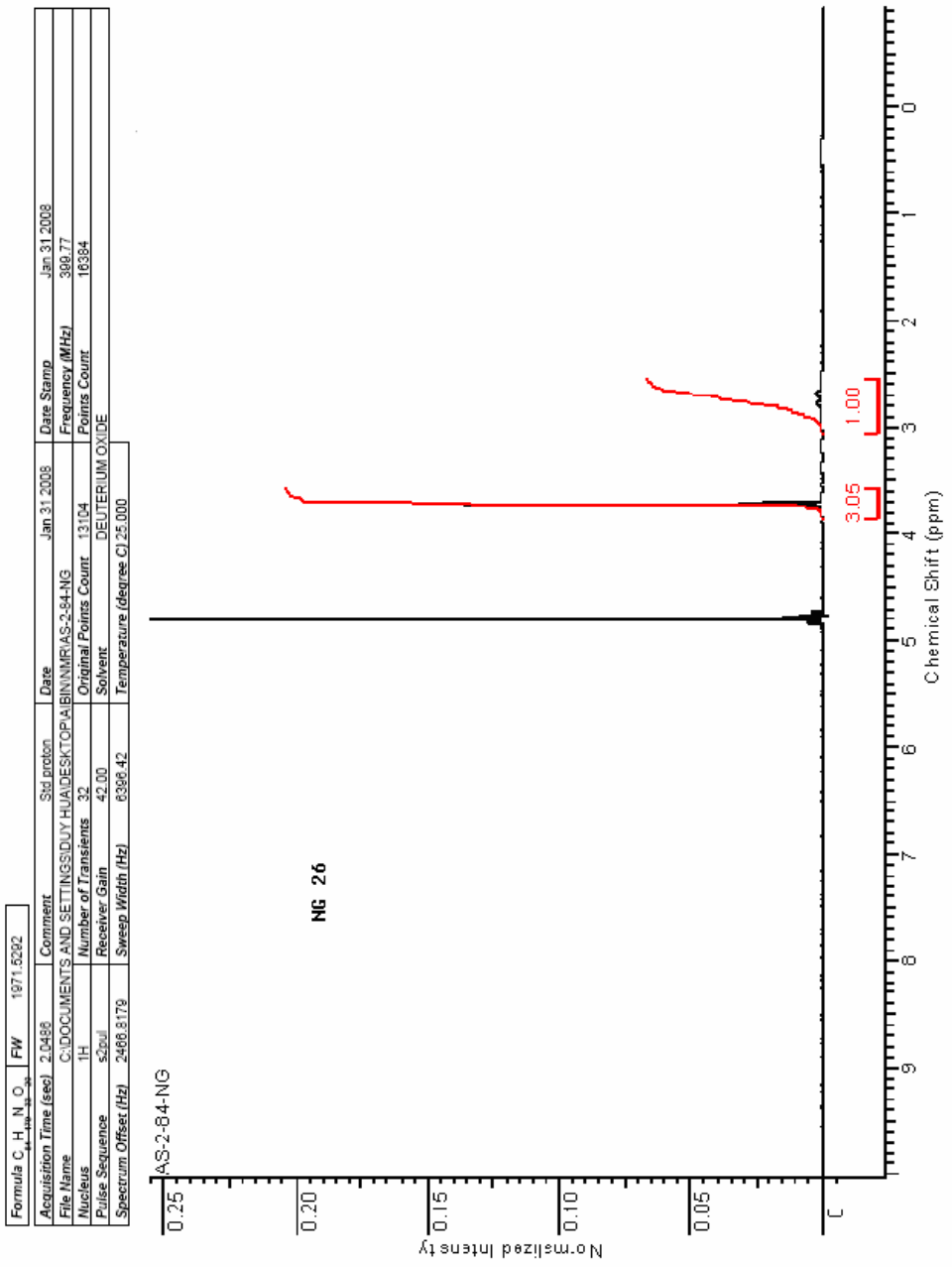
Formula C H N O FW 1971.5292
Acquisition Time (sec) 2.0498 Comment Std proton Date Jan 31 2008 Date Stamp Jan 31 2008
File Name C:\DOCUMENTS AND SETTINGS\DUY HUA\DESKTOP\AIBIN\NMR\AS-2-84-NG Frequency (MHz) 399.77
Nucleus 1H Number of Transients 32 Original Points Count 13104 Points Count 16384
Pulse Sequence s2pul Receiver Gain 42.00 Solvent DEUTERIUM OXIDE
Spectrum Offset (Hz) 2486.8179 Sweep Width (Hz) 6396.42 Temperature (degree C) 25.000
AS-2-84-NG
NG 26
3.05
1.00
Normalized Intensity
Chemical Shift (ppm)

Formula $C_{80}H_{160}N_{22}O_{23}$	FW	2097.6392					
Acquisition Time (sec)	2.0486	Comment	Std proton	Date	Dec 12 2007	Date Stamp	Dec 12 2007
File Name	C:\DOCUMENTS AND SETTINGS\DUY HUA\DESKTOP\AIBIN\NMR\AS-2-44-NG-AC2O					Frequency (MHz)	399.77
Nucleus	1H	Number of Transients	32	Original Points Count	13104	Points Count	16384
Pulse Sequence	s2pul	Receiver Gain	42.00	Solvent	DEUTERIUM OXIDE		
Spectrum Offset (Hz)	2467.4038	Sweep Width (Hz)	6396.42	Temperature (degree C)	25.000		

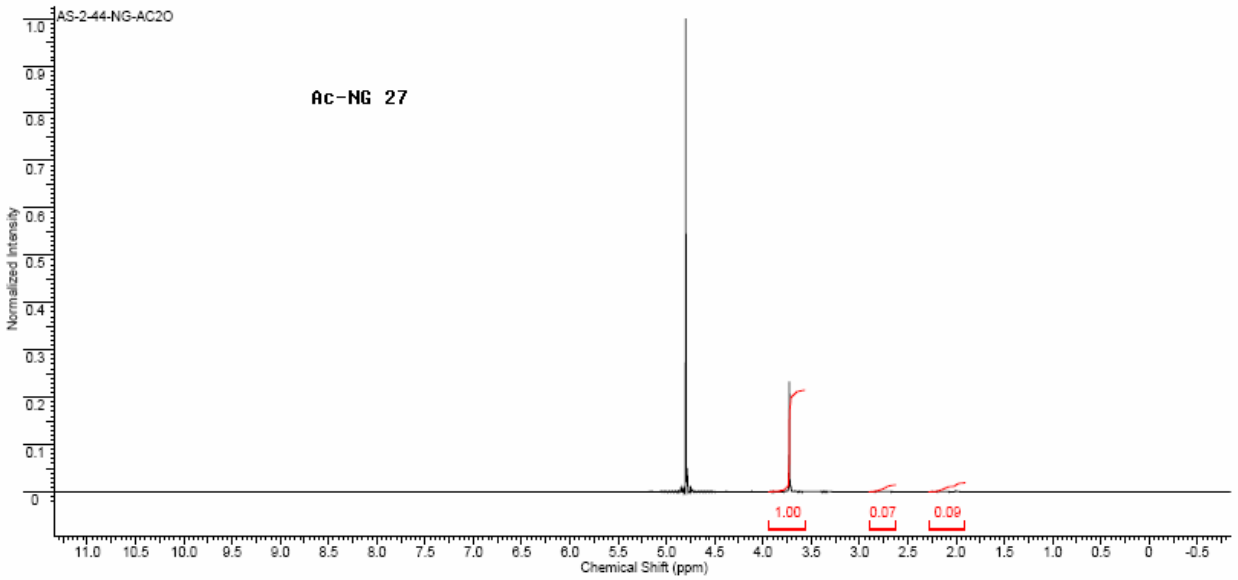

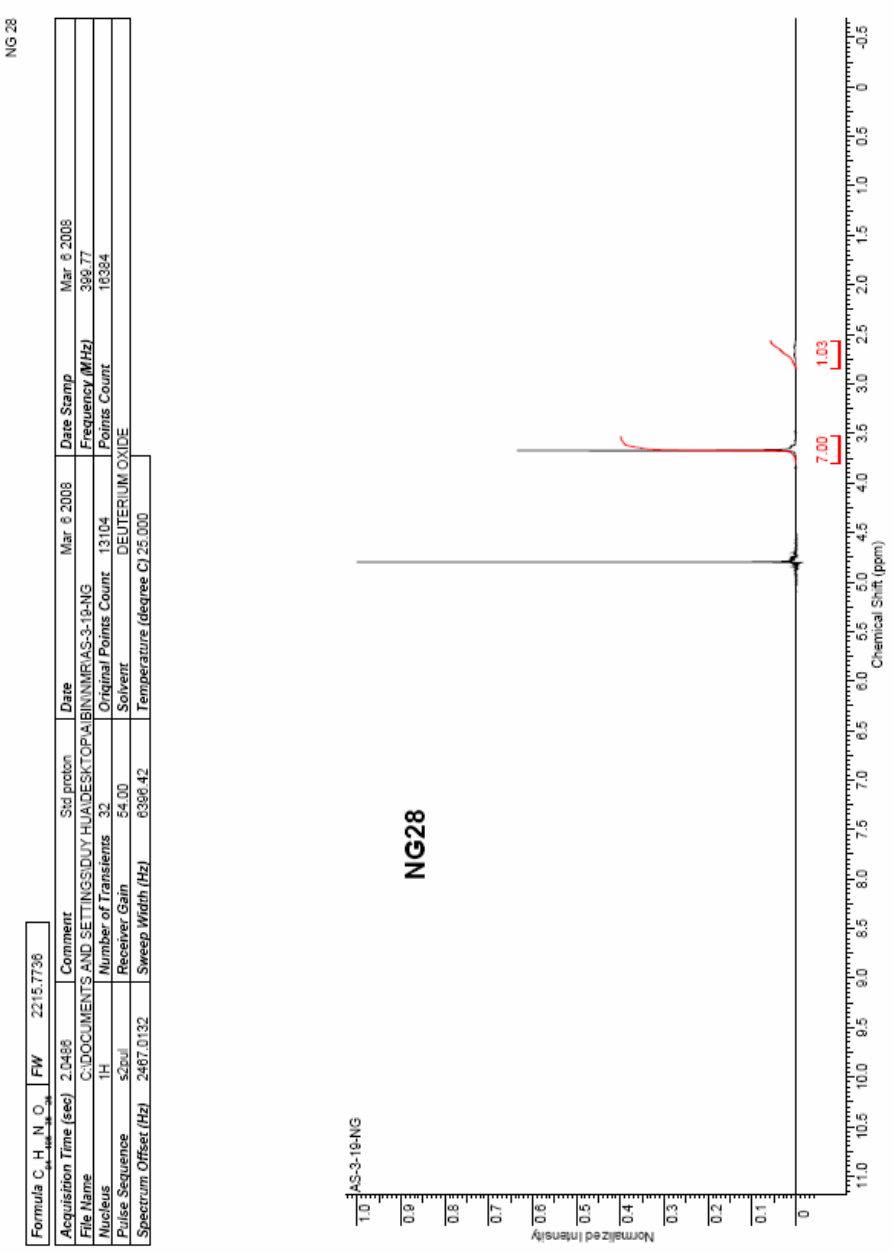
NG 28
Formula C H N O FW 2215.7736
Acquisition Time (sec) 2.0486 Comment Std proton Date Mar 6 2008 Date Stamp Mar 6 2008
File Name C:\DOCUMENTS AND SETTINGS\DUY HUA\DESKTOP\AIBIN\NMR\AS-3-19-NG Frequency (MHz) 399.77
Nucleus 1H Number of Transients 32 Original Points Count 13104 Points Count 16384
Pulse Sequence s2pul Receiver Gain 54.00 Solvent DEUTERIUM OXIDE
Spectrum Offset (Hz) 2467.0132 Sweep Width (Hz) 6398.42 Temperature (degree C) 25.000
NG28
AS-3-19-NG
Normalized Intensity
Chemical Shift (ppm)
7.00
1.03

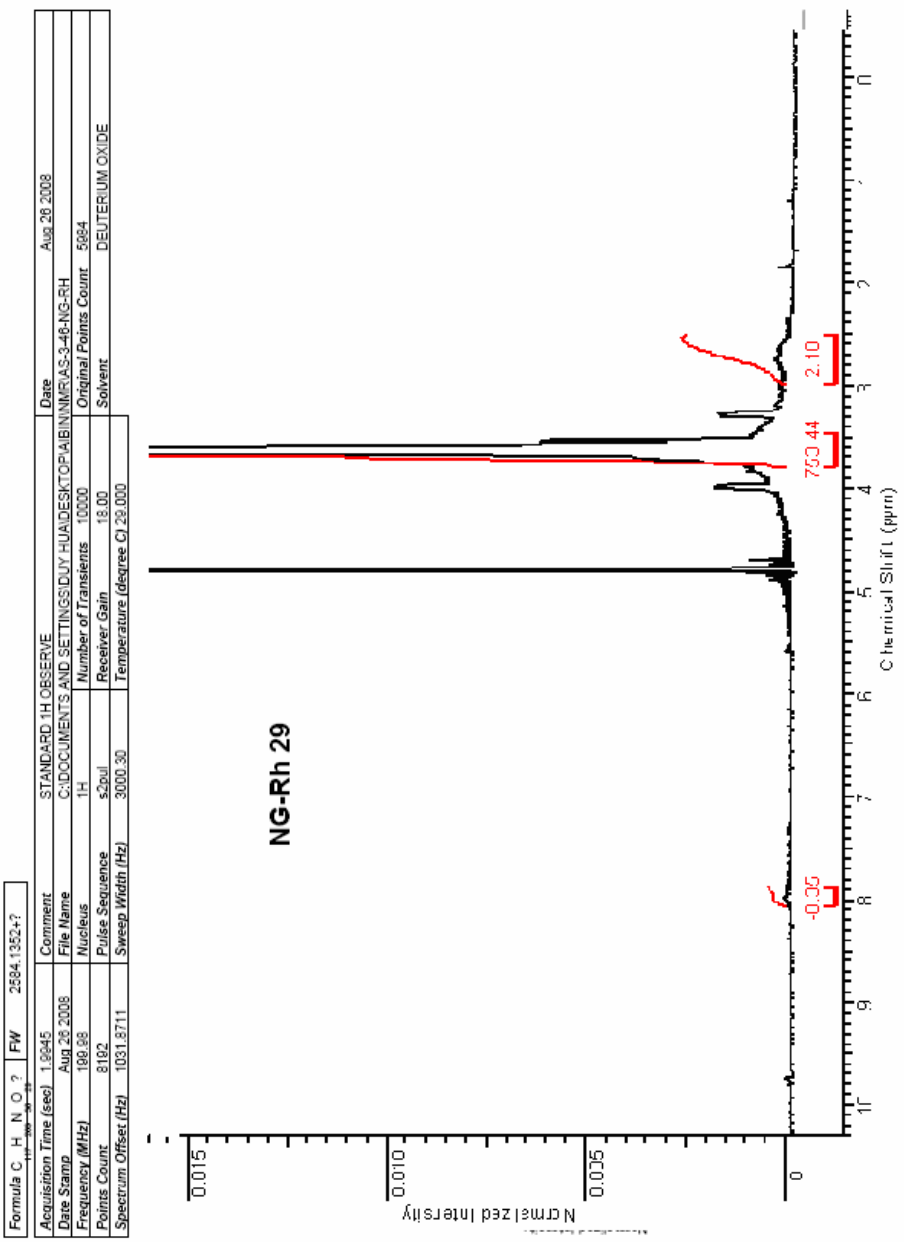
Formula C H N O ? FW 2584.1352+?
Acquisition Time (sec) 1.9945
Comment STANDARD 1H OBSERVE
Date Aug 28 2008
Date Stamp Aug 28 2008
File Name C:\DOCUMENTS AND SETTINGS\DUY HUA\DESKTOP\ALBIN\NMR\AS-3-48-NG-RH
Frequency (MHz) 199.98
Nucleus 1H
Number of Transients 10000
Original Points Count 5984
Points Count 8192
Pulse Sequence s2pul
Receiver Gain 18.00
Solvent DEUTERIUM OXIDE
Spectrum Offset (Hz) 1031.8711
Sweep Width (Hz) 3000.30
Temperature (degree C) 29.000
NG-Rh 29
Normalized Intensity
0.015
0.010
0.005
0
-0.05
7.44
2.10
Chemical Shift (ppm)

Formula $C_{42}H_{46}DTBN_2O_4PS$				FW	470.2766		
Acquisition Time (sec)	2.0467	Comment	Std proton	Date	Nov 3 2008	Date Stamp	Nov 3 2008
File Name	C:\DOCUMENTS AND SETTINGS\DUY HUA\DESKTOP\WB\NNMR\AS-4-64-PURE					Frequency (MHz)	399.76
Nucleus	1H	Number of Transients	128	Original Points Count	13103	Points Count	16384
Pulse Sequence	s2pul	Receiver Gain	54.00	Solvent	CHLOROFORM-d		
Spectrum Offset (Hz)	2414.4705	Sweep Width (Hz)	6395.91	Temperature (degree C)	25.000		

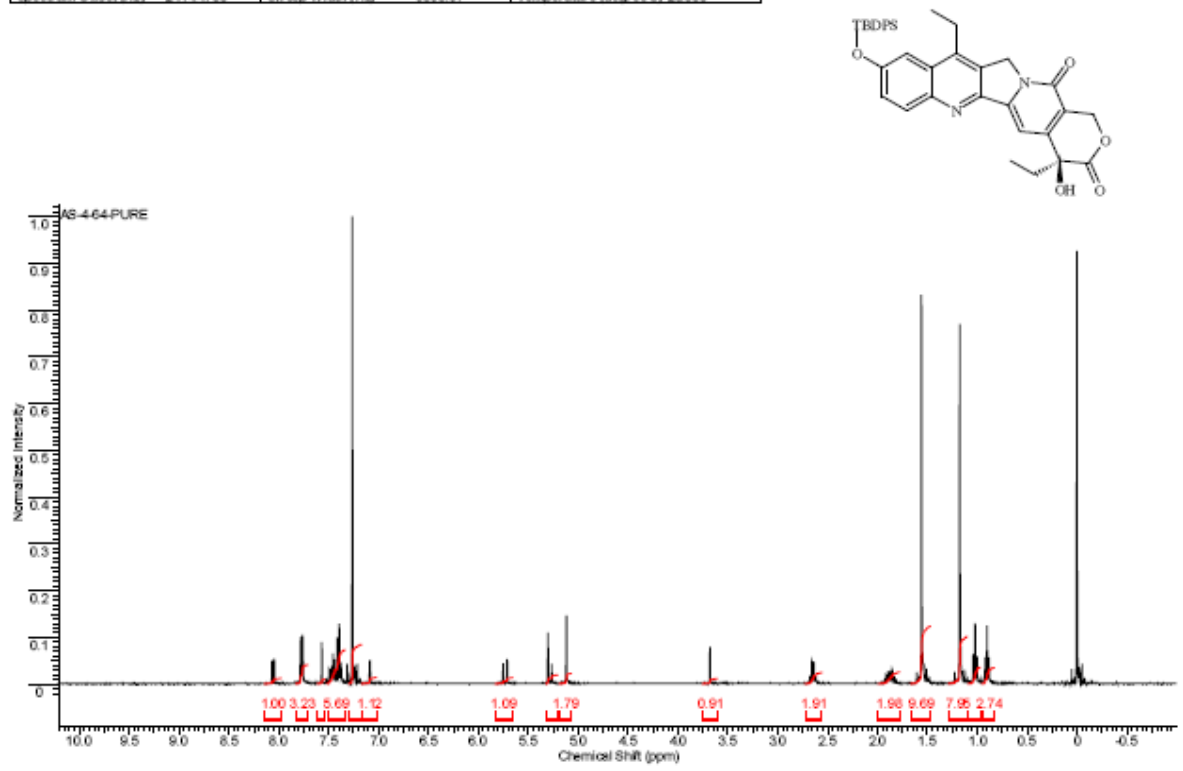

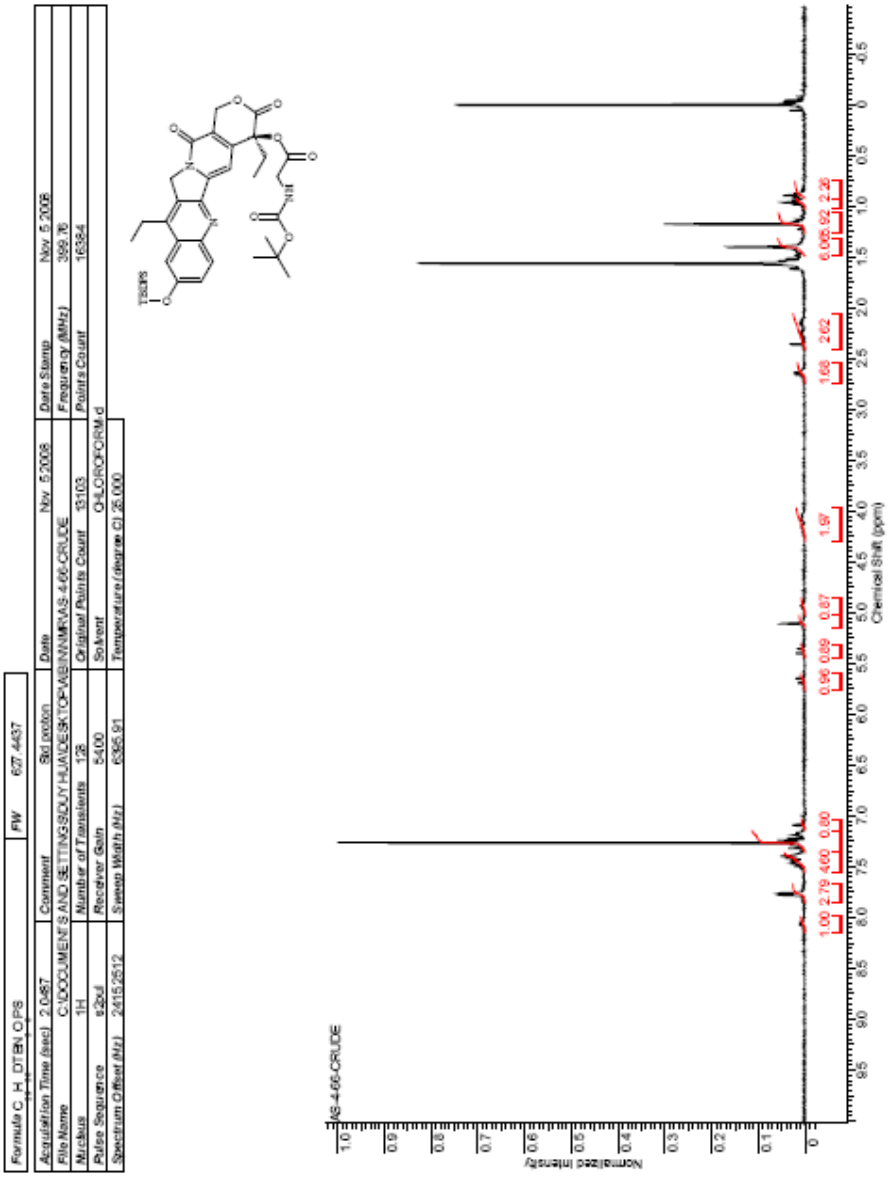
Formula C_H_DTBI_O_PS
FW 627.4437
Acquisition Time (sec) 2.0487
Comment Std proton
Date Nov 5 2008
Date Stamp Nov 5 2008
File Name C:\DOCUMENTS AND SETTINGS\DOUYHUA\DESKTOP\ABINNMR\AS-4-66-CRUDE
Frequency (MHz) 399.76
Nucleus 1H
Number of Transients 128
Original Points Count 15103
Points Count 16384
Pulse Sequence s2pul
Receiver Gain 5400
Solvent CHLOROFORM-d
Spectrum Offset (Hz) 2415.2512
Sweep Width (Hz) 6365.91
Temperature (degree C) 26.000
TBDPS
AS-4-66-CRUDE
Normalized Intensity
Chemical Shift (ppm)
1.00 2.79 4.60 0.80
0.96 0.89 0.87 1.97
1.68 2.62
6.06 5.92 2.26

Formula $C_{44}H_{57}DTBN_4O_7Si$		FW	827.3279				
Acquisition Time (sec)	2.0467	Comment	Std proton	Date	Nov 6 2008	Date Stamp	Nov 6 2008
File Name	C:\DOCUMENTS AND SETTINGS\DUY HUA\DESKTOP\AB\NMR\AS-4-68-CRUDE					Frequency (MHz)	399.76
Nucleus	1H	Number of Transients	128	Original Points Count	13103	Points Count	16384
Pulse Sequence	s2pul	Receiver Gain	5400	Solvent	CHLOROFORM-d		
Spectrum Offset (Hz)	2413.8848	Sweep Width (Hz)	6395.91	Temperature (degree C)	25.000		

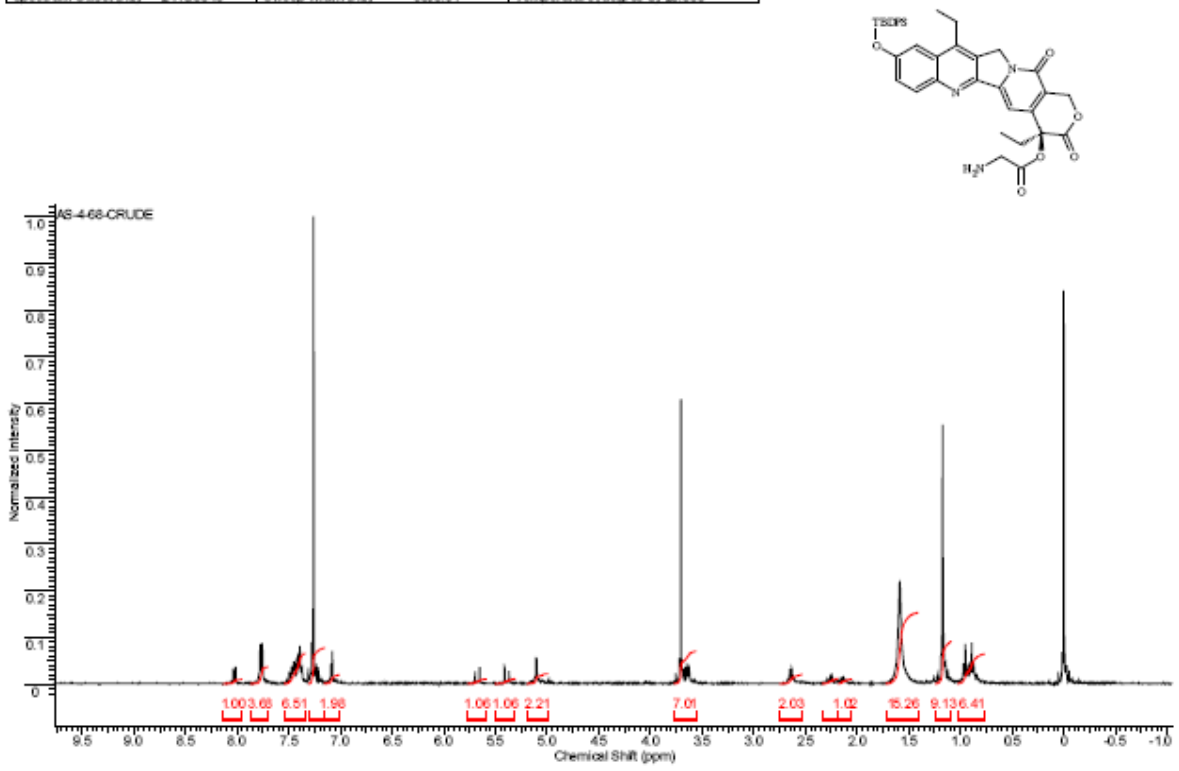

Formula $C_{42}H_{47}DTBN_4O_7PS$				FW 627.4007			
Acquisition Time (sec)	1.4976	Comment	13C OBSERVE	Date	Feb 26 2009	Date Stamp	Feb 26 2009
File Name	C:\DOCUMENTS AND SETTINGS\DUY HUA\DESKTOP\AB\NMR\AS-5-SN380-COOH-C13					Frequency (MHz)	50.29
Nucleus	13C	Number of Transients	20000	Original Points Count	18720	Points Count	32768
Pulse Sequence	s2pul	Receiver Gain	40.00	Solvent	CHLOROFORM-d		
Spectrum Offset (Hz)	4875.8877	Sweep Width (Hz)	12500.00	Temperature (degree C)	29.000		

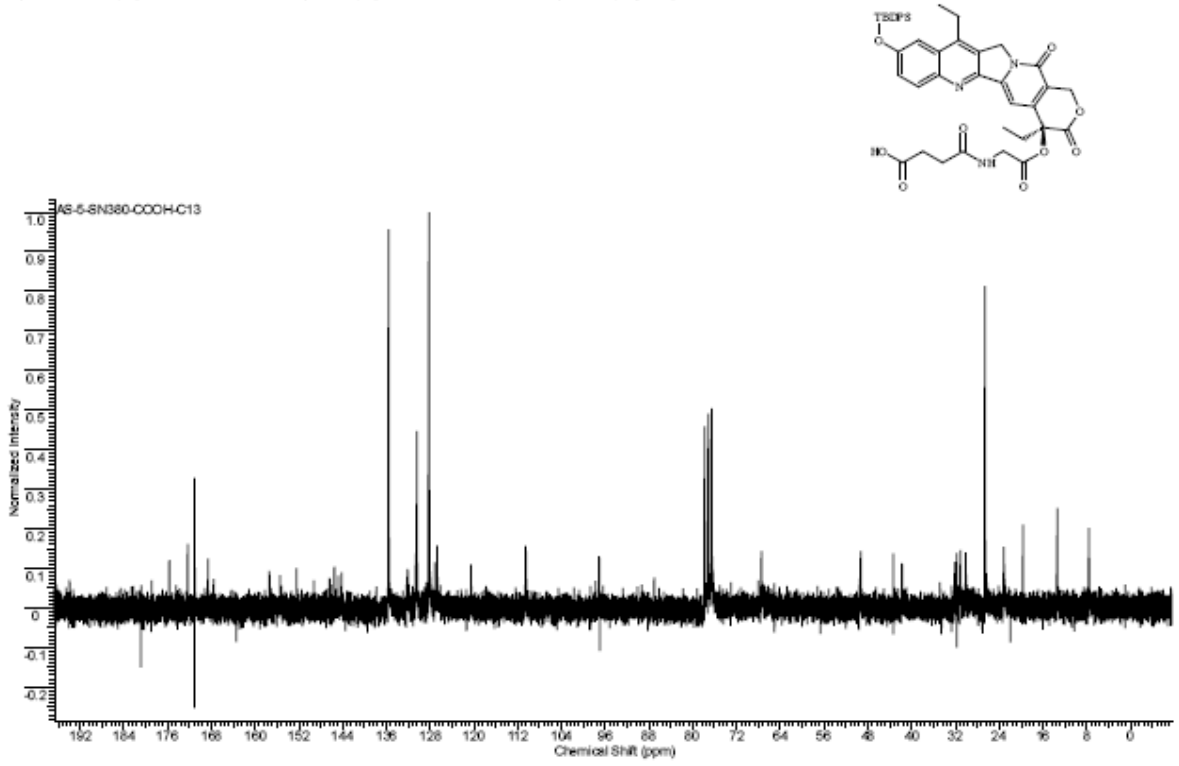

Formula $C_{42}H_{47}DTBN_4O_7PS$		FW	627.4007				
Acquisition Time (sec)	2.0457	Comment	Std proton	Date	Nov 10 2006	Date Stamp	Nov 10 2006
File Name	C:\DOCUMENTS AND SETTINGS\DUY HUA\DESKTOP\AB\NNMR\AS-4-69-CRUDE					Frequency (MHz)	399.76
Nucleus	1H	Number of Transients	128	Original Points Count	13103	Points Count	16384
Pulse Sequence	s2pul	Receiver Gain	54.00	Solvent	CHLOROFORM-d		
Spectrum Offset (Hz)	2413.6897	Sweep Width (Hz)	6396.91	Temperature (degree C)	25.000		

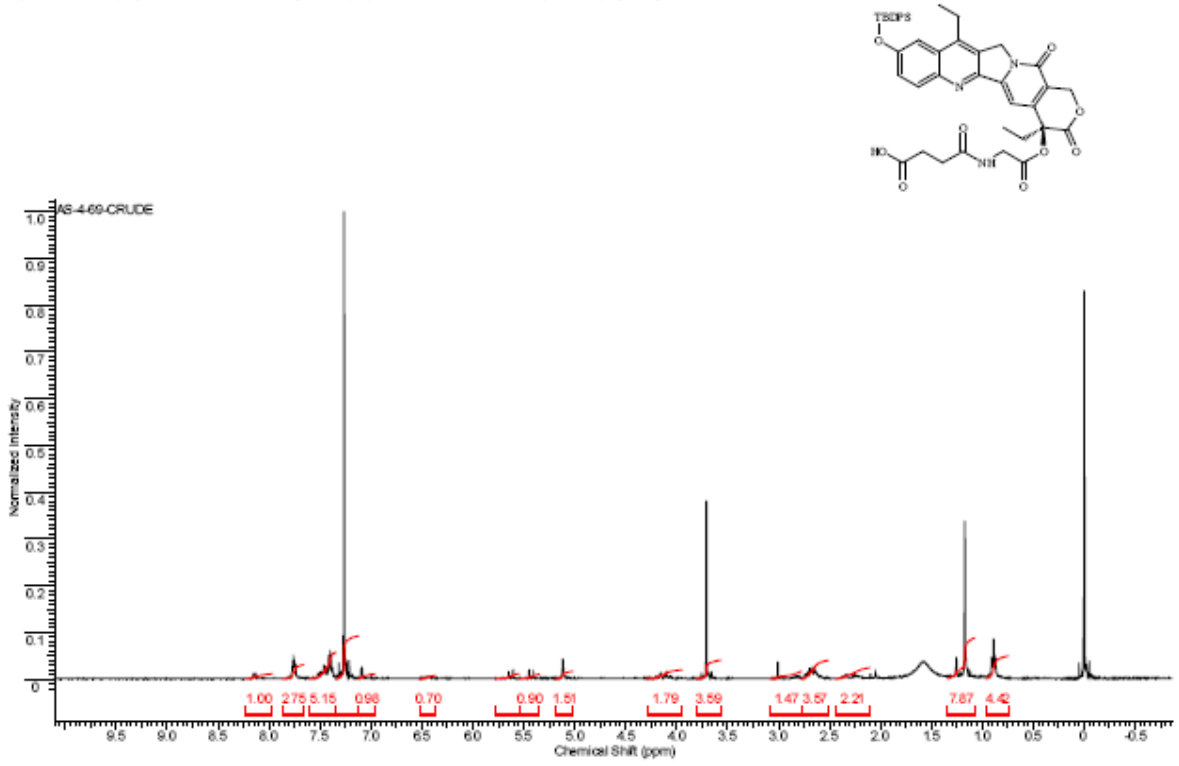

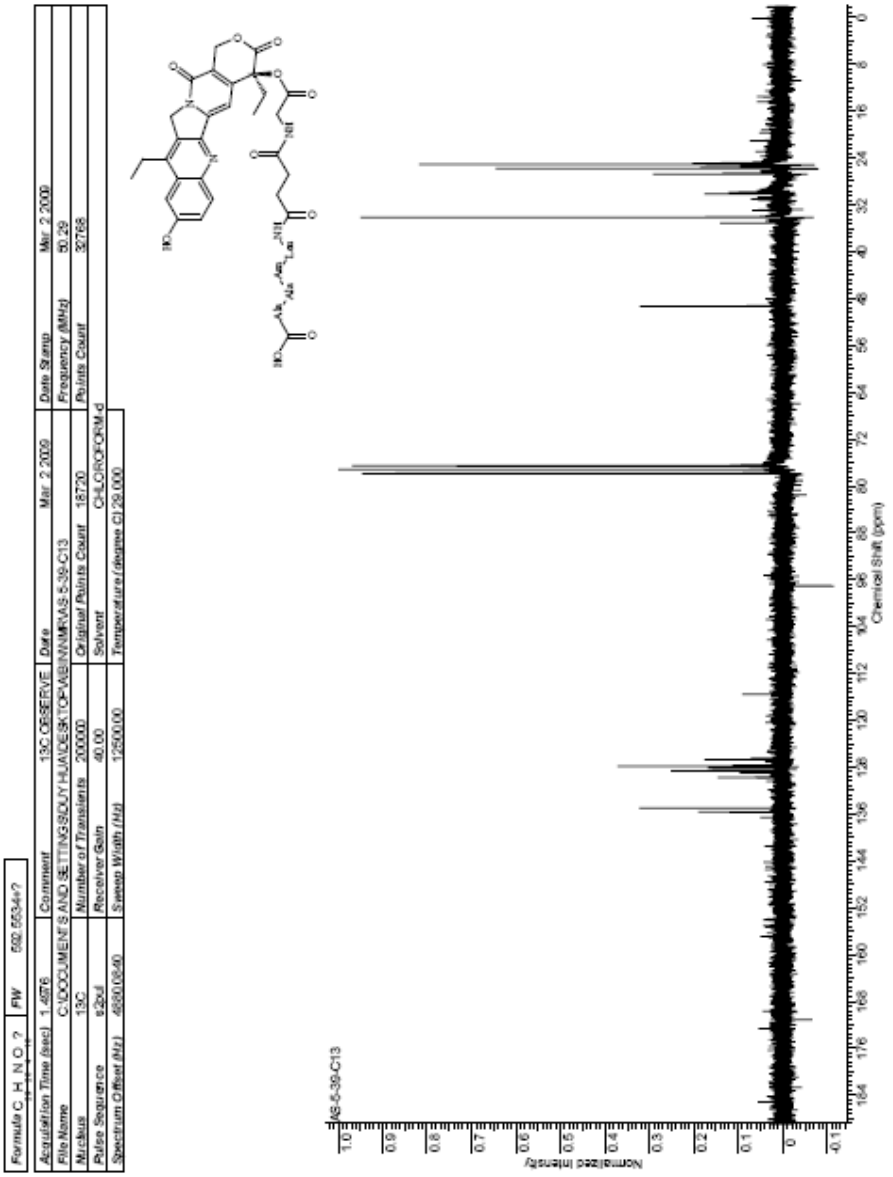
Formula C H N O ? FW 592.6534+?
Acquisition Time (sec) 1.4976 Comment 13C OBSERVE Date Mar 2 2009 Date Stamp Mar 2 2009
File Name C:\DOCUMENTS AND SETTINGS\DUY HUA\DESKTOP\ABI\NMR\AS-5-39-C13 Frequency (MHz) 50.29
Nucleus 13C Number of Transients 200000 Original Points Count 16720 Points Count 32768
Pulse Sequence s2pul Receiver Gain 40.00 Solvent CHLOROFORM-d
Spectrum Offset (Hz) 4600.0840 Sweep Width (Hz) 12500.00 Temperature (degree C) 29.000
AS-5-39-C13
Normalized Intensity
Chemical Shift (ppm)

Formula $C_{38}H_{48}N_4O_{10}$?	FW	592.6534+?					
Acquisition Time (sec)	2.0487	Comment	Std proton	Date	Dec 12 2008	Date Stamp	Dec 12 2008
File Name	C:\DOCUMENTS AND SETTINGS\DUY HUA\DESKTOP\A\BIN\NMR\AS-4-90-3					Frequency (MHz)	399.75
Nucleus	1H	Number of Transients	128	Original Points Count	13103	Points Count	16384
Pulse Sequence	s2pul	Receiver Gain	54.00	Solvent	CHLOROFORM-d		
Spectrum Offset (Hz)	2400.8074	Sweep Width (Hz)	6395.91	Temperature (degree C)	25.000		

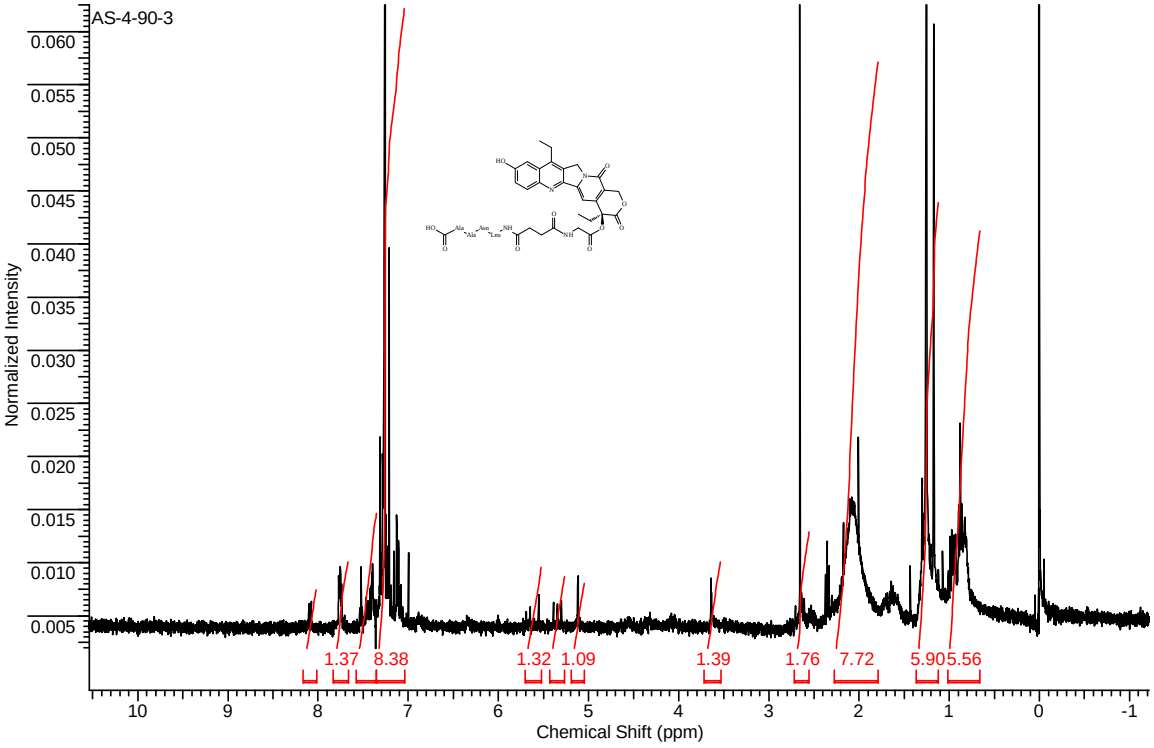

Formula C H N O S	FW 341.3628

Acquisition Time (sec)	1.9945	Comment	STANDARD 1H OBSERVE	Date	Jul 29 2008
Date Stamp	Jul 29 2008	File Name	C:\DOCUMENTS AND SETTINGS\DOYI HUA\DESKTOP\ASBNNMR\AS-3-98-DMSO		
Frequency (MHz)	199.98	Nucleus	1H	Number of Transients 32	Original Points Count 5984
Points Count	8192	Pulse Sequence	s2pul	Receiver Gain 34.00	Solvent DMSO-d6
Spectrum Offset (Hz)	1004.5566	Sweep Width (Hz)	3000.30	Temperature (degree C) 29.000	

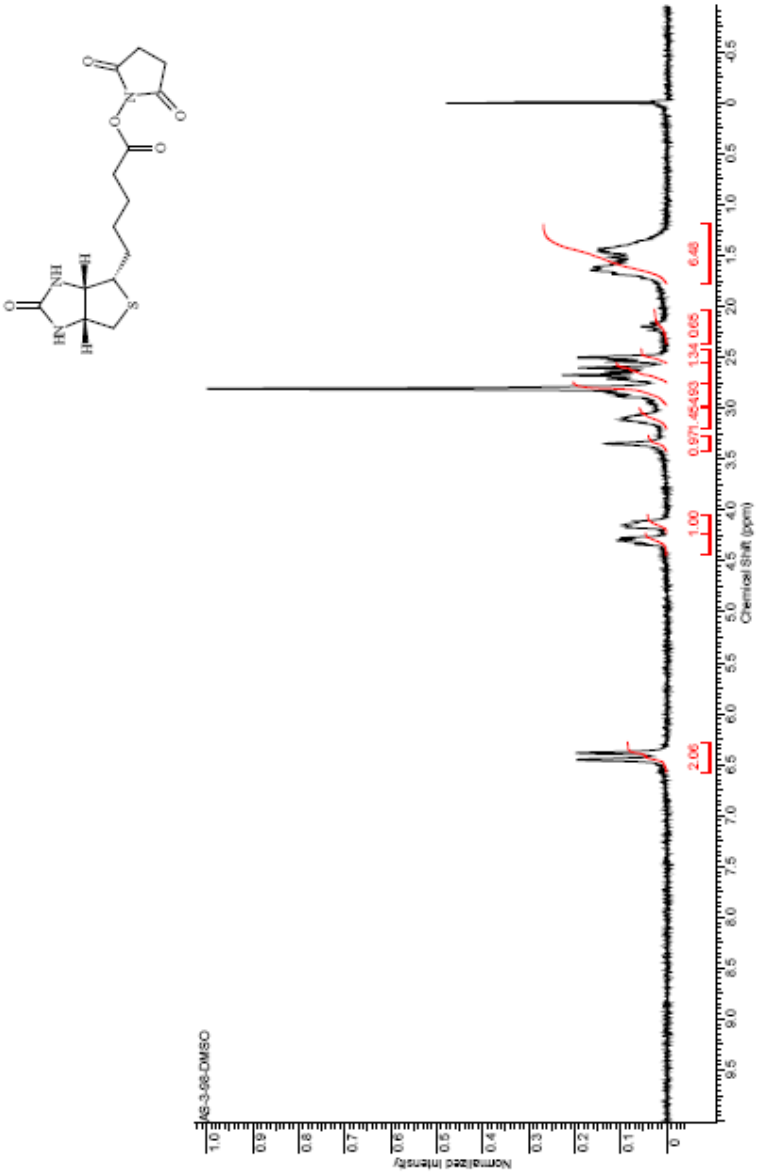

Acquisition Time (sec)	2.0487	Comment	Std proton	Date	Aug 11 2008	Date Stamp	Aug 11 2008
File Name	C:\DOCUMENTS AND SETTINGS\DUY HUA\DESKTOP\AIBN\NMR\AS-3-100-NG-BIOTIN					Frequency (MHz)	399.76
Nucleus	1H	Number of Transients	1000	Original Points Count	13103	Points Count	16384
Pulse Sequence	s2pul	Receiver Gain	48.00	Solvent	DEUTERIUM OXIDE		
Spectrum Offset (Hz)	2472.8893	Sweep Width (Hz)	6395.91	Temperature (degree C)	25.000		

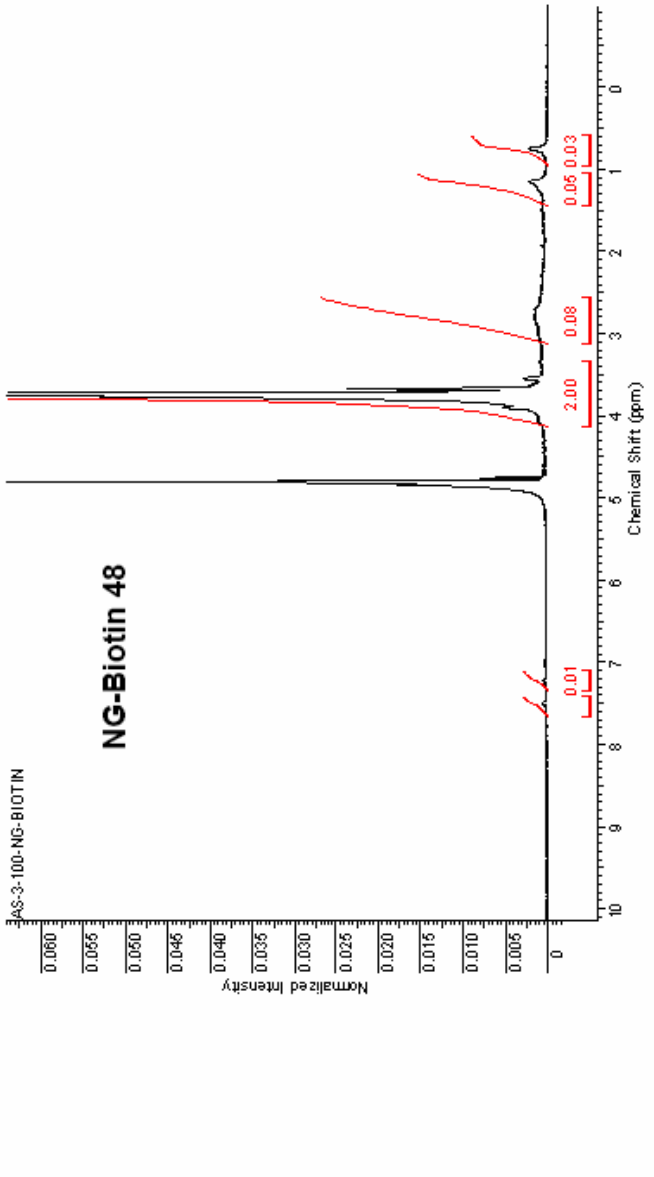

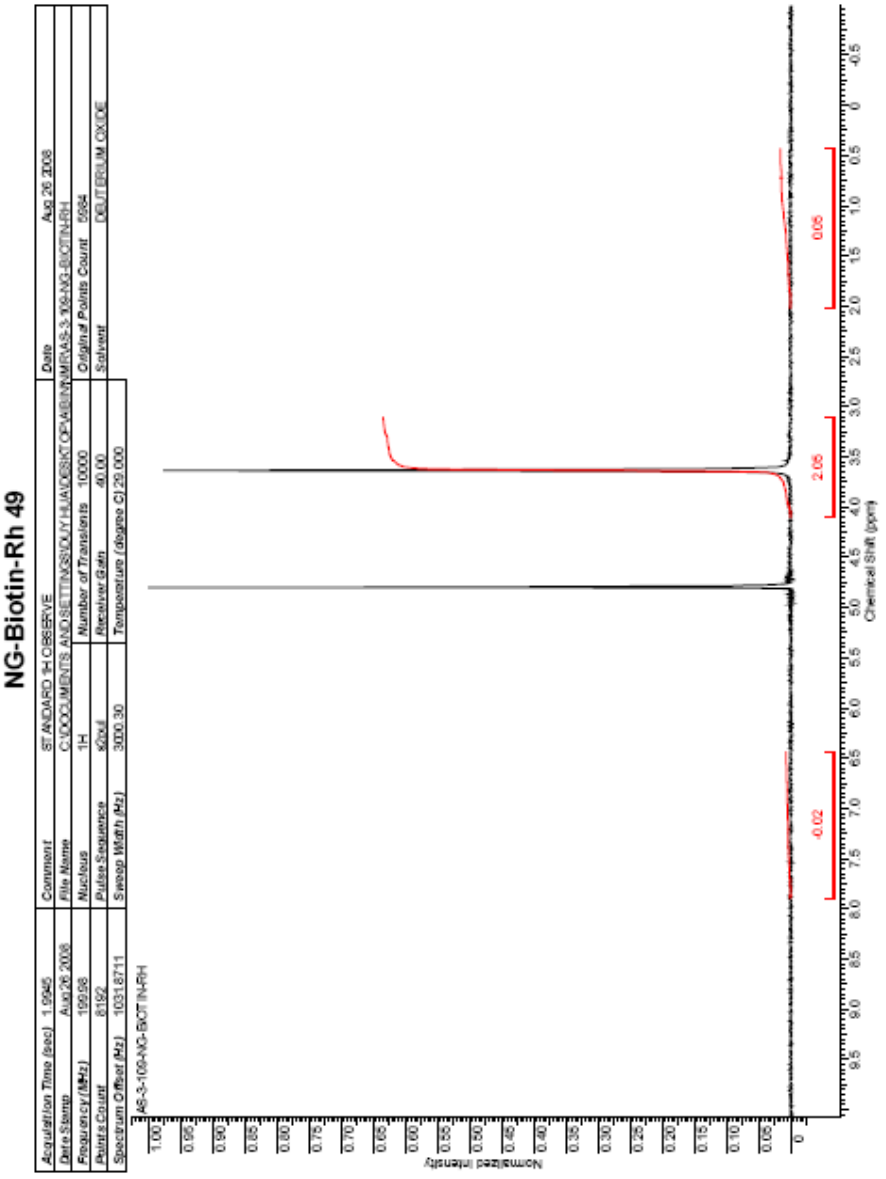
NG-Biotin-Rh 49
Acquisition Time (sec) 1.9945
Comment STANDARD 1H OBSERVE
Date Aug 26 2006
Date Stamp Aug 26 2006
File Name C:\DOCUMENTS AND SETTINGS\DJY\MIJA\DESKTOP\ARBUMRAS-3-109-NG-BIOTIN-RH
Frequency (MHz) 199.98
Nucleus 1H
Number of Transients 10000
Original Points Count 5984
Points Count 8192
Pulse Sequence s2pul
Receiver Gain 40.00
Solvent DEUTERIUM OXIDE
Spectrum Offset (Hz) 1031.8711
Sweep Width (Hz) 3000.30
Temperature (degree C) 29.000
AS-3-109-NG-BIOT IN-RH
Normalized Intensity
Chemical Shift (ppm)
0.02
2.05
0.05

Formula $C_5H_{10}N_2O_2S$	FW	176.2367

Acquisition Time (sec)	1.4576	Comment	13C OBSERVE			Date	May 13 2009
Date Stamp	May 13 2009	File Name	C:\DOCUMENTS AND SETTINGS\DUY HUA\DESKTOP\ABINNMR\DB-1-27-C13				
Frequency (MHz)	50.29	Nucleus	13C	Number of Transients	1000	Original Points Count	16720
Points Count	32768	Pulse Sequence	s2pul	Receiver Gain	40.00	Solvent	DMSO-d6
Spectrum Offset (Hz)	4922.0527	Sweep Width (Hz)	12500.00	Temperature (degree C)	29.000		

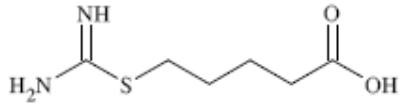

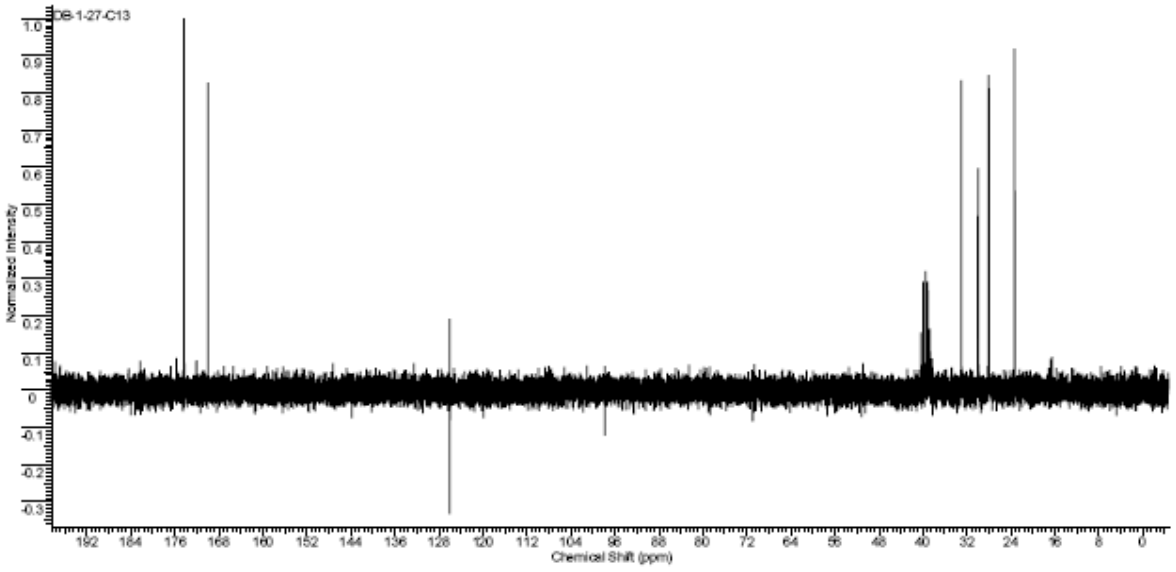

Formula $C_5H_{10}N_2O_2S$	FW	176.2367

Acquisition Time (sec)	1.9965	Comment	STANDARD 1H OBSERVE			Date	May 13 2009
Date Stamp	May 13 2009	File Name	C:\DOCUMENTS AND SETTINGS\DUY HUA\DESKTOP\AS\NMR\DB-1-27				
Frequency (MHz)	199.98	Nucleus	1H	Number of Transients	32	Original Points Count	5984
Points Count	8192	Pulse Sequence	s2pul	Receiver Gain	12.00	Solvent	DMSO-d6
Spectrum Offset (Hz)	962.1274	Sweep Width (Hz)	3000.30	Temperature (degree C)	29.000		

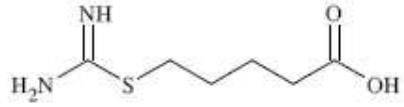

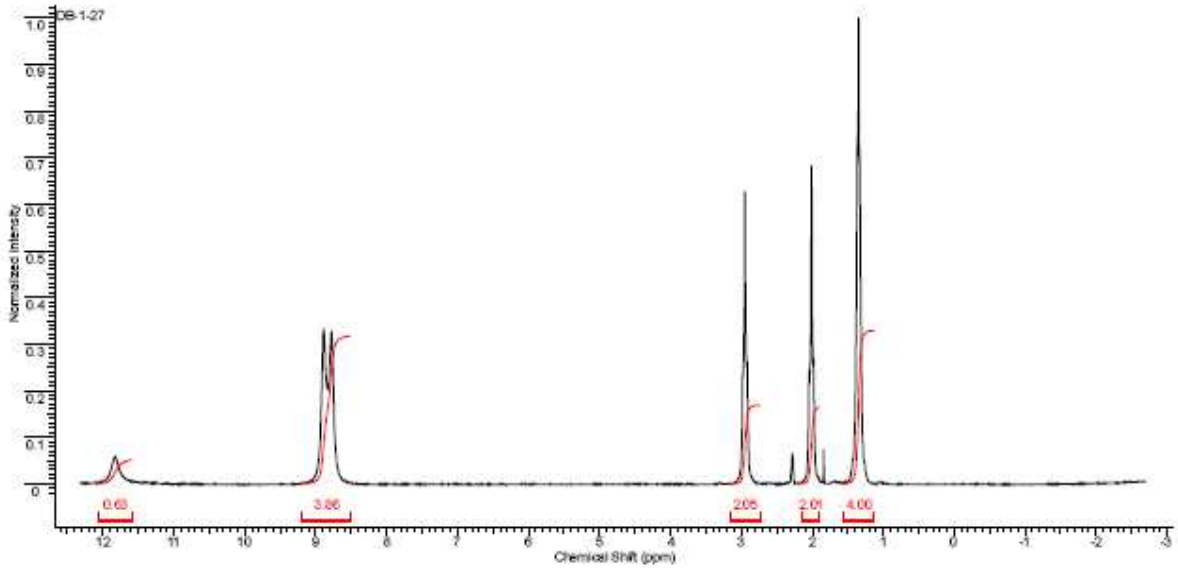

Formula $C_5H_{10}O_2S$	FW	134.1967

Acquisition Time (sec)	1.4976	Comment	13C OBSERVE			Date	Jun 2 2009	Date Stamp	Jun 2 2009
File Name	G:\AIBINA\BIN\DB-1-29-C13			Frequency (MHz)	50.29	Nucleus	13C	Number of Transients	10000
Original Points Count	18720	Points Count	32768	Pulse Sequence	s2pul	Receiver Gain	40.00		
Solvent	CHLOROFORM-d			Spectrum Offset (Hz)	4877.4136	Sweep Width (Hz)	12500.00	Temperature (degree C)	29.000

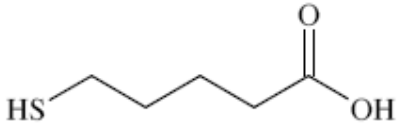

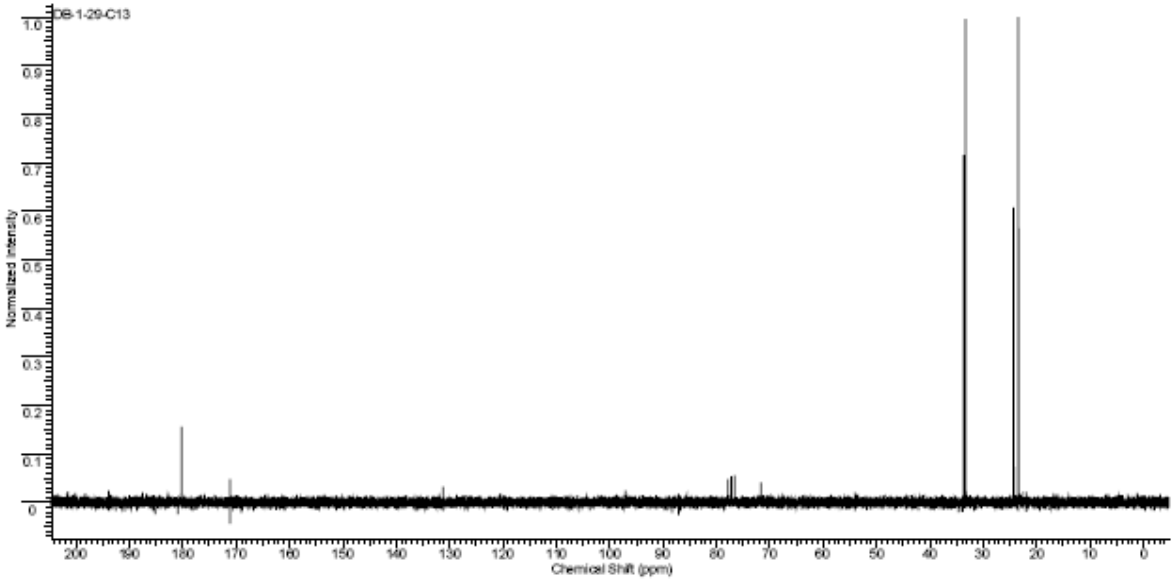

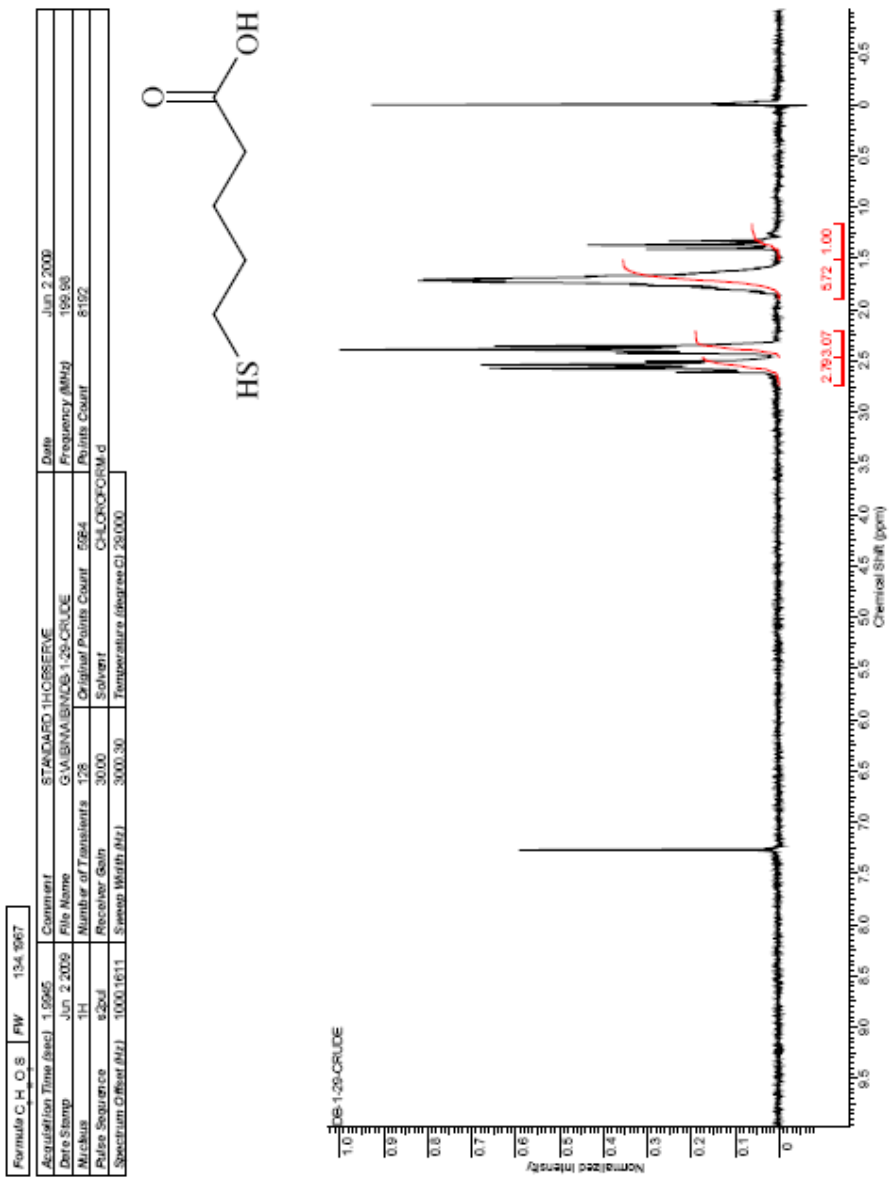
Formula C H O S FW 134.1967
Acquisition Time (sec) 1.9945 Comment STANDARD 1HOBSERVE Date Jun 2 2009
Date Stamp Jun 2 2009 File Name GVABINAB/NDB 1-29-CRUDE Frequency (MHz) 199.98
Nucleus 1H Number of Transients 128 Original Points Count 5984 Points Count 8192
Pulse Sequence s2pul Receiver Gain 3000 Solvent CHLOROFORM-d
Spectrum Offset (Hz) 1000.1611 Sweep Width (Hz) 3000.30 Temperature (degree C) 25.000
HS
O
OH
NDB-1-29-CRUDE
Normalized Intensity
Chemical Shift (ppm)
2.793
5.72
1.00

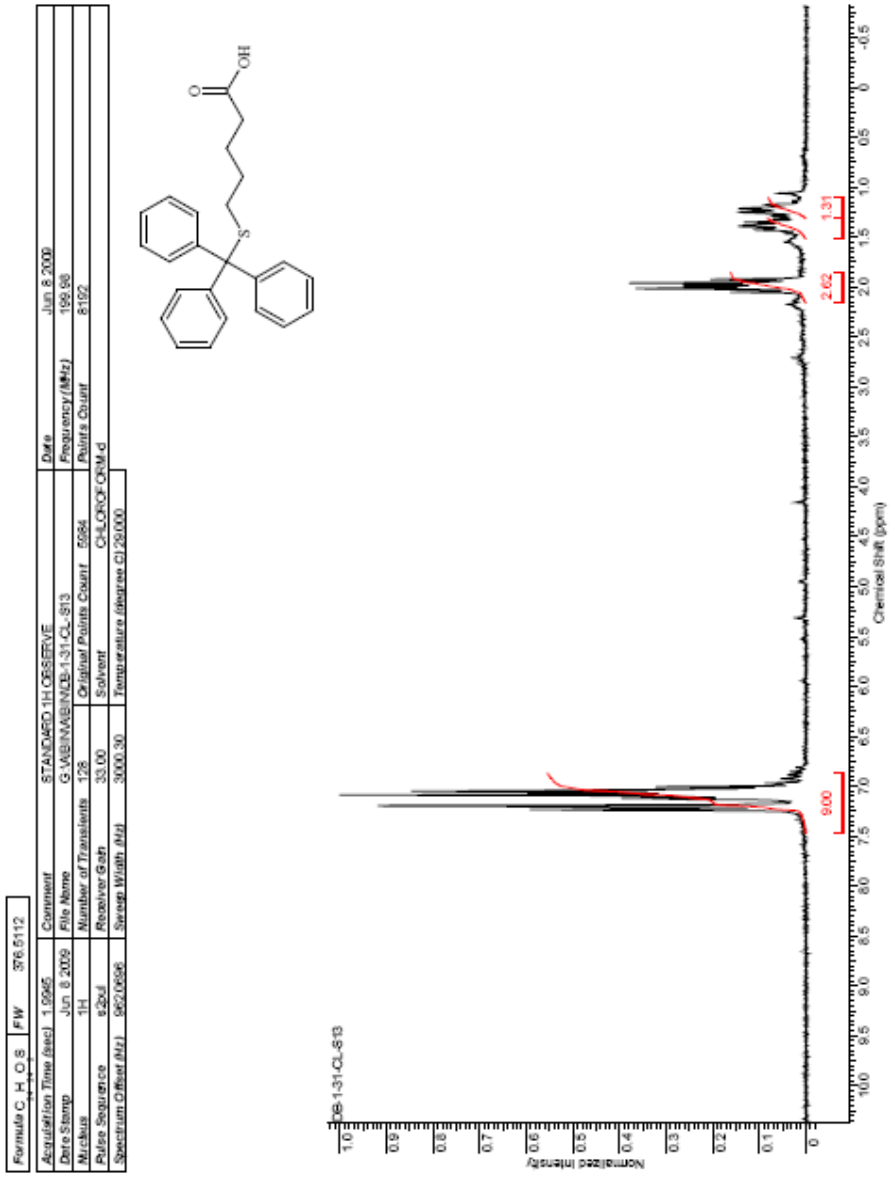
Formula C H O S
FW 376.5112
Acquisition Time (sec) 1.9945
Date Stamp Jun 8 2009
Nucleus 1H
Pulse Sequence s2pul
Spectrum Offset (Hz) 962.0996
Comment STANDARD 1H OBSERVE
File Name G:\VEENA\BENCE-1-31-CL-813
Number of Transients 128
Receiver Gain 33.00
Sweep Width (Hz) 3000.30
Date Jun 8 2009
Frequency (MHz) 199.98
Points Count 8192
Original Points Count 5984
Solvent CHLOROFORM-d
Temperature (degree C) 29.000
OH
O
S
BE-1-31-CL-813
Normalized Intensity
Chemical Shift (ppm)
9.00
2.62
1.31

Acquisition Time (sec)	2.0487	*Comment*	Std proton			*Date*	Jun 17 2009
Date Stamp	Jun 17 2009			*File Name*	F:\AS-4-95	*Frequency (MHz)*	399.75
Nucleus	1H	*Number of Transients*	128	*Original Points Count*	13103	*Points Count*	16384
Pulse Sequence	s2pul	*Receiver Gain*	20.00	*Solvent*	DEUTERIUM OXIDE	*Spectrum Offset (Hz)*	2460.2393
Sweep Width (Hz)	6395.91	*Temperature (degree C)*	25.000				

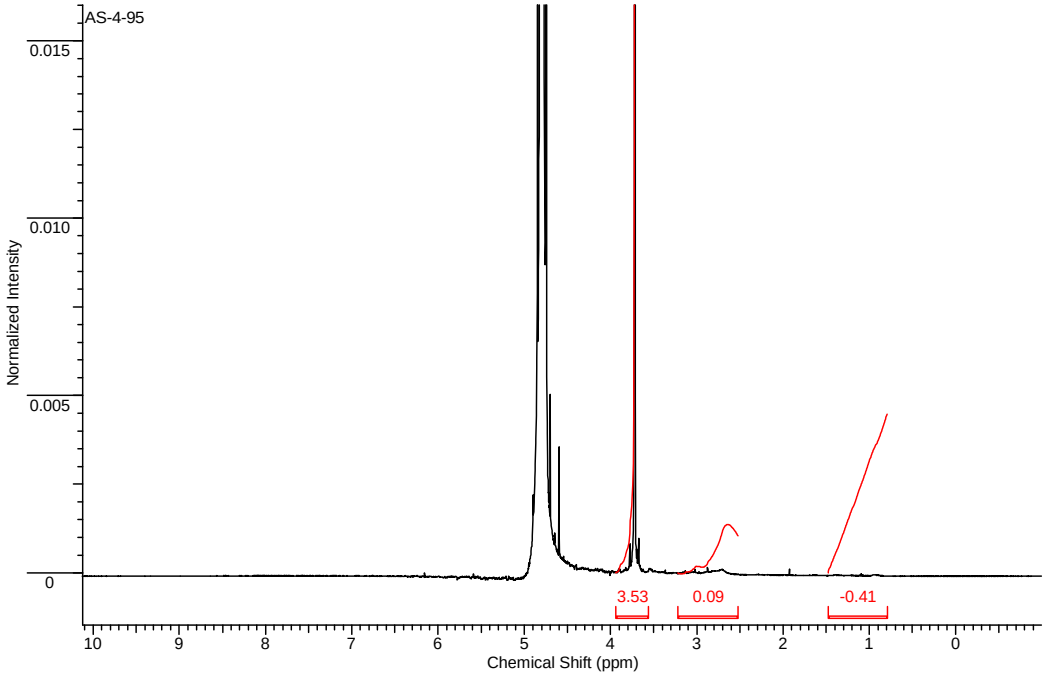

Acquisition Time (sec)	2.0487	*Comment*	Std proton			*Date*	Jun 17 2009
Date Stamp	Jun 17 2009			*File Name*	[illegible]	*Frequency (MHz)*	399.75
Nucleus	1H	*Number of Transients*	128	*Original Points Count*	13103	*Points Count*	16384	*Pulse Sequence*	s2pul
Receiver Gain	20.00	*Solvent*	DEUTERIUM OXIDE			*Spectrum Offset (Hz)*	2460.2393		
Sweep Width (Hz)	6395.91	*Temperature (degree C)*	25.000						

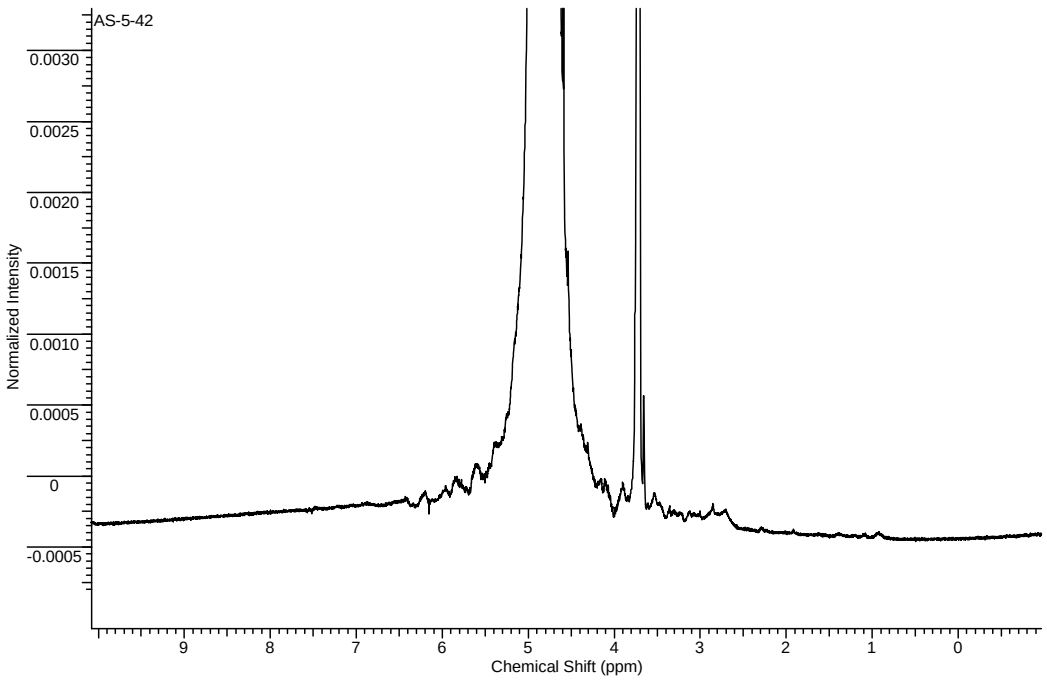

Acquisition Time (sec)	2.0487	*Comment*	Std proton		*Date*	Jun 17 2009	
Date Stamp	Jun 17 2009			*File Name*		*Frequency (MHz)*	399.75
Nucleus	1H	*Number of Transients*	128	*Original Points Count* 13103	*Points Count*	16384	*Pulse Sequence* s2pul
Receiver Gain	20.00	*Solvent*	DEUTERIUM OXIDE		*Spectrum Offset (Hz)*	2460.2393	
Sweep Width (Hz)	6395.91	*Temperature (degree C)*	25.000